AD NUMBER

ADB259877

NEW LIMITATION CHANGE

TO

Approved for public release, distribution unlimited

FROM

Distribution authorized to U.S. Gov't. agencies only; Proprietary Information; Aug 2000. Other requests shall be referred to U.S. Army Medical Research and Material Command, 504 Scott Street, Fort Detrick, MD 21702-5012

AUTHORITY

USAMRMC ltr, 1 Jun 2001.

AD_____

Award Number: DAMD17-96-1-6029

TITLE: Immunobiological Aspects of erbB Receptors in Breast Cancer

PRINCIPAL INVESTIGATOR: Mark Greene, M.D., Ph.D.

CONTRACTING ORGANIZATION: University of Pennsylvania
Philadelphia, Pennsylvania 19104-3246

REPORT DATE: August 2000

TYPE OF REPORT: Final

PREPARED FOR: U.S. Army Medical Research and Materiel Command
Fort Detrick, Maryland 21702-5012

NOTICE

USING GOVERNMENT DRAWINGS, SPECIFICATIONS, OR OTHER DATA INCLUDED IN THIS DOCUMENT FOR ANY PURPOSE OTHER THAN GOVERNMENT PROCUREMENT DOES NOT IN ANY WAY OBLIGATE THE U.S. GOVERNMENT. THE FACT THAT THE GOVERNMENT FORMULATED OR SUPPLIED THE DRAWINGS, SPECIFICATIONS, OR OTHER DATA DOES NOT LICENSE THE HOLDER OR ANY OTHER PERSON OR CORPORATION; OR CONVEY ANY RIGHTS OR PERMISSION TO MANUFACTURE, USE, OR SELL ANY PATENTED INVENTION THAT MAY RELATE TO THEM.

LIMITED RIGHTS LEGEND

Award Number: DAMD17-96-1-6029
Organization: University of Pennsylvania

Those portions of the technical data contained in this report marked as limited rights data shall not, without the written permission of the above contractor, be (a) released or disclosed outside the government, (b) used by the Government for manufacture or, in the case of computer software documentation, for preparing the same or similar computer software, or (c) used by a party other than the Government, except that the Government may release or disclose technical data to persons outside the Government, or permit the use of technical data by such persons, if (i) such release, disclosure, or use is necessary for emergency repair or overhaul or (ii) is a release or disclosure of technical data (other than detailed manufacturing or process data) to, or use of such data by, a foreign government that is in the interest of the Government and is required for evaluational or informational purposes, provided in either case that such release, disclosure or use is made subject to a prohibition that the person to whom the data is released or disclosed may not further use, release or disclose such data, and the contractor or subcontractor or subcontractor asserting the restriction is notified of such release, disclosure or use. This legend, together with the indications of the portions of this data which are subject to such limitations, shall be included on any reproduction hereof which includes any part of the portions subject to such limitations.

THIS TECHNICAL REPORT HAS BEEN REVIEWED AND IS APPROVED FOR PUBLICATION.

Annina Maria Minn
10/19/00

_____

_____

_____

REPORT DOCUMENTATION PAGE

Form Approved
OMB No. 074-0188

1. AGENCY USE ONLY (Leave blank)	2. REPORT DATE	3. REPORT TYPE AND DATES COVERED
	August 2000	Final (15 Jul 96 - 14 Jul 00)

4. TITLE AND SUBTITLE
Immunobiological Aspects of erbB Receptors in Breast Cancer

5. FUNDING NUMBERS
DAMD17-96-1-6029

6. AUTHOR(S)
Mark Greene, M.D., Ph.D.

7. PERFORMING ORGANIZATION NAME(S) AND ADDRESS(ES)
University of Pennsylvania
Philadelphia, Pennsylvania 19104-3246
E-MAIL:
greene@reo.med.upenn.edu

8. PERFORMING ORGANIZATION REPORT NUMBER

9. SPONSORING / MONITORING AGENCY NAME(S) AND ADDRESS(ES)
U.S. Army Medical Research and Materiel Command
Fort Detrick, Maryland 21702-5012

10. SPONSORING / MONITORING AGENCY REPORT NUMBER

11. SUPPLEMENTARY NOTES
Report contains color photos

12a. DISTRIBUTION / AVAILABILITY STATEMENT
Distribution authorized to U.S. Government agencies only (proprietary information, Aug 00). Other requests for this document shall be referred to U.S. Army Medical Research and Materiel Command, 504 Scott Street, Fort Detrick, Maryland 21702-5012.

12b. DISTRIBUTION CODE

13. ABSTRACT ***(Maximum 200 Words)***

The purpose of our studies was to define basic features of receptor complex formation relevant to breast cancer. Our efforts are to determine the amino acid residues required to form a transforming receptor assembly so as to develop an understanding of a subset of human aggressive breast cancers characterized by erbB receptor ensembles. Moreover, knowledge of the role of the kinase containing endodomain of these receptors is desirable as therapeutic intervention of breast cancer becomes more oncoprotein specific. In addition, the activity of ligand-like molecules that modulate p185 her2/neu receptor complex activity has been studied. We have defined principles of erbB receptor assembly and modulation by ligand.

14. SUBJECT TERMS	15. NUMBER OF PAGES
Breast Cancer erbB receptors	97
	16. PRICE CODE

17. SECURITY CLASSIFICATION OF REPORT	18. SECURITY CLASSIFICATION OF THIS PAGE	19. SECURITY CLASSIFICATION OF ABSTRACT	20. LIMITATION OF ABSTRACT
Unclassified	Unclassified	Unclassified	Unlimited

FOREWORD

Opinions, interpretations, conclusions and recommendations are those of the author and are not necessarily endorsed by the U.S. Army.

MF Where copyrighted material is quoted, permission has been obtained to use such material.

___ Where material from documents designated for limited distribution is quoted, permission has been obtained to use the material.

___ Citations of commercial organizations and trade names in this report do not constitute an official Department of Army endorsement or approval of the products or services of these organizations.

MF In conducting research using animals, the investigator(s) adhered to the "Guide for the Care and Use of Laboratory Animals," prepared by the Committee on Care and use of Laboratory Animals of the Institute of Laboratory Resources, national Research Council (NIH Publication No. 86-23, Revised 1985).

MF For the protection of human subjects, the investigator(s) adhered to policies of applicable Federal Law 45 CFR 46.

MF In conducting research utilizing recombinant DNA technology, the investigator(s) adhered to current guidelines promulgated by the National Institutes of Health.

MF In the conduct of research utilizing recombinant DNA, the investigator(s) adhered to the NIH Guidelines for Research Involving Recombinant DNA Molecules.

___ In the conduct of research involving hazardous organisms, the investigator(s) adhered to the CDC-NIH Guide for Biosafety in Microbiological and Biomedical Laboratories.

Mark C Frere 7/26/00

PI - Signature Date

Table of Contents

5) INTRODUCTION:

Our efforts were concerned with a general understanding of two processes that are important for assembly and peptidic signals needed for triggering of a transforming receptor complex. In the assembly studies we determined the role of sub domains of the p185^{neu} receptor that were needed to organize a receptor complex and to permit heterodimer formation betweeen p185 neu and the epidermal growth factor receptor (EGFR). In the study of peptidic forms that might modify receptor function we were able to clone an isoform of neuregulin, and we also evaluated a small exocyclic peptide that affected the transforming functions of p185.

6) BODY:

There were two general hypotheses and two tasks approved for study.

We hypothesized that we can better understand receptor assemblies by analysis of areas of the subdomain of p185^{neu} involved in stabilizing or forming the receptor complex. The purpose of the first task was to provide molecular understanding of heteromer formation fashioned from mutant forms of p185 and the EGFR and determine their responses to recombinant ligands, their growth and transforming properties, and responses to anti-receptor antibodies.

Initial studies performed (documented in Reference 1) at the time of the grant's submission dealt with definition of many of the molecules that became associated with the endodomain of a transforming receptor complex built of p185 homomers or p185/EGFR heterodimers. We were able to show, as seen in the accompanying paper, that a variety of unique substrates became associated with distinct endodomains created by p185 homomers or p185/EGFR heteromers. Moreover, through the use of p185 endodomain mutants that lacked an active kinase domain, we noticed that many substrates could still associate with them after receiving trans-phosphorylation signals from the associated EGFR.

In the next set of studies (Reference 2) we developed a molecular and atomic level understanding of the kinase-kinase association mechanism by developing homology models of the p185 and EGFR kinase domains. We were able to define the surface interactions that govern kinase-kinase associations. Moreover, we found that the auto-phosphorylation sites found within the kinase domain itself most likely regulate substrate selection, thereby affecting signal transduction. Another critical insight from these efforts was the ready assembly of tetrameric forms of the receptor complex.

We extended these structural studies (Reference 3) to examine the auto phosphorylation sites that exist within the kinase domain of neu in biochemical and molecular assays to verify our modeling predictions. Previous analysis of p185^{neu} indicated that there are at least five tyrosine autophosphorylation sites: Y882, Y1028, Y1143, Y1226/7, and Y1253, of which Y882 might be important because of its location in the kinase activity domain. We specifically analyzed the effect of a Y882F (phenylalanine substituted for tyrosine at position 882) mutation in the enzymatic active domain. We also deleted the carboxyl terminal 122 amino acids of the endodomain which contained three other autophosphorylation sites (TAPstop) and combined mutants of that deletion with Y882F (Y882F/APstop). Both *in vitro* and *in vivo* transformation assays showed that substitution of tyrosine^{882} by phenylalanine significantly decreased the transforming

potential of activated, oncogenic p185^{neu}, although no significant difference in the total phosphotyrosine levels of the mutant proteins were observed.

To analyze mitogenic signaling in response to ligand, the intracellular domains of p185 p185^{neu} and Y882F were fused with the extracellular domain of the EGF receptor. The proliferation of cells expressing these chimeric receptors was EGF-dependent, and cells expressing EGFR/Y882F chimeric receptors were less responsive to EGF stimulation than those expressing EGFR/neu receptors. In vitro kinase assays demonstrated that abolishing the autophosphorylation site Y882 diminished the enzymatic tyrosine kinase activity of p185^{neu}. These studies indicated that the tyrosine^{882} residue may be important for p185^{neu}-mediated transformation by affecting the enzymatic kinase function of the p185^{neu} receptor.

In the next set of studies (Reference 3) we examined how EGFR and p185 endodomain mutants interacted with an ectodomain mutant form of EGFR. Mutant Epidermal Growth Factor Receptor (ΔEGFR, also referred to as EGFRvIII) oncoproteins lack most of subdomains I and II of the extracellular region, a deletion which includes most of the first of two cysteine-rich regions. ΔEGFR oncoproteins confer increased tumorigenicity in vivo and are often co-expressed with full-length EGFR in human tumors.

We expressed an ectodomain-derived, carboxyl-terminal deletion mutant of the p185^{neu} oncogene (T691stop) in human glioblastoma cells coexpressing endogenous EGFR and activated ΔEGFR oncoproteins (Reference 4). The p185^{neu} ectodomain formed heterodimers with ΔEGFR proteins and reduced the phosphotyrosine content of ΔEGFR monomers. As a consequence of T691stop neu expression, cell proliferation in conditions of full growth and reduced serum and anchorage-independent growth in soft agar was reduced in glioblastoma cells expressing either endogenous EGFR alone or coexpressing EGFR and elevated levels of ΔEGFRs. T691stop neu mutant receptors abrogated the dramatic growth advantage conferred by ΔEGFR in vivo, suggesting that physical associations primarily between subdomains III and IV of the p185^{neu} and EGFR ectodomains are sufficient to modulate signaling from activated EGFR complexes.

We also determined (Reference 4) the consequences of disabling oncogenic erbB receptors with this form of endodomain mutant of p185. In these studies we evaluated whether disabling oncoproteins of the erbB receptor family would sensitize transformed human cells to the induction of genomic damage by gamma irradiation. Radioresistant human tumor cells in which erbB receptor signaling was inhibited exhibited increased growth arrest and apoptosis in response to DNA damage. Apoptosis was observed after radiation in human tumor cells containing either a wild-type or mutated p53 gene product and suggested that both p53-dependent and p53–independent mechanisms may be responsible for the more radiosensitive phenotype. Because cells exhibiting increased radiation-induced apoptosis were also capable of growth arrest in serum-deprived conditions and in response to DNA damage, apoptotic cell death was not induced simply as a result of impaired growth arrest pathways.

The issue of subdomains was further studied (Reference 5). Contributions made by various p185^{neu} subdomains to signaling induced by a heterodimeric erbB complex were analyzed. Co-expression of full-length EGFR and oncogenic p185^{neu} receptors resulted in an increased EGF-induced phosphotyrosine content of p185^{neu}, increased cell proliferation to limiting concentrations of EGF, and increases in both EGF-induced

MAPK and phosphatidylinositol 3-kinase (PI3-kinase) activation. Intracellular domain-deleted p185^{neu} receptors (T691stop neu) were able to associate with full-length EGFR but induced antagonistic effects on EGF-dependent EGF receptor down-regulation, cell proliferation, and activation of MAPK and PI3-kinase pathways.

Extracellular domain-deleted p185^{neu} forms failed to augment activation of MAPK and PI 3-kinase in response to EGF. Association of the EGFR with a carboxyl-terminally truncated p185^{neu} mutant (TAPstop) form did not increase transforming efficiency and phosphotyrosine content of the TAPstop species, and proliferation of EGFR/TAPstop-co-expressing cells in response to EGF was similar to cells containing the EGFR only. We found that the formation of potent homodimer assemblies composed of oncogenic p185^{neu} requires the ectodomains for ligand-dependent physical association and the intracellular domain contacts for efficient intermolecular kinase activation.

Disabling p185 receptor complexes was studied using both monoclonal antibodies and the endodomain p185 mutant. We used differential display to find novel genes that became expressed during phenotype reversion. As shown in Reference 6, we isolated a 325-bp cDNA fragment that, as determined by Northern analysis, was expressed at higher levels in anti-p185^{neu}-treated tumor cells but not in cells expressing internalization defective p185^{neu} receptors. This cDNA fragment was identical to the HIV tat-binding protein-1 (TBP1). TBP1 mRNA levels were found to be elevated on inhibition of the oncogenic phenotype of transformed cells expressing erbB family receptors. TBP1 overexpression diminished cell proliferation, reduced the ability of the parental cells to form colonies in vitro, and almost completely inhibited transforming efficiency in athymic mice when stably expressed in human tumor cells containing erbB family receptors. Disabling erbB tyrosine kinases by antibodies or by trans-inhibition represents an initial step in triggering a TBP1 pathway which itself is a negative regulator of the 26S proteasome.

Hypothesis 2: The second hypothesis linked to the first involved the study of erbB and p185$^{c\text{-}neu}$ function in vitro and in vivo using ligand like molecules. Previously we isolated a Neu Activating Factor (NAF) and characterized it biochemically and in terms of some of its activities. We intended to characterize neu activating peptides in terms of sequence and tissue distribution.

In our next set of studies we began to examine peptidic ligand signals that modulate erbB function (Reference 7). We showed that cytokines, including EGF, are able to induce tyrosine phosphorylation of Signal Regulatory Proteins (SIRPs) that can inhibit erbB function. We overexpressed human SIRPα1 in U87MG cells in order to examine how SIRPα1 modulates erbB signaling pathways. Overexpression of the SIRPα1 cDNA diminished EGF-induced phosphoinositide-3-OH kinase (PI3-K) activation in U87MG cells. Reduced EGF-stimulated activation of PI3-K was mediated by interactions between the carboxyl terminus of SIRPα1 and the Src homology-2 (SH2)-containing phosphotyrosine phosphatase, SHP2. Furthermore, SIRPα1-overexpressing U87MG cells displayed reduced cell migration and cell spreading that was mediated by association between SIRPα1 and SHP2. However, SIRPα1-overexpressing U87MG clonal derivatives exhibited no differences in cell growth or levels of mitogen-activated protein kinase (MAPK) activation. These data reveal a pathway that negatively regulates erbB-induced PI3-K activation in tumor cells and involves interactions between SHP2 and tyrosine phosphorylated SIRPα1.

We also identified a neuregulin or NRG-like gene using the NRG transmembrane primers. The level of homology suggested that we have identified a human NRG-2 or NRG-2-like gene. Expression in the ATL-2 cell line of our RT-PCR fragment was 97% identical at the nucleotide level (102/106 nucleotides) and 100% identical (34/34) at the amino acid level with the reported NRG-2 transmembrane region. The minor differences at the nucleotide level may reflect a sequencing artifact, Taq polymerase infidelity, a naturally occurring polymorphism in the human NRG-2 gene, or a possible ATL-2-derived sequence that is distinct from NRG-2.

We used this probe to screen an oligo-dt primed ATL-2 cDNA library but only identified several false positives using the transmembrane domain as a probe. We feel the short length of this probe (only 100 nucleotides in length) and the possible promiscuity of the probe binding to any clone that has transmembrane spanning regions has caused us to obtain inappropriate clones in our first round of ATL-2 cDNA library screening.

New primers were designed that correspond exactly to conserved regions outside the region encoding the transmembrane domain. Using this renewed RT-PCR strategy, we were able to amplify a clone, designated 'SK1', approximately 1000 nucleotides in length that extends from the middle of the immunoglobulin-like domain to just beyond the transmembrane region and into the intracellular domain of the NRG-2_{ATL-2} molecule from the ATL-2 cDNA. The SK1 clone exactly matched the reported sequence for the corresponding region of the NRG-2 sequence in the Genbank database. This suggested that the NRG-2_{ATL-2} molecule is an isoform of NRG-2 and apparently not a new neuregulin-related gene.

We created a peptidic form (Reference 8) designed from an antibody reported to have agonisitc activities including the induction of phosphorylation of p185 followed by inactivation of p185 function. We term this peptide Anti-Her2/Neu Peptide (AHNP). Treatment of human cancer cells expressing HER2/neu (either alone or in combination with the EGFR) with an AHNP peptide derived from the anti-HER2/neu monoclonal antibody 4D5, resulted in increased inhibition of cell growth in vitro and in vivo. Levels of apoptosis induced by gamma-irradiation or doxorubicin were enhanced in these same cells *in vitro* by incubation with AHNP. Short-term (0-6 h) AHNP treatment resulted in increased tyrosine phosphorylation of signal-regulatory proteins (SIRPs/SHPS-1) and in differential binding of endogenous SIRPα proteins to SHP-2, suggesting that AHNP1 modulated apoptosis by inducing SIRP/SHPS-1 function. In combination studies, treatment with doxorubicin and AHNP *in vivo* resulted in greater inhibition of tumor growth than that observed with either agent alone.

Therefore, ligand-like small aromatic modified exocyclic (AME) peptide mimetics of anti-receptor antibodies modulate the response of HER2-expressing cancer cells to DNA-damaging agents and enhance the effects of cytotoxic therapies. AHNP peptide mimetics, such as AHNP, represent an alternative way to target erbB receptor oncoproteins.

7) KEY RESEARCH ACCOMPLISHMENTS:

- Definition of the role of subdomains in receptor complex assembly and function.
- Determination of the induction of a negative regulator of the 26S proteasome as a consequence of disabling of erbB function.
- Determination of a structural model of kinase associations that favor the formation of tetrameric assemblies.
- Isolation of a neuregulin isoform that may have peptide ligand properties.
- Creation of a cyclic peptide fashioned from an agonistic antibody that disables erbB complexes.

8) REPORTABLE OUTCOMES:

A) Manuscript list:

1) Zhang, H.T., O'Rourke, D., Zhao, H., Murali, R., Mikami, Y., Davis, J.G., Greene, M.I. and Qian, X.: Absence of autophosphorylation site Y882 in the p185^{neu} oncogene product correlates with a reduction of transforming potential. Oncogene, 16:2835-2842, 1998.

2) O'Rourke, D., Kao, G.D., Singh, N., Park, B., Muschel, R.J., Wu, C. and Greene, M.I.: Conversion of a radioresistant phenotype to a more sensitive one by disabling erbB receptor signaling in human cancer cells. Proc. of the Nat'l Acad. of Sci. (USA), 95:10842-10847, 1998.

3) Qian, X., O'Rourke, D.M., Fei, Z., Zhang, H., Kao, C. and Greene, M.I.: Domain-specific interactions between the p185^{neu} and epidermal growth receptor kinases determine differential signaling outcomes. Journal of Biological Chemistry, 274(2):574-583, 1999.

4) Park, B., O'Rourke, D., Wang, Q., Davis, J., Post, A., Qian, X. and Greene, M.I.: Induction of the Tat-binding protein-1 accompanies the disabling of oncogenic erbB receptor tyrosine kinases. Proc. of the Nat'l Acad. of Sci. (USA), 96:6434-6438, 1999.

5) Wu, C., Chen, Z., Ullrich, A., Greene, M.I., O'Rourke, D.:Inhibition of EGFR-mediated phosphoinositide-3-OH (PI3-K) signaling and glioblastoma phenotype by Signal-Regulatory Proteins (SIRPs). Oncogene, accepted, 2000.

6) Park, B.W., Berezov, A., Wu, C.W., Zhang, X., Dua, R., Zhang, H.T., Wang, Q., Kao, G., O'Rourke, D., Greene, M.I. and Murali, R.: Rationally designed anti-HER2/neu peptide mimetic disables p185$^{HER2/neu}$ tyrosine kinases *in vitro* and *in vivo*. Nature (Biotechnology), 18: 194-198, 2000

B) Thesis: Chih-Ching Kao received Ph. D. UNIVERISTY OF PENNSYLVANIA. Thesis title: Studies of the interaction of novel forms of the p185$^{c\text{-}neu}$ receptor domain

C) Presentations: Presentation at the Era of Hope Army meeting in Atlanta, Georgia 2000 – Receptor ensembles in transformation

D) Patent for the AHNP mimetic and irradiation - submitted

E) Development of the AHNP peptides and the HER2/neu endodomain mutant cell lines

9) CONCLUSIONS:

We have made significant progress in understanding the roles of the subdomains of the endodomain of p185^{neu}. It is clear from our work that the assembly of erbB homomeric and heteromeric complexes able to transform human breast tumors involves multiple subdomain interactions and likely is mediated through tetrameric erbB polypeptides. Furthermore, we have shown that disabling erbB complexes involves activation of regulators of the 26S proteasome. Other pathways triggered by disabling erbB include the SIRP pathways that inhibit PI3 kinase function and lead to phenotype reversal.

In addition we have created a novel ligand-like peptide which was fashioned from the HERCEPTIN antibody's three-dimensional structure. The AHNP peptide may have clinical utility.

10) REFERENCES:

1)Dougall, W.C., Qian, X., Miller, M., and M.I. Greene.: Association of signaling proteins with a nonmitogenic heterodemeric complex composed of Epidermal Growth Factor Receptor and kinase-inactive p185$^{c\text{-}neu}$. *DNA and Cell Biology* **15**, 31-40, 1996.

2)Murali, R., Brennan, P.J., Kieber-Emmons, T., and M.I. Greene.: Structural analysis of p185$^{c\text{-}neu}$ and epidermal growth factor receptor tyrosine kinases: Oligomerization of kinase domains. *Proc. Natl. Acad. Sci.* **93**, 652-657, 1996.

3)Zhang, H.T., O'Rourke, D., Zhao, H., Murali, R., Mikami, Y., Davis, J.G., Greene, M.I. and Qian, X.: Absence of autophosphorylation site Y882 in the p185^{neu} oncogene product correlates with a reduction of transforming potential. Oncogene, 16:2835-2842, 1998.

4)O'Rourke, D., Kao, G.D., Singh, N., Park, B., Muschel, R.J., Wu, C. and Greene, M.I.: Conversion of a radioresistant phenotype to a more sensitive one by disabling erbB receptor signaling in human cancer cells. Proc. of the Nat'l Acad. of Sci. (USA), 95:10842-10847, 1998.

5) Qian, X., O'Rourke, D.M., Fei, Z., Zhang, H., Kao, C. and Greene, M.I.: Domain-specific interactions between the p185^{neu} and epidermal growth receptor kinases determine differential signaling outcomes. Journal of Biological Chemistry, 274(2):574-583, 1999.

6)Park, B., O'Rourke, D., Wang, Q., Davis, J., Post, A., Qian, X. and Greene, M.I.: Induction of the Tat-binding protein-1 accompanies the disabling of oncogenic erbB receptor tyrosine kinases. Proc. of the Nat'l Acad. of Sci. (USA), 96:6434-6438, 1999.

7) Wu, C., Chen, Z., Ullrich, A., Greene, M.I., O'Rourke, D.:Inhibition of EGFR-mediated phosphoinositide-3-OH (PI3-K) signaling and glioblastoma phenotype by Signal-Regulatory Proteins (SIRPs). Oncogene, accepted, 2000.

8) Park, B.W., Berezov, A., Wu, C.W., Zhang, X., Dua, R., Zhang, H.T., Wang, Q., Kao, G., O'Rourke, D., Greene, M.I. and Murali, R.: Rationally designed anti-HER2/neu peptide mimetic disables p185$^{HER2/neu}$ tyrosine kinases *in vitro* and *in vivo*. Nature (Biotechnology), 18: 194-198, 2000.

11) APPENDICES:

Final Bibliography

1) Zhang, H.T., O'Rourke, D., Zhao, H., Murali, R., Mikami, Y., Davis, J.G., Greene, M.I. and Qian, X.: Absence of autophosphorylation site Y882 in the p185^{neu} oncogene product correlates with a reduction of transforming potential. Oncogene, 16:2835-2842, 1998.

2) O'Rourke, D., Kao, G.D., Singh, N., Park, B., Muschel, R.J., Wu, C. and Greene, M.I.: Conversion of a radioresistant phenotype to a more sensitive one by disabling erbB receptor signaling in human cancer cells. Proc. of the Nat'l Acad. of Sci. (USA), 95:10842-10847, 1998.

3) Qian, X., O'Rourke, D.M., Fei, Z., Zhang, H., Kao, C. and Greene, M.I.: Domain-specific interactions between the p185^{neu} and epidermal growth receptor kinases determine differential signaling outcomes. Journal of Biological Chemistry, 274(2):574-583, 1999.

4) Park, B., O'Rourke, D., Wang, Q., Davis, J., Post, A., Qian, X. and Greene, M.I.: Induction of the Tat-binding protein-1 accompanies the disabling of oncogenic erbB receptor tyrosine kinases. Proc. of the Nat'l Acad. of Sci. (USA), 96:6434-6438, 1999.

5) Wu, C., Chen, Z., Ullrich, A., Greene, M.I., O'Rourke, D.:Inhibition of EGFR-mediated phosphoinositide-3-OH (PI3-K) signaling and glioblastoma phenotype by Signal-Regulatory Proteins (SIRPs). Oncogene, accepted, 2000.

6) Park, B.W., Berezov, A., Wu, C.W., Zhang, X., Dua, R., Zhang, H.T., Wang, Q., Kao, G., O'Rourke, D., Greene, M.I. and Murali, R.: Rationally designed anti-HER2/neu peptide mimetic disables p185$^{HER2/neu}$ tyrosine kinases *in vitro* and *in vivo*. Nature (Biotechnology), 18: 194-198, 2000

Abstract: Presentation at the Era of Hope Army meeting in Atlanta, Georgia 2000 – Receptor ensembles in transformation

List of personnel receiving pay from this research effort:

James Davis
Mark Greene
Chih Ching Kao
Kiichi Kajino
Toru Kumagai
Jennifer Peavey
Huizhen Zhao

DNA AND CELL BIOLOGY
Volume 15, Number 1, 1996
Mary Ann Liebert, Inc.
Pp. 31–40

Association of Signaling Proteins with a Nonmitogenic Heterodimeric Complex Composed of Epidermal Growth Factor Receptor and Kinase-Inactive p185$^{c\text{-}neu}$

WILLIAM C. DOUGALL,[1] XIAOLAN QIAN, MARSHA J. MILLER, and MARK I. GREENE

ABSTRACT

The functional consequences of heterodimer formation between the epidermal growth factor receptor (EGFr) and the p185$^{c\text{-}neu}$ receptor tyrosine kinase include increased mitogenic and transformation potencies. To determine the possible alteration of signal transduction pathways resulting from this heteromeric complex, the capacity of several signaling proteins to associate with the heterodimeric receptors has been assayed. The *in vivo* interaction with the EGFr/p185$^{c\text{-}neu}$ heterodimer of several signal transduction proteins, including phospholipase C-γ1 (PLC-γ1), the p85 subunit of phosphotidylinositol 3-kinase, the *ras* GTPase activating protein, SHC, NCK, p72RAF, and the tyrosine phosphatase SHPTP2, was measured by coimmunoprecipitation. The binding of these signaling proteins to a complex composed of EGFr and a kinase-inactive form of p185 (p185K757M) was not impaired, even though the mitogenic and transformation activity of this complex had been abrogated. In addition, the EGF-induced phosphorylation of GAP, p85, and PLC-γ1 did not correlate with the dominant-negative action of p185K757M on EGFr function. Thus, substrate association and phosphorylation do not correlate stringently with the mitogenic and transforming activity of this receptor complex, suggesting additional pathways or mechanisms vital to EGFr/p185$^{c\text{-}neu}$ heterodimeric signaling.

INTRODUCTION

RECEPTOR TYROSINE KINASES transmit signals resulting from polypeptide ligand binding by the phosphorylation and activation of cellular proteins. Two prototypic type I transmembrane receptors, the epidermal growth factor receptor (EGFr) and the product of the rat c-*neu* or the human c-*erbB-2* gene (p185$^{c\text{-}neu/c\text{-}erbB\text{-}2}$) affect signal transduction mechanisms by ligand-induced receptor oligomerization, which results in the activation of the intrinsic tyrosine kinase and receptor autophosphorylation (Weiner *et al.*, 1989a,b; Ullrich and Schlessinger, 1990). This ligand-induced mechanism has been deregulated in the oncogenic p185^{neu} protein as a result of a point mutation in the transmembrane region leading to constitutive oligomerization, enzymatic activation, and cellular transformation (Bargmann and Weinberg, 1988; Weiner *et al.*, 1989a,b).

The overexpression of the human c-*erbB-2* protein has been observed in a large number of human adenocarcinomas (including breast, ovarian, stomach, pancreatic, and bladder) and correlates with a poor clinical prognosis (Slamon *et al.*, 1987). The hypothesis that human c-*erbB-2* gene amplification and protein overexpression causes cellular transformation by receptor oligomerization and subsequent tyrosine kinase activation in a ligand-independent manner has been confirmed experimentally (Di Fiore *et al.*, 1987; Chazin *et al.*, 1992; LeVea *et al.*, 1993; Samanta *et al.*, 1994).

A third mechanism for cellular transformation by type I growth factor receptors results from the hetero-oligomeric interaction of two different receptor proteins (EGFr and p185$^{c\text{-}neu}$). Expression of moderately high levels of EGFr and p185 proteins together in rat fibroblasts led to enhanced activation of the receptor tyrosine kinase complex (Qian *et al.*, 1992), enhanced proliferative response to EGF (Wada *et al.*, 1990), and transformation of fibroblasts in the absence of exogenously added growth factor (Kokai *et al.*, 1989). The critical role for EGFr/p185 heteroreceptor interactions in signal transduction has been shown in two ways: (i) the inhibition of transformation by down-modulation of either receptor protein by monoclonal antibodies (Wada *et al.*, 1989); (ii) the loss of EGF-induced responses in cells that express kinase-

Center for Receptor Biology and Division of Immunology, Department of Pathology and Laboratory Medicine, University of Pennsylvania School of Medicine, Philadelphia, PA 19104.
[1]Present address: Department of Molecular Biology, Immunex Corporation, 51 University St., Seattle, WA 98101.

deficient forms of p185 (Qian *et al.*, 1994a,b). The regulation of receptor kinase function by hetero-receptor interactions has been suggested to be a general mechanism by which signal transduction pathways are modulated in different differentiation, growth, and transformation circumstances (for review, see Dougall *et al.*, 1994; Lemmon and Schlessinger, 1994; Heldin, 1995).

Receptor tyrosine kinase signaling is initially mediated by a number of tyrosine kinase substrates containing Src homology 2 (SH2) domains including phospholipase C-γ (PLC-γ), phosphatidylinositol-3 kinase, GTPase activating protein, SHPTP-2 tyrosine phosphatase, and the JAK/STAT proteins (van der Geer *et al.*, 1994; Marshall, 1995). In addition, the activation of the *ras* pathway by receptor tyrosine kinases leads to the regulation of serine/threonine protein cascades including Raf and the MAP kinase (MAPK) pathway (for review, see Johnson and Vallaincourt, 1994). The specificity of the growth factor signaling can thus be mediated at several levels: the initial ligand signal; the relative expression and hetero-interaction of growth factor receptors; the relative strength or duration of substrate activation; and/or the availability of cellular substrates responding to this signal.

A central question in attempting to understand how hetero-receptors (such as the EGFr and p185 tyrosine kinases) mediate enhanced and/or altered signaling pathways is to determine which cellular substrates couple with the receptor complex. Recent evidence has suggested the importance of cross-phosphorylation of associated receptor proteins as a mechanism for enhanced signal transduction (Soltoff *et al.*, 1994; Qian *et al.*, 1995). The dominant negative effect of a kinase-inactive $p185^{c\text{-}neu}$ mutant protein on EGFr function suggests that normal signal pathways have been disrupted (Qian *et al.*, 1994a,b). In the present study we have utilized the interaction of the kinase-inactive p185 protein (p185K757M) with the wild-type EGFr as a model system to determine the efficiency of substrate association with the heterodimeric complex. These results indicate that although EGF-induced functions (including mitogenesis) were abrogated in these cells, the association and phosphorylation of several cellular signaling molecules with the p185/EGFr heterodimer still operates efficiently in an EGF-dependent fashion.

MATERIALS AND METHODS

Cell-lines and antibodies

NR6 cells (Pruss and Herschman, 1977) were devoid of endogenous EGFr and $p185^{c\text{-}neu}$ expression and were used as the parental cell line for further transfection. M1 cells express the wild-type human EGFr and wild-type rat $p185^{c\text{-}neu}$ (Kokai *et al.*, 1989). NEN757 cells express wild-type human EGFr and a kinase inactive form of rat $p185^{c\text{-}neu}$ (p185K757M) in which the lysine at position 757 was altered to a methionine. All cell lines utilized in this study were characterized periodically for correct expression of receptors by flow cytometry and immunoprecipitation/Western blotting.

Monoclonal antibody (mAb) 7.16.4 against the extracellular domain of rat $p185^{c\text{-}neu}$ was produced from hybridoma cells as described previously (Drebin *et al.*, 1984) and did not cross-react with EGFr or other members of the EGFr family (Dougall and Qian, unpublished). Anti-p185 carboxyl-terminal antiserum NCT (LeVea *et al.*, 1993) was specific for p185; anti-EGFr antisera CT was specific for EGFr (kindly provided by Stuart Decker); anti-Bacneu antiserum against rat $p185^{c\text{-}neu}$ intracellular domain (Myers *et al.*, 1992) recognized both p185 and EGFr; anti-phosphotyrosine monoclonal antibody 4G10, and polyclonal antisera against PLC-g, SHPTP2, GAP, and p85 (PI3-kinase) were purchased from UBI (Lake Placid, NY). Polyclonal anti-Shc antisera was purchased from Transduction Laboratories (Lexington, KY). Each of these antibodies were tested for cross-reactivity to baculovirus-expressed rat p185 protein.

EGF treatment of cells

Cells were cultured in DMEM supplemented with 10% heat-inactivated fetal calf serum and 1% penicillin/streptomycin. Cells were plated at a density of 1×10^6/10-cm dish and cultured for 2 days; the media was decanted, cells were washed with PBS and media minus serum for 16 hr. Murine EGF (GIBCO/BRL) was added to the various concentrations indicated.

Immunoprecipitation and Western blotting

Cells were washed twice with cold phosphate-buffered saline (PBS) and lysed with 1 ml of PLCLB (PLC lysis buffer: 50 m*M* HEPES pH 7.5, 150 m*M* NaCl, 10% glycerol, 1% Triton X-100, 1 m*M* EGTA, 1.5 m*M* $MgCl_2$, 100 m*M* NaF, 10 m*M* sodium pyrophosphate) supplemented with 2 m*M* sodium orthovanadate, 1 m*M* phenylmethylsufonyl fluoride, 10 μg/ml aprotinin, and 10 μg/ml leupeptin. Lysates were clarified by centrifugation at 14,000 $\times$ *g* for 15 min at 4°C and supernatants were immunoprecipitated with the various antibodies for 1 hr at 0°C. Immune complexes were purified with Protein A–Sepharose and washed twice with HNTG buffer (20 m*M* HEPES pH 7.5, 150 m*M* NaCl, 10% glycerol, 0.1% Triton X-100, 1 m*M* sodium orthovanadate, and protease inhibitors as described above), once with HNTG buffer containing 500 m*M* NaCl, and finally with HNTG buffer containing 150 m*M* NaCl. Controls demonstrated that the antibodies/antisera used were not limiting. Samples were boiled for 5 min in $NaDodSO_4$ sample buffer prior to $NaDodSO_4$-PAGE. Western blotting was performed as described previously (Wada *et al.*, 1990) and developed with anti-mouse or anti-rabbit coupled to horseradish peroxidase (Boehringer Mannheim) using enhanced chemiluminescence (ECL, Amersham). The intensity of the bands was analyzed using a Phosphorimager (Molecular Dynamics, Inc.). To determine the amount of coimmunoprecipitated receptor proteins proportional to the total receptor protein content, both receptors were simultaneously immunoprecipitated with specific antisera and serial dilutions of the immune complexes were blotted with anti-receptor antibodies.

*Expression and purification of glutathione-S-transferase fusion protein/*in vitro *SH2 binding assays*

The plasmid encoding the recombinant glutathione-*S*-transferase/p85 SH2 fusion protein (GST-p85SH2) was provided by

Dr. Ed Wood (Burroughs Wellcome Co.). This fusion protein was expressed using the pGEX2T vector and has been described previously (Yamamoto, 1992). It encodes amino acids 330–724 of the human p85 protein and includes both SH2 domains. The glutathione-*S*-transferase fusion protein was purified by glutathione affinity chromatography according to published procedures (Yamamoto *et al.*, 1992). The proteins were analyzed by $NaDodSO_4$-PAGE and a single band at the predicted molecular weight (70 kD) was identified. Protein concentration was determined using the Bradford assay.

Binding of GST fusion proteins to cellular proteins was performed in 1% Triton X-100 lysates (PLCLB). Five micrograms of the GST fusion protein was mixed with total cellular lysates at 4°C for 1 hr. Protein complexes were recovered by adding 40 μl of glutathione-agarose (Pharmacia) and continued mixing by rotation at 4°C for 30 min. The complexes were washed as described above. These data indicate that the p85 subunit of PI3-kinase associates (by virtue of its SH2 domains) with phosphorylated EGFr and $p185^{c\text{-}neu}$ after EGF treatment.

RESULTS

EGF-induced tyrosine phosphorylation

Alteration of the ATP binding site of p185 at position 757 from a lysine to methionine (K757M) results in the inactivation of the tyrosine kinase activity and the loss of tyrosine autophosphorylation (Weiner *et al.*, 1989; Qian *et al.*, 1994a). Recently, we have shown that stable co-expression of this kinase-inactive p185 (p185K757M) with the wild-type EGFr has profound effects on various EGF-induced functions, including receptor down-modulation and degradation, DNA synthesis, EGFr affinity for EGF, and cellular transformation (Qian *et al.*, 1994b). Both p185K757M and the 170-kD EGFr protein become rapidly phosphorylated on tyrosine residues following EGF treatment as shown by anti-phosphotyrosine immunoprecipitation followed by Western blotting with anti-receptor antibodies (Fig. 1, lanes 1, 2, 5, and 6). Approximately the same percentage (50%) of the cellular pool of EGFr and p185K757M become phosphorylated in NEN757 cells as in M1 cells co-expressing EGFr and wild-type p185 (Qian *et al.*, 1992). These data confirm that transphosphorylation of the kinase-inactive p185K757M by EGFr and autophosphorylation of EGFr were not significantly impaired in these cells. Immunoprecipitation with receptor-specific antisera demonstrated that the total levels of protein did not change during EGF treatment (Fig. 1, lanes 3, 4, 7, and 8), although the mobility of EGFr and p185 was reduced due to the increased phosphorylation.

Co-expression of the p185K757M protein with EGFr (in the NEN757 cell line) reduces the percentage of high-affinity ($K_d = 1.3\text{–}7.5 \times 10^{-11}$ *M*) EGF receptors seen in cells expressing only EGFr (NE91 cells) or cells expressing both wild-type $p185^{c\text{-}neu}$ and EGFr (M1 or NENB2 cells) from 5% to 0.5%, while the low-affinity ($k_d = 5 \times 10^{-9}$ *M*) EGF-binding subclass was unaltered (Qian *et al.*, 1994b). Accordingly, it was necessary to demonstrate the relative efficiency of total tyrosine phosphorylation in NEN757 cells relative to the other cell lines. Figure 2 illustrates an EGF dose–response curve of total cellular tyrosine phosphorylation in the cell lines M1 and

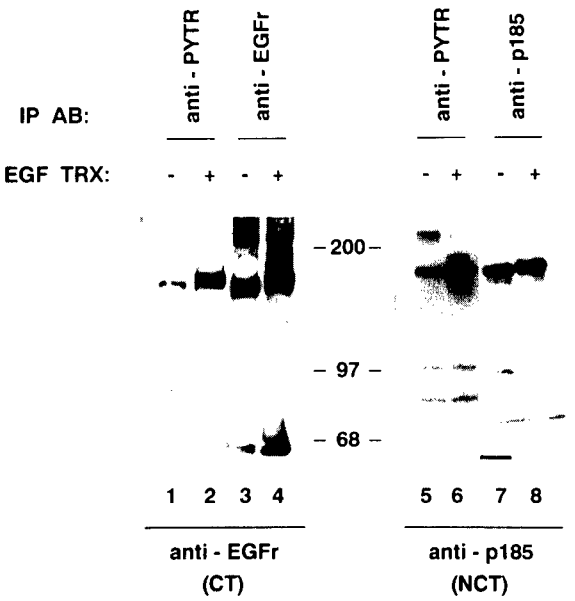

FIG. 1. Tyrosine phosphorylation of EGFr and $p185^{c\text{-}neu}$ receptor tyrosine kinases in NEN757 cells. Serum-starved cells were treated with 100 ng/ml of EGF for 15 min at 37°C before lysis with 1% Triton X-100-containing buffer. Immunoprecipitated proteins were separated by $NaDodSO_4$-PAGE (8% gel) and analyzed by anti-receptor or anti-PTYR antibodies. EGF-dependent tyrosine phosphorylation of the EGFr was demonstrated by anti-PTYR precipitation followed by immunoblotting with specific anti-sera (CT) against p170 EGFr (lanes 1 and 2). EGFr was directly immunoprecipitated with anti-EGFr antisera and immunoblotting with anti-EGFr antibodies (lanes 3 and 4). EGF-dependent tyrosine phosphorylation of the p185K757M was demonstrated by anti-PTYR precipitation followed by immunoblotting with specific anti-sera against $p185^{c\text{-}neu}$ (NCT) (lanes 5 and 6). Lanes 7 and 8 indicate direct immunoprecipitation of p185K757M followed by immunoblotting with NCT anti-sera.

NEN757. Both cell lines appear to respond efficiently to EGF in terms of tyrosine phosphorylation, and optimal tyrosine phosphorylation was observed at EGF concentrations of 50–100 ng/ml. Both cell lines also responded similarly over a defined time course to EGF treatment (unpublished data). The presence of the high-affinity EGFr in M1 cells does not appear to affect significantly the pattern of proteins phosphorylated after EGF treatment. Differences in phosphotyrosine-containing proteins were mostly quantitative, although some qualitative differences were also observed between the two cell lines upon longer exposures of the anti-phosphotyrosine immunoblots (Fig. 3). In each subsequent experiment, cells were treated with 100 ng/ml (16 n*M*) of EGF for 15 min unless indicated otherwise.

Shc, Grb2, and p72Raf proteins are bound by the phosphorylated EGFr/$p185^{c\text{-}neu}$ heterodimeric complex

The total level of tyrosine phosphorylation observed in the NEN757 cell line indicated that EGF-inducible kinase activity was still operable, which is in agreement with our previous re-

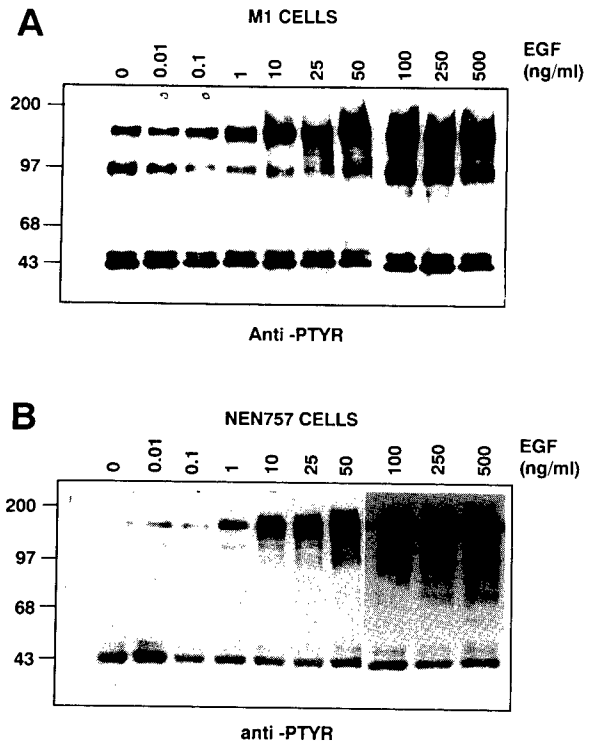

FIG. 2. Tyrosine phosphorylation of cellular proteins as a function of EGF dosage. Serum-starved cells were treated with indicated concentrations of EGF for 15 min at 37°C before lysis with 1% Triton X-100-containing buffer. Phosphotyrosine-containing proteins were precipitated with anti-PTYR antibodies, separated by NaDodSO$_4$-PAGE (8% gel), and analyzed by anti-PTyr immunoblotting. Molecular weight markers are indicated at left of each panel. The prominent band at 55 kD is the Ig heavy chain. A. M1 cells that express both wild-type rat p185$^{c\text{-}neu}$ and human EGFr proteins (Kokai *et al.*, 1989). B. NEN757 cells that express wild-type EGFr and a mutant form of p185$^{c\text{-}neu}$ (p185K757M), which lacks functional kinase activity.

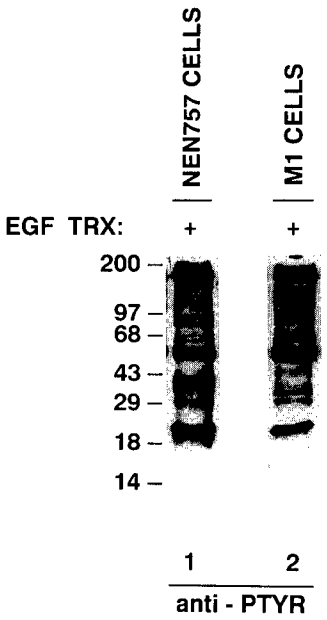

FIG. 3. Tyrosine phosphorylation substrates of the active (M1 cells) and inactive (NEN757 cells) EGFr/p185 heterodimeric complex. Cell lines were treated with EGF (100 ng/ml) for 15 min and tyrosine phosphorylated proteins were identified by anti-phosphotyrosine immunoprecipitation and anti-phosphotyrosine immunoblotting. Proteins were resolved on a gradient 4–20% NaDodSO$_4$-PAGE.

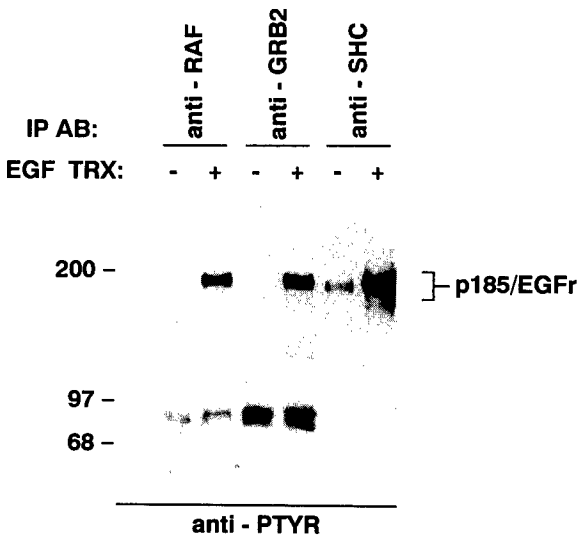

FIG. 4. EGF-induced complex formation of EGFr and p185$^{c\text{-}neu}$ proteins with RAF, GRB2, and SHC. NEN757 cells were treated with 100 ng/ml of EGF for 15 min as indicated. Total cellular lysates were immunoprecipitated (as described in Materials and Methods) with polyclonal antisera against the human RAF or SHC proteins or monoclonal antibodies reactive with the rat GRB2 protein. Proteins were fractionated on NaDodSO$_4$-PAGE (8%) and immunoblotted with antibodies against phosphotyrosine. The tyrosine-phosphorylated EGFr/p185 heterodimer was visualized at 170–190 kD. The sizes of marker proteins are indicated in kilodaltons.

port (Qian *et al.*, 1994a) and indicates that the loss of EGF-induced mitogenesis in these cells was not due to a loss of kinase activity or protein phosphorylation. To examine whether effector/substrate proteins were coupled to the EGFr and p185K757M heterodimer, co-precipitation experiments were performed with anti-substrate antibodies. We initially examined three proteins implicated in the *ras* signaling pathway and subsequent activation of the MAP kinase system: Grb2, Shc, and p72Raf.

Lysates from NEN757 cells that were either treated with EGF or untreated were subjected to immunoprecipitation with antibodies specific for Grb2, SHC, and p72Raf. After resolution of proteins by NaDodSO$_4$-PAGE, samples were immunoblotted with antisera specific for either phosphotyrosine (clone 4G10), EGFr (anti-CT sera), or p185$^{c\text{-}neu}$ (anti-NCT sera). Figure 4 illustrates that a tyrosine-phosphorylated protein complex of approximately 170–190 kD is coimmunoprecipitated with each of these substrate/effector proteins after EGF treatment. Blotting with specific anti-receptor antisera confirmed that both EGFr

and p185$^{c\text{-}neu}$ were present in this complex (data not shown and Qian *et al.*, 1994a). The size heterogeneity of the p185/EGFr complex is due to the differential tyrosine phosphorylation of each receptor, as shown in Fig. 1. The amount of tyrosine phosphorylated EGFr/p185 complex associated with Shc, Grb2, and p72Raf proteins was estimated to be approximately 5% of the total tyrosine phosphorylated EGFr/p185 receptors. The kinetics of inducible association between the EGFr/p185$^{c\text{-}neu}$ heterodimer and these proteins was rapid occurring within 1 min of EGF treatment, only Shc demonstrated constitutive binding in the absence of EGF. Although p72Raf could form a complex with tyrosine-phosphorylated EGFr and p185 after EGF treatment, altered p72Raf mobility in NaDodSO$_4$-PAGE or increased p72 tyrosine phosphorylation (previously associated with the activation of p72Raf; (Morrison *et al.*, 1990) could not be demonstrated.

Grb2 does not appear to be a favored substrate for the EGFr tyrosine kinase (data not shown and Lowenstein *et al.*, 1992), and instead functions to link activated receptor tyrosine kinases to the mSOS1 protein (Egan *et al.*, 1993). However, the phosphorylation of Shc and formation of a protein complex composed of Sch and Grb2 have been shown to correlate with proliferative signals (Rozakis-Adcock *et al.*, 1993; Salcini *et al.*, 1994). To examine the role of SHC and GRB2 proteins in heterodimeric signaling proteins were immunoprecipitated after EGF treatment from a cell line expressing EGFr with wild-type p185 (M1) or cells expressing EGFr with the kinase inactive p185K757M (NEN757). Two proteins of molecular weight 46 and 52 kD contained low levels of phosphotyrosine from serum-starved cells, and showed increased phosphotyrosine content after EGF treatment in both cell lines (Fig. 5). These proteins were identified as p46 and p52 Shc by direct blotting with anti-SHC antisera. EGF-induced tyrosine phosphorylation of SHC was not negatively effected by the expression of the kinase-inactive p185K757M protein. The phosphorylation of p46 and p52 Shc correlated with the association with and tyrosine phosphorylation of the 170 to 180-kD EGFr/p185 complex (Fig. 5).

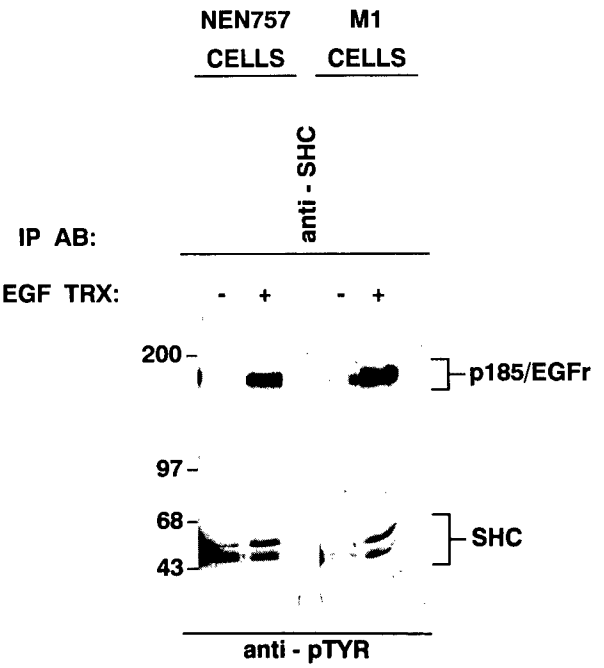

FIG. 5. Phosphorylation of SHC proteins. M1 cells that express both wild-type rat p185$^{c\text{-}neu}$ and human EGFr proteins or NEN757 cells, which express wild-type EGFr and a mutant form of p185$^{c\text{-}neu}$ (p185K757M) which lacking functional kinase activity, were treated with 100 ng/ml of EGF for 15 min and lysates were immunoprecipitated with polyclonal antisera against SHC as described in Materials and Methods. After NaDodSO$_4$-PAGE (8%) and transfer to nitrocellulose, the membrane was immunoblotted with anti-phosphotyrosine. Phosphorylated SHC proteins were visualized at 46, 52, and 66 kD.

Association of the heterodimeric EGFr/p185$^{c\text{-}neu}$ complex with PLC-g, PI-3 kinase, GAP, NCK, and SHPTP2

The formation of complexes between the EGFr/p185 heteromer and additional potential substrates including PLC-γ, the p85 subunit of phosphotidylinositol 3-kinase (PI3-kinase), NCK, the tyrosine phosphatase SHPTP2, and the GTPase activating protein (p120GAP) was examined next. The association and tyrosine phosphorylation of these proteins with activated receptors has previously been shown to correlate with positive, mitogenic signals (for review, see van der Geer *et al.*, 1994). The EGFr/p185$^{c\text{-}neu}$ heterodimeric complex (170–190 kD) associates with each of these substrate/effector proteins in an EGF-dependent fashion as illustrated by phosphotyrosine immunoblotting after anti-substrate immunoprecipitation (Fig. 6). Again, the presence of both EGFr and p185$^{c\text{-}neu}$ was confirmed by blotting with specific anti-receptor antisera. The association between receptor and substrate/effectors was ligand-inducible and rapid, occurring within 1 min.

The tyrosine phosphorylation of SH2-containing substrates was determined by analysis of the phosphotyrosine western blots. PLC-γ (145 kD) was phosphorylated by the heterodimer composed of EGFr and kinase inactive p185K757M, as demonstrated by the phosphorylation of a 145-kD band (Fig. 6, lane 6), which was subsequently demonstrated to be PLC-γ by blotting with PLC-γ-specific antisera (data not shown). The tyrosine phosphorylation of GAP (120 kD) was undetectable in anti-substrate immunoprecipitations. However, EGF-inducible tyrosine phosphorylation was demonstrated in these cells by Western blotting with substrate-specific antisera after anti-phosphotyrosine immunoprecipitation. p120GAP (Fig. 7A) showed enhanced tyrosine phosphorylation after EGF treatment. Phosphorylation of the p85 subunit of PI3-kinase was detectable at comparable levels in cell lines expressing EGFr with either wild-type p185 or kinase-inactive p185 (p185K757M) (Fig. 7B). The phosphorylation of the p72 SHPTP2 phosphatase could not be reproducibly demonstrated, even though phosphate inhibitors were included in the lysis and immunoprecipitations.

The p185$^{c\text{-}neu}$/EGFr heterodimer directly associates with the SH2 domains of PI3 kinase p85 subunit

Immunoprecipitation using antisera against PI-3 kinase also coprecipitated a phosphorylated protein of 150 kD in addition to the EGFr/p185c-*neu* heterodimeric complex present at 170–190 kD. Using Western blotting, this protein did not cross-

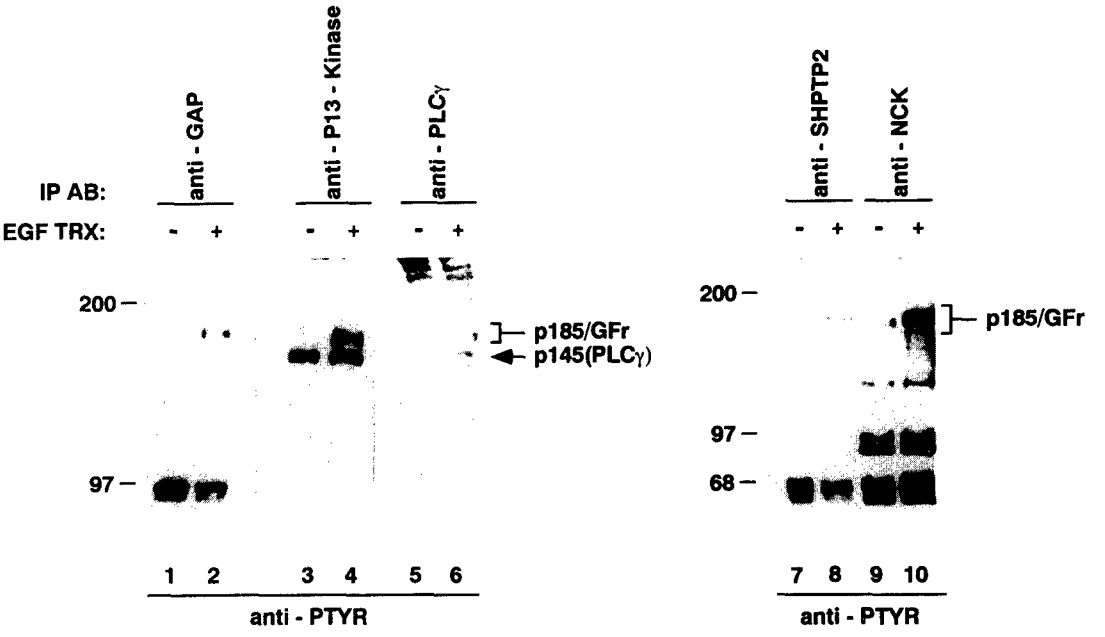

FIG. 6. EGF-induced association of the EGFr/p185 heterodimer with GAP, PI3-kinase, PLC-γ, SHPTP2, and NCK in NEN757 cells. Coprecipitation experiments were used to define association of cytoplasmic proteins with the EGFr/p185$^{c\text{-}neu}$ heterodimer. NEN757 cells were serum-starved overnight and treated with 100 ng/ml of EGF for 15 min as indicated. Triton X-100 (1%) lysates were immunoprecipitated with polyclonal antisera against the human GAP (lanes 1 and 2), rat PI3-kinase (lanes 3 and 4), bovine PLC-γ1 (lanes 5 and 6), and murine SHPTP2/SYP (tyrosine phosphatase) (lanes 7 and 8) and or monoclonal antibodies against the bovine NCK protein (lanes 9 and 10). Immunoprecipitations were processed as described in the Materials and Methods section and fractionated on NaDodSO$_4$-PAGE (8%) followed by immunoblotting with anti-phosphotyrosine antibodies. The phosphorylated EGFr and p185K757M proteins were visualized at 170–190 kD; the phosphorylated PLC-γ1 was visualized at 145 kD (lane 6). The constitutively phosphorylated 150-kD band in anti-PI3-kinase immunoprecipitates (lanes 3 and 4) was not identified.

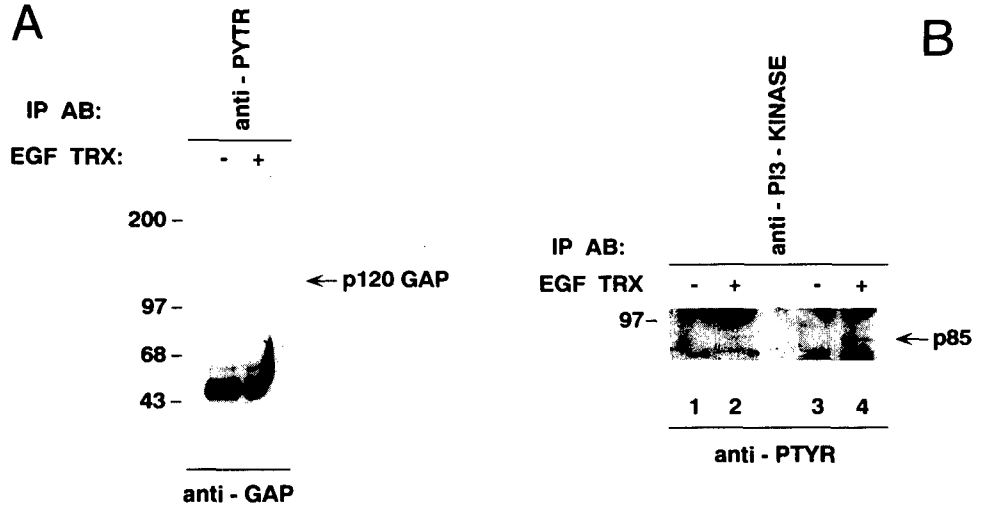

FIG. 7. EGF-induced phosphorylation of p120 GAP and the p85 subunit of PI3-kinase after EGF treatment of NEN757 or M1 cells. A. NEN757 cells were treated with 100 ng/ml of EGF for 15 min or left untreated as indicated, and total cellular lysates were immunoprecipitated with anti-phosphotyrosine antibodies. Immunoprecipitated complexes were fractionated on a 8% NaDodSO$_4$-PAGE and immunoblotted with polyclonal sera raised against GTPase-activating protein (GAP). The GAP protein was visualized at 120 kD. The prominent band at 55 kD is the Ig heavy chain. B. Either NEN757 cells (lanes 1 and 2) expressing wt EGFr with kinase-inactive p185K757M or M1 cells (lanes 3 and 4) expressing both wt EGFr and p185$^{c\text{-}neu}$ were serum-starved overnight, treated with 100 ng/ml of EGF for 15 min, and cellular lysates were prepared. Immunoprecipitation with anti-PI3-kinase antibodies was performed as described in Materials and Methods and was identical to that described for Fig. 5 (lanes 3 and 4). Proteins were fractionated by NaDodSO$_4$-PAGE and immunoblotted with anti-phosphotyrosine antibodies. Phosphotyrosine-containing proteins were detected by incubation with an anti-mouse IgG coupled to horseradish peroxidase and visualized by ECL (see Materials and Methods). The image was intentionally overexposed to detect faint signals. The phosphorylated p85 subunit of PI3-kinase was visualized at 85 kD after EGF treatment in both cell lines.

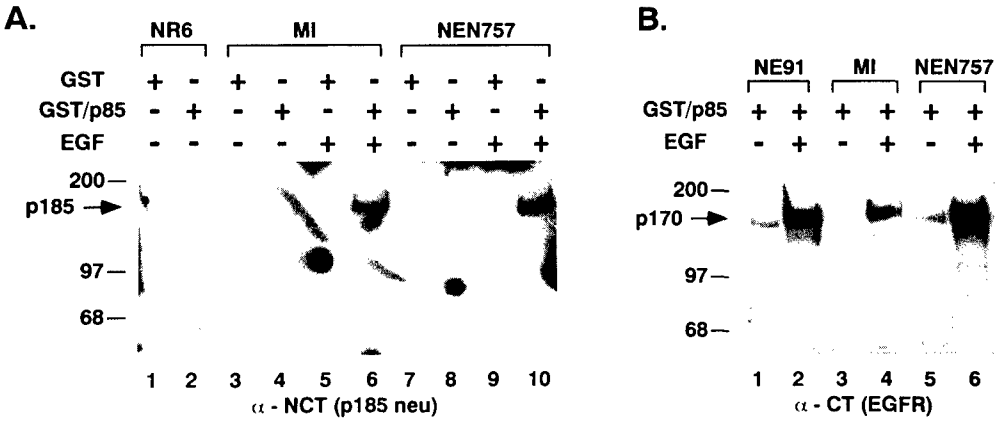

FIG. 8. Association of p85PI3 kinase SH2 domains with both the EGFr and p185 forms after EGF treatment A. Association of the p85 SH2 domains with the tyrosine phosphorylated EGFr and p185K757M proteins was determined using GST-fusion protein binding and anti-p185 immunoblotting with anti-NCT antisera as described in the Methods and Materials. Lanes 1 and 2, Reactivity of GST/p85 SH2 domains with proteins in the parental NR6 cell line, which lacks endogenous EGFr and $p185^{c\text{-}neu}$; lanes 3 and 4, binding of GST/p85 SH2 proteins with p185 protein in the M1 cell lines, which express both wild-type EGFr and p185; lanes 5 and 6, binding to p185 in the NEN757 cell line, which expresses EGFr with the kinase-inactive p185K757M. B. Association of GST/p85 SH2 domains with the EGFr was determined using antiserum (CT) specific for EGFr in the Western blotting. Lanes 1 and 2, EGF-inducible binding in a control cell line NE91, which expresses only EGFr; lanes 3 and 4, bining of the GST/p85 SH2 protein in the M1 cells; binding to EGFr in NEN757 cells. Each cell line represented expresses approximately equivalent EGFr or p185 protein ($2.5–7.5 \times 10^5$ receptors/cell) (Qian *et al.*, 1994a).

react with PLC-γ antisera or antisera raised against the p85 subunit of PI3 kinase (data not shown). To demonstrate the specificity of interaction between PI3 kinase and the EGFr/p185 heterodimer, the ability of the receptor proteins to bind glutathione-*S*-transferase (GST) fusion proteins containing the amino- and carboxy-terminal SH2 domains of the p85 subunit of PI3 kinase (GST/p85) was examined.

GST/p85 fusion protein or control GST proteins without p85 SH2 domains were purified from bacteria and added to cell lysates following EGF treatment. Association of the GST/p85 SH2 protein with EGFr or $p185^{c\text{-}neu}$ was measured by Western blotting using receptor-specific antisera (Fig. 8). EGF treatment for 15 minutes mediated an increased association of GST/p85 SH2 domains with both wild-type $p185^{c\text{-}neu}$ expressed in M1 cells (Fig. 8A, lanes 4 and 6) and the kinase-inactive p185K757M expressed in NEN757 cells (lanes 8 and 10). Comparable levels of either wild-type p185 or p185K757M were coprecipitated with GST/p85 after activation and phosphorylation after EGF treatment (compare lanes 6 and 10).

In a similar fashion, EGF treatment induced the efficient association between EGFr and p85 SH2 protein in the same cell lines (Fig. 8B, lanes 3–6). There was no apparent reduction in the amount of EGFr associated with GST/p85 from NEN757 cells (EGFr expressed with p185K757M), M1 cells (wild-type EGFr and p185), or NE91 cells (wild-type EGFr only). The relative total amounts of EGFr expressed in the cell lines were approximately equal (Qian *et al.*, 1994a and data not shown). The control GST protein did not specifically bind either EGFr or $p185^{c\text{-}neu}$ forms.

DISCUSSION

Ligand-induced dimerization or oligomerization is a requisite step in the activation and signaling of most growth factor receptors (Weiner *et al.*, 1989 and reviewed in Heldin, 1995). Heterodimerization (or oligomerization) of related tyrosine kinase receptors may profoundly expand the potential repertoire of substrate binding sites and subsequent substrate activation. The intermolecular association of the EGFr cytoplasmic domain with the p185 tyrosine kinase has been shown to enhance substrate binding and transformation (Qian *et al.*, 1995) suggesting the amplification of tyrosine kinase signaling through additional substrate binding site availability. Likewise, p160c-erbB-3, which has a low or nonexistent kinase activity (Prigent and Gullick, 1994), provides additional binding motifs for the p85 subunit of PI3-kinase that may be amplified through heterodimerization of p160c-erbB-3 and p185c-erbB-2 (Carraway and Cantley, 1994; Soltoff *et al.*, 1994). The heterodimerization between p160c-erbB-3 and p185c-erbB-2 or p160c-erbB-3 and p180c-erbB-4 also may provide for high-affinity binding of the heregulin family of ligands (Plowman *et al.*, 1993; Slikowski *et al.*, 1994). Heterodimerization within the EGFr family thus appears to be a general mechanism that provides for an increased intensity or diversity of ligand-induced signaling responses (Kokai *et al.*, 1989; Wada *et al.*, 1990; and reviewed in Lemmon and Schlessinger, 1994).

Heterodimerization between the EGFr and $p185^{c\text{-}neu}$ tyrosine kinase receptors has been well characterized in transfected mouse cell lines (Wada *et al.*, 1990; Spivak-Kroizman *et al.*, 1992) and human adenocarcinoma cell lines (Goldman *et al.*, 1990). The significance of the formation of this heterodimeric complex between EGFr family members is indicated by: (i) the resulting transformation of fibroblasts in the absence of exogenously added growth factor (Kokai *et al.*, 1989); (ii) the predominance of heterodimeric EGFr/p185 species over homodimeric forms (Qian *et al.*, 1994a); and (ii) the loss of EGF-induced responses in cell lines coexpressing wt EGFr with a kinase-inactive form of p185 (Qian *et al.*, 1994a,b, and this paper). To explore the potential defects in the signal transduc-

tion pathway(s) mediated by EGFr and a kinase-inactive p185 heterodimer, we characterized the receptor association and phosphorylation of several known substrates for receptor tyrosine kinases.

The hypothesis that EGFr and $p185^{c\text{-}neu}$ can couple with distinct signal transduction pathways has been based on several observations. The distinct phosphorylation patterns of intracellular substrates by EGFr and p185 tyrosine kinases (Fazioli *et al.*, 1991) argues for the direct phosphorylation of unique substrates including the EGFr-specific eps15 (Fazioli *et al.*, 1993), or the activation of unique pathways by the two receptors. Moreover, the two receptors have demonstrated differential mitogenic potency in different cell lines (Di Fiore *et al.*, 1990), suggesting that the utilization of alternative substrate pathways is important for signaling through members of the EGFr family.

In the model system used in the present study, we derived cell lines transfected with EGFr or p185 forms from a common parental clone, therefore there should be no differences in the content of intracellular kinase substrates. The coexpression of EGFr with either wild-type p185 or the kinase inactive p185K757M had profound effects on the mitogenic or transforming potency of EGF signaling. Expression of the p185K757M protein with EGFr has been shown to functionally inactivate EGF-inducible DNA synthesis, receptor turnover, and cellular transformation in NEN757 cells (Qian *et al.*, 1994b). However, the present study demonstrates that the EGFr tyrosine kinase in these cells was still active and capable not only of phosphorylating p185 but was also active in total cellular substrate phosphorylation (Figs. 1 and 2). The dose-dependent response to EGF in terms of tyrosine phosphorylation was qualitatively and quantitatively the same whether wild-type p185 (M1 cells) or the kinase-inactive form (NEN757 cells) was expressed with EGFr (Fig. 2). The defective mitogenic signaling in NEN757 cells was then not due to a disruption of tyrosine kinase and phosphorylation activity, but rather may be due to the loss of phosphorylation or activation of a specific subset of intracellular signal transducers. The possibility that the activity of the p185 tyrosine kinase coexpressed with EGFr couples with alternative substrate pathways is suggested by the phosphorylation of different substrate proteins, as shown in Fig. 3.

Considerable effort has demonstrated that the phosphorylation and activation of putative tyrosine kinase substrates correlates with positive mitogenic signals. However, it is unclear whether the protein–protein association between substrate and activated receptor or the actual substrate phosphorylation is a more important determinant for substrate activation. PLC-γ1 and PI3 kinase have been shown to be associated with activated receptors and subsequently phosphorylated and activated by receptor tyrosine kinases (Nishibe *et al.*, 1990). p120 GAP has also been shown to be associated with activated tyrosine kinase receptors (Ellis *et al.*, 1990) and to become phosphorylated (Morrison *et al.*, 1990). In the present study, PLC-γ1, the p85 subunit of PI3-kinase, Shc, and p120 GAP became associated with the phosphorylated EGFr/p185K757M complex and were phosphorylated themselves after EGF treatment (Figs. 4 and 6). The stoichiometry of substrate phosphorylation appeared to be equally efficient in cells with the kinase inactive p185K757M as with the wild-type p185 (Figs. 5 and 7). However, the enzymatic activation of the respective substrate proteins was not analyzed directly. Shc, NCK, and Grb2 were shown to form EGF-inducible complexes with the EGFr/p185 heterodimer, suggesting that these adapter proteins can functionally couple with downstream signals (Fig. 4 and 6).

Because the catalytic activity of SHPTP2 has been demonstrated to be enhanced by an EGFr-dependent phosphorylation (Lechleider *et al.*, 1993; Vogel *et al.*, 1993) and an inhibitory antibody against SHPTP2 reduced EGF-stimulated DNA synthesis (Xiao *et al.*, 1994), this substrate protein is a good candidate for further analysis in the defective signaling pathway presented here. The tyrosine phosphatase SHPTP2 also became associated with the phosphorylated EGFr/p185K757M complex (Fig. 6); however, increased phosphotyrosine content on SHPTP2 could not be detected. The specific activation of p72RAF has also been correlated with growth factor activation (Morrison *et al.*, 1990). Further analysis of the activation status of p72RAF and SHPTP2 in NEN757 cells is currently being performed.

An additional explanation for the defect responsible for the inactivated EGF response in these cells is the improper subcellular localization or enzymatic activation of each of these putative substrate proteins. The association of PLC-γ1, p120GAP, PI3-kinase, and p72RAF with the membrane-bound receptor proteins suggests that these substrates are properly located for their respective activities. It has been demonstrated that the subcellular localization of a complex between tyrosine-phosphorylated Shc, Grb2, and mSOS correlates with distinct signaling responses (Di Gugliemo *et al.*, 1994); the proper association of p72Raf, Grb2, and Shc with the membrane-bound receptor complex (Fig. 4) also suggests that substrate localization is not an issue with the NEN757 cells.

The particular relevance of individual substrates for certain signaling pathways is questionable. For instance, the relative mitogenic potency of EGFr and p185 does not necessarily correlate with the relative phosphorylation levels of two substrates p120GAP and PLC-γ1 (Fazioli *et al.*, 1991). There have been several observations of alternative EGF-dependent signaling pathways that may require uncharacterized substrate/enzyme pathways. Some initial findings of EGFr tyrosine kinase-independent pathways (Campos-Gonzales and Glenney, 1992; Selva *et al.*, 1993) may be due to activation of endogenous murine EGFr in transfected cells (Hack *et al.*, 1993). However it is impossible to exclude as yet unidentified EGF-activated kinases. The particular relevance of the JAK/STAT pathway for EGFr-mediated signaling is still not clear, although in preliminary analysis we have demonstrated EGF-inducible association of stat1α and stat3 with the EGFr/p185K757M complex as well as EGF-inducible activation of STAT DNA binding activity (Dougall, Samanta, and Greene, manuscript in preparation), indicating that the JAK/STATs are probably not essential for EGFr signaling.

DiFiore and colleagues have identified novel substrates by virtue of their tyrosine phosphorylation after EGF treatment (Fazioli *et al.*, 1992). Two of these substrates (eps8 and eps15) have been shown (in the NEN757 cells used in the present study) to become tyrosine phosphorylated and coprecipitate with EGFr and p185K757M in an EGF-dependent manner (W. Dougall, W. Wong, and M. Greene, unpublished observations).

The transforming capacity of the p185 tyrosine kinase has

been linked to the activation of the MAP kinase and *ras* pathway (Ben-Levy *et al.*, 1994). The specific activation of the ERK family of MAP kinases is likely to be a critical trigger in the signaling through receptor tyrosine kinases (Marshall, 1995). The distinction between mitogenic/transformation signals and differentiation signals may be mediated by the duration of ERK activation. Direct analyses of the activation of the MAP kinase enzymes were not performed in the present study, however, we demonstrated that three proteins involved in the upstream regulation of the MAP kinase pathway (p72Raf, Grb2, and Shc) are correctly associated with the heterodimer expressed in the NEN757 cells.

Future studies in this model system will focus on a comparison between EGF-responsive and nonresponsive EGFr/p185 heterodimers with regard to specific activation of MAP kinases. It is interesting to note that the EGF-inducible internalization rate of the complex formed between EGFr and p185K757M is significantly retarded (as compared to a complex between wild-type proteins) (Qian *et al.*, 1994b), raising the possibility that the activation of downstream signaling pathways is improperly sustained at the plasma membrane, thereby altering the normal mitogenic signal. Alternatively, certain signals initiated by the p185/EGFr heterodimer may be routed through heterologous kinase pathways independent of the MAPK and *ras* pathways, as has been observed for EGF-dependent signaling in neuroendocrine cells (Pickett and Gutierrez-Hartmann, 1994).

Several questions remain as to the nature of the functional inactivation of EGF-inducible DNA synthesis, receptor turnover, and transformation seen in NEN757 cells coexpressing EGFr with the kinase-inactive p185K757M. The present study demonstrates that the activation of the EGFr tyrosine kinase and the tyrosine phosphorylation of several substrates proceeds in an accurate and stoichiometric manner in cells with abnormal heterodimeric receptors. Thus, substrate association and phosphorylation do not stringently correlate with the mitogenic and transforming activity of this receptor complex, suggesting additional pathways or mechanisms vital to EGFr/p185$^{c\text{-}neu}$ heterodimeric signaling. It is also likely that the defective signaling may then be attributable to defects in the specific activation of downstream enzymes or effector molecules.

ACKNOWLEDGMENTS

The authors wish to acknowledge Maud Lemercier and Steve Szabo for technical assistance, and Drs. Norman Peterson and Kumar Navaratnam for a critical reading of the manuscript. This work was supported in part by the University of Pennsylvania's Cancer Center Pilot Project Program (W.C.D.), the NIH, NCI, and CTR. (M.I.G.).

REFERENCES

BARGMANN, C.I., and WEINBERG, R.A. (1988). Oncogenic activation of the *neu*-encoded receptor protein by point mutation and deletion. EMBO J. **7,** 2043–2052.

BEN-LEVY, R., PATERSON, H.F., MARSHALL, C.J., and YARDEN, Y. (1994). A single autophosphorylation site confers oncogenicity to the Neu/ErbB-2 receptor and enables coupling to the MAP kinase pathway. EMBO J. **13,** 3302–3311.

CAMPOS-GONZALES, R., and GLENNEY, J.R. (1992). Tyrosine phosphorylation of mitogen-activated protein kinase in cells with tyrosine kinase-negative epidermal growth factor receptors. J. Biol. Chem. **267,** 14535–14538.

CARRAWAY, K.L., and CANTLEY, L. (1994). A neu acquaintance for erbB3 and erbB4: A role for receptor heterodimerization in growth signaling. Cell **78,** 5–8.

CHAZIN, V.R., M. KALEKO, et al. (1992). Transfection mediated by the human Her-2 gene independent of the epidermal growth factor receptor. Oncogene **7,** 1859–1866.

DI GUGLIEMO, G.M., BAASS, P., OU, W.J., POSNER, B.I., and BERGERON, J.J. (1994). Compartmentalization of SHC, GRB2 and mSOS, and hyperphosphorylation of Raf-1 by EGF but not insulin in liver parenchyma. EMBO J. **13,** 3302–3311.

DI FIORE, P.P., PIERCE, J.H., et al. (1987). *erbB-2* is a potent oncogene when overexpressed in NIH/3T3 cells. Science **237,** 178–182.

DI FIORE, P., SEGATTO, O., et al. (1990). The carboxy-terminal domains of *erbB-2* and epidermal growth factor receptor exert different regulatory effects on intrinsic receptor tyrosine kinase function and transforming activity. Mol. Cell. Biol. **10,** 2749–2756.

DOUGALL, W.C., QIAN, X., PETERSON, N.C., MILLER, M.J., SAMANTA, A., and GREENE, M.I. (1994). The neu-oncogene: signal transduction pathways, transformation mechanisms and evolving therapies. Oncogene **9,** 2109–2123.

DREBIN, J., STERN, D., et al. (1984). Monoclonal antibodies identify a cell-surface antigen associated with an activated cellular oncogene. Nature **312,** 545–548.

EGAN, S.E., GIDDINGS, B., BROOKS, M., BUDAY, L., SIZELAND, A., and WEINBERG, R.A. (1993). Association of Sos Ras exchange protein with Grb2 is implicated in tyrosine kinase signal transduction and transformation [see comments]. Nature **363,** 45–51.

ELLIS, C., MORAN, M., et al. (1990). Phosphorylation of GAP and GAP-associated proteins by transforming and mitogenic tyrosine kinases. Nature **343,** 377–381.

FAZIOLI, F., KIM, U.H., et al. (1991). The erbB-2 mitogenic signaling pathway—Tyrosine phosphorylation of phospholipase-C-gamma and GTPase-activating protein does not correlate with erbB-2 mitogenic potency. Mol. Cell. Biol. **11,** 2040–2048.

FAZIOLI, F., BOTTARO, D.P., et al. (1992). Identification and biochemical characterization of novel putative substrates for the epidermal growth factor receptor kinase. J. Biol. Chem. **267,** 5155–5161.

FAZIOLI, F., MINICHIELLO, L., MATOSKOVA, B., WONG, W.T., and DI FIORE, P.P. (1993). eps15, a novel tyrosine kinase substrate, exhibits transforming activity. Mol. Cell. Biol. **13,** 5814–5828.

GOLDMAN, R., BENLEVY, R., et al. (1990). Heterodimerization of the erbB-1 and erbB-2 receptors in human breast carcinoma cells—A mechanism for receptor transregulation. Biochemistry **29,** 11024–11028.

HACK, N., QUAN, A.S.A., MILLIS, G.B., and SKORECKI, K.L. (1993). Expression of human tyrosine kinase-negative epidermal growth factor receptor amplifies signaling through endogenous murine epidermal growth factor receptor. J. Biol. Chem. **268,** 26441–26446.

HELDIN, C.H. (1995). Dimerization of cell surface receptors in signal transduction. Cell **80,** 213–223.

JOHNSON, G.L., and VAILLANCOURT, R.R. (1994). Sequential protein kinase reactions controlling cell growth and differentiation. Curr. Opin. Cell Biol. **6,** 230–238.

KOKAI, Y., MYERS, J.N., et al. (1989). Synergistic interaction of p185c-neu and the EGF receptor leads to transformation of rodent fibroblasts. Cell **58,** 287–292.

LECHLEIDER, R.J., FREEMAN, R.M., and NEEL, B.G. (1993). Tyrosyl phosphorylation and growth factor receptor association of the human corkscrew homologue, SH-PTP2. J. Biol. Chem. **268,** 13434–13438.

LEMMON, M.A., and SCHLESSINGER, J. (1994). Regulation of signal transduction and signal diversity by receptor oligomerization. Trends Biol. Sci. **19,** 459–463.

LEVEA, C.M., MYERS, J.N., et al. (1993). Structural and kinetic comparisons of proto-oncogenic and oncogenic Neu holo-receptors expressed in insect cells. Receptor **3,** 287–303.

MARSHALL, C.J. (1995). Specificity of receptor tyrosine kinase signaling: Transient versus sustained extracellular signal-regulated kinase activation. Cell **80,** 179–185.

MORRISON, D., KAPLAN, D., et al. (1990). Platelet-derived growth factor (PDGF)-dependent association of phospholipase-C-gamma with the PDGF receptor signaling complex. Mol. Cell. Biol. **10,** 2359–2366.

MYERS, J.N., LEVEA, C.M., et al. (1992). Expression, purification, and characterization of bacneu. Receptor **2,** 1–16.

NISHIBE, S., WAHL, M.I., HERNANDEZ-SOTOMAYOR, S.M.T., TONKS, N.K., RHEE, S.G., and CARPENTER, G. (1990). Increase of the catalytic activity of phospholipase C-gamma 1 by tyrosine phosphorylation. Science **250,** 1253–1256.

PICKETT, C.A., and GUTIRREZ-HARTMANN, A. (1994). Ras mediates Src but not epidermal growth factor-receptor tyrosine kinase signaling pathways in GH4 neuroendocrine cells. Proc. Natl. Acad. Sci. USA **91,** 8612–8616.

PLOWMAN, G.D., GREEN, J.M., CULOUSCOU, J.M., CARLTON, G.W., ROTHWELL, V.M., and BUCKLEY, S. (1993). Heregulin induces tyrosine phosphorylation of HER4/p180erbB4. Nature **366,** 473–475.

PRIGENT, S.A., and GULLICK, W.J. (1994). Identification of c-erbB-3 binding sites for phosphatidylinositol 3′-kinase and SHC using an EGF receptor/c-erbB-3 chimera. EMBO J. **13,** 2831–2841.

PRUSS, R.M., and HERSCHMAN, H.R. (1977). Variants of 3T3 cells lacking mitogenic response to epidermal growth factor. Proc. Natl. Acad. Sci. USA **74,** 3918–3921.

QIAN, X., DECKER, S.J., et al. (1992). p185c-neu and EGF receptor associate into a novel structure composed of activated kinases. Proc. Natl. Acad. Sci. USA **89,** 1330–1334.

QIAN, W., LEVEA, C.M., FREEMAN, J.K., DOUGALL, W.C., and GREENE, M.I. (1994a). Heterodimerization of EGFR and wild type or kinase deficient Neu: A mechanism of inter-receptor kinase activation and trans-phosphorylation. Proc. Natl. Acad. Sci. USA **91,** 1500–1504.

QIAN, X., DOUGALL, W.C., HELLMAN, M., and GREENE, M.I. (1994b). Kinase deficient Neu proteins suppress EGFR function and abolish cell transformation. Oncogene **9,** 1507–1514.

QIAN, X., DOUGALL, W.C., FEI, Z., and GREENE, M.I. (1995). Intermolecular association and trans-phosphorylation of different neu-kinase forms permit SH2-dependent signaling and oncogenic transformation. Oncogene **10,** 211–219.

ROZAKIS-ADCOCK, M., McGLADE, J., MBAMALU, G., PELICCI, G., LI, R., DALY, W., BATZER, A., THOMAS, S., BRUGGE, J., PELICCI, P.G., SCHLESSIGER, J., and PAWSON, T. (1993). The SH2 and SH3 domains of mammalian Grb2 couple the EGF receptor to the Ras activator mSos1. Nature **363,** 83–85.

SALCINI, A.E., McGLADE, J., PELICCI, G., NICOLLETTI, I., PAWSON, T., and PELICCI, P.G. (1994). Formation of Shc-Grb2 complexes is necessary to induce neoplastic transformation by overexpression of Shc proteins. Oncogene **9,** 2827–2836.

SAMANTA, A., LEVEA, C.M., et al. (1994). Ligand and $p185^{c\text{-}erbB2}$ density govern receptor interactions and tyrosine kinase activation. Proc. Natl. Acad. Sci. USA **91,** 1711–1715.

SELVA, E., RADEN, D.L., and DAVIS, R.J. (1993). Mitogen-activated protein kinase stimulation by a tyrosine kinase-negative epidermal growth factor receptor. J. Biol. Chem. **268,** 2250–2254.

SLAMON, D.J., CLARK, G.M., et al. (1987). Human breast cancer: Correlation of relapse and survival with amplification of the HER-2/neu oncogene. Science **235,** 177–182.

SLIKOWSKI, M.X., SCHAEFER, G., AKITA, R.W., LOFGREN, J.A., FITZPATRICK, V.D., NUIJENS, A., FENDLY, B., CERRIONE, R.A., VANDLEN, R.L., and CARRAWAY, K.L. (1994). Coexpression of erbB2 and erbB3 proteins reconstitutes a high affinity receptor for heregulin. J. Biol. Chem. **269,** 14661–14665.

SOLTOFF, S.P., CARRAWAY III, K.L., PRINGENT, S.A., GULLICK, W.G., and CANTLEY, L.C. (1994). ErbB3 is involved in activation of phosphatidylinositol 3-kinase by epidermal growth factor. Mol. Cell. Biol. **14,** 3550–3558.

SPIVAK-KROIZMAN, T., D. ROTIN, et al. (1992). Heterodimerization of c-erbB2 with different epidermal growth factor receptor mutants elicits stimulatory or inhibitory responses. J. Biol. Chem. **267,** 8056–8063.

ULLRICH, A., and SCHLESSINGER, J. (1990). Signal transduction by receptors with tyrosine kinase activity. Cell **61,** 203–212.

VAN DER GEER, P., HUNTER, T., and LINDBERG, R.A. (1994). Receptor protein-tyrosine kinases and their signal transduction pathways. Annu. Rev. Cell Biol. **10,** 251–337.

VOGEL, W., LAMMERS, R.E., HUANG, J., and ULLRICH, A. (1993). Activation of a phosphotyrosine phosphatase by tyrosine phosphorylation. Science **259,** 1611–1614.

WADA, T., MYERS, J.N., et al. (1989). Anti-receptor antibodies reverse the phenotype of cells transformed by two interacting proto-oncogene encoded receptor proteins. Oncogene **4,** 489–494.

WADA, T., QIAN, X., et al. (1990). Intermolecular association of the p185c-neu protein and the EGF receptor modulates EGF receptor function. Cell **61,** 1339–1347.

WEINER, D.B., KOKAI, Y., et al. (1989a). Linkage of tyrosine kinase activity with transforming ability of the p185neu oncoprotein. Oncogene **4,** 1175–1183.

WEINER, D.B., LIU, J., et al. (1989b). A point mutation in the neu oncogene mimics ligand induction of receptor aggregation. Nature **339,** 230–231.

XIAO, S., ROSE, D.W., SADSAOKA, T., MAEGAWA, H., BURKE, T.R., ROLLER, P.P., SHOELSON, S.E., and OLEFSKY, J.M. (1994). Syp (SH-PTP2) is a positive mediator of growth factor-stimulated mitogenic signal transduction. J. Biol. Chem. **269,** 21244–21248.

YAMAMOTO, K., ALTSHULER, D., WOOD, E., HORLICK, K., JACOBS, S., and LAPETINA, E.G. (1992). Association of phosphorylated insulin-like growth factor-I receptor with the SH2 domains of phosphatidylinositol 3-kinase p85. J. Biol. Chem. **267,** 11337–11343.

Address reprint requests to:
Dr. Mark I. Greene
Center for Receptor Biology and Division of Immunology
Department of Pathology and Laboratory Medicine
University of Pennsylvania School of Medicine
Philadelphia, PA 19104

Received for publication August 15, 1995; accepted September 12, 1995.

Proc. Natl. Acad. Sci. USA
Vol. 93, pp. 6252–6257, June 1996
Biochemistry

Structural analysis of p185$^{c\text{-}neu}$ and epidermal growth factor receptor tyrosine kinases: Oligomerization of kinase domains

(receptor dimerization/molecular modeling/enzyme structure-function/autophosphorylation)

RAMACHANDRAN MURALI*, PATRICK J. BRENNAN, THOMAS KIEBER-EMMONS, AND MARK I. GREENE

Department of Pathology and Laboratory of Medicine, University of Pennsylvania, Philadelphia, PA 19104

Communicated by Peter C. Nowell, University of Pennsylvania School of Medicine, Philadelphia, PA, February 27, 1996 (received for review November 27, 1995)

ABSTRACT **The epidermal growth factor receptor (EGFR) and p185$^{c\text{-}neu}$ proteins associate as dimers to create an efficient signaling assembly. Overexpression of these receptors together enhances their intrinsic kinase activity and concomitantly results in oncogenic cellular transformation. The ectodomain is able to stabilize the dimer, whereas the kinase domain mediates biological activity. Here we analyze potential interactions of the cytoplasmic kinase domains of the EGFR and p185$^{c\text{-}neu}$ tyrosine kinases by homology molecular modeling. This analysis indicates that kinase domains can associate as dimers and, based on intermolecular interaction calculations, that heterodimer formation is favored over homodimers. The study also predicts that the self-autophosphorylation sites located within the kinase domains are not likely to interfere with tyrosine kinase activity, but may regulate the selection of substrates, thereby modulating signal transduction. In addition, the models suggest that the kinase domains of EGFR and p185$^{c\text{-}neu}$ can undergo higher order aggregation such as the formation of tetramers. Formation of tetrameric complexes may explain some of the experimentally observed features of their ligand affinity and hetero-receptor internalization.**

p185$^{c\text{-}neu}$ and its human homologue p185$^{c\text{-}erbB\text{-}2}$ are related to the epidermal growth factor receptor (EGFR) and possess intrinsic tyrosine kinase activity. Overexpression of these receptors has been correlated with poor prognosis of human adenocarcinoma of breast, ovarian, and pancreatic cancers (1–3). These receptor-tyrosine kinases (RTK) are characterized by an ectodomain, a transmembrane domain, and an endodomain. The endodomain consists of a kinase domain and a carboxyl-terminal tail, which contains most of the autophosphorylation sites (4). Many RTK receptors, except insulin receptor, appear to undergo oligomerization upon ligand binding (4–6). Oligomerization can occur between the same receptors, forming a homodimer, or different members of the same receptor family, thus forming a heterodimer (6, 13). When ligand binds to the ectodomain of the receptor, conformational changes are propagated through the transmembrane domain to the cytoplasmic domain, resulting in receptor activation (7). The net effects of oligomerization are enhanced kinase activity and initiation of signal transduction (5). A similar scenario has been proposed for several cytokines and their receptor complexes (6). Thus, oligomerization seems to be a common pathway leading to signal propagation (7).

The ectodomain has been postulated to bring the cytoplasmic domains into proximity and orient them for favorable kinase activity (4, 8). The role of the transmembrane region in RTK seems to stabilize the cytoplasmic domain (4). p185$^{c\text{-}neu}$, on the other hand, has been shown to undergo dimerization caused by a point mutation (Val-664 → Glu) in the transmembrane region (8, 9). An analogous transmembrane position in p185$^{c\text{-}erbB\text{-}2}$, mutation of Val-659 → Glu, also leads to dimerization (10). The linker region between the transmembrane region and the kinase domain seems relevant for kinase activity, though no specific role has yet been assigned to this area. Mutations in this region appear to affect kinase activity (4).

p185$^{c\text{-}neu}$ and EGFR can associate and undergo dimerization (11–13). Upon dimerization, enhanced kinase activity ensues and the receptors transphosphorylate each other (12, 14). The ectodomain is necessary for association of p185$^{c\text{-}neu}$ and EGFR, and this heteromer formation is increased in a ligand-dependent manner (12, 14). An active heterodimeric complex of EGFR and p185$^{c\text{-}neu}$ proteins was able to contribute to cellular transformation (12–15). However, cells transfected with EGFR and a kinase-deficient p185$^{c\text{-}neu\ K758M}$ inhibited the kinase activity of EGFR, abolished cellular transformation, and reduced EGF-stimulated mitogenesis (14, 16). These results further suggest that kinase activation requires an association of the cytoplasmic domains of the respective receptors, and that this feature is indispensable to receptor activation and signal transduction.

Although the ectodomain has been shown to be involved in oligomerization, it is not known whether the kinase domains can form dimers in the cytoplasm of cell. We have explored this aspect by using homology modeling. We have analyzed structural features of the monomeric, dimeric, and tetrameric forms of p185$^{c\text{-}neu}$ and EGFR kinase domains. Our study shows that formation of dimers and tetramers within cells is plausible, and this oligomeric state might be a strategy used to recruit diverse substrates in a structure dependent manner and may, as suggested (13), represent a novel diversification mechanism for nonpolymorphic receptors.

MATERIALS AND METHODS

The sequences of the kinase domain of p185$^{c\text{-}neu}$, EGFR, and cAMP-dependent kinase (cAPK) were aligned using the multiple sequence alignment program CLUSTALV (17). The alignment was then adjusted manually, conserving the overall secondary structure and positioning the residues known to be critical in binding adenosine triphosphate (ATP) and in the catalytic site. We modeled both p185$^{c\text{-}neu}$ and EGFR by using the crystal structure of cAPK (18). The modeling was carried out by using QUANTA (Molecular Simulations, Cambridge, MA), and energy minimization was performed using both QUANTA and XPLOR 3.1 (19). CHARMM energy parameters were used in both the programs. The models were analyzed by using QUANTA, O (20), and GRASP (21).

The publication costs of this article were defrayed in part by page charge payment. This article must therefore be hereby marked "*advertisement*" in accordance with 18 U.S.C. §1734 solely to indicate this fact.

Abbreviations: RTK, receptor tyrosine kinase(s); EGF, epidermal growth factor; EGFR, EGF receptor; cAPK, cAMP-dependent kinase; rms, root mean square; ATP, adenosine triphosphate; IRK, insulin receptor kinase.

*To whom reprint requests should be addressed.

A trial structure was built based on the sequence alignment. Insertions, deletions, and mutations were incorporated into the template structure to build an initial model. For both p185$^{c\text{-}neu}$ and EGFR, the sequence alignment led to trial structures with two large insertions and four small deletions in the kinase domain. At the loops where insertions and deletions occur, we used a knowledge-based approach for loop conformation construction (22, 23) because the sizes of the loops were small (five to six residues). The structural data base was created with QUANTA by using the latest coordinates from the Brookhaven National Laboratory data bank. The search was performed with a minimum of two residues included at the termini. The fragments were selected based upon sequence homology and the avoidance of steric contacts. When several satisfactory loops were found, an average structure was accepted. The fragments were annealed and regularized to the template by using QUANTA. The trial structure, with insertion fragments and deletions, was then subjected to energy minimization followed by molecular dynamics. Mutated side chains were screened for steric contacts and, if necessary, remodeled either by using the rotamer library data base (24) or by manually rotating the side chains.

The regions of insertion and deletion were minimized while holding the remainder of the structure fixed, thus preserving the overall structure. The entire structure was then subjected to conjugate gradient energy minimization for 2000 cycles to convergence, followed by an equilibration and production run of molecular dynamics at 300 K for 60 ps. Molecular dynamics was performed to remove any steric contacts and to allow a change in the conformation of inserted loops, if more favorable. All energy calculations were performed at a dielectric constant of 1. Final energy values were calculated by using CHARMM for monomers and XPLOR 3.1 (19) for oligomers. Average root mean square (rms) deviations between the alpha carbon positions of the final models were calculated by using QUANTA. Parameters for MnATP were built from CHARMM and used in all calculations. The consistency of the model was checked by using profile 3-D (25).

Aggregation states were predicted through manual docking of one subunit while holding the remaining subunit(s) fixed. The best-shape complementarity between the kinase domains was obtained by rotation of 165° and translation of 10–12 Å of one of the monomers with respect to its counterpart. The area of surface buried was calculated by using QUANTA with a probe radius of 1.4 Å. Number and type of contacts were evaluated by the program CONTACT (26), with a distance cut-off of 4.5 Å. A tetramer was constructed from the homodimers with 2-fold symmetry operation about an axis parallel to the pseudo-dimer axis of the homodimers. Individual monomers were then adjusted to maximize the complementarity, followed by 40 cycles of rigid body minimization by using XPLOR (19). Electrostatic calculations were performed with GRASP. Charged amino acid groups were assigned full charges as provided in GRASP and charges for MnATP were obtained from CHARMM19, which is part of QUANTA. The electrostatic calculations were performed with distance-dependent dielectric constants, from 1 at the interior to 80 at the outer surface.

RESULTS

Structural and Sequence Alignment of Tyrosine Kinase Domains. Crystal structures of cAPK with and without MgATP show that the ATP binding domain can rotate away from the catalytic domain such that the cleft is either wide open or closed (27). Thus, the kinase domain may exist in either an open form (inactive) or closed form (active). While the active form of cAPK requires bound MgATP, we have shown that Mn^{2+} is preferred over Mg^{2+} by p185$^{c\text{-}neu}$ and EGFR for kinase activity (28). We therefore used MnATP for our calculations. The residues in the ATP binding domain and catalytic region are conserved in all kinases but the activation loop (184–200 of cAPK) is the most variable region among kinases. Choosing an alignment for the autophosphorylation tyrosine residues in p185$^{c\text{-}neu}$ and EGFR (Tyr-882 in p185$^{c\text{-}neu}$ and Tyr-845 in EGFR) proved difficult, and the tyrosines were aligned in two ways within the activation loop: the tyrosine residues were aligned with Thr-197 of cAPK, shown to be phosphorylated in the crystal structure, and alternatively, as an insert in the activation loop (Fig. 1). In both cases, the conformation of the activation loop and the orientation of tyrosines were very similar, suggesting that the alignment of these tyrosines was not critical. The final alignment (Fig. 1) is in agreement with an alignment developed by Knighton *et al.* (29).

Tyrosine Kinase Domain. The overall structure of the kinase domain in p185$^{c\text{-}neu}$ and EGFR is very similar to that of cAPK. The conserved parts of EGFR and p185$^{c\text{-}neu}$ have an rms deviation of 0.43 Å and 0.34 Å and the overall rms deviation is 1.9 Å (Fig. 2). The secondary structures are

```
cAPK    43  FDRIKTLGTGSFGRVMLVKHKESG----NHYAMKI  73
EGFR   688  FKKIKVLGSGAFGTVYKGLWIPEGEKVKIPVAIKE 722
Neu    725  LRKVKVLGSGAFGTVYKGIWIPDGENVKIPVAIKV 759

cAPK    74  LDKQKVVKLKQIEHTLNEKRILQAVNFFFLVKLEF 108
EGFR   723  LREATSP--KANKEILDEAYVMASVDNPHVCRLLG 755
Neu    760  LRENTSP--KANKEILDEAYVMAGVGSPYVSRLLG 792

cAPK   109  SFKDNSNLYMVMEYVAGGEMFSHLRRIGRFSEPHA 143
EGFR   756  ICLTSTVQLITQLMPFGCLLDYVREHKDNIGSQYL 790
Neu    793  ICLTSTVQLVTQLMPYGCLLDHVRENRGRLGSQDL 827

cAPK   144  RFYAAQIVLTFEYLHSLDLIYRDLKPENLLIDQQG 178
EGFR   791  LNWCVQIAKGMNYLEDRRLVHRDLAARNVLVKTPQ 825
Neu    828  LNWCVQIAKGMSYLEDVRLVHRDLAARNVLVKSPN 862

cAPK   179  YIQVTDFGFAKRVKGRTWT-----LCGTPEYLAPE 208
EGFR   826  HVKITDFGLAKLLGAEEKEYHAEGGKVPIKWMALE 860
Neu    863  HVKITDFGLARLLDIDETEYHADGGKVPIKWMALE 897

cAPK   209  IILSKGYNKAVDWWALGVLIYEMAAGYPPFFADQP 243
EGFR   861  SILHRIYTHQSDVWSYGVTVWELMTFGSKPYDGIP 895
Neu    898  SILRRRFTHQSDVWSYGVTVWELMTFGAKPYDGIP 932

cAPK   244  IQIYEKIVSGKVRFPSH-FSSDLKDLLRNLLQV-D 276
EGFR   896  ASEISSILEKGERLPQPPICTIDVYMIMVKCWMID 930
Neu    933  AREIPDLLEKGERLPQPPICTIDVYMIMVKCWMID 967

cAPK   277  LTKRFGNLKNGVNDIKNHKWF                297
EGFR   931  ADSRP-KFRELIIEFSKMARD                950
Neu    968  SECRP-RFRELVSEFSRMARD                987
```

FIG. 1. Sequence alignment of cAPK, p185$^{c\text{-}neu}$, and EGFR. The amino acid sequences were aligned based on the crystal structure of cAPK (18). The alignment was made such that the secondary structures were conserved. The insertions and deletions were allowed only at the loops. The identical amino acids are boxed.

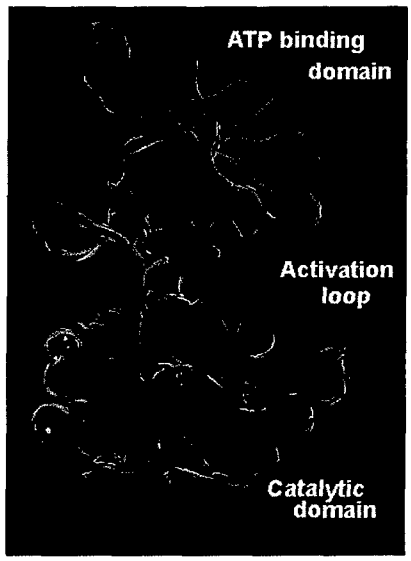

FIG. 2. Comparison of the models of p185$^{c\text{-}neu}$ and EGFR kinase domains. p185$^{c\text{-}neu}$ (red) and EGFR (magenta) kinase domain are shown as trace. The kinase domain is comprised of a smaller lobe or a ATP binding domain and a catalytic domain. The activation loop is located between catalytic domain and the ATP binding domain. Overall secondary structure is similar in both the models of p185$^{c\text{-}neu}$ and EGFR kinase domains. The most variable and flexible region is the activation loop where the autophosphorylation tyrosines are located. The ATP binding domain (the small lobe) is more conserved than the catalytic domain.

conserved in EGFR, p185$^{c\text{-}neu}$, and cAPK with only minor changes. Naming of secondary structures follows that used for cAPK (18). The smaller lobe at the N terminus or ATP binding domain is rich in β strands, and the large lobe at the C terminus or the catalytic domain is rich in α helices. Based upon the alignment, the p185$^{c\text{-}neu}$ and EGFR models lack the β1 strand, β4 is short, and the β5 strand is longer. The region β4 to β5 contains sequences that are not conserved with respect to cAPK. One of the two helices observed in the small lobe, the αB helix, is distorted from that seen in cAPK in both p185$^{c\text{-}neu}$ and EGFR due to the insertions in that region. The helix αD, which is close to the hinge region in cAPK, is also distorted in p185$^{c\text{-}neu}$ and EGFR.

Homodimers and Heterodimers. *Substrate binding region.* Dimers are stabilized by β strands at the top and by the two helices αEF and αG at the bottom (Fig. 3*c*). The homodimers of p185$^{c\text{-}neu}$ and EGFR are shown in Fig. 3 *a* and *b*, and the heterodimers are shown in Fig. 3*d*, which shows that dimers have a similar interface geometry. In our model, the heterodimer interface is formed by six segments from p185$^{c\text{-}neu}$ (727–740, 760–771, 795–799, 880–891, 899–901, and 929–937) and five segments from EGFR (696–701, 722–731, 845–864, and 891–904). The substrate binding region in the dimers is formed at the interface of the two monomers with their MnATP facing each other. Both the heterodime and p185$^{c\text{-}neu}$ homodimer have similar binding pocket size. The substrate binding region is 20.6 Å wide, and the interior narrows down to 7.2 Å and then widens in the back to 10.2 Å. Distance between the dimers (as measured from C$^{\gamma}$ of ATP) is about 20.6 Å. The EGFR-homodimer is 28.9 Å wide near the substrate binding region and narrows down to 14.2 Å near the center of the cavity and in the back widens to 17.9 Å. The EGFR dimers are separated by 16.1 Å.

Association of dimers and tetramers. Studies on protein–protein interaction have identified three major characteristics associated with these interactions: complementarity of shapes, a large area buried (or loss of accessible surface area upon dimerization), and finally, contacts are often dominated by hydrophobic interactions (30, 31). In this study we assumed minimal structural change in the monomer proteins upon oligomerization. The oligomerization of p185$^{c\text{-}neu}$ and EGFR was analyzed by using conformational energy calculations and accessible surface area. The results obtained from the calculations of accessible surface area for the oligomers and molecular energy calculation are shown in Table 1. Surprisingly, the nature of the surface at the interface upon oligomerization is very similar in both homodimers and the heterodimer. The surface is predominately formed by nonpolar atoms at the interface. Heterodimer association leads to a loss of surface area, which is about 2% greater than in the homodimers. In addition, the total energy of the heterodimer is lower than that of the homodimers (Table 1). Clearly, the total energy is dominated by electrostatic interactions. This major electrostatic energy was contributed by the clustering of charges on the surface and the interior of the molecules. The core is negatively charged, and one end of the molecule contains a positively charged cluster (Fig. 4). In the heterodimer, the positive charges span from one side of EGFR to the interface of the p185$^{c\text{-}neu}$. The positively charged surface patch is formed by residues from EGFR (His-749, Arg-752, Lys-822, and His-826) and p185$^{c\text{-}neu}$ (Arg-726, Lys-727, and His-818). The features of p185$^{c\text{-}neu}$ and EGFR tetramers are similar to that of dimers (data not shown). Energetic and surface area calculations suggest that the tetrameric association of p185$^{c\text{-}neu}$ and EGFR is less stable than the heterodimer.

DISCUSSION

Protein kinases share a high degree of homology in the catalytic domain, whether they are Ser/Thr kinases or tyrosine kinases (32). Several crystal structures of Ser/Thr kinases have now been determined, including the cAMP dependent kinase (18), mitogen-activating kinase ERK-2 (33), twitchin kinase (34). Recently, the kinase domain of insulin receptor (IRK), a member of the tyrosine kinase family was determined (35). These protein structures reveal that the kinase domains not only share sequence homology but also have very similar topologies. Sequence homology among the kinase family members has helped to develop an informative model of the EGFR kinase domain (29). p185$^{c\text{-}neu}$ belongs to class I type receptors and is very similar to EGFR, sharing 82% amino acid sequence homology in the tyrosine kinase domain.

The ATP binding domain is mostly conserved in both cAMP-dependent kinases and in the kinase domains of RTK. The sequence alignments of kinases show that the Ser/Thr kinases contain a flexible hinge sequence (Gly-125–Gly-126) near the ATP binding region (Fig. 1). This has been replaced by Gly–Cys in tyrosine kinases. Structurally, this indicates that p185$^{c\text{-}neu}$ and EGFR have less freedom to open and close than Gly–Gly-containing kinases. In comparison to cAPK (a Ser/Thr kinase), there is an additional helix, disposed near the activation loop of p185$^{c\text{-}neu}$ and the EGFR tyrosine kinases. The minor changes in the secondary structural features of p185$^{c\text{-}neu}$ and EGFR kinase domains are consistent with characteristics observed in both the IRK (35) and EGFR models (29). The amino acid residues involved in ATP binding are conserved in all the tyrosine kinases, including p185$^{c\text{-}neu}$ and EGFR. In p185$^{c\text{-}neu}$, the ligand ATP is neutralized by two charged residues, Lys-758 and Arg-854, in comparison to only Lys-72 in cAPK. The role of Lys-758 in p185$^{c\text{-}neu}$ has been shown to be critical for kinase activity. Mutation of this residue abolishes the kinase activity and also abrogates cellular transformation (9). In EGFR, Lys-721 and Arg-817 may play a similar role.

The catalytic site, where phospho-group transfer occurs, is located between the ATP binding and catalytic domains. The putative catalytic site in p185$^{c\text{-}neu}$ is formed by Lys-758, Glu-775, Asp-850, Arg-854, and Asp-868, as discerned from

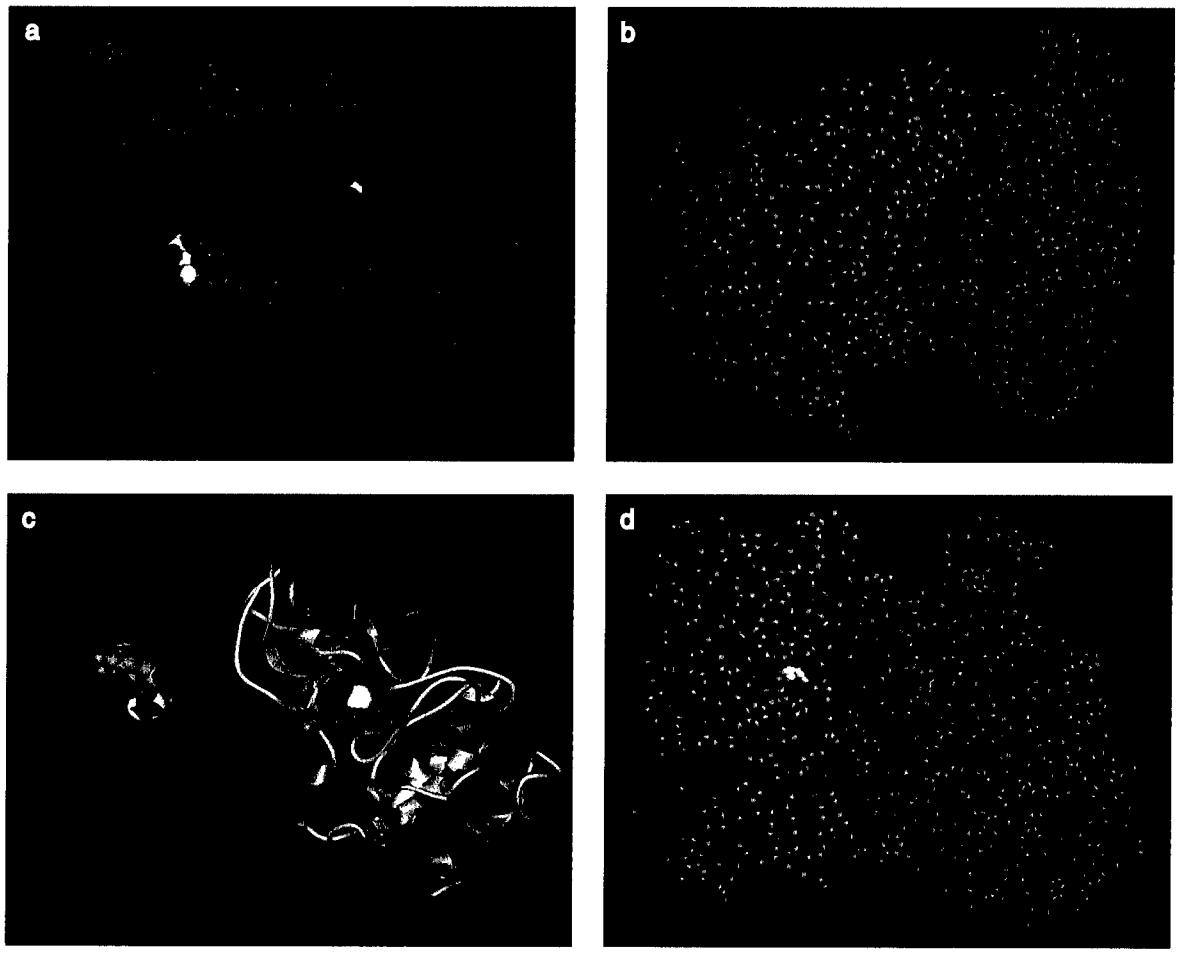

FIG. 3. Oligomerization of the kinase domains of p185$^{c\text{-}neu}$ and EGFR. The molecules are viewed down the autophosphorylation tyrosines. Each molecule within a given homodimer is shown in different color. The autophosphorylation tyrosine is shown in pink, and MnATP moiety is shown in yellow. The space-filling model of p185$^{c\text{-}neu}$ homodimer shows that the autophosphorylation tyrosine is close to the substrate binding domain and fully exposed (*a*), while in homodimer of EGFR the autophosphorylation site is partially buried and much closer to the substrate binding region (*b*) (see text for discussion). (*c*) Heterodimer formation is shown as ribbon model to highlight the complementarity between the p185$^{c\text{-}neu}$ and EGFR. The p185$^{c\text{-}neu}$ monomer is shown in purple and EGFR by yellow. The two molecules are stabilized by a pair of β sheets in the ATP binding domain and by an α helix in the catalytic domain. (*d*) Space-filling model of heterodimer of EGFR (red) and p185$^{c\text{-}neu}$ (blue). In the heterodimer, the intermolecular interactions are different than those of the homodimers, and based on energetic, heterodimer formation is more stable than homodimers. The autophosphorylation tyrosines (pink) are poised in such a fashion that, in heterodimers, these tyrosines might act like a gate to modulate and control signal transduction by altering structure and selection of substrate (see text for details).

crystal structures of kinases. In the catalytic region of both p185$^{c\text{-}neu}$ and EGFR, the Lys-Pro-Glu of cAPK has been substituted by Ala-Ala-Arg, a feature suggested to be characteristic of the tyrosine kinase family proteins (29). The structural features of the ATP binding domain is conserved despite the fact residues Lys-168 and Glu-170 in cAPK are changed to alanine and arginine in both p185$^{c\text{-}neu}$ and EGFR. The arginine residue in p185$^{c\text{-}neu}$ and EGFR may play a different role in stabilizing charge distribution in the substrate binding domain.

Nonconserved residues in the kinase domains of p185$^{c\text{-}neu}$ and EGFR are located near the activation loop and near the surface of the molecule. The most variable region, the activation loop, is distinct in both p185$^{c\text{-}neu}$ and the EGFR and remains flexible in both (Fig. 2). We consider the activation loop as perhaps the most defining region of a particular kinase. The activation loop contains some of sites for autophosphorylation. In the case of EGFR, the Tyr-845 is partially oriented toward the active site, whereas in p185$^{c\text{-}neu}$, Tyr-882 appears to

Table 1. Results of energy and surface calculations for oligomers of the kinase domains of p185$^{c\text{-}neu}$ and EGFR

Surface accessibility	neu–neu	EGFR–EGFR	neu-EGFR	Tetramer*
Buried, Å^2	1653	1553	2536	5670
Hydrophilic	458 (28%)	477 (31%)	581 (23%)	1481 (26%)
Hydrophobic	1195 (72%)	1075 (69%)	1955 (77%)	4189 (74%)
Energy, kcal/mol				
VDW contribution	−2870	−2560	−3201	−414
Electrostatic	−30874	−29686	−31028	−47113

Surface accessibility and intermolecular energy were calculated by using QUANTA (Molecular Simulations) with a probe radius of 1.4 Å.
*Calculations were performed by using XPLOR (19).

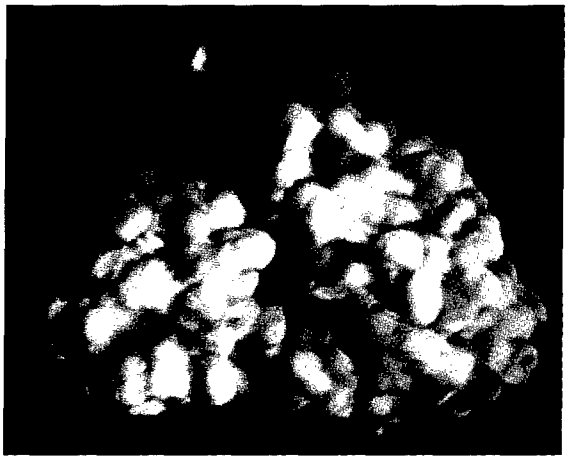

FIG. 4. Surface model of heterodimer of the kinase domains of p185$^{c\text{-}neu}$ and EGFR. Blue color represents the distribution of positive charges, and red represents the negative charges. The surface charge distribution shows separation of charge clusters. A dipole induced by the charge separation might initiate oligomerization when kinase domains approach within close proximity and also act as a stabilizing force.

be disposed on the surface. This feature was rather unexpected given the observation that in the crystal structures of cAPK and IRK, the equivalent self-phosphorylation sites oriented toward the active site. The environment of the Tyr-882, the autophosphorylation site, is more negative in p185$^{c\text{-}neu}$ than the autophosphorylation site of cAPK or IRK. In the activation loop, the autophosphorylation sites in p185$^{c\text{-}neu}$, EGFR, and cAPK are preceded by an amino acid sequence Asp-Glu-Thr-Glu, Glu-Glu-Lys-Glu, and Gly-Arg-Thr-Trp, respectively (Fig. 1). Lack of a positive charge near the autophosphorylation site leaves the activation loop in p185$^{c\text{-}neu}$ negative, and this feature disposes Tyr-882 on the surface pointing toward the active site. The IRK activation loop has been observed to be very mobile as judged by high thermal factors (35). The mobility of the activation loop is consistent with large movement of this region observed in p185$^{c\text{-}neu}$ and EGFR during the short molecular dynamics calculation we have undertaken. During the dynamics calculation, we observed that some autophosphorylation tyrosines could fold inwards for cis-

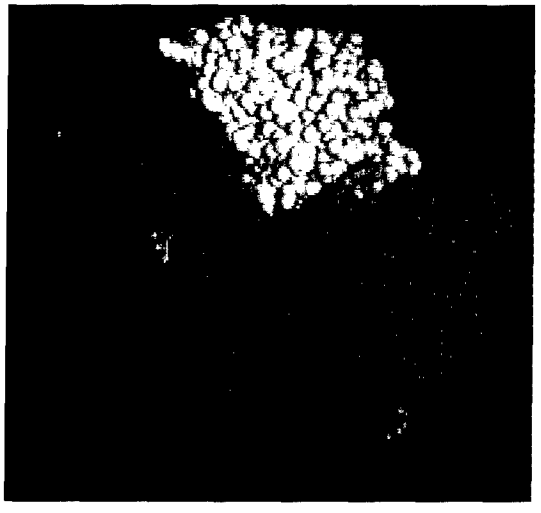

FIG. 5. Space-filling model of tetrameric association of the kinase domains of p185$^{c\text{-}neu}$ and EGFR. The tetramer is viewed down the pseudo-4-fold axis, tilted toward the viewer. The autophosphorylation tyrosines of p185$^{c\text{-}neu}$ and EGFR are more involved in tetrameric structural integrity, where any change, such as phosphorylation or mutation, might induce an allosteric-related structural change.

phosphorylation. The positively charged residue preceding Tyr-845 in the EGFR is attracted toward the negatively charged catalytic site, favoring the activation loop to fold inwards. No such force was exerted on the activation loop of p185$^{c\text{-}neu}$ to fold inwards. This results in the autophosphorylation site of EGFR (Tyr-845) being partially buried, while the autophosphorylation tyrosine Tyr-882 of p185$^{c\text{-}neu}$ appears on the surface. In ERK-2, one of the autophosphorylation sites, Thr-183, preceded by uncharged residues, is also observed on the surface and is phosphorylated.

The substrate binding pocket in dimers of p185$^{c\text{-}neu}$ and EGFR is wide near the substrate binding region of the monomer, narrow near the active sites, and wide again at the back. Although the substrate binding pocket in dimers has similar shape, the dimension of the pocket is different. Both the p185$^{c\text{-}neu}$ homodimer and the heterodimer have smaller binding pockets compared to the binding pocket of EGFR. The substrate binding pocket of the EGFR homodimers is widened by the presence of Tyr-891 located near the interface. The difference in the size of binding pockets among the dimers suggests that the dimers might be used to recruit different substrates of different sizes in a structure dependent manner.

Jones and Thornton (36), in a recent survey of protein–protein interactions of dimers, suggest that the amino acid composition at the interface of dimers can be hydrophilic, resembling the surface of a protein. Nevertheless, the interface is stabilized by hydrophobic interactions rather than hydrophilic interactions. In general, the protein dimers are stabilized by an average of 8 hydrogen bonds per 1000 Å^2 buried surface (36). Results from our analysis of p185$^{c\text{-}neu}$–EGFR dimers are consistent with their results. Our data also indicate that the interfaces of homodimers and heterodimers of p185$^{c\text{-}neu}$ and EGFR are equally rich in hydrophobic residues. The distribution of hydrophobic residues at the interface would increase the avidity to form dimers and energetically act like a glue (37). The dimeric surface of p185$^{c\text{-}neu}$ and EGFR is stabilized by an average of 15 hydrogen bonds. The average area of surface lost on dimer formation of p185$^{c\text{-}neu}$ and EGFR is 1696 Å, and it is contributed by 68.1% of nonpolar atoms and 21.9% by polar atoms. These values are also in the range with that observed for other protein dimers surveyed by Jones and Thornton (36).

Results from the conformational energy calculations indicate that heterodimers would be preferred over homodimers. In addition, the larger area of buried surface in forming heterodimers over homodimers suggests that the heteromer would be more stable than the homomer. Thus, if a cell expresses both p185$^{c\text{-}neu}$ and EGFR, then heterodimer formation would be favored over homodimer formation. This is in agreement with our biochemical observations (14) that coexpression of truncated p185$^{c\text{-}neu}$ and full length EGFR results in a predominant intermediate size heterodimer over either p185$^{c\text{-}neu}$ or an EGFR homodimer.

Fig. 4 shows the surface charge distribution in the heterodimer. The core is negatively charged, and one end of the molecule contains a positively charged cluster. The positive charge spans from one side of EGFR to the interface of the p185$^{c\text{-}neu}$. A similar charge distribution is observed in the homodimers. The separation of charges suggests that the dimers might be stabilized by a net dipole–dipole interaction when the two kinase domains are juxtaposed. Thus, the distance within which the kinase domains must be brought into juxtaposition would be critical. In support of this concept, bivalent monoclonal antibodies have been shown to induce dimerization where as the Fab fragment derived from the monoclonal alone failed to do so (38). It is structurally possible that the antibody, with two Fab fragments disposed apart at least by about 36 Å, can bind to two receptors and bring them within a distance that might induce a favorable dipole–dipole interaction between the kinase domains.

It is known that autophosphorylation plays a crucial role in signal transduction (39). Various receptors have a tendency to phosphorylate both cis and trans on either Ser/Thr or Tyr. In the case of $p185^{c\text{-}neu}$ and EGFR, most of the autophosphorylation sites are located outside of the kinase domain, at the C terminus of the receptor. The complete role of the autophosphorylation sites in the kinase domain is not known definitively, but autophosphorylated tyrosines have been implicated as binding site for Src homology 2 domain-containing substrates (44). The autophosphorylation sites Tyr-882 in $p185^{c\text{-}neu}$ and Tyr-845 in EGFR are located in the activation loop and near the interface of the dimer. The orientation of these tyrosine are very different in $p185^{c\text{-}neu}$ and EGFR, although they are located at the same place within the activation loop. In the $p185^{c\text{-}neu}$ homodimer, the autophorylation tyrosine (Tyr-882) is pointing outwards (Fig. 3*a*), suggesting that this tyrosine may not be involved in the cis-phosphorylation and would not affect kinase activity. In contrast, the autophosphorylation tyrosine in EGFR (Tyr-845) is partially buried (Fig. 3*b*), suggesting that the tyrosine can undergo cis-autophosphorylation. These tyrosines in EGFR are located about 15 Å away from the interface of the dimer and oriented toward the substrate binding region, such that they could influence substrate binding. Thus, the model suggests that in the case of $p185^{c\text{-}neu}$, that autophosphorylation of Tyr-882 might not be critical to kinase activity. However, this residue may be phosphorylated by other proteins, provided it is not buried by the C-terminal residues. Thus, the location and orientation of these tyrosines implies that they play a critical role in the selection of substrates in various protein aggregation states.

The C terminus of the cytoplasmic domain is not conserved within the tyrosine kinase family receptors (40). Lack of sequence homology limits modeling of this fragment. In the crystal structure of cAPK (18) and twitchin kinase (34), the C terminus (regions outside the kinase domain) folds back close to the active site of the enzyme. It is possible that nonhomologous proteins within a family will have similar structures (41). Based on such observations, the C terminus of both $p185^{c\text{-}neu}$ and EGFR might fold back and approximate to the active site.

EGFR and $p185^{c\text{-}neu}$ may also undergo higher orders of aggregation (42). Yarden and Schlessinger (38) have demonstrated that noncovalent forces appear relevant to EGFR oligomerization using nondenaturing gel analysis. Lax *et al.* (43) have shown that EGFR can undergo higher order of oligomerization upon binding to EGF. Formation of dimers and tetramers have been deduced from electron microscopic analysis. Assuming the aggregation is ordered and specific for dimers, the next higher order of aggregation would be a tetramer. Model building shows that such a possibility exists. The substrate binding region in the tetrameric form is very similar to that of the dimers. However, the interactions among the subunits of $p185^{c\text{-}neu}$ and EGFR are very different. In a tetramer, the role of these tyrosines may even involve structural changes induced by an allosteric effect (Fig. 5). One of the important consequences is that the autophosphorylation tyrosines are positioned at the interface like a gate, resulting in less freedom of movement among the subunits. Thus, it is possible that in a cell expressing both $p185^{c\text{-}neu}$ and EGFR, dimers would be formed initially, and over time the dimers could associate as tetramers. This transition, then, might be used to regulate signals and to provide unique scaffolds for adaptor molecules

Our modeling investigated several features of homodimeric and heteromeric complexes of $p185^{c\text{-}neu}$ and EGFR kinase domains. Our study demonstrates the propensity of kinase domains to complex within a cell and features of the nature of these complexes. Consistent with observed biochemical data, our model confirms that heterodimers would be preferred over homodimers. Our models also suggest that the autophosphorylation tyrosine in the kinase domains might be involved in altering the oligomeric structure by allosteric mechanism to recruit different substrates without altering kinase activity. These models may facilitate the design and development of inhibitors of heteromeric kinase complexes that are relevant to neoplastic disease.

We would like to thank Drs. James Davis, Navaratnam Kumar, and Xiaolan Qian for discussion. The work was supported by grants from Astral Corporation, Frontiers of Science, and the National Institutes of Health (M.I.G.), and the U.S. Army Medical Research Acquisition Activity (T.K.E.) Breast Cancer Initiative.

1. Kokai, Y., Cohen, J. A., Drebin, J. A. & Greene, M. I. (1987) *Proc. Natl. Acad. Sci. USA* **84,** 8498–8501.
2. Mori, S., Akiyama, T., Yamada, Y., Morishita, Y., Sugawara, I., Toyoshima, K. & Yamamoto, T. (1989) *Lab. Invest.* **61,** 93–97.
3. Press, M. F., Cordon-Cardo, C. & Slammon, D. (1990) *Oncogene* **5,** 953–962.
4. Ullrich, A. & Schlessinger, J. (1990) *Cell* **61,** 203–212.
5. Schlessinger, J. (1988) *Trends Biochem. Sci.* **13,** 443–447.
6. Lemmon, M. A. & Schlessinger, J. (1994) *Trends Biochem. Sci.* **19,** 459–463.
7. Heldin, C. H. (1995) *Cell* **80,** 213–223.
8. Weiner, D. B., Liu, J., Cohen, J. A., Williams, W. V. & Greene, M. I. (1989) *Nature (London)* **339,** 230–231.
9. Weiner, D. B., Kokai, Y., Wada, T., Cohen, J. A., Williams, W. V. & Greene, M. I. (1989) *Oncogene* **4,** 1175–1183.
10. Segatto, O., King, R. C., Pierce, J. H., Di Fiore, P. P. & Aaronson, S. A. (1988) *Mol. Cell. Biol.* **8,** 5570–5574.
11. Goldman, R., Benlevy, R., Peles, E. & Yarden, Y. (1990) *Biochemistry* **29,** 11024–11028.
12. Qian, X. L., Decker, S. J. & Greene, M. I. (1992) *Proc. Natl. Acad. Sci. USA* **89,** 1330–1334.
13. Wada, T., Qian, X. & Greene, M. (1990) *Cell* **61,** 1339–1347.
14. Qian, X., LeVea, C. M., Freeman, J. K., Dougall, W. C. & Greene, M. I. (1994) *Proc. Natl. Acad. Sci. USA* **91,** 1500–1504.
15. Kokai, Y., Myers, J. N., Wada, T., Brown, V. I., LeVea, C. M., Davis, J. G., Dobashi, K. & Greene, M. I. (1989) *Cell* **58,** 287–292.
16. Qian, X., Dougall, W. C., Hellman, M. E. & Greene, M. I. (1994) *Oncogene* **9,** 1507–1514.
17. Higgins, D. G., Bleasby, A. J. & Fuchs, R. (1992) *Comput. Appl. Biosci.* **8,** 189–191.
18. Knighton, D. R., Zheng, J. H., Ten, E. L. F., Ashford, V. A., Xuong, N. H., Taylor, S. S. & Sowadski, J. M. (1991) *Science* **253,** 407–414.
19. Brünger, A. T. (1992) X-PLOR: A System for X-Ray Crystallography and NMR (Yale Univ. Press, New Haven, CT), Version 3.1.
20. Jones, T. A., Zou, J.-Y & Cowan, S. W. (1991) *Acta Crystallogr. A* **47,** 110–119.
21. Nicholls, A., Sharp, K. A. & Honig, B. (1991) *Proteins* **11,** 281–296.
22. Jones, T. A. & Thirup, S. (1986) *EMBO J.* **5,** 819–822.
23. Blundell, T. L., Sibanda, B. L., Sternberg, M. J. & Thornton, J. M. (1987) *Nature (London)* **326,** 347–352.
24. Ponder, J. W. & Richards, F. M. (1987) *J. Mol. Biol.* **193,** 775–791.
25. Luthy, R., Bowie, J. U. & Eisenberg, D. (1992) *Nature (London)* **356,** 83–85.
26. CCP4 (1994) *Acta Crystallogr. D* **50,** 760–763.
27. Zheng, J., Knighton, D. R., Xuong, N. H., Taylor, S. S., Sowadski, J. M. & Ten, E. L. (1993) *Protein Sci.* **2,** 1559–1573.
28. Myers, J. N., LeVea, C. M., Smith, J. E., Kallen, R. G., Tung, L. & Greene, M. I. (1992) *Receptor* **2,** 1–16.
29. Knighton, D. R., Cadena, D. L., Zheng, J., Ten, E. L. F., Taylor, S. S., Sowadski, J. M. & Gill, G. N. (1993) *Proc. Natl. Acad. Sci. USA* **90,** 5001–5005.
30. Janin, J. & Chothia, C. (1990) *J. Biol. Chem.* **265,** 16027–16030.
31. Wodak, S. J., Crombrugghe, M. D. & Janin, J. (1987) *Prog. Biophys. Mol. Biol.* **49,** 29–63.
32. Hanks, S. K., Quinn, A. M. & Hunter, T. (1988) *Science* **241,** 42–52.
33. Zhang, F., Strand, A., Robbins, D., Cobb, M. H. & Goldsmith, E. J. (1994) *Nature (London)* **367,** 704–711.
34. Hu, S. H., Parker, M. W., Lei, J. Y., Wilce, M. C., Benian, G. M. & Kemp, B. E. (1994) *Nature (London)* **369,** 581–584.
35. Hubbard, S. R., Wei, L., Ellis, L. & Hendrickson, W. A. (1994) *Nature (London)* **372,** 746–754.
36. Jones, S. & Thornton, J. M. (1995) *Prog. Biophys. Mol. Biol.* **63,** 31–65.
37. Argos, P. (1988) *Protein Eng.* **2,** 101–113.
38. Yarden, Y. & Schlessinger, J. (1987) *Biochemistry* **26,** 1434–1442.
39. Downward, J., Parker, P. & Waterfield, M. D. (1984) *Nature (London)* **311,** 483–485.
40. Dougall, W. C., Qian, X., Peterson, N. C., Miller, M. J., Samanta, A. & Greene, M. I. (1994) *Oncogene* **9,** 2109–2123.
41. Sali, A., Overington, J. P., Johnson, M. S. & Blundell, T. L. (1990) *Trends Biochem. Sci.* **15,** 235–240.
42. Samanta, A., LeVea, C. M., Dougall, W. C., Qian, X. & Greene, M. I. (1994) *Proc. Natl. Acad. Sci. USA* **91,** 1711–1715.
43. Lax, I., Mitra, A. K., Ravera, C., Hurwitz, D. R., Rubinstein, M., Ullrich, A., Stroud, R. M. & Schlessinger, J. (1991) *J Biol. Chem.* **266,** 13828–13833.
44. Cantley, L. C., Auger, K. R., Carpenter, C., Duckworth, B., Graziani, A., Kapeller, R. & Soltoff S. (1991) *Cell* **64,** 281–302.

Oncogene (1998) 16, 2835–2842

http://www.stockton-press.co.uk/onc

Absence of autophosphorylation site Y882 in the p185^{neu} oncogene product correlates with a reduction of transforming potential

Hong-Tao Zhang[1], Donald M O'Rourke[2], Huizhen Zhao[1], Ramachandran Murali[1], Yasunori Mikami[1], James G Davis[1], Mark I Greene[1] and Xiaolan Qian[3]

[1]*Departments of Pathology and Laboratory Medicine and* [2]*Neurosurgery, University of Pennsylvania, School of Medicine, 36th and Hamilton Walk, Philadelphia, PA, 19104;* [3]*Laboratory of Cellular Oncology, National Cancer Institute, Bethesda, Maryland, 20892, USA*

Autophosphorylation of type I receptor tyrosine kinases (RTKs) comprises one step in the signaling events mediated by erbB receptors such as p185^{neu} and EGFR. Previous analysis of p185^{neu} has indicated that there are at least five tyrosine autophosphorylation sites, Y882, Y1028, Y1143, Y1226/7 and Y1253, of which Y882 might be important because of its location in the kinase activity domain. We have specifically analysed the effect of a Y882F (phenylalanine substituted for tyrosine at position 882) mutation in the enzymatic active domain. We also deleted the carboxyl terminal 122 amino acids which contained three other autophosphorylation sites (TAPstop) and combined mutants of that deletion with Y882F (Y882F/APstop). Both *in vitro* and *in vivo* transformation assays showed that substitution of tyrosine^{882} by phenylalanine significantly decreased the transforming potential of activated, oncogenic p185^{neu}, although no significant difference in the total phosphotyrosine levels of the mutant proteins were observed. To analyse mitogenic signaling in response to ligand, the intracellular domains of p185^{neu} and Y882F were fused with the extracellular domain of the EGF receptor. The proliferation of cells expressing these chimeric receptors was EGF-dependent, and cells expressing EGFR/Y882F chimeric receptors were less responsive to EGF stimulation than those expressing EGFR/neu receptors. *In vitro* kinase assays demonstrated that abolishing the autophosphorylation site Y882 diminished the enzymatic tyrosine kinase activity of p185^{neu}. These studies, taken together with the phenotypic inhibition observed with cells expressing Y882F, suggest that the tyrosine^{882} residue may be important for p185^{neu}-mediated transformation by affecting the enzymatic kinase function of the p185^{neu} receptor.

Keywords: p185^{neu}; tyrosine kinase; Y882; transformation

Introduction

Activation of erbB receptor tyrosine kinases, such as p185^{neu} and the EGFR, involves oligomerization of receptors (reviewed in Heldin, 1995). Mutation and overexpression of erbB family receptors has been found to lead to receptor activation by inducing the formation of dimeric and oligomeric forms (Weiner *et al.*, 1989; Samanta *et al.*, 1994). The net effects of oligomerization are both enhanced kinase activity and subsequent signal transduction (Samanta *et al.*, 1994). Activation of erbB family receptors results in self-phosphorylation of receptors by an intermolecular mechanism and in the phosphorylation of substrates which are critical in initiating signal transduction events required for cell growth and differentiation (Ullrich and Schlessinger, 1990; Carraway and Cantley, 1994). The interactions between receptor tyrosine kinases and specific signaling proteins is in part governed by phosphorylation at particular tyrosine residues in the carboxyl terminus of these receptors (see Carter and Kung, 1994; Dougall *et al.*, 1994). Receptor autophosphorylation is therefore not only required for direct interaction and phosphorylation of protein substrates, but also is felt to be important in the regulation of the enzymatic tyrosine kinase activity.

In the case of EGFR, self-phosphorylation of the cytoplasmic domain is known to occur at five tyrosine residues located in the carboxyl terminus outside of the enzymatic kinase domain (Y992, Y1068, Y1086, Y1148 and Y1173) (see Carter and Kung, 1994). Many kinases are also activated by phosphorylation of a conserved Thr or Tyr site that lies within the catalytic core of the kinase domain. For example, a conserved tyrosine residue within the kinase domain of the v/c-*src* kinase has been located at position Y416 (Hanks *et al.*, 1988). Autophosphorylation of this site is important for regulating kinase enzymatic function and biological activity of the *src* kinase (Kmiecik and Shalloway, 1987; Piwnica *et al.*, 1987). The corresponding tyrosine residue is important for regulating kinase function in many other receptor and cytoplasmic tyrosine kinases, including v-*fps* (Weinmaster *et al.*, 1984), the insulin receptor (Ellis *et al.*, 1986), the colony stimulating factor I-receptor (CSF-IR) (Roussel *et al.*, 1990; Van de Geer and Hunter, 1991), and the platelet-derived growth factor receptor (PDGFR) (Fantl *et al.*, 1989; Morrison *et al.*, 1990). However, the analogous site within the catalytic core of the EGFR kinase domain, Y845, has been reported to be less relevant for tyrosine autophosphorylation of the mature 170 kDa EGFR, EGF-induced stimulation of DNA synthesis, or EGF-dependent transformation of NIH3T3 cells (Gotoh *et al.*, 1992). Nevertheless, mutations in charged residues adjacent to Y845 decrease the Vmax for receptor self-phosphorylation, suggesting that this surface region stabilizes the catalytic core of the kinase domain and is important for maximal self-phosphorylation activity of the kinase domain (Timms *et al.*, 1995).

Correspondence: MI Green
Received 17 September 1997; revised 30 December 1997; accepted 30 December 1997

p185^{neu} is also tyrosine-phosphorylated on five sites, Y882, Y1028, Y1143, Y1226/7 and Y1253 (see Dougall *et al*., 1994). Residue Y882 corresponds to position Y845 of the EGFR and we have deduced its position through molecular modeling of the kinase domain (Murali *et al*., 1996). In order to address whether position Tyr-882 is important for p185^{neu} receptor autophosphorylation and transformation mediated by oncogenic p185^{neu}, we constructed a mutant neu cDNA encoding the rat neu activating transmembrane point mutation and a phenylalanine (F) residue at position 882 (Y882F). In another pair of mutants, we deleted the carboxyl terminal 122 amino acids which included the last three autophosphorylation sites in the carboxyl terminal (TAPstop) (Mikami *et al*., 1992) and also combined it with Y882F (Y882F/APstop). Tyr-882 residue appears important for both the regulation of enzymatic kinase function of p185^{neu} and for some downstream signaling events mediated by p185^{neu} receptors. These studies may facilitate the development of site-specific inhibitors of kinase activation which inhibit signal transduction events contributing to oncogenic transformation.

Results

Tyrosine autophosphorylation of oncogenic p185^{neu} (Tneu) and mutant neu derivatives in vivo

Schematic representation of rat p185^{neu} and derived mutant protein structures are shown in Figure 1. Tneu refers to the full-length oncogenic p185^{neu} receptor which contains the activating transmembrane point mutation (V664E). All mutant neu constructs were derived from Tneu and therefore contain the activating transmembrane point mutation. Site-directed mutagenesis was used on the Tneu construct to generate a phenylalanine (F) at position 882 instead of a tyrosine (Y). Tneu and Y882F were used to generate an additional set of mutants, TAPstop and Y882F/APstop, respectively, by deleting 122 amino acids from the carboxyl terminus. Additionally, a mutant chimera, EGFR/Y882F, was generated from the EGFR/neu chimeric receptor. These mutant proteins were expressed in NR6 cells, a fibroblast cell line which lacks endogenous EGF receptors (Pruss and Herschman, 1977). Stable cell lines expressing each mutant

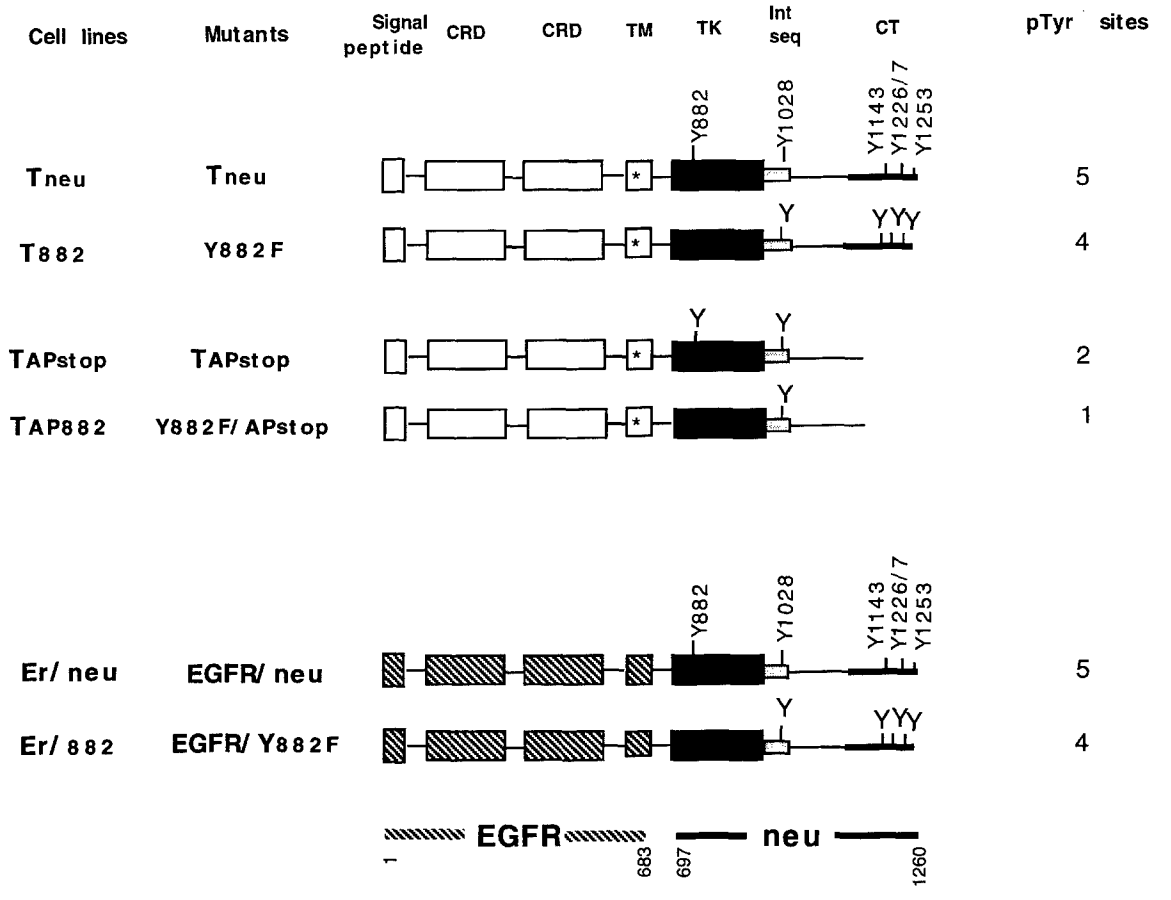

Figure 1 Schematic representation of rat p185^{neu} and derived mutant protein structures. The cell lines derived to express various p185^{neu} mutant receptors are listed in addition to the individual mutant receptors. Location of simplified ectodomain, including two cysteine-rich subdomains (CRD), transmembrane region (TM), tyrosine kinase domain (TK), internalization sequence (Int seq), and potential autophosphorylation sites of carboxyl terminal tyrosine residues (Y) are indicated. Tneu refers to full-length oncogenic p185^{neu} containing the transmembrane point mutation, V664E (*). Y882F has a phenylalanine substitution for tyrosine at the 882 residue. TAPstop and Y882F/APstop are derived from Tneu and Y882, respectively, by deleting 122 amino acid residues from carboxyl terminus (CT). EGFR/neu, a gift from K Alitalo (University of Helsinki), is a wild-type chimera containing the ectodomain and transmembrane region of EGFR, and the intracellular domain of p185^{neu}. The mutant chimera, EGFR/Y882F was derived from EGFR/neu and Y882F by subcloning. The number of potential tyrosine autophosphorylation sites for each mutant is also listed

constructs were established and designated as shown in Figure 1.

Immunoprecipitation of mutant p185^{neu} forms followed by immunoblotting with an anti-phosphotyrosine antibody was performed in order to assess whether substitution of tyrosine-882 was associated with a reduction in total phosphotyrosine content of oncogenic p185^{neu} immuno-complexes (Figure 2, lanes 1–4). The same blot was stripped and re-probed with the anti-Neu antibody α-Bacneu to verify the receptor protein level (Figure 2, lanes 5–8). The phosphotyrosine content was estimated by scanning densitometry (not shown). Cells expressing Y882F (designated T882) appeared to have comparable levels of total phospho-tyrosine content of the receptor compared with oncogenic neu expressing cells (designated Tneu) (Figure 2, lanes 1–2 and 5–6). Comparable levels were also observed in a comparison between mutants TAPstop (TAPstop cells) and Y882F/APstop (TAP882 cells) (Figure 2, lanes 3–4 and 7–8).

It is noteworthy that the mutant TAP882, although missing four out of five known tyrosine phosphorylation sites, still exhibited a high phospho-tyrosine content (Figure 2, lane 4). This observation supports the notion that there exist some cryptic tyrosine phosphorylation sites other than the known ones of the *erb*B family of RTKs. Notably, replacing all the five known sites in EGFR could not completely eliminate tyrosine phosphorylation of the receptor upon ligand stimulation (Decker, 1993; Li *et al*., 1994).

In cells expressing the full-length p185^{neu} mutants (Tneu and T882 lines), an additional faster migrating form of the protein was observed which presumably represents a precursor form of p185^{neu} (Figure 2, lanes 1–2 and 3–4). We and others have noted these protein forms, particularly in quiescent cells expressing proto-oncogenic p185^{neu} (Kiyokawa *et al*., 1995), and has been interpreted as a form of the receptor with altered phosphorylation of serine and/or threonine residues.

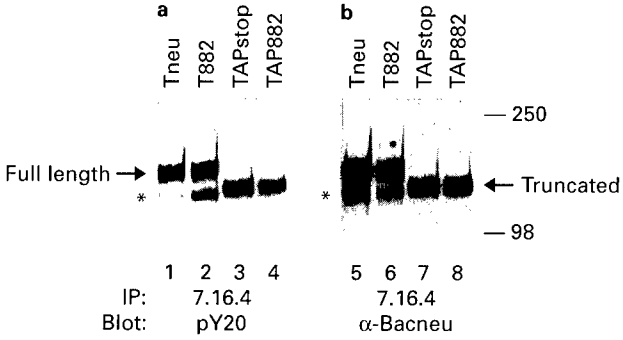

Figure 2 Immunodetection of mutant p185^{neu} proteins. The total phosphotyrosine level of p185^{neu} is not significantly changed by the substitution of tyrosine-882 with phenylalanine. Cell lysates were prepared from cell lines indicated above (Figure 1) and were subjected to immunoprecipitation using anti-neu mAb 7.16.4. The protein samples were separated by 6% SDS–PAGE and transferred onto nitrocellulose membranes followed by immunoblotting with anti-phosphotyrosine antibody pY20 (Santa Cruz) (**a**) or the anti-p185^{neu} antibody Bacneu (**b**). All protein signals were visualized using the enhanced chemiluminescence (ECL) technique (Amersham). Molecular weight markers (in kDa) are indicated on the right of the panel and the positions of full length (p185) and truncated p185^{neu} proteins are shown (arrow). The slightly high-mobility precursor forms of full length neu proteins (lanes 1, 2, 5 and 6) were also denoted (*)

Our results indicate that this precursor form of p185^{neu} is also differentially phosphorylated on tyrosine residues. The greater abundance of the tyrosine phosphorylated precursor form of Y882F may be of relevance to the biologic data described below. Deletion of the carboxyl-terminal 122 amino acids produced a protein of approximately 170–175 kDa and resulted in the detection of only one form of mutant p185^{neu} receptor.

Effect of Y882F substitution on in vitro *kinase activity of p185*^{neu}

Anti-neu immuno-complexes from cell lines expressing p185^{neu}-derived mutant proteins were suspended in kinase reaction buffer containing [γ^{32}P]ATP and protein samples were then separated by 8% SDS–PAGE (Figure 3a). Y882F mutant neu proteins expressed in T882 cells have a dramatically reduced total phosphorylation content in this assay compared to oncogenic p185^{neu} (Figure 3a, lanes 1 and 2). Additionally, deletion of the carboxyl terminal 122 amino acids caused a similar reduction of total phosphotyrosine content (Figure 3a, lanes 3 and 4) of mutant neu proteins of 170–175 kDa, suggesting that the reduced autophosphorylation of Y882F could not be explained by decreased autophosphorylation of the three terminal autophosphorylation sites. In addition to decreased autophosphorylation of p185^{neu} receptors, substitution of tyrosine-882 resulted in decreased phosphorylation of exogenous substrates Histone III (Figure 3b). Differences were more pronounced between cells expressing Tneu and Y882F (Figure 3b, lanes 1 and 2) than between cells expressing TAPstop and Y882F/APstop (Figure 3b, lanes 3 and 4).

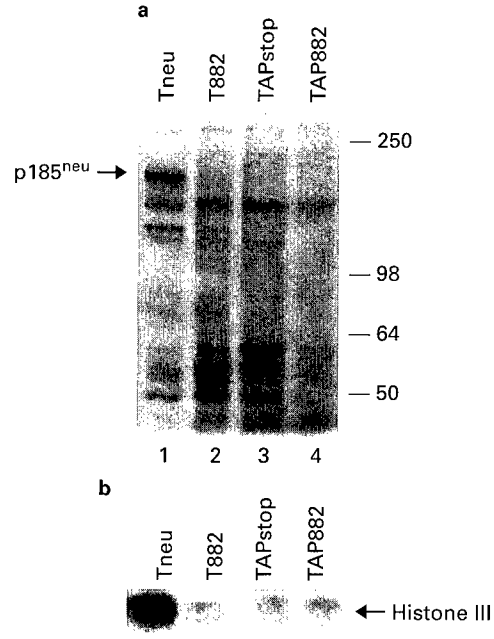

Figure 3 *In vitro* kinase assay. (**a**). Anti-neu immune complexes from various transfected cells were suspended in 50 ml of kinase reaction buffer containing 0.2 mCi [γ^{32}P]ATP at room temperature for 30 min. Protein samples were separated by 6% SDS–PAGE and analysed by autoradiography. Phosphorylation of exogenous substrate histone III by immune complexes from each cell line are shown in the bottom panel (15% SDS–PAGE) (**b**)

TAPstop also showed reduced kinase activity compared with the full length oncogenic Tneu. This result suggests that the conformational changes resulting from the deletion of the carboxyl terminal 122 amino acids influences substrate accessibility to the activation loop of the p185^{neu} kinase domain, although this may not be generalizable to all biological substrates. Decreased tyrosine *in vitro* kinase activity of p185^{neu} mutant receptor proteins was consistently observed in lysates derived from various Y882F mutant cells lines (T882, TAP882).

Y882F substitution inhibits EGF-induced cell proliferation of cell lines expressing EGFR/p185^{neu} chimeric receptors

To analyse mitogenic signaling in response to ligand, the intracellular domains of p185^{neu} and Y882F were independently fused with the extracellular domain of the EGF receptor (Figure 1). Using the MTT assay, we determined that the proliferation of cell lines expressing these chimeric receptors was EGF-dependent (Figure 4). We had previously shown that the EGF dose needed for a proliferative response to ligand-induced DNA synthesis (Qian *et al*., 1994) or cell proliferation (O'Rourke *et al*., 1997) was in the ng/ml range in fibroblasts and human transformed cell lines expressing EGFR only. In the presence of EGF (1–50 ng/ml), the growth of Er/882 cells expressing EGFR/Y882F chimeric receptors was less than those expressing EGFR/neu receptors (Er/neu cell line) (Figure 4). At a concentration of 100 ng/ml, EGF mediated an inhibitory effect on the growth of Er/neu cells, which we previously observed in fibroblasts expressing high levels of human EGFR (Qian *et al*., 1994). However, this high EGF dose had no similar influence on Er/882 cells, indicating that some regulatory mechanism was impaired by the Y882F mutation. As a negative control, a chimeric construct with all five tyrosine phosphorylation sites replaced was also transfected into fibroblasts, which, not unexpectedly, responded only modestly to EGF stimulation (data not shown).

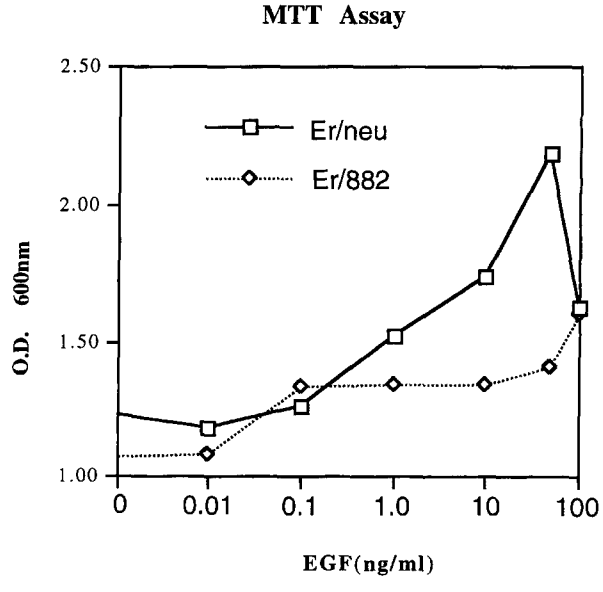

Figure 4 MTT assay: response of different cell lines to EGF treatment. On day 1, individual 96-well plates were seeded with 5000 cells/well of cells expressing EGFR/neu or EGFR/Y882F mutant receptors in 5% FBS medium and incubated overnight at 37°C. On day 2, the medium was changed to serum-free medium with different concentration of EGF and the microplates were incubated at 37°C for 48 h. On day 4, MTT was added (1 mg/ml) and after 4 h incubation at 37°C, cells were lysed by buffer containing SDS and DMSO at pH 4.7. The OD was then measured on day 5 at 600 nm using an ELISA reader

Substitution of Y882 inhibits transformation of cell lines expressing oncogenic p185^{neu} and EGFR/neu chimeric receptors. Anchorage-independent cell growth

The ability of murine fibroblasts to form colonies in soft agar was addressed in order to determine whether tyrosine-882 was relevant to the transforming activity of p185^{neu}. As is shown in Figure 5 (and Table 1), cells expressing Y882F were inhibited in their transforming

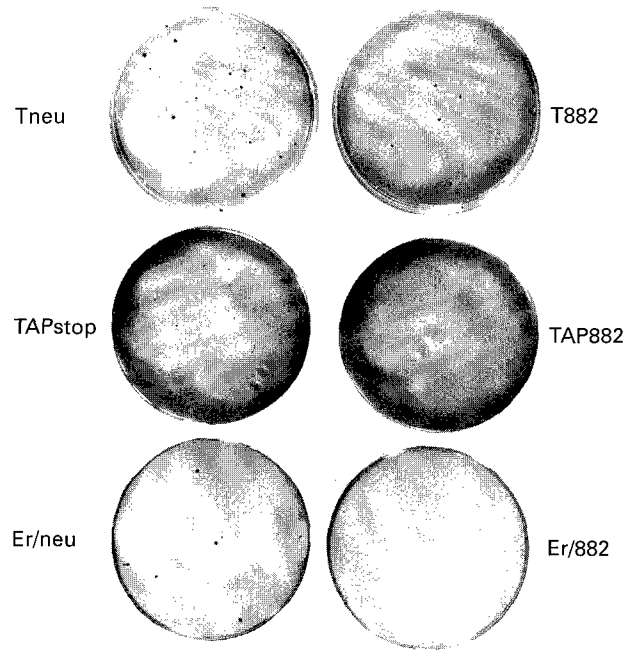

Figure 5 Colony growth in soft agar. Two hundred and fifty cells of each line were seeded in soft agar dishes and fed with 5% FBS-DMEM with (EGFR/neu and EGFR/882F) or without (Tneu, Y882F, TAPstop, and Y882F/APstop) EGF (10 ng/ml) twice a week for 3 weeks. Colonies were then visualized after staining with *p*-iodnitrotetrazolium violet (1 mg/ml) and counted

Table 1 Reduce of transforming activity in cells carrying Y882→F mutation

Cell lines	*Colonies on soft agar*[a] (mean±s.d.)
Tneu	52±4.9
T882	10±5.7
TAPstop	12±3.2
TAP882	1±0.6
Er/neu[b]	6±0.7
Er/882[b]	1±0.7

[a] Based on experiments performed in duplicate or triplicate. [b] Cells were treated with 10 ng/ml EGF as described in Materials and methods

efficiency *in vitro*. Elimination of the three carboxyl terminal autophosphorylation sites (TAPstop) resulted in reduced oncogenicity relative to full-length oncogenic Tneu which was further reduced by substituting tyrosine-882 with phenylalanine (Y882F/APstop). In order to assess the effect of tyrosine-882 substitution on ligand-dependent transformation, EGFR/neu and EGFR/882 chimeric proteins were expressed in murine fibroblasts. When these cells were examined for their growth capability, colony growth in soft agar of EGF-dependent fibroblasts was inhibited by the Y882F substitution in the p185^{neu} intracellular region. The *in vitro* transforming activity of Tneu and Y882F were also examined by an assay of focus formation in mass culture. In this study, significantly less foci were observed in Y882F-transfected cells (data not shown). These data confirmed that the Y882F mutant had a reduced transforming activity.

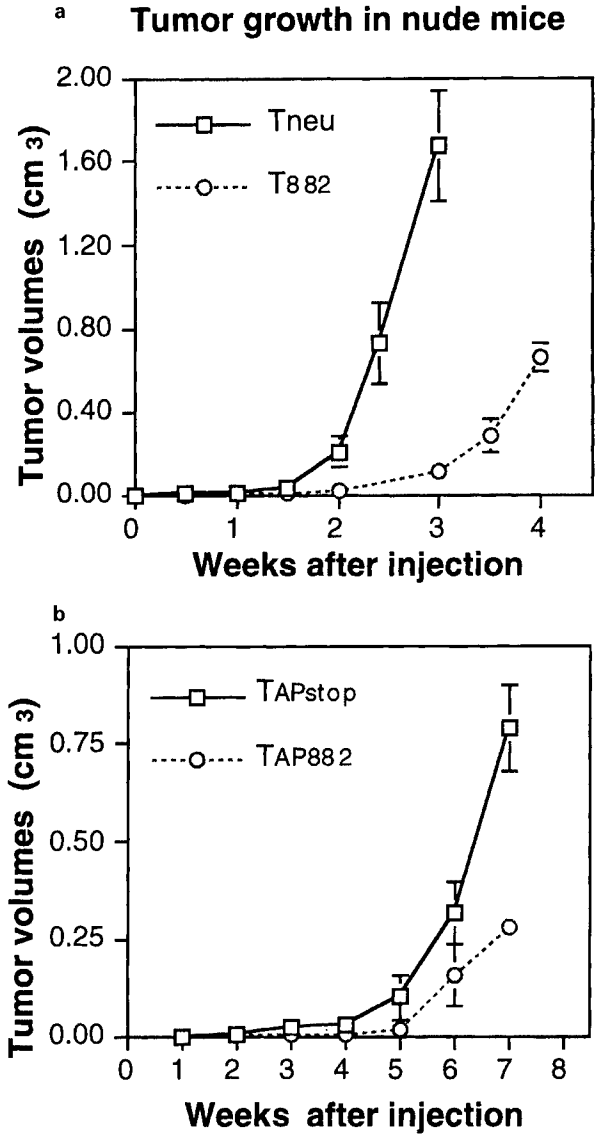

Figure 6 Comparison of tumor growth efficiency in nude mice. 1×10^6 cells from cell lines Tneu and T882 (**a**), TAPstop and TAP882 (**b**), were injected intradermally into BALB/C nude mice. Tumor volume (mean$\pm$s.d.) from a group of five injections of each cell line is plotted against time after injection

In vivo *tumorigenicity*

A comparison of tumor growth in athymic mice was then performed with the Y882F mutant cell lines. Oncogenic p185^{neu}-expressing fibroblasts (Tneu) form rapidly growing tumors when implanted subcutaneously in nude mice (Figure 6). Full-length Y882F mutant receptors are inhibited in their ability to mediate transformation *in vivo* (Figure 6a). Deletion of the carboxyl terminal three autophosphorylation sites in p185^{neu} proteins containing the activating transmembrane point mutation (TAPstop) resulted in a significant diminution of tumor forming efficiency (Figure 6b). Visible tumor growth did not occur in these animals until 4 weeks, which was beyond the time point that animals implanted with Tneu cells (Qian *et al*., 1996) were sacrificed from tumor burden. Again, substitution of tyrosine-882 was associated with further inhibition of transforming efficiency *in vivo* (Figure 6b).

Discussion

Dimerization of *erb*B family receptors results in activation of the enzymatic kinase by an incompletely understood intermolecular allosteric mechanism (Ullrich and Schlessinger, 1990; Wada *et al*., 1990), although an intramolecular mechanism contributing to kinase activation has not been excluded (Groenen *et al*., 1997). It is thought that contacts in the ectodomain in *erb*B family receptors initiate the formation of dimers thereby bringing the kinase domains in proximity with one another, which is required for catalytic activation (Weiner *et al*., 1989; Ullrich and Schlessinger, 1990). The use of dominant-negative mutant receptors has established that ectodomain interactions alone are sufficient for *erb*B family homo- and heterodimerization (Qian *et al*., 1994; O'Rourke *et al*., 1997), although cytoplasmic interactions determine receptor signaling outcome (Qian *et al*., 1995). Using co-immunoprecipitation experiments, truncated EGFRs lacking the extracellular region were shown to oligomerize with holo-EGFRs, resulting in constitutively phosphorylated receptors (Chantry, 1995). Deletion analysis showed that intracellular contacts within the kinase domain were most important in these interactions. Kinase domain oligomerization was also suggested to occur between truncated EGFRs and HER2/neu (Chantry, 1995), which was predicted by molecular modeling (Murali *et al*., 1996). The carboxyl terminal autophosphorylation sites in the EGFR (Y1086, Y1148 and Y1173) are not required for enzymatic kinase activation (Walton *et al*., 1990). The structural requirements and regulation of kinase domain interactions necessary for catalytic activation and transphosphorylation of substrates have not been defined.

Protein kinases share a high degree of homology in the catalytic domain, whether they are serine/threonine kinases or tyrosine kinases (Hanks *et al*., 1988). p185^{neu} and EGFR, members of the erbB family of type I RTKs, share 82% amino acid homology in the tyrosine kinase domain (Murali *et al*., 1996). In contrast, the carboxyl terminus of the cytoplasmic domain is not significantly conserved within tyrosine kinase receptor families. The kinase domain of *erb*B family kinases can be subdivided into an ATP-binding domain, an

activation loop, and a catalytic domain (Knighton *et al.*, 1991; Murali *et al.*, 1996). The ATP-binding domain is more conserved between kinase family members than the catalytic domain. Interestingly, the most variable region within the kinase domain is the activation loop where the autophosphorylation tyrosines are located. The activation loop may be critical for permitting access to different substrates and facilitating subsequent attachment.

Molecular modeling of the kinase domains of EGFR and p185^{neu} reveals that the orientation of the tyrosines within the activation loop, tyrosine-845 and tyrosine-882, respectively, are oriented differently, which might account for the different phenotypic consequences of substitution of these residues in the corresponding receptors (Murali *et al.*, 1996). It has been reported that Y845 is not required for either the tyrosine autophosphorylation of the mature 170 kDa EGFR, the initiation of EGF-induced DNA synthesis, or for EGF-dependent transformation of NIH3T3 cells (Gotoh *et al.*, 1992). However, mutations in charged residues adjacent to Y845 decrease the Vmax for receptor self-phosphorylation, suggesting that these residues stabilize the catalytic core of the kinase domain and are important for maximal self-phosphorylation activity of the kinase domain.

Although both tyrosines within the activation loop (Y845 in EGFR and Y882 in p185^{neu}) lie within a stretch of acidic residues (EGFR: EEKEY^{845}HAE; p185^{neu}: DETEY^{882}HAD), a feature observed with most tyrosine phosphorylation sites, the basic residue K^{843} in the EGFR loop alters this negatively charged structural feature. It has been reported this basic residue prevented peptides derived from the activation loop of EGFR from being phosphorylated by some protein tyrosine kinases (Cola *et al.*, 1989). However, in p185^{neu}, T^{880} at the corresponding position should not influence this structural feature, thus making the activation loop accessible for p185^{neu} or other tyrosine kinases capable of phosphorylating Y882. These differences between EGFR and p185^{neu} may account for the different biological effects of similar mutations on EGFR and p185^{neu} (Y845F and Y882F, respectively).

In our studies, substitution of tyrosine-882 in the full-length oncogenic p185^{neu} receptor did not appreciably alter the level of tyrosine phosphorylation of p185^{neu} *in vivo*. This observation supports the notion of cryptic or supplemental phosphotyrosine sites in EGFR and p185^{neu}. It has been reported that replacing all the identified tyrosine autophosphorylation sites in EGFR did not completely eliminate tyrosine phosphorylation of EGFR upon EGF stimulation, or EGF stimulation of mitogen-activated protein kinase activity (Decker, 1993). In our experiments, *in vivo* tyrosine phosphorylation was detected in the mutant with deletion of four autophosphorylation sites (Y882F/APstop). Although the *in vitro* kinase activity for p185^{neu} receptor self-phosphorylation and phosphorylation of exogenous substrate was decreased in all cell lines expressing Y882F, other kinases or signaling molecules could be involved to account for our inability to detect receptor phosphotyrosine content differences at this level of analysis.

Germline mutations in the tyrosine kinase domain of the RET proto-oncogene, in particular a Met->Thr substitution at position 918, are associated with the familial cancer syndrome multiple endocrine neoplasia (MEN) type 2B (Carlson *et al.*, 1994; Hofstra *et al.*, 1994). M918T has been shown to be an activating mutation by altering the substrate specificity in the tyrosine kinase domain of RET (Santoro *et al.*, 1995). A shift in the substrate specificity which would be transforming in certain tissues depending on the differentially expressed profile of available substrates capable of regulating RET catalytic activity. Position 918 in RET is located in the substrate binding domain of the activation loop, and is predicted by homology modeling to be approximately 15Å from a tyrosine analogous to Y882 in p185^{neu}.

Mutation of tyrosine-882 was associated with a diminution of transforming efficiency mediated by oncogenic p185^{neu} *in vitro* and *in vivo*. Upon ligand stimulation, the *erb*B family of RTKs transduce signals by creating: (1) an active form of tyrosine kinases which can phosphorylate signaling molecules including the receptor *per se*; (2) phosphorylated tyrosines as docking sites for SH2/SH3 domain containing proteins. It is unlikely that Y882 acts as one docking site, since there is no homology in this region to SH2 or SH3 binding motif and this site has never been shown able to associate with other molecules. Our data suggest that Y882 plays an important role in the transforming potential and tumorigenicity of oncogenic p185^{neu} by regulating the kinase activity of this receptor tyrosine kinase. By having a distinct phosphorylation status, Y882 could alter the accessibility of particular substrates to the kinase catalytic cleft. In support of this, we found that some proteins are not phosphorylated in the *in vitro* kinase assay as a result of the Y882F substitution (Figure 3), although the identities of these potential substrates are not known at present.

The corresponding residue in EGFR, Y845, has been found phosphorylated by c-*Src* in an EGF-dependent manner both *in vivo* and *in vitro* (Sato *et al.*, 1995). Further examination of the structural features of p185^{neu} and EGFR kinase domain activation may facilitate the understanding of cross-talking between signaling pathways and the development of site-specific inhibitors of *erb*B receptor catalytic function contributing to oncogenesis.

Materials and methods

Construction of mutants and expression vectors, and derivation of stably transfected cell lines

All the following mutant p185^{neu} cDNAs were derived from rat oncogenic neu cDNA (Tneu) containing a single mutation (V664E) in the transmembrane region. Briefly, the mutant Y882F was derived from Tneu by site-directed mutagenesis by substituting a phenylalanine for Tyrosine-882. The TAP/stop mutant was also made by site-directed mutagenesis by introducing a stop codon at position 1139, which was 122 amino acids from the carboxyl terminus (Mikami *et al.*, 1992). The T882F/APstop mutant was made by a subcloning strategy to generate both the Y882F substitution and carboxyl terminal deletion. To make a chimeric mutant of EGFr and TneuY882F, a 6.7 kb *Sal*I–*Xba*I fragment from an EGFR-neu expression vector, pSV2EGFR/neu (Lehvaslaiho *et al.*, 1989), was ligated to a 2.3 kb fragment containing the 3′ region of the Y882F mutant. All the mutant constructs were verified by DNA sequencing.

The wild type or mutant *neu* cDNAs were subcloned into the pMuLVLTRneo^r expression vector and then transfected into NR6 fibroblasts lacking endogenous EGFRs with neomycin selection to generate mutant neu-expressing subclones. The expression of mutant neu proteins in resultant colonies was confirmed by flow cytometry using an anti-p185^{neu} monoclonal antibody (mAb) 7.16.4 (Qian *et al.*, 1994). The resultant transfected cell lines were designated Tneu(T-2), T882, TAP/stop, TAP882, Er/neu and Er/882 (Figure 1). Using flow cytometric analysis, it was determinated that neu-derived proteins were expressed at comparable levels in Tneu and T882 cells, and in TAP/stop and TAP882 cells, although the latter two cell lines had higher surface expression levels than the Tneu and T882 cell lines. These transfected clones were maintained in Dulbecco's Modified Eagle's medium (DMEM) containing 5% fetal bovine serum (FBS, Hyclone).

Analysis of transforming characteristics

Anchorage-independent growth was determined by assessing the colony forming efficiency of cells suspended in soft agar (O'Rourke *et al.*, 1997). Cells (250–1000) were suspended in 0.18% agarose/5% FBS-DMEM and plated on 0.25% of basal agar in 60 mm tissue culture plates. 0.5 ml of DMEM medium (5% FBS, 20 mM HEPES, pH 7.5) was added to soft-agar cultures once a week for the duration of the experiment. Colonies (>0.3 mm) were visualized on day 21 for all cell lines after staining with *p*-iodnitrotetrazolium violet (1 mg/ml). Each cell line was examined in triplicate for three separate experiments. Number of colonies reported represented the mean of triplicate samples.

To analyse tumor growth in athymic mice, cells (1×10^6) of each line were suspended in 0.1 ml of PBS and injected intradermally in the mid-dorsum of NCR nude mice. PBS alone was also injected as a control. Animals used in this study were maintained in accordance with the guidelines of the Committee on Animals of the University of Pennsylvania and those prepared by the Committee on Care and Use of Laboratory Animals of the Institute of Laboratory Animal Resource. Tumor growth was monitored every 2–3 days up to 8 weeks. Tumor size was calculated by this formula: 3.14/6 × (length × width × thickness).

Antibodies

The monoclonal antibody (mAb) 7.16.4 against the ectodomain of p185^{neu} was produced from hybridoma cells as described previously (Drebin *et al.*, 1984). The polyclonal rabbit antiserum reactive with the neu intracellular domain, designated anti-Bacneu, was also utilized (Myers *et al.*, 1992). A monoclonal anti-phosphotyrosine antibody (pY20) was purchased from Santa Cruz, Biotechnology (Santa Cruz, CA).

In vitro *kinase assay*

Cells were plated in 100 mm culture dishes and the next day were washed twice in ice cold PBS and lysed in 1 ml of lysis buffer (50 mM Hepes, pH 7.5, 150 mM NaCl, 3% Brij-35, 2 mM EDTA, 0.02 mg/ml Aprotinin, 10% glycerol, 1.5 mM $MgCl_2$). Cell lysates were centrifuged at 20000 *g* for 15 min. Protein concentrations of cell lysate were measured with the Dc Protein Assay (Bio-Rad). Lysates that contained comparable amounts of neu-derived proteins (as determined by Western blotting) were used for immunoprecipitation with the anti-neu mAb, 7.16.4. 40 μl of 50% (vol/vol) protein A-sepharose were used to collect the immune complexes, which were then washed three times with wash buffer (50 mM HEPES, 150 mM NaCl, 0.1% Brij-35, 2 mM EDTA, 0.01 mg/ml Aprotinin, 0.03 mM Na_3VO_4). The pellets were suspended in 20 μl of 20 mM HEPES (pH 7.4, 5 mM $MnCl_2$, 0.1% Brij-35, 0.03 mM Na_3VO_4, 0.02 mg/ml Aprotinin) containing 5 μCi of [γ^{32}P]ATP, and incubated at room temperature for 30 min. The reaction were terminated by the addition of 3 × electrophoresis sample buffer containing 2 mM ATP. After incubation at 100°C for 3 min, samples were then analysed by SDS–PAGE.

MTT (3,(4,5-dimethylthiazol-2-yl)2,5-diphenyl-tetrazolium bromide) assay of cell proliferation

The MTT assay for measuring cell growth has been reported previously (Hansen *et al.*, 1989). Briefly, cells (5000) of each cell line were seeded in 96-well plates overnight in DMEM containing 5% FBS. Cells were starved in ITS-DMEM for 48 h, then cultured in 100 μl of the same medium plus various concentrations of EGF for 48 h. 25 μl of MTT solution (5 mg/ml in PBS) were added to each well, and after 2 h of incubation at 37°C, 100 microliters of the extraction buffer (20% w/v of SDS, 50% *N*,*N*-dimethyl formamide, pH 4.7) was added. After an overnight incubation at 37°C, the optical density at 600 nm were measured using an ELISA reader. Each value represented a mean of four samples.

Acknowledgements
We thank Dr Kari Alitalo for the EGFR-neu expression vector, pSV2EGFR/neu. This work was supported by grants awarded to MIG by CaPCURE, NIH, and the US Army.

References

Carlson KM, Dou S, Chi D, Scavarda N, Toshima K, Jackson CE, Wells SJ, Goodfellow PJ and Donis KH. (1994). *Proc. Natl. Acad. Sci. USA*, **91,** 1579–1583.
Carraway KL and Cantley LC. (1994). *Cell*, **78,** 5–8.
Carter TH and Kung HJ. (1994). *Crit. Rev. Oncog.*, **5,** 389–428.
Chantry A. (1995). *J. Biol. Chem.*, **270,** 3068–3073.
Cola C, Brunati AM, Borin G, Ruzza P, Calderan A, De CR and Pinna LA. (1989). *Biochim. Biophys. Acta*, **1012,** 191–195.
Decker SJ. (1993). *J. Biol. Chem.*, **268,** 9176–9179.
Dougall WC, Qian X, Peterson NC, Miller MJ, Samanta A and Greene MI. (1994). *Oncogene*, **9,** 2109–2123.
Drebin JA, Stern DF, Link VC, Weinberg RA and Greene MI. (1984). *Nature*, **312,** 545–548.
Ellis L, Clauser E, Morgan DO, Edery M, Roth RA and Rutter WJ. (1986). *Cell*, **45,** 721–732.
Fantl WJ, Escobedo JA and Williams LT. (1989). *Mol. Cell. Biol.*, **9,** 4473–4478.
Gotoh N, Tojo A, Hino M, Yazaki Y and Shibuya M. (1992). *Biochem. Biophys. Res. Commun.*, **186,** 768–774.
Groenen LC, Walker F, Burgess AW and Treutlein HR. (1997). *Biochemistry*, **36,** 3826–3836.
Hanks SK, Quinn AM, Hunter T. (1988). *Science*, **241,** 42–52.
Hansen MB, Nielsen SE and Berg K. (1989). *J. Immunol. Methods*, **119,** 203–210.
Heldin CH. (1995). *Cell*, **80,** 213–223.

Hofstra RM, Landsvater RM, Ceccherini I, Stulp RP, Stelwagen T, Luo Y, Pasini B, Hoppener JW, van AH, Romeo G, Lips CJM and Buys CHCM. (1994). *Nature,* **367,** 375–376.

Kiyokawa N, Yan DH, Brown ME and Hung MC. (1995). *Proc. Natl. Acad. Sci. USA,* **92,** 1092–1096.

Kmiecik TE and Shalloway D. (1987). *Cell,* **49,** 65–73.

Knighton DR, Zheng JH, Ten Eyck LF, Ashford VA, Xuong NH, Taylor SS and Sowadski JM. (1991). *Science,* **253,** 407–414.

Lehvaslaiho H, Lehtola L, Sistonen L and Alitalo K. (1989). *EMBO. J.,* **8,** 159–166.

Li N, Schlessinger J and Margolis B. (1994). *Oncogene,* **9,** 3457–3465.

Mikami Y, Davis JG, Dobashi K, Dougall WC, Myers JN, Brown VI and Greene MI. (1992). *Proc. Natl. Acad. Sci. USA,* **89,** 7335–7339.

Morrison DK, Kaplan DR, Rhee SG and Williams LT. (1990). *Mol. Cell. Biol.,* **10,** 2359–2366.

Murali R, Brennan PJ, Kieber ET and Greene MI. (1996). *Proc. Natl. Acad. Sci. USA,* **93,** 6252–6257.

Myers JN, LeVea CM, Smith JE, Kallen RG, Tung L and Greene MI. (1992). *Receptor,* **2,** 1–16.

O'Rourke DM, Qian X, Zhang H-T, Davis JG, Nute E, Meinkoth J and Greene MI. (1997). *Proc. Natl. Acad. Sci. USA,* **94,** 3250–3255.

Piwnica WH, Saunders KB, Roberts TM, Smith AE and Cheng SH. (1987). *Cell,* **49,** 75–82.

Pruss RM and Herschman HR. (1977). *Proc. Natl. Acad. Sci. USA,* **74,** 3918–3921.

Qian X, Dougall WC, Hellman ME and Greene MI. (1994). *Oncogene,* **9,** 1507–1514.

Qian X, Dougall WC, Fei Z and Greene MI. (1995). *Oncogene,* **10,** 211–219.

Qian X, O'Rourke DM, Zhao H and Greene MI. (1996). *Oncogene,* **13,** 2149–2157.

Roussel MF, Shurtleff SA, Downing JR and Sherr CJ. (1990). *Proc. Natl. Acad. Sci. USA,* **87,** 6738–6742.

Samanta A, LeVea CM, Dougall WC, Qian X and Greene MI. (1994). *Proc. Natl. Acad. Sci. USA,* **91,** 1711–1715.

Santoro M, Carlomagno F, Romano A, Bottaro DP, Dathan NA, Grieco M, Fusco A, Vecchio G, Matoskova B, Kraus MH and Di Fiore PP. (1995). *Science,* **267,** 381–383.

Sato K, Sato A, Aoto M and Fukami Y. (1995). *Biochem. Biophys. Res. Commun.,* **215,** 1078–1087.

Timms JF, Noble ME and Gregoriou M. (1995). *Biochem. J.,* **308,** 219–229.

Ullrich A and Schlessinger J. (1990). *Cell,* **61,** 203–212.

Van der Geer P and Hunter T. (1991). *Mol. Cell. Biol.,* **11,** 4698–4709.

Wada T, Qian XL and Greene MI. (1990). *Cell,* **61,** 1339–1347.

Walton GM, Chen WS, Rosenfeld MG and Gill GN. (1990). *J. Biol. Chem.,* **265,** 1750–1754.

Weiner DB, Liu J, Cohen JA, Williams WV and Greene MI. (1989). *Nature,* **339,** 230–231.

Weinmaster G, Zoller MJ, Smith M, Hinze E and Pawson T. (1984). *Cell,* **37,** 559–568.

Proc. Natl. Acad. Sci. USA
Vol. 95, pp. 10842–10847, September 1998
Medical Sciences

Conversion of a radioresistant phenotype to a more sensitive one by disabling erbB receptor signaling in human cancer cells

(apoptosis/epidermal growth factor receptor/glioblastoma/p185neu/*trans*-receptor inhibition)

DONALD M. O'ROURKE*†‡§, GARY D. KAO¶, NATASHA SINGH†, BYEONG-WOO PARK†, RUTH J. MUSCHEL†¶, CHUAN-JIN WU†, AND MARK I. GREENE†‡

Departments of *Neurosurgery, †Pathology and Laboratory Medicine, ¶Radiation Oncology and ‡Cancer Center, University of Pennsylvania School of Medicine, Philadelphia, PA 19104

Communicated by James M. Sprague, University of Pennsylvania School of Medicine, Philadelphia, PA, June 12, 1998 (received for review March 6, 1998)

ABSTRACT **Inhibition of cell growth and transformation can be achieved in transformed glial cells by disabling erbB receptor signaling. However, recent evidence indicates that the induction of apoptosis may underlie successful therapy of human cancers. In these studies, we examined whether disabling oncoproteins of the erbB receptor family would sensitize transformed human glial cells to the induction of genomic damage by γ-irradiation. Radioresistant human glioblastoma cells in which erbB receptor signaling was inhibited exhibited increased growth arrest and apoptosis in response to DNA damage. Apoptosis was observed after radiation in human glioma cells containing either a wild-type or mutated p53 gene product and suggested that both p53-dependent and -independent mechanisms may be responsible for the more radiosensitive phenotype. Because cells exhibiting increased radiation-induced apoptosis were also capable of growth arrest in serum-deprived conditions and in response to DNA damage, apoptotic cell death was not induced simply as a result of impaired growth arrest pathways. Notably, inhibition of erbB signaling was a more potent stimulus for the induction of apoptosis than prolonged serum deprivation. Proximal receptor interactions between erbB receptor members thus influence cell cycle checkpoint pathways activated in response to DNA damage. Disabling erbB receptors may improve the response to γ-irradiation and other cytotoxic therapies, and this approach suggests that present anticancer strategies could be optimized.**

The molecular parameters that determine how a cell becomes more or less sensitive to DNA damage induced by radiation or chemotherapeutic agents are poorly understood. Status of cell cycle checkpoint-signaling pathways has been argued to be an important determinant of the response to DNA damage, and mutations in checkpoint components are prevalent in human cancers (reviewed in refs. 1 and 2). A recently introduced paradigm suggests that tumor cells exhibit growth arrest or apoptosis in response to cytotoxic therapies depending on the functional state of checkpoint pathways and that radiation-induced apoptosis may result from impaired growth arrest pathways (3). Similarly, in other systems using nontransformed cells, incomplete mechanisms of DNA repair, occurring during checkpoint phase delay, increase the tendency to apoptosis (4).

Human glioblastomas exhibit many genetic alterations, including amplification and/or mutation of the gene encoding the epidermal growth factor receptor (EGFR) (reviewed in refs. 5 and 6) in some cases resulting in expression of a constitutively activated EGF receptor kinase (7–9). We have shown that expression of a *trans*-receptor inhibitor of the EGFR, derived from the ectodomain of the p185neu oncogene (T691stop neu), forms heterodimers with both full-length EGFR and a constitutively activated extracellular-deleted mutant EGFR form (ΔEGFR) commonly observed in human glial tumors, particularly those of higher pathologic grade (9, 10). Cell growth and transformation of EGFR-positive or EGFR/ΔEGFR-coexpressing human glioma cells is inhibited by kinase-deficient deletion mutants of p185neu (9, 10). The surface-localized T691stop neu mutant/EGFR heterodimeric receptor complex has decreased affinity for the EGF ligand, impaired internalization kinetics, reduced phosphotyrosine content, and diminished enzymatic kinase activity relative to full-length EGFR and ΔEGFR homodimeric complexes (9, 10).

The specific pathways mediating oncogenic transformation in EGFR positive-transformed human cells have not been characterized completely. Naturally occurring ΔEGFR oncoproteins may increase constitutive activity of a Grb2/Shc/Ras pathway (11) and signaling through phosphatidyl inositol-3 (PI-3) kinases (12), presumably by binding to distinct adaptor proteins (13). Particular mitogen-activated protein kinases, such as those of the c-jun amino terminal kinase family, may be constitutively activated by ligand-independent oncogenic ΔEGF receptors (14). Although holo-EGFRs have been found to be weakly transforming only in a ligand-dependent manner at high levels of receptor expression in fibroblasts, many human tumors exhibit elevated levels of EGFR and this may contribute to unregulated kinase activity in transformed cells (15, 16).

We sought to address whether specific inhibition of signaling through the overexpressed EGFR in radioresistant human glioma cells would alter the physiologic response of these cells to the induction of genomic damage. γ-irradiation combined with erbB receptor inhibition resulted in a greater degree of radiation-induced growth arrest and apoptosis in cancer cells normally resistant to ionizing radiation. These results have implication for the design of receptor-specific agents capable of sensitizing cells to cytotoxic therapies and suggest that erbB receptor-specific inhibition combined with cytotoxic treatments may improve the response to anticancer regimens.

MATERIALS AND METHODS

Vector Construction. The derivation of the T691stop neu mutant receptor construct has been detailed previously (10).

The publication costs of this article were defrayed in part by page charge payment. This article must therefore be hereby marked "*advertisement*" in accordance with 18 U.S.C. §1734 solely to indicate this fact.

Abbreviations: DAPI, 4′,6-diamidino-2-phenylindole dihydrochloride hydrate; EGFR, epidermal growth factor receptor; RT, radiation treatment.

§To whom reprint requests should be addressed. e-mail: orourked@mail.med.upenn.edu.

Maintenance of Cells and Development of Stably Transfected Cell Lines. The U87MG human glioblastoma cell line was obtained from Webster Cavenee (Ludwig Cancer Institute, San Diego). U373MG human glioma cells, originally isolated from a human anaplastic astrocytoma, were obtained through the American Type Tissue Collection (ATCC; Rockville, MD). Maintenance of cells lines, methods for deriving subclones expressing p185neu-derived proteins and transfection procedures have been described previously (9, 10).

Flow Cytometric Analysis of Cell Cycle Distribution. Cells were stained for flow cytometry by sequential treatment with 0.003% trypsin solution, followed by 0.05% trypsin inhibitor, 0.01% RNase A solution, and then 0.0416% propidium iodide and 5 mM spermine tetrachloride solution. Each treatment was performed for 10 min with continuous shaking at room temperature. All reagents were ordered from Sigma. Cell cycle analysis was performed within 2 h of staining on a Becton Dickinson FACScan flow cytometer. Ten thousand events were collected for each sample and the data analyzed by using the MODFIT cell cycle analysis program (Becton Dickinson, version 2.0).

Nuclei Staining and Morphologic Analysis of Apoptosis. Cells were plated onto coverslips for at least 12 h before irradiation. Irradiation was performed in conditions identical to the colony formation assays. Coverslips were then washed twice with PBS at the indicated times and fixed in 50:50 mix of ice-cold methanol/acetone for 1 min. Coverslips were subsequently stained with 4′,6-diamidino-2-phenylindole dihydrochloride hydrate (DAPI) (Sigma) at a concentration of 0.1–.25 μg/ml in PBS. Inter-observer consistency in apoptosis counts was confirmed with terminal deoxynucleotidyl transferase-mediated dUTP nick end labeling-staining and by three independent observers.

Cell counts were performed within 30 min of staining, and photographs were taken on a Zeiss Axioplan epifluorescence microscope. At least three independent fields of 100 cells were counted for each sample.

Colony Formation Assay. Cell survival after irradiation was assessed by the colony formation assay. The number of cells to be plated was calculated to form 20–200 colonies per dish at each radiation dose and plated into 10-cm culture dishes (Fisher Scientific). By using a J. L. Shepherd (San Fernando, CA) model 30 Mark I Cesium-137 irradiator, 12.8 Gy/min of irradiation was delivered to the cells on a rotating platform to ensure uniform dosing. Cells were incubated after irradiation at 37°C with 5% CO_2 for 7–10 days and then stained with crystal violet. Colonies containing >50 cells were counted under a dissecting microscope. The surviving fraction is the ratio of the number of colonies formed to the number of cells plated and was corrected for plating efficiency. At least three cell concentrations were used for each radiation dose.

Western Blotting. For each time point, 10^5 cells per 6-cm plate were harvested by lysis in 400 μl of sample buffer (10% glycerol/2% SDS/100 mM DTT/50 mM Tris, pH 6.8). Thirty microliters of each lysate was loaded per lane and separated by electrophoresis on a 15% SDS-polyacrylamide gel before overnight transfer to a nitrocellulose membrane (Bio-Rad). Membranes were probed with mouse anti-human p53 mAb (NeoMarkers, Fremont, CA), followed by goat anti-mouse Ig secondary antibody coupled to horseradish peroxidase (Amersham). To reduce background antibody binding, incubation with secondary antibody in 2.5% powdered milk in PBS was performed. Detection was performed by enhanced chemiluminescence (ECL, Amersham). Relative levels of p53 expression were determined by scanning the blots using a scanning densitometer (Molecular Dynamics).

Antibodies. The mAb 7.16.4 reactive against the p185neu ectodomain has been described (10). Polyclonal antibodies reactive with p53 and p21 were obtained from NeoMarkers. Antibodies reactive with bcl-2, bax, and bcl-x_L were obtained from Oncogene Science.

RESULTS

Cell Cycle Distribution of Cycling Human Glioblastoma Cells Treated with γ-Irradiation: Effects of Disabling erbB Signaling on Growth Arrest. For both U87MG and U87/T691 cells, prolonged serum starvation alone (72–100 h) led to increased accumulation of cells in G_0/G_1, with modest reductions in both the S and G_2/M populations. U87/T691 cells exhibited a higher G_0/G_1 fraction than parental U87MG cells either in the presence of serum (Fig. 1 *A* and *C*) or after prolonged serum deprivation (data not shown). The relative increase in growth arrest induced by expression of the T691stop neu mutant receptor in U87MG cells was thus not overcome by growth in full serum.

Induction of growth arrest by exposure of asynchronously cycling transformed human glial cell populations to γ-irradiation was greater than that induced by prolonged serum deprivation alone. In both U87MG and U87/T691 cells, irradiation of cells grown under full serum growth conditions caused robust increases in G_0/G_1 and G_2/M, and a decrease in the percentage of cells in S phase, as determined by flow cytometric staining for DNA content (Fig. 1 *B* and *D*). Reduction of the S phase fraction and accumulation of cells in G_2 is characteristic of cells sustaining DNA damage (4, 17). The data in Fig. 1 depict a representative experiment of cells analyzed 72 h after γ-irradiation. Earlier time points indicated similar trends, but analysis 72 h after irradiation was chosen to be consistent with subsequent experiments (see below). An analysis of three independent experiments revealed the following changes in cell cycle distribution [mean percent of cells ± SEM; ± radiation treatment (RT)]: (*i*) U87MG parental cells: G_0/G_1: 26 ± 2.8, +RT 51.5 ± 2.1; S: 66 ± 4.2, +RT 21 ± 2.8; G_2/M: 8 ± 1.4, +RT 28.5 ± 0.7; (*ii*) U87/T691 cells: G_0/G_1: 34.5 ± 4.9, +RT 71 ± 7.1; S: 57.5 ± 4.9, +RT 16 ± 4.2; G_2/M: 7.5 ± 0.7, +RT 12.5 ± 3.5. U87/T691 cells exhibited a higher G_0/G_1 fraction and reduced S and G_2/M

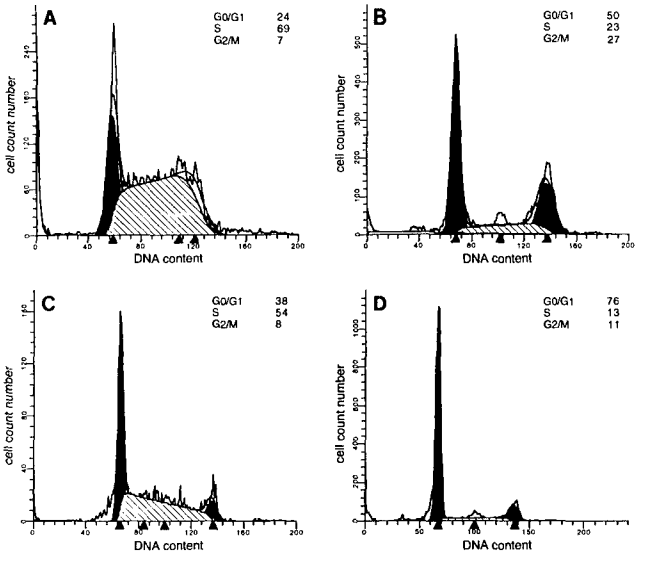

FIG. 1. Cell cycle distribution of human glioblastoma cells with or without radiation treatment in 10% serum. Parental U87MG cells (*A* and *B*) and U87/T691 transfectants (*C* and *D*) were studied. Cells were plated in 60-mm dishes and allowed to attach before either being γ-irradiated (10 Gy) (*B* and *D*) or mock-irradiated (*A* and *C*). After 72 h, cells were than analyzed by flow cytometry after propidium iodide staining. The distributions of cells according to DNA content are indicated in each panel. The data shown in this experiment are representative of four independent experiments.

populations when compared with parental glioblastoma cells when grown asynchronously in culture either with or without radiation treatment, and the largest difference was in the G_0/G_1 population. Radiation-induced increases in the G_2/M fraction were seen in both U87MG and U87/T691 cells, although to a greater degree in parental U87MG cells. Serum deprivation and radiation treatment in these cell populations was not additive and did not appreciably alter the cell cycle distributions in either cell line from that observed with radiation treatment in full serum (data not shown). Thus, disabling EGFR-mediated signaling appears to induce a growth arrest by a mechanism distinct from that observed with prolonged serum deprivation.

***Trans*-Receptor Inhibition Sensitizes Human Glioblastoma Cells to Radiation-Induced Apoptosis.** Human glioblastoma cells have been shown to be especially resistant to radiation treatment both experimentally and clinically. EGFR overexpression and/or mutation has been correlated with particularly aggressive human glial tumors and oncogenicity was suggested to be caused by reduced apoptosis *in vitro* and *in vivo* (18). We examined whether inhibition of EGFR-mediated signaling in human glioblastoma cells by the T691stop neu mutant receptor could sensitize cells to apoptotic cell death.

With prolonged serum deprivation, we observed only 0–1% apoptosis in U87MG parental cells by either 4′-6-diamidino-2-phenylindole (DAPI) staining or terminal deoxynucleotidyl transferase-mediated dUTP nick end-labeling staining, which was less than that observed in other studies (18). We found that U87MG-derived cells do not exhibit a sub-G_0 peak by flow cytometric analysis after propidium iodide staining under conditions causing apoptosis, which is in agreement with others (19). Expression of the T691stop neu inhibitor in U87MG cells resulted in only 0–2% apoptosis with prolonged serum deprivation as determined by immunohistochemical identification of apoptotic nuclei with DAPI.

Apoptosis was maximal in repeated studies at 72 h, and this time point was selected for all additional experiments. Expression of the T691stop neu protein in the U87MG cell background increased the level of radiation-induced apoptosis to 23 ± 7.9% (mean ± SEM) at 72 h in four independent experiments in full growth media (Fig. 2*A*). Prolonged serum deprivation combined with radiation resulted in 33 ± 10.6% apoptosis in U87/T691 cells and in 11 ± 1.5% apoptosis in parental U87MG cells, a comparable increase in both populations above that observed with radiation of cells in full growth media. These data indicate that T691stop neu expression induced greater apoptosis than prolonged serum deprivation in U87MG cells. The morphological changes of nuclear blebbing and fragmentation characteristic of apoptosis are shown by immunohistochemical analysis of U87MG-derived cultured cells stained with DAPI (Fig. 3*A–D*). The apoptotic indices represent an underrepresentation of total cell death after radiation in U87/T691 cells because we were unable to examine floating cells immunohistochemically.

Clonogenic Survival of Irradiated Human Glioblastoma Cells. We measured the number of cells that escape growth arrest or death and are able to go on to form a colony, an assay commonly used to determine radiosensitivity. In certain cases, clonogenic growth assays have not correlated with sensitivity to radiation or chemotherapy (3), presumably because the fate of the dead or stably arrested cells is not determined in this assay (20). As shown in Fig. 4, U87/T691 cells exhibited increased sensitivity to radiation across a range of radiation concentrations (2–10 Gy). U87/T691 cells were approximately one-half log more sensitive to radiation than their untransfected parental counterparts at all radiation doses tested. These data suggest a correlation between increases in growth arrest and apoptosis and increased radiosensitivity after inhibition of erbB signaling in irradiated human glioma cells. We

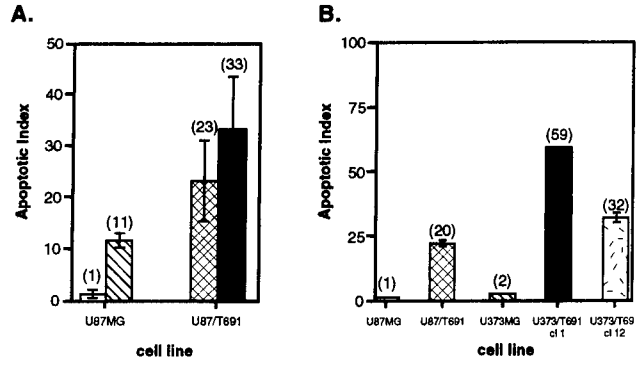

FIG. 2. Determination of apoptosis and clonogenic survival after γ-irradiation of human glioblastoma cells. (*A*) Cells were plated and allowed to attach before being exposed to γ-irradiation (10 Gy) in 10% serum or serum-free media. After 72 h, quantitation of apoptosis was conducted by two independent observers. The apoptotic index is the percentage of apoptotic cells with morphologic evidence of apoptosis as determined by staining of nuclei with DAPI. Results presented are mean ± SEM of four independent experiments, and the mean is indicated in parentheses. U87MG cells were grown in 10% serum (□) or serum-free media (▨) and U87/T691 cells were grown in 10% serum (▩) or serum-free media (■). (*B*) U87MG and U373MG human glioma cells and derivatives were stained with DAPI and analyzed for apoptotic morphology 72 h after γ-irradiation. The mean is indicated in parentheses, and the index shown in this representative experiment is mean ± SD. These results are representative of two additional experiments. Apoptotic indices were felt to be an underestimate because floating cells could not be assayed by this technique.

confirmed these results by analysis of additional T691stop neu-expressing subclones.

Relationship of Radiation Sensitivity of Human Glioblastoma Cells to p53 Status. U87MG cells and their derivatives contain wild-type p53 and p21 proteins. p53 status has been shown to influence the response to ionizing radiation in a number of transformed and nontransformed cell types (21–23). Western analysis of cell lysates obtained at distinct time points after radiation treatment indicated persistent increases in p53 protein levels detected at all times between 6 and 72 h after radiation in both U87MG and their T691stop neu-transfected derivatives (Fig. 5). The zero time point indicates cells which were γ-irradiated and immediately lysed for analysis. p53 densities were comparable at this time point to mock-irradiated, cycling cells (data not shown). We observed a 10-fold increase in p53 density 12 h after radiation in U87/T691 cells, as compared with only 1.5- to 3-fold increases in both U87MG cells and U87/T691 cells at all other time points examined. This trend was consistently observed (four experiments), and was seen in U87/T691 cells as early as 6 h after radiation in some experiments, and suggests that p53-dependent signaling pathways may be more efficiently activated by disabling the EGFR in the presence of genomic damage. Alterations in p53-regulated checkpoint proteins have been observed 12 h after the induction of genomic damage by γ-irradiation (24) Growth inhibition and differentiation of human breast cancer cells after ligation of erbB receptors has been associated with activation of a p53-dependent pathway (25).

p21 was induced in both U87MG and U87/T691 cells after radiation treatment, with highest levels seen 24 h after radiation exposure in both cell lines. In both U87MG cells and U87/T691 cells, p21 protein density 6–24 h after radiation was comparable (data not shown). Although others (18) have suggested that up-regulation of bcl-x_L is associated with reduced apoptosis in human glioma cells, we detected no changes in bcl-x_L protein expression after radiation in either U87MG or U87/T691 cells. Both constitutive and radiation-induced bcl-x_L levels were comparable in U87MG and U87/T691 cells

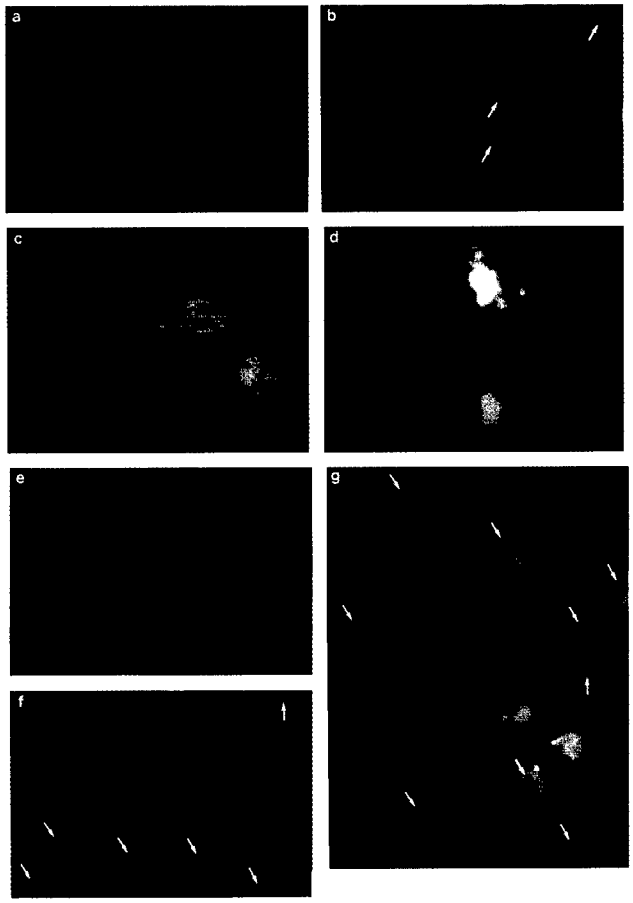

FIG. 3. Morphologic assessment of apoptosis in human glioma cells after γ-irradiation. All cells were stained with DAPI 72 h after being exposed to γ-irradiation. Parental U87MG cells (*a* and *c*) and U87/T691 clonal derivatives (*b* and *d*) are depicted at two magnifications. Nuclei exhibiting apoptotic morphology are indicated by the arrows. Parental U373MG cells (*e*) and U373/T691 subclones 1 (*g*) and 12 (*f*) are shown after staining with DAPI.

(data not shown). Examination of bax and bcl-2 protein levels did not reveal differences between glioblastoma cells and their inhibited subclones.

Apoptosis in p53-Mutated Human Glioblastoma Cells. U373MG human glioma cells contain a mutated p53 gene product, have undetectable levels of the p21 protein (26, 27), and display a comparable elevation of surface EGFR to U87MG cells by flow cytometric analysis. These cells were used to determine whether the observed apoptosis after inhibition of EGFR-mediated signaling and γ-irradiation was dependent on a wild-type p53 protein. U373MG cells exhibited increases in levels of a mutated p53 protein after γ-irradiation but do not express p21 constitutively or after radiation treatment (data not shown, ref. 27).

We expressed the truncated T691stop neu protein in U373MG glioma cells and confirmed expression at levels comparable with U87/T691 cells in four U373/T691 subclones by metabolic labeling and flow cytometic analysis (data not shown). Surface levels for the T691stop neu mutant receptor was equivalent in U87/T691, U373/T691 cl 1 and U373/T691 cl 12 subclones, and two additional T691stop neu-expressing U373MG derivatives. U373/T691 subclones were capable of growth arrest in low serum and displayed a lawn of confluent cells without the development of morphologically transformed foci *in vitro* (data not shown), indicating that wild-type p53 and p21 proteins were not required to arrest growth or inhibit transformation of glioma cells in which erbB signaling was disabled.

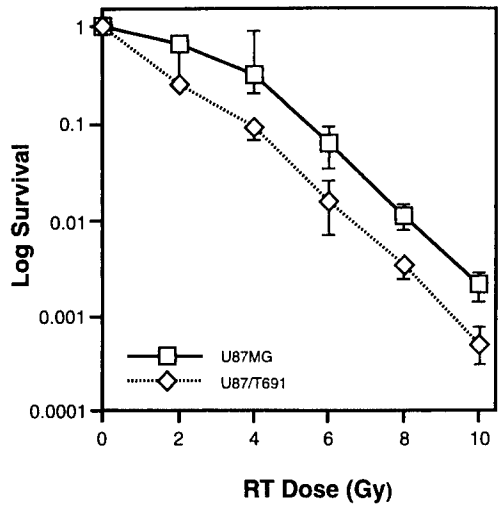

FIG. 4. Clonogenic survival after irradiation. Cells were plated and γ-irradiated with varying doses of radiation followed by incubation for 7–10 days at 37°C with 5% CO_2. Colonies were then stained and those with >50 cells were counted under a dissecting microscope. The log survival was then determined by calculating the ratio of the number of colonies formed to the number of cells plated, after correcting for plating efficiency. Similar experiments were performed three times.

U373/T691 cl 1 and U373/T691 cl 12 subclones exhibited increased levels of apoptosis over parental U373MG cells after radiation (Figs. 2*B* and 3*E-G*). In the representative experiment shown, two U373/T691 subclones exhibited 32% and 59% apoptosis, respectively, 72 h after γ-irradiation, compared with 2% apoptosis in parental U373MG cells and 20% apoptosis in U87/T691 cells. Disabling EGFR signaling by expression of T691stop neu in two distinct human glioma cell lines containing differences in p53 and p21 status resulted in increased radiation-induced apoptosis in each case. Sensitization of human glioblastoma cells to genomic damage can thus occur in the absence of wild-type p53 and p21 proteins. Taken together, these data suggest that both p53-dependent (Fig. 5) and p53-independent pathways may mediate sensitization to cell death induced by a combination of *trans*-receptor inhibition and genomic damage. Of note, human glioblastoma cells in which EGFR signaling is disabled do not appear to be more sensitive to either prolonged serum deprivation or tumor necrosis factor α-mediated cell death than parental cells (data not shown).

DISCUSSION

Specific inhibition of EGFR signaling inhibits cell growth and transformation and also sensitizes radioresistant human glioma cells to radiation-induced genomic damage. Glioblastoma cells expressing a *trans*-dominant p185neu-derived mutant receptor exhibit a greater G_1 phase arrest and higher levels of apoptosis after radiation than their parental counterparts. In

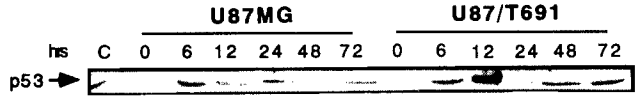

FIG. 5. Analysis of p53 induction in human glioblastoma cells after γ-irradiation. 10^5 U87MG and U87/T691 cells containing a wild-type p53 gene product were plated and γ-irradiated (10 Gy) after attachment overnight. Lysates were then taken at the indicated times after radiation, subjected to SDS/PAGE and immunoblotted with an antibody reactive with p53. Control (C) cells were MCF-7 breast cancer cells containing immunoreactive p53 protein. We consistently demonstrated more robust induction of the p53 protein at 12 h after γ-irradiation in U87/T691 subclones on four independent occasions.

mammalian fibroblasts (28) and in specialized neuronal cells (29, 30), serum or growth factor deprivation can lead to apoptosis under particular conditions. Prolonged serum deprivation alone did not induce apoptosis in human glioblastoma cells in these studies. DNA damage combined with either disabling of erbB receptor signaling or serum deprivation was required to induce apoptosis. Apoptosis was induced by radiation in 23% of U87MG derivatives and in 32–59% of U373MG-derived subclones in which EGFR was disabled (compared with only 1–2% in parental cells) in full growth media, indicating that inhibition of EGFR signaling by *trans*-receptor inhibition could not be overcome by growth in serum. Serum deprivation combined with radiation damage increased observed levels of apoptosis in both parental U87MG cells and T691stop neu-expressing human glioblastoma derivatives to the same degree. Notably, after DNA damage, the apoptosis observed by disabling erbB receptor signaling at the cell surface was greater than that seen with serum deprivation. Counterintuitively, these data also reveal that growth-inhibited glioma cells are more sensitive to radiation-induced cell death. Induction of an inhibitory pathway occurring as a result of EGFR inhibition may thus sensitize cancer cells to radiation-induced growth arrest and/or cell death.

Resistance of γ-irradiated cells is affected by the functional state of distinct oncogenes. Expression of oncogenic Ras or Raf diminishes radiosensitivity in NIH 3T3 cells (31–34) and expression of the Ras^H plus either c- or v-myc oncogenes conferred resistance to rat embryo fibroblasts exposed to γ-irradiation (35). It is also true that expression of various oncogenes can sensitize cells to apoptosis, upon exposure to low serum (28) or to anticancer agents (21, 36). Division delay occurring in both the G_1 and G_2 phases of the cell cycle is influenced by the expression of dominant oncoproteins such as H-ras (17). Expression of a wild-type p53 protein has been associated with decreased survival after γ-irradiation, due to the induction of a higher fraction of apoptosis over cells containing a mutated p53 protein (21, 22). However, tumor cells containing a mutated p53 protein (37) and proliferating lymphoid cells derived from $p53^{-/-}$ mice (38) have been shown to undergo apoptosis after radiation, suggesting p53-independent mechanisms of cell death following genomic damage.

We have shown that p53-dependent mechanisms may influence the response of inhibited glioma cells to undergo relative growth arrest and/or apoptosis. Our results in U373MG-derived cells also indicate that apoptotic cell death occurring after genomic damage in transformed human cells in which EGFR signaling is inhibited involves mechanisms that do not require wild-type p53 and p21 proteins. $p21^{-/-}$ mice develop normally and do not appear to have defects in programmed cell death required for normal organ development, indicating that p21 is not likely to be required for apoptosis (39). $p53^{-/-}$ mice display genetic instability and contain elevated c-myc levels (40). These mice undergo significant levels of apoptosis *in vivo*, indicating that p53-independent mechanisms of apoptosis are functional in both normal tissues (40) and transformed cells (37).

Interestingly, recent work demonstrates that the absence of p21 in isogenically matched colorectal carcinoma cells resulted in reduced growth arrest when compared with p21-positive derivatives of the same cell line and this was correlated to more inhibited tumor growth *in vivo* (3). These observations were ascribed to increased apoptosis due to defects in p21-mediated checkpoint growth arrest, though the increased tendency to apoptose by $p21^{-/-}$ cells was not directly shown in this work. Induction of apoptosis was suggested to be preferable to growth arrest as a response to anticancer therapy *in vivo* (3). In our studies, unlike those of Waldmann *et al.* (3), there was a correlation between apoptosis, increased growth arrest, and reduction in clonogenic survival after radiation. Pathways distal to the specific inhibitory interaction between the T691stop mutant neu protein and the EGF receptor determine tumor responsiveness to genomic damage and these pathways can be modulated by proximal erbB receptor associations. Specific inhibitory pathways initiated at the level of the cell membrane and associated with growth arrest and/or apoptosis may modulate subsequent checkpoint outcomes in response to DNA damage.

Under certain circumstances, particularly in cancer cells, apoptosis may be favored after genomic damage if defects in pathways mediating growth arrest are present (3). Additionally, when cells are capable of undergoing both growth arrest and apoptosis, as in the case of p21-containing and -deficient human glioma cells in which EGFR signaling was disabled in these studies, apoptosis may be induced after certain signals, such as radiation. The ability or inability to induce growth arrest *per se* does not appear to be a major determinant of radiosensitivity because both radioresistant parental human glioblastoma cell lines and more radiosensitive derivatives exhibited growth arrest with prolonged serum deprivation or exposure to radiation, and radiosensitive subclones displayed a greater degree of growth arrest.

Our data indicate that the relative proportion of growth arrest or apoptosis induced by genomic damage is influenced by both the integrity of specific checkpoints and alterations in erbB-signaling pathways. Notably, modulating receptor tyrosine kinase signaling pathways may influence checkpoint outcomes after DNA damage in transformed cells. Others (41) have shown that activation of erbB-signaling pathways in breast cancer cells contributes to radioresistance, suggesting that erbB family-signaling pathways influence the response to DNA damage in many tumor types. By combining biologic inhibition of signaling with agents capable of specifically inhibiting receptor oncoproteins of the tyrosine kinase family, we may be able to influence the kinetics of tumor cell response to standard cytotoxic agents. The timing of administration of cytotoxic therapies may be optimized in such combination therapies ,and these data suggest that selective antitumor effects of presently available anticancer regimens could be improved, even in the treatment of advanced human malignancies containing alterations in multiple checkpoint signal transduction pathways.

This work was supported by a Merit Review Grant from the Veterans Administration (to D.M.O.), by grants from the Lucille P. Markey Trust and the American Association of Neurological Surgeons Research Foundation (to D.M.O.), and by grants from the National Cancer Institute, the National Institutes of Health, the American Cancer Society, the U.S. Army, and the Abramson Institute to M.I.G.

1. Paulovich, A. G., Toczyski, D. P. & Hartwell, L. H. (1997) *Cell* **88,** 315–321.
2. Nurse, P. (1997) *Cell* **91,** 865–867.
3. Waldman, T., Zhang, Y., Dillehay, L., Yu, J., Kinzler, K., Vogelstein, B. & Williams, J. (1997) *Nat. Med.* **3,** 1034–1036.
4. Orren, D. K., Petersen, L. N. & Bohr, V. A. (1997) *Mol. Biol. Cell* **8,** 1129–1142.
5. Louis, D. N. & Gusella, J. F. (1995) *Trends Genet.* **11,** 412–415.
6. Westermark, B. & Nister, M. (1995) *Curr. Opin. Oncol.* **7,** 220–225.
7. Nishikawa, R., Ji, X. D., Harmon, R. C., Lazar, C. S., Gill, G. N., Cavenee, W. K. & Huang, H. J. (1994) *Proc. Natl. Acad. Sci. USA* **91,** 7727–7731.
8. Moscatello, D. K., Montgomery, R. B., Sundareshan, P., McDanel, H., Wong, M. Y. & Wong, A. J. (1996) *Oncogene* **13,** 85–96.
9. O'Rourke, D. M., Nute, E. J. L., Davis, J. G., Wu, C., Lee, A., Murali, R., Zhang, H.-T., Qian, X., Kao, C.-C. & Greene, M. I. (1998) *Oncogene* **16,** 1197–1207.
10. O'Rourke, D. M., Qian, X., Zhang, H.-T., Davis, J. G., Nute, E., Meinkoth, J. & Greene, M. I. (1997) *Proc. Natl. Acad. Sci. USA* **94,** 3250–3255.

11. Prigent, S. A., Nagane, M., Lin, H., Huvar, I., Boss, G. R., Feramisco, J. R., Cavenee, W. K. & Huang, H.-J. S. (1996) *J. Biol. Chem.* **271,** 25639–25645.
12. Moscatello, D. K., Holgado, M. M., Emlet, D. R., Montgomery, R. B. & Wong, A. J. (1998) *J. Biol. Chem.* **273,** 200–206.
13. Holgado-Madruga, M., Moscatello, D. K., Emlet, D. R., Dieterich, R. & Wong, A. J. (1997) *Proc. Natl. Acad. Sci. USA* **94,** 12419–12424.
14. Antonyak, M. A., Moscatello, D. K. & Wong, A. J. (1998) *J. Biol. Chem.* **273,** 2817–2822.
15. Samanta, A., LeVea, C. M., Dougall, W. C., Qian, X. & Greene, M. I. (1994) *Proc. Natl. Acad. Sci. USA* **91,** 1711–1715.
16. Kiyokawa, N., Yan, D. H., Brown, M. E. & Hung, M. C. (1995) *Proc. Natl. Acad. Sci. USA* **92,** 1092–1096.
17. McKenna, W. G., Bernhard, E. J., Markiewicz, D. A., Rudoltz, M. S., Maity, A. & Muschel, R. J. (1996) *Oncogene* **12,** 237–245.
18. Nagane, M., Coufal, F., Lin, H., Bogler, O., Cavenee, W. K. & Huang, H.-J. S. (1996) *Cancer Res.* **56,** 5079–5086.
19. Haas, K. D., Yount, G., Haas, M., Levi, D., Kogan, S. S., Hu, L., Vidair, C., Deen, D. F., Dewey, W. C. & Israel, M. A. (1996) *Int. J. Radiat. Oncol. Biol. Phys.* **36,** 95–103.
20. Lamb, J. R. & Friend, S. H. (1997) *Nat. Med.* **3,** 962–963.
21. Lowe, S. W., Ruley, H. E., Jacks, T. & Housman, D. E. (1993) *Cell* **74,** 957–967.
22. Lowe, S. W., Bodis, S., McClatchey, A., Remington, L., Ruley, H. E., Fisher, D. E., Housman, D. E. & Jacks, T. (1994) *Science* **266,** 807–810.
23. Levine, A. J. (1997) *Cell* **88,** 323–331.
24. Hermeking, H., Lengauer, C., Polyak, K., He, T.-C., Zhang, L., Thiagalingam, S., Kinzler, K. & Vogelstein, B. (1997) *Mol. Cell* **1,** 3–11.
25. Bacus, S. S., Yarden, Y., Oren, M., Chin, D. M., Lyass, L., Zelnick, C. R., Kazarov, A., Toyofuku, W., Gray, B. J., Beerli, R. R., Hynes, N. E., Nikiforov, M., Haffner, R., Gudkov, A. & Keyomarsi, K. (1996) *Oncogene* **12,** 2535–2547.
26. Russell, S. J., Ye, Y. W., Waber, P. G., Shuford, M., Schold, S. J. & Nisen, P. D. (1995) *Cancer* **75,** 1339–1342.
27. Chen, J., Willingham, T., Shuford, M., Bruce, D., Rushing, E., Smith, Y. & Nisen, P. D. (1996) *Oncogene* **13,** 1395–1403.
28. Evan, G. I., Wyllie, A. H., Gilbert, C. S., Littlewood, T. D., Land, H., Brooks, M., Waters, C. M., Penn, L. Z. & Hancock, D. C. (1992) *Cell* **69,** 119–128.
29. Greene, L. A. (1978) *J. Cell Biol.* **78,** 747–755.
30. Batistatou, A. & Greene, L. A. (1993) *J. Cell Biol.* **122,** 523–532.
31. Chang, E. H., Pirollo, K. F., Zou, Z. Q., Cheung, H. Y., Lawler, E. L., Garner, R., White, E., Bernstein, W. B., Fraumeni, J. J. & Blattner, W. A. (1987) *Science* **237,** 1036–1039.
32. Kasid, U., Pfeifer, A., Weichselbaum, R. R., Dritschilo, A. & Mark, G. E. (1987) *Science* **237,** 1039–1041.
33. Kasid, U., Pfeifer, A., Brennan, T., Beckett, M., Weichselbaum, R. R., Dritschilo, A. & Mark, G. E. (1989) *Science* **243,** 1354–1356.
34. Sklar, M. D. (1988) *Science* **239,** 645–647.
35. McKenna, W. G., Weiss, M. C., Endlich, B., Ling, C. C., Bakanauskas, V. J., Kelsten, M. L. & Muschel, R. J. (1990) *Cancer Res.* **50,** 97–102.
36. Harrington, E. A., Fanidi, A. & Evan, G. I. (1994) *Curr. Opin. Genet. Dev.* **4,** 120–129.
37. Bracey, T. S., Miller, J. C., Preece, A. & Paraskeva, C. (1995) *Oncogene* **10,** 2391–2396.
38. Strasser, A., Harris, A. W., Jacks, T. & Cory, S. (1994) *Cell* **79,** 329–339.
39. Deng, C., Zhang, P., Harper, J. W., Elledge, S. J. & Leder, P. (1995) *Cell* **82,** 675–684.
40. Fukasawa, K., Wiener, F., Vande, W. G. & Mai, S. (1997) *Oncogene* **15,** 1295–1302.
41. Wollman, R., Yahalom, J., Maxy, R., Pinto, J. & Fuks, Z. (1994) *Int. J. Radiat. Oncol. Biol. Phys.* **30,** 91–98.

THE JOURNAL OF BIOLOGICAL CHEMISTRY
Vol. 274, No. 2, Issue of January 8, pp. 574–583, 1999
Printed in U.S.A.

Domain-specific Interactions between the p185^{neu} and Epidermal Growth Factor Receptor Kinases Determine Differential Signaling Outcomes*

(Received for publication, March 23, 1998, and in revised form, September 15, 1998)

Xiaolan Qian‡§, Donald M. O'Rourke¶, Zhizhong Fei‡‖, Hong-Tao Zhang‡, Chih-Ching Kao, and Mark I. Greene‡ ‡‡**

*From the ‡Department of Pathology and Laboratory Medicine, and the ¶Department of Neurosurgery, University of Pennsylvania School of Medicine, and the **Department of Pathology, University of Pennsylvania School of Veterinary Medicine, Philadelphia, Pennsylvania 19104*

We expressed the epidermal growth factor receptor (EGFR) along with mutant p185^{neu} proteins containing the rat transmembrane point mutation. The work concerned the study of the contributions made by various p185^{neu} subdomains to signaling induced by a heterodimeric ErbB complex. Co-expression of full-length EGFR and oncogenic p185^{neu} receptors resulted in an increased EGF-induced phosphotyrosine content of p185^{neu}, increased cell proliferation to limiting concentrations of EGF, and increases in both EGF-induced MAPK and phosphatidylinositol 3-kinase (PI 3-kinase) activation. Intracellular domain-deleted p185^{neu} receptors (T691stop neu) were able to associate with full-length EGFR, but induced antagonistic effects on EGF-dependent EGF receptor down-regulation, cell proliferation, and activation of MAPK and PI 3-kinase pathways. Ectodomain-deleted p185^{neu} proteins (TΔ5) were unable to physically associate with EGFR, and extracellular domain-deleted p185^{neu} forms failed to augment activation of MAPK and PI 3-kinase in response to EGF. Association of EGFR with a carboxyl-terminally truncated p185^{neu} mutant (TAPstop) form did not increase transforming efficiency and phosphotyrosine content of the TAPstop species, and proliferation of EGFR·TAPstop-co-expressing cells in response to EGF was similar to cells containing EGFR only. Thus, neither cooperative nor inhibitory effects were observed in cell lines co-expressing either TΔ5 or TAPstop mutant proteins. Unlike the formation of potent homodimer assemblies composed of oncogenic p185^{neu}, the induction of signaling from p185^{neu}·EGFR heteroreceptor assemblies requires the ectodomain for ligand-dependent physical association and intracellular domain contacts for efficient intermolecular kinase activation.

The ErbB family includes four members of homologous receptor tyrosine kinases, the epidermal growth factor receptor (EGFR[1] or ErbB-1) (1), ErbB-2·p185^{neu} (2, 3), ErbB-3 (4), and ErbB-4 (5). ErbB family proteins are widely expressed in epithelial, mesenchymal, and neuronal tissues, and play important roles in normal growth and development (6–9). Aberrant expression of these ErbB proteins is frequently observed in human malignancies (10).

The transmembrane mutation in rat p185^{neu} (also termed Tneu) (12) serves as a paradigm for receptor dimerization that leads to constitutive kinase activation contributing to oncogenic transformation (11–13). Additional support for this mechanism has come from the identification of a naturally occurring activated EGFR oncoprotein (ΔEGFR or EGFRvIII) in human tumors, which forms constitutive dimers and confers increased tumorigenicity (14, 15). Gene amplification and overexpression of ErbB-2 have been observed in a high frequency of human adenocarcinomas, including those of the breast and ovary, and these features correlate with poor clinical prognosis (16, 17). Experimental support for this model is provided by *in vitro* transformation assays using cell lines overexpressing either protooncogenic rat p185$^{c\text{-}neu}$ or human ErbB-2 at levels of 10^6 receptors/cell (18, 19). Biochemical and biophysical analysis of baculovirus-expressed p185^{neu} proteins further support the notion of receptor oligomerization as a mechanism of kinase activation of normal holoreceptors (20, 21).

Heterodimeric interactions govern many signaling properties within the ErbB receptor family. Co-expression of EGFR and p185$^{c\text{-}neu}$ at modestly elevated levels (10^5/cell) (but not either receptor independently) results in synergistic transformation (22), due to increase of the ligand binding affinity and catalytic kinase activity (23, 24). Heterodimerization of EGFR and ErbB-2 has also been observed in human breast tumor lines (25). Moreover, ligand treatment promotes the assembly of an activated p185$^{c\text{-}neu}$·EGFR kinase complex in many cells (24), resulting in novel distinct cellular signaling events (26). Therefore, the receptor tyrosine kinase ensemble can be activated not only by homodimer formation, but also by heterodimeric associations. In this regard, endodomain interactions between p185^{neu} and EGFR appear to influence

* This work was supported by a National Research Service Award (to X. Q.); by grants from the Veterans Administration Merit Review Program, the Lucille Markey Charitable Trust, and the American Cancer Society (IRG-135P) (to D. M. O.); and by grants from National Cancer Institute, the Lucille Markey Charitable Trust, the United States Army, American Cancer Society, and the Abramson Institute for Cancer Research (to M. I. G.). The costs of publication of this article were defrayed in part by the payment of page charges. This article must therefore be hereby marked "*advertisement*" in accordance with 18 U.S.C. Section 1734 solely to indicate this fact.

§ Present address: Laboratory of Cellular Oncology, NCI, National Institutes of Health, Bethesda, MD 20892.

‖ Present address: Cardiology Branch, NHLBI, National Institutes of Health, Bethesda, MD 20892.

‡‡ To whom correspondence should be addressed: 252 John Morgan Bldg., Dept. of Pathology and Laboratory Medicine, 36th and Hamilton Walk, Philadelphia, PA 19104. Tel.: 215-898-2868; Fax: 215-898-2401; E-mail: greene@reo.med.upenn.edu.

[1] The abbreviations used are: EGFR, epidermal growth factor receptor; EGF, epidermal growth factor; PI 3-kinase, phosphatidylinositol 3-kinase; HA, hemagglutinin; PAGE, polyacrylamide gel electrophoresis; MAP, mitogen-activated protein; MAPK, MAP kinase; mAb, monoclonal antibody; aa, amino acid(s); DMEM, Dulbecco's modified Eagle's medium; FBS, fetal bovine serum; PBS, phosphate-buffered saline; MTT, 3,(4,5-dimethylthiazol-2-yl)2,5-diphenyl tetrazolium bromide); ERK, extracellular signal-regulated kinase; BS^3, bis(sulfosuccinimidyl) suberate.

functional signaling outcomes (27).

In response to EGF or Neu differentiating factor/heregulin (a ligand for ErbB-3 and ErbB-4) family ligands (28, 29), EGFR and ErbB-2 both form heterodimers with ErbB-3 and ErbB-4 (30–34). Heterodimers between p185^{neu}·ErbB-2 and ErbB-3 are associated with activated signaling and the transformed phenotype in primary human cancer cells (35). Existence of an ErbB-3·ErbB-4 heterodimer has not been convincingly demonstrated to date. More recent data support the notion that p185^{neu}·ErbB-2 is the preferred heterodimerization partner of *all* ErbB receptors and a mediator for divergent cellular signaling in many distinct cell types (34, 36).

The structural basis for ErbB receptor heterodimerization has not been completely defined and crystallographic information on dimerized ErbB receptor kinases is currently unavailable. Previous work has revealed that ectodomain interactions are sufficient to stabilize dimer formation between p185^{neu} and EGFR in fibroblasts and transformed cells (5, 37, 38), which is supported by observations showing that a partial deletion of the EGF receptor ectodomain still allow dimer formation and receptor activation (14, 15). Although the transmembrane alone can stabilize the formation of p185^{neu} homodimers, the relative contributions of the transmembrane region and the ectodomain have not been directly compared regarding the formation of signaling heterodimers.

In this study, we have constructed various p185^{neu} deletion mutants in order to specifically compare signaling events resulting from associations between EGF receptors and either p185^{neu} ectodomain- or endodomain-derived mutant receptors. We have co-expressed EGFR with *low* levels of p185^{neu} proteins, or their mutant derivatives, to monitor p185^{neu}-mediated enhancement of cell growth and transformation *in vitro* and *in vivo*, and to analyze the influence of EGF-induced heterodimeric receptor interactions on downstream signaling effectors. Signaling resulting from heterodimeric associations between full-length EGFR and mutant p185^{neu} proteins has revealed the functional importance of p185^{neu} subdomains in the induction of Ras/extracellular signal-regulated kinase (ERK) and phosphatidylinositol 3-kinase (PI 3-kinase) pathways contributing to cell growth and transformation.

EXPERIMENTAL PROCEDURES

Antibodies—As described previously (20, 39, 40), monoclonal antibody 7.16.4, polyclonal antiserum α-Bacneu, and NCT are reactive with the ectodomain, intracellular domain, and carboxyl terminus of p185^{neu}, respectively. mAb 225 reactive with the ectodomain of EGFR was obtained from Dr. John Mendelsohn (M. D. Anderson Cancer Center, Dallas, TX). A polyclonal rabbit antiserum specifically against the COOH terminus of EGFR (termed CT) was provided by Dr. Stuart Decker (40). The anti-phosphotyrosine monoclonal antibody, PY20, was obtained from Santa Cruz Biotechnology (Santa Cruz, CA.).

DNA Constructs—All the deletion mutants were derived from the rat oncogenic p185^{neu} cDNA containing a single point mutation (V664G) in the transmembrane region. The TAPstop mutant, containing a 122-aa truncation of the COOH terminus was prepared as described previously (41). A T691stop species was prepared by site-directed mutagenesis and substitution of a stop codon for Thr-691, resulting in a large cytoplasmic deletion (42, 43). The ectodomain-deleted mutant TΔ5 neu protein was described previously (27). These cDNAs encoding for mutant p185^{neu} forms were all cloned into the pSV2neo^{r}/DHFR vector as described (44) for expression in murine fibroblasts. These wild-type or mutant p185^{neu} cDNAs were also subcloned into pcDNA3 vector for transient expression in COS7 cells. pSRαEGFR/hyg^{r} vector (44) was used for full-length EGFR expression.

Transfection and Maintenance of Cell Lines—Ten micrograms of the p185^{neu} constructs were transfected into NR6 cells, a mouse fibroblast cell line devoid of endogenous EGF receptors (43), or NE91 cells expressing human EGFR (37) by calcium phosphate precipitation. After 2–3 weeks of selection with Geneticin (0.9 mg/ml), the established stable clones were screened and characterized. Gene amplification by methotrexate was used to increase the p185^{neu} receptor level. Expression of p185^{neu} and its derivatives in resultant subclones was examined by flow cytometric analysis following anti-p185^{neu} mAb 7.16.4 staining. Surface expression of p185^{neu} proteins was then estimated by comparing the mean channel fluorescent intensity with that of B104-1-1 cells, as the level of p185^{neu} in B104-1-1 cells was previously determined by ^{125}I-labeled anti-neu mAb binding assay (22). EGFR numbers in NE91 cells and mutant p185^{neu} co-transfected cells were determined by Scatchard assays as described (37). These transfected clones were maintained in Dulbecco's modified Eagle's medium (DMEM) containing 5% fetal bovine serum (FBS, HyClone) at 37 °C in a 5% CO_2 atmosphere.

Cross-linking, Immunoprecipitation, and Immunoblotting Procedures—Subconfluent cells in 10-cm dishes were washed and starved in cysteine-free DMEM for 1 h, and grown in low cysteine-containing 5% FBS-DMEM containing 55 μCi/ml [^{35}S]cysteine (Amersham Pharmacia Biotech) for 16 h for metabolic labeling. Alternatively, the unlabeled cells were cultured overnight in 10-cm Petri dishes. After treatment with or without EGF, cells were washed twice with cold phosphate-buffered saline (PBS) and treated with PBS containing 2 mM membrane-impermeable cross-linker bis(sulfosuccinimidyl) suberate (BS^{3}, Pierce), for 30 min. After quenching the cross-linking reaction with a buffer containing 10 mM Tris-HCl (pH 7.6), 0.9% NaCl, and 0.1 M glycine, cells were washed twice with cold PBS and solubilized with PI/RIPA buffer as described (24). The immunocomplexes were washed and solubilized, then separated by gradient SDS-PAGE gels (4–7.5%). Proteins from metabolically labeled cells were analyzed by autoradiography. Proteins from unlabeled cells were transferred onto nitrocellulose and then immunoblotted with anti-phosphotyrosine mAb PY20, anti-EGFR CT, or anti-p185 antiserum as indicated in the figures. The protein signals were identified by the binding of ^{125}I-labeled protein A (NEN Life Science Products), or by enhanced chemiluminase (ECL) using ECL kit from Amersham Pharmacia Biotech.

Receptor Down-regulation Studies—Cells (1×10^{5}) were plated in a six-well dish with DMEM containing 5% FBS overnight. Cells were then treated with EGF (50 ng/ml) for 0–4 h and were harvested and washed with cold PBS containing 0.5% bovine serum albumin and 0.1% sodium azide. Cell preparations were then incubated with a saturating amount (0.5 μg/reaction) of anti-neu mAb 7.16.4 or anti-EGFR mAb 225, or an irrelevant mAB (such as 9BG5 against the hemagglutinin of reovirus receptor), at 4 °C for 30 min, restained with fluorescein isothiocyanate-conjugated anti-mouse IgG (Sigma) for another 30 min after extensive washing. Cells were then fixed with 2% paraformaldehyde and analyzed by flow cytometry (FACScan, Becton Dickinson), as described previously (37). Briefly, after subtracting the nonspecific background staining with 9BG5, the mean channel values from each time point were used to determine the percentage of surface expression of EGFR or p185^{neu} proteins at the various time points after EGF treatment.

In Vitro and in Vivo Transformation Assays—Anchorage-independent growth ability was determined by assessing the colony forming efficiency of cells suspended in soft agar (15, 37). Cells (1000/dish) were suspended in 7% FBS-DMEM containing 0.18% agarose, and plated on 0.25% basal agar in each dish. Cells were fed with DMEM supplemented with 7% FBS-DMEM, 20 mM HEPES (pH 7.5). Colonies (>0.3 mm) were visualized at day 21 for all cell lines after stained with *p*-iodonitrotetrazolium violet (1 mg/ml). Each cell line was examined in triplicate samples for separate experiments.

To analyze the tumor growth in athymic mice, cells (1×10^{6}) of each line were suspended in 0.1 ml of PBS and injected intradermally in the mid-dorsum of NCR nude mice. PBS alone was also injected as a control. Animals used in this study were maintained in accordance with the guidelines of the Committee on Animals of the University of Pennsylvania and those prepared by the Committee on Care and Use of Laboratory Animals of the Institute of Laboratory Animal Resource. Tumor growth was monitored twice a week up to 10 weeks. Tumor size was calculated by this formula: 3.14/6 × (length × width × thickness) as described (27).

EGF-dependent Cell Proliferation Assay—The 3,(4,5-dimethylthiazol-2-yl)2,5-diphenyl tetrazolium bromide) (MTT) assay for measuring cell growth has been described previously (38). Briefly, cells (3000/well) of each cell line were seeded in 96-well plates overnight in DMEM containing 5% FBS. Cells were starved in serum-free ITS-DMEM for 48 h, then cultured in 100 μl of the same medium plus various concentrations of EGF for another 48 h. 25 μl of MTT solution (5 μg/ml in PBS) were added to each well, and after 2 h of incubation at 37 °C, 100 μl of the extraction buffer (20% w/v SDS, 50% *N,N*-dimethyl formamide, pH 4.7) was added. After an overnight incubation at 37 °C, the optical density at 600 nm was measured using an enzyme-linked immunosorbent assay reader. Each value represents a mean of four samples.

MAP Kinase and PI 3-Kinase Immune Complex Kinase Assays—COS7 cells were transiently transfected with pcDNA3-HA-ERK2 (a gift from Silvio Gutkind, National Institutes of Health, Bethesda, MD) and pSRαEGFR/hyg^r, along with either empty vector or plasmids expressing wild-type or mutant p185$^{c\text{-}neu}$ using LipofectAMINE (Life Technologies, Inc.) according to the manufacturer's instructions and assayed 48 h after transfection. Cells deprived of serum for 16–20 h were treated with or without EGF (50 ng/ml) for 5 min. For MAP kinase assay, cells were lysed with RIPA buffer (25 mM Tris-HCl (pH 7.5), 0.3 M NaCl, 1.5 mM $MgCl_2$, 1 mM $MgCl_2$, 0.2 mM EDTA, 0.5 mM dithiothreitol, 1% Triton X-100, 0.5% sodium deoxycholate, 0.1% SDS, 20 mM β-glycerophosphate, 1 mM sodium orthovanadate, 10 μg/ml aprotinin, 1 mM phenylmethylsulfonyl fluoride, 10 μg/ml leupeptin). Protein concentrations were determined by the BCA kit (Pierce). Equal amounts of protein (100 μg) from cell extracts were immunoprecipitated with anti-HA (BabCo). After washing extensively, the immunocomplexes were then incubated with 50 μl of reaction buffer (30 mM HEPES (pH 7.4), 10 mM $MaCl_2$, 1 mM dithiothreitol, 5 μM ATP) containing 1 μCi of [γ-^{32}P]ATP (NEN Life Science Products) and 2 μg of myelin basic protein (Upstate Biotechnology Inc.). After incubation for 20 min at 30 °C, kinase reactions were terminated by the addition of 2× Laemmli sample buffer. The samples were then resolved by SDS-PAGE, and the phosphorylated myelin basic protein was visualized by autoradiography.

PI 3-kinase immune complex assays were carried out as described (45) with slight modifications. Cells were lysed in Nonidet P-40 lysis buffer (20 mM Tris-HCl (pH 7.4), 137 mM NaCl, 1 mM $MgCl_2$, 1 mM $CaCl_2$, 10% glycerol, 1% Nonidet P-40, 1 mM sodium orthovanadate, 10 μg/ml aprotinin, 1 mM phenylmethylsulfonyl fluoride, 1 μg/ml leupeptin). Equal amounts of protein (600 μg) from cell extracts were immunoprecipitated with anti-phosphotyrosine 4G10 (Upstate Biotechnology Inc.) for 3 h. Protein A-Sepharose was then added and rotated at 4 °C for overnight. Immunocomplexes were washed twice with lysis buffer; twice with 100 mM Tris (pH 7.4), 0.5 M LiCl, 0.2 mM sodium orthovanadate, plus 0.2 mM adenosine; and twice with reaction buffer (10 mM HEPES (pH 7.5), 5 mM EDTA, 150 mM NaCl). The beads were resuspended in 40 μl of reaction buffer containing substrate mixture (phosphatidylinositol, phosphatidylinositol 4-phosphate, and phosphatidylserine dispersed by sonication in 10 mM HEPES (pH 7.5), 1 mM EGTA). The tubes were incubated at room temperature for 10 min and reaction were initiated by adding 5 μCi of [γ-^{32}P]ATP (NEN Life Science Products) per reaction in 5 μl of 500 mM ATP and terminated by addition of 80 μl of $CHCl_3$:CH_3OH (1:1) after another 10 min. Phospholipids were extracted, desiccated, and redissolved as described (45). The samples were the chromatographed on thin layer chromatography plates (precoated with potassium oxalate and baked at 100 °C for 1 h before use) in $CHCl_3$:CHOH:2.5 M NH_4OH:H_2O (45:35:2.7:7.3). Spots corresponding to phosphatidylinositol 3-phosphate and phosphatidylinositol 3,4-bisphosphate were visualized after autoradiography. Unlabeled phospholipid standards were included and were visualized by exposure to iodine vapor.

RESULTS

Expression of EGFR and/or Mutant p185^{neu} Proteins—Cell lines expressing EGFR and various p185^{neu} deletion mutant proteins derived from full-length transforming p185^{neu} were all generated in the NR6 cell background (43). In addition, stable transfectants derived from NR6 fibroblasts expressing human EGFR (termed NE91 cells) were also generated. NE91 cells, as well as NR6 parental cells, were then transfected with various p185^{neu} cDNA constructs to express one of the following mutant p185^{neu} proteins with or without EGFR, respectively (Fig. 1): (*a*) Er/p185^{neu} or p185^{neu} (full-length oncogenic p185^{neu} product), (*b*) Er/T691stop or T691stop (lacking 591 aa from the carboxyl terminus), (*c*) Er/TAPstop or TAPstop (a 122-aa truncation at carboxyl terminus), and (*d*) Er/TΔ5 or TΔ5 (an ectodomain deleted p185^{neu} product, also termed TΔ5). A schematic representation of the oncogenic p185^{neu} protein and its mutant derivative species is shown in Fig. 1.

B104-1-1 murine fibroblasts transformed by the expression of oncogenic p185^{neu} were used as a positive control, since surface expression of p185^{neu}, biochemical features of p185^{neu} homodimerization and p185^{neu} transforming potency have been characterized previously (13, 22, 27). As shown in Table I, relative expression levels of various p185^{neu} mutant proteins in

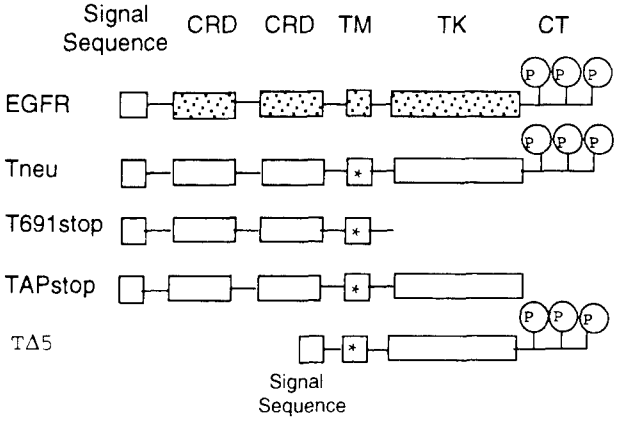

FIG. 1. **Schematic representation of EGFR and mutant p185^{neu} proteins.** Locations of cysteine-rich subdomains (*CRD*), transmembrane region (*TM*) containing the point mutation V664E (*), tyrosine kinase domain (*TK*), and carboxyl-terminal region (*CT*) are indicated. *Tneu* is the full-length transforming rat p185^{neu}. *T691stop* contains a stop codon substituting for Thr-691 at the amino terminus to the TK domain. *TAPstop* contains a 120-aa truncation within the carboxyl terminus of p185^{neu}. *TΔ5* is generated by the deletion of ectodomain of p185^{neu} but retains ~10 aa and the signal sequence. These mutant p185^{neu} proteins were either expressed alone or co-expressed with EGFR in NR6 transfected cells.

selected clones were estimated by a comparison with B104-1-1 cells, while the expression of EGFR in these cells was estimated by Scatchard analysis. In order to observe an enhancement of EGFR-mediated cellular signaling and transformation, clone Er/p185^{neu} expressing a moderately low level of both receptors (~10^4/cell) was chosen. In other subclones, the expression of EGFR and/or mutant p185^{neu} proteins was approximately ~10^5 receptors/cell.

The Ectodomain of p185^{neu} Is Required for Heterodimerization with EGFR—Stable cell lines expressing EGFR and/or mutant p185^{neu} proteins were used to assess dimer formation using the chemical cross-linker BS^3. As shown in Fig. 2, B104-1-1 cells expressing oncogenic p185^{neu} contained p185^{neu} homodimers (~370 kDa) independent of ligand stimulation (Fig. 2*A*, *lane 1*), due to the activating transmembrane mutation (12). A cell line expressing the ectodomain-derived T691stop neu alone was used as a control to demonstrate the sizes of the monomer and dimer of this truncated p185^{neu} protein, which migrated at approximately 115 kDa (Fig. 2*A*, *lanes 2* and *3*), and at ~230 kDa in the presence of a chemical cross-linker (Fig. 2*A*, *lane 3*).

In the presence of EGF, the 170-kDa monomeric form and the 340-kDa homodimer of EGFR were both detected in NE91 cells expressing EGFR alone, and in Er/T691stop cells (Fig. 2*A*, *lanes 4* and *5*, respectively). An additional intermediate band of ~285 kDa representing the heterodimer of EGFR and T691stop was clearly detectable upon anti-EGFR immunoprecipitation (Fig. 2*A*, *lane 5*). The 285-kDa intermediate complex was similar to the heterodimer composed of EGFR and truncated N691stop derived from proto-oncogenic p185$^{c\text{-}neu}$ as described previously (44), except that the heterodimeric EGFR·N691stop complex was even more predominant than the EGFR homodimer in those studies. Notably, T691stop is still able to complex with EGFR (*lane 5*) even under conditions favorable for T691stop homodimerization (*lane 3*). Densitometric analysis suggested that at least 50% of the EGFR associated with T691stop neu in a heterodimeric complex in Er/T691stop cells (Fig. 2*A*, *lane 5*), further suggesting the strong preference for EGFR·p185^{neu} heterodimerization.

We have previously studied complex formation between the p185^{neu} and EGFR holoreceptors (22, 24, 37) and heterodimer-

TABLE I

Transformation parameters and relative receptor expression levels of cell lines

The number of EGFR on NE91 and other transfected cells was determined by Scatchard assays. Cell surface expression of neu proteins were estimated by comparing the mean channel fluorescent intensity with that from B104–1-1 cells using flow cytometry analysis. p185^{neu} on B104–1-1 cells was originally determined by an ^{125}I-labeled anti-neu mAb binding assay (22). For the tumor growth assay, individual clones (1×10^6 cells/site) were injected intradermally into athymic mice. NT, no tumor after 10 weeks; ND, not determined.

Cells	Colony in soft agar	Tumor growth			Receptor expression	
		Incidence	Latency	mm^3 (at week 6)	Neu protein	EGFR
	% efficiency		*week*			
B104–1-1	33.7 ± 0.6	6/6	1	sacrificed	1.5×10^5	0
NE91	<0.1	0/4		NT	0	2.8×10^5
Tneu	5.4 ± 0.4	4/4	4–5	158.5	3.7×10^4	0
Er/neu	10.2 ± 0.6	6/6	2–2.5	663	3.9×10^4	3.8×10^4
T691stop	<0.1	0/4		NT	4.5×10^5	0
Er/T691stop	<0.1	0/4		NT	4.3×10^5	2.5×10^5
TAPstop	6.5 ± 0.5	6/6	4–5	177.6	1.2×10^5	0
Er/TAP/stop	5.5 ± 0.6	4/4	4–5	168.7	1.3×10^5	4.6×10^5
TΔ5	5.7 ± 0.3	6/6	3	545.7	ND	0
Er/TΔ5	6.6 ± 0.4	4/4	3	593.4	ND	1.6×10^5

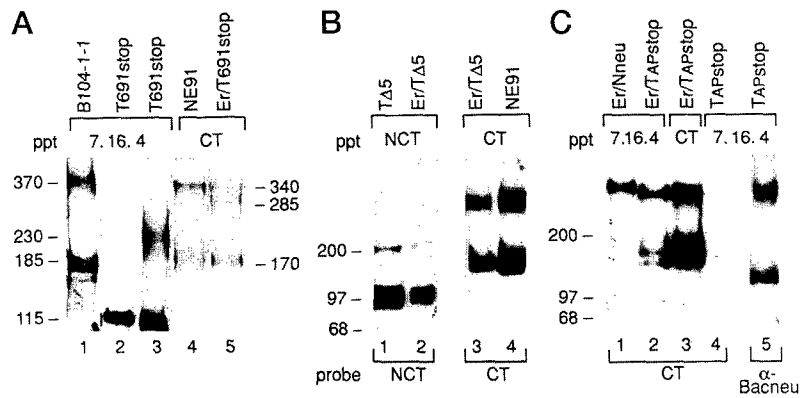

FIG. 2. **Homodimerization and heterodimerization of EGFR and p185^{neu} proteins.** *A*, cells were labeled with [^{35}S]cysteine overnight. Cell lines expressing EGFR (*lanes 4* and *5*) were then stimulated with EGF (200 ng/ml) at 37 °C for 10 min. All cells (except *lane 2*) were treated with the chemical cross-linker BS^3 (2 mM). Cell lysates were then immunoprecipitated with anti-neu mAb 7.16.4 or anti-EGFR antiserum CT as indicated. Proteins were separated by 4–8% gradient SDS-PAGE and analyzed by autoradiography. The estimated molecular weight of monomers and dimers is indicated. *B* and *C*, cell lines expressing EGFR (NE91, Er/TΔ5, and Er/TAPstop) were stimulated with EGF. After BS^3 treatment, all the cells were lysed and subjected to immunoprecipitation with either anti-neu (7.16.4 or NCT) or anti-EGFR (CT) antibodies, then immunoblotted with either the anti-neu (NCT or α-Bacneu) or anti-EGFR probe (CT) as indicated.

ization between ectodomain p185^{neu} and either full-length (37, 44) EGFR or a form of EGFR that lacks the majority of subdomains 1 and 2 (15) by immunoprecipitation and immunoblotting using anti-receptor specific antibodies following EGF and chemical cross-linker treatment.

In this next set of studies, we extended these observations to novel species of p185^{neu}. Er/Nneu cells expressing higher levels of EGFR and normal p185$^{c\text{-}neu}$ served as a positive control to examine the physical association of EGFR with truncated mutant p185^{neu} receptor forms (Fig. 2*C*, *lane 1*). The heterodimer between full-length p185^{neu} with EGFR in Er/neu cells could not be detected due to low expression levels of each receptor (data not shown). Abundant levels of the EGFR monomer and dimer were detected in Er/TAPstop cells by anti-EGFR immunoprecipitation and immunoblotting (Fig. 2*C*, *lane 3*). Analysis of anti-p185^{neu} immunoprecipitates by immunoblotting with anti-EGFR antisera indicated EGF-induced heterodimerization of EGFR and TAPstop in Er/TAPstop cells (Fig. 2*C*, *lane 2*). As expected, the size of this complex was slightly smaller when compared with the heterodimer of EGFR and full-length normal p185^{neu} in Er/Nneu cells (Fig. 2*C*, *lane 1*). The control cell line expressing TAPstop alone showed that TAPstop was only recognized by an anti-neu antibody (Fig. 2*C*, *lane 5*), but not by anti-EGFR antibody CT (Fig. 2*C*, *lane 4*).

Heterodimerization between EGFR and the ectodomain-deleted TΔ5 p185^{neu} mutant was also analyzed. TΔ5 can be recognized by either the α-Bacneu or anti-NCT polyclonal antisera reactive with the intracellular domain or carboxyl terminus of the p185^{neu} protein, respectively. Immunoblotting showed that the size of the TΔ5 neu mutant was approximately 95–97 kDa, and the detectable dimeric form was about ~200 kDa (Fig. 2*B*, *lane 1*). Er/TΔ5 cells express a high level of EGFR and TΔ5, as homodimers of either form were clearly detected in the presence of cross-linker (Fig. 2*B*, *lanes 2* and *3*), when compared with control cell lines NE91 and TΔ5 (Fig. 2*B*, *lanes 1* and *4*). However, unlike Er/T691stop and Er/TAPstop cells, the heterodimer between EGFR and TΔ5 in Er/TΔ5 cells was undetectable following EGF and BS^3 treatment since the predicted intermediate size (~270 kDa) complex representing EGFR and TΔ5 heterodimer was not observed (Fig. 2*B*, *lanes 2* and *3*). In an attempt to identify the association of EGFR with this ectodomain-deleted TΔ5 protein, several alternative assays were performed, such as using the membrane-permeable chemical cross-linker DSP (Pierce), or a mild detergent digitonin lysis buffer. These methods were sensitive enough to detect the complex formation between full-length p185^{neu} and TΔ5 (27).

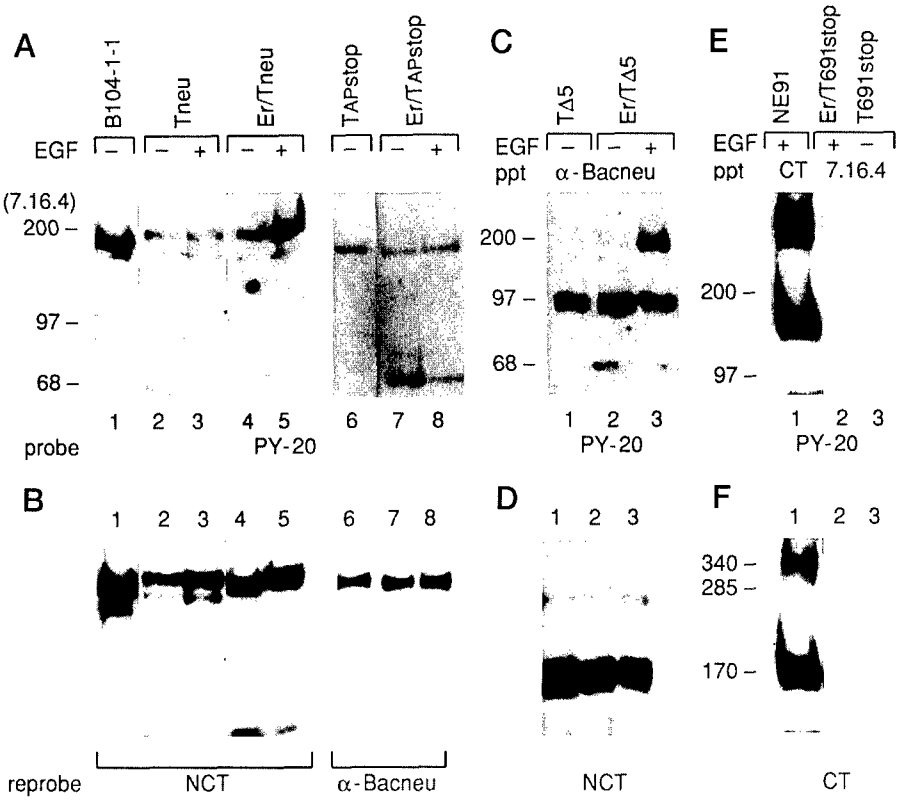

FIG. 3. **Tyrosine phosphorylation of EGFR and mutant p185^{neu} proteins in living cells.** Cells in *panels A*, *C*, and *E* were treated with or without EGF as indicated. Cells in *panel E* were also treated with the chemical cross-linker BS^3 (2 mM). Cell lysates were then immunoprecipitated with anti-neu antibodies, 7.16.4, α-Bacneu, or anti-EGFR CT as indicated. Proteins were separated by 6% (*A* and *C*) or 4–8% (*E*) gradient SDS-PAGE followed by immunoblotting with anti-phosphotyrosine mAb PY-20. After stripping the PY20 signals presented in *top panels*, these nitrocellulose membranes were reprobed with anti-neu NCT (*B*, *lanes 1–5*, and *D*), α-Bacneu (*B*, *lanes 6–8*) or α-EGFR CT (*F*) to compare protein amounts used in each sample.

However, the association of EGFR and TΔ5 was still undetectable (data not shown). Taken together, these results strongly suggest that the ectodomain of the p185^{neu} receptor is necessary and sufficient for heterodimerization with holoreceptor EGFR.

Tyrosine Kinase Activity in Living Cells—It has been well documented that EGF, in an EGFR-dependent manner, stimulated phosphorylation of the p185$^{c\text{-}neu}$ and c-ErbB-2 gene products with a concomitant increase in their tyrosine kinase activities (46–49). Heterodimerization of p185 and EGFR facilitates cross-phosphorylation (24, 25), since a full-length, kinase-deficient p185^{neu} mutant (K757M) is trans-phosphorylated upon physical association with EGFR (37). We next examined the tyrosine phosphorylation level of p185^{neu} derivatives in living cells in response to EGF treatment. After the addition of EGF, oncogenic p185^{neu} and its derivatives were immunoprecipitated by anti-neu antibodies, and receptor phosphotyrosine content *in vivo* was detected by immunoblotting with an anti-phosphotyrosine antibody (PY20) (Fig. 3). Full-length p185^{neu} from control B104-1-1 fibroblasts displayed constitutive kinase activity (Fig. 3*A*, *lane 1*). Upon EGF stimulation, there was indeed an additional increase in tyrosine kinase activity of p185^{neu} in Er/neu cells expressing lower amounts of the p185^{neu} protein (Fig. 3*A*, *lanes 4* and *5*), but not in cells expressing p185^{neu} alone (*lanes 2* and *3*). A weak tyrosine phosphorylation signal was detected in TAPstop cells (Fig. 3*A*, *lane 6*). EGF stimulation did not appreciably increase the tyrosine phosphorylation of TAPstop in EGFR-co-expressing cells (Fig. 3*A*, *lanes 7* and *8*), although the association of EGFR and TAPstop was evident (Fig. 2*C*). Truncation of the p185^{neu} carboxyl terminus, and deletion of at least three known critical tyrosine residues, was associated with the failure to trans-phosphorylate the p185^{neu} mutant protein. Elimination of the ectodomain did not impair the intrinsic kinase activity of p185^{neu}-derived TΔ5, since the TΔ5 mutant receptor was still a competent tyrosine kinase (Fig. 3*C*, *lane 1*). However, unlike the full-length p185^{neu}, no further increase in tyrosine phosphorylation of TΔ5 was detected in Er/TΔ5 cells with EGF stimulation (Fig. 3*C*, *lane 2* and *3*). In Er/TΔ5 cells, the EGFR was also immunoprecipitated by the anti-Bacneu antisera and still autophosphorylated after EGF treatment (Fig. 3*C*, *lane 3*). These results correlated with failure to detect physical interactions between EGFR and TΔ5 proteins (Fig. 2). Reprobing with anti-neu antibodies (Fig. 3, *A* and *C*) confirmed equivalent protein loading in paired samples with or without EGF treatment (Fig. 3, *B* and *D*). These experiments indicated that the full-length p185^{neu} receptor, but not mutant p185^{neu} proteins with NH_2-terminal or distal COOH-terminal truncations, was able to interact with activated EGFR functionally, resulting in trans-phosphorylation.

We next analyzed tyrosine kinase activation in EGFR-positive NE91 cells with or without T691stop neu co-expression. Treatment with EGF and a chemical cross-linking reagent resulted in heavy tyrosine phosphorylation of EGFR monomers and homodimers in NE91 cells (Fig. 3*E*, *lane 1*). No detectable tyrosine phosphorylation of cytoplasmic domain-deleted T691stop neu was seen in cells with or without EGFR co-expression (Fig. 3*E*, *lanes 2* and *3*, respectively). In addition, the tyrosine phosphorylation signal of an intermediate band (~285 kDa) representing EGFR·T691stop heterodimeric complex was also undetectable (Fig. 3*E*, *lane 2*), although a significant portion of EGFR forms a heterodimer with T691stop under these conditions (Fig. 2*A*, *lane 5*). Tyrosine kinase activation of full-length EGFR was thus completely inhibited when EGFR was physically associated with the T691stop neu mutant protein, which correlates with reduction of the transformed phenotype of primary EGFR-positive glioma cells expressing T691stop neu (42). Moreover, these results are consistent with the observation from cells co-expressing EGFR with N691stop neu derived from normal p185^{neu} (37).

Re-probing the membrane with an anti-EGFR antibody (CT) showed total EGFR levels in NE91 cells (Fig. 3*F*, *lane 1*), and confirmed the presence of the EGFR·T691stop heterodimer (~285 kDa), since this complex was recognized by anti-neu in

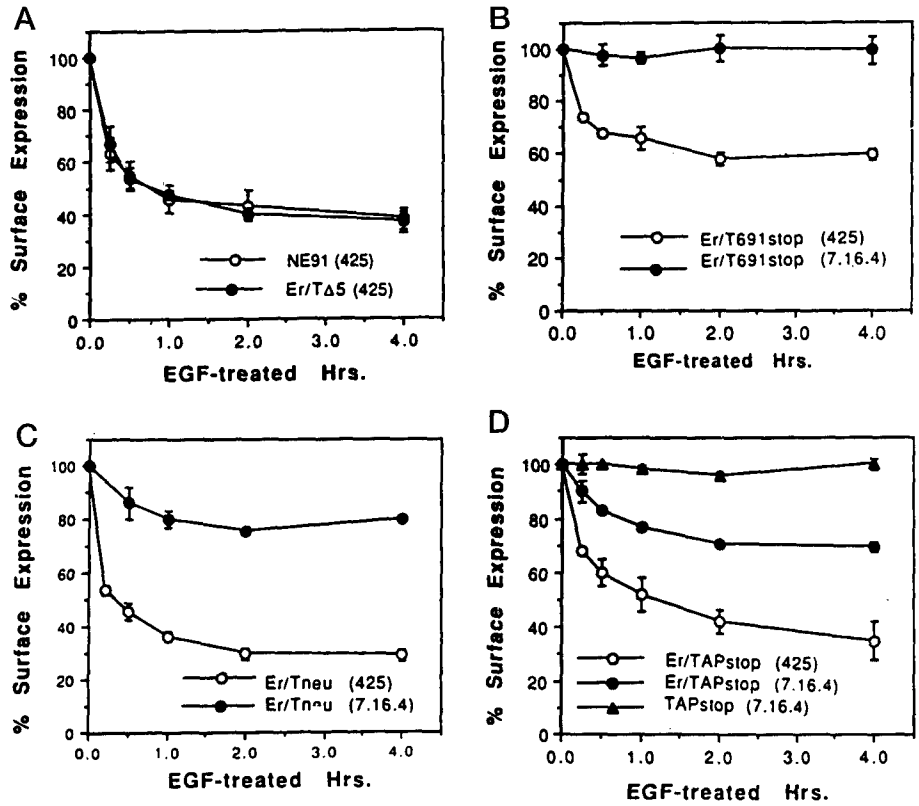

FIG. 4. **EGF-mediated receptor down-regulation.** Cells were plated in six-well dishes overnight and treated with EGF (50 ng/ml) for 0–4 h at 37 °C. Cells were then washed with fluorescence-activated cell sorting buffer and stained with anti-neu mAb 7.16.4 or anti-EGFR mAb 425 as indicated. After subtracting the background staining with irrelevant mAb 9BG5, the percentage of cell surface receptor expression reflected by the mean fluorescent intensity from each treated sample verses that from a non-treated sample was plotted against EGF treatment time. *A*, NE91 and Er/TΔ5; *B*, Er/T691stop; *C*, Er/neu; *D*, TAPstop and Er/TAPstop.

immunoprecipitation and anti-EGFR in immunoblotting (Fig. 3*F*, *lane 2*). Lysates obtained from T691stop neu-expressing cells did not react with the anti-EGFR CT probe (Fig. 3*F*, *lane 3*). Although the cytoplasmic domain deletion in T691stop did not impair heterodimerization with EGFR, the undetectable phosphotyrosine content of the intermediate heterodimer suggested that EGFR kinase activity was reduced when associated with T691stop neu. These experiments further support our model that the heteroreceptor assembly mediated primarily by ectodomain interactions facilitates kinase trans-activation and trans-phosphorylation caused by interactions between cytoplasmic domains (15, 27, 37).

EGF-induced Receptor Down-regulation from the Cell Surface—Numerous studies indicate that ligand-mediated receptor endocytosis and degradation is a kinase-dependent process for many types of growth factor receptors (50). We found that the efficiency of receptor down-regulation and degradation in cells co-expressing EGFR and p185^{neu} correlated well with heterodimeric kinase activities (37). We used this method as an alternative assay to examine the kinase activity of various heterodimers.

Cells were incubated with EGF (50 ng/ml) for various times prior to cell surface staining with anti-neu mAb 7.16.4 or anti-EGFR mAb 225 followed by the staining with fluorescein isothiocyanate-conjugated anti-mouse-IgG. Cell surface expression of each receptor was analyzed using flow cytometric analysis. EGF treatment of NE91 cells (expressing EGFR only) resulted in a reduction of cell surface EGFR, and over 60% of EGF receptors disappeared from the cell surface after 4 h of treatment (Fig. 4*A*). Normal EGFR down-regulation was not affected by the co-expression of TΔ5, as the efficiency of EGFR down-regulation in Er/TΔ5 cells was very similar to that seen in NE91 cells (Fig. 4*A*). A similar EGFR down-regulation curve was observed in Er/neu and Er/TAPstop cells (Fig. 4, *C* and *D*, respectively), indicating that the EGFR behaves as an active receptor kinase in these cells. Moreover, about ~20% of p185^{neu} or 25% TAPstop was co-down-regulated with EGFR upon EGF stimulation (Fig. 4, *C* and *D*). As illustrated above, the low expression of p185^{neu} and EGFR in Er/neu cells was insufficient to demonstrate the physical association of the two receptors biochemically. The current assay was more sensitive in determining EGF-mediated receptor interactions. Control cells expressing TAPstop alone did not respond to EGF treatment, and the surface expression of TAPstop remained unchanged within the period of EGF treatment (Fig. 4*D*).

Analysis using an EGF-mediated pulse-chase assay showed that the down-regulated EGFR and co-down-regulated TAPstop proteins efficiently went into the degradation pathway (data not shown), similar to the cells overexpressing EGFR and p185^{neu} (37). Our data suggested that EGFR and either p185^{neu} or TAPstop associated into an active kinase complex and that these receptor assemblies exhibited comparable kinetics of receptor endocytosis.

However, co-expression of T691stop with EGFR resulted in diminished EGF-induced down-regulation of EGFR. The maximal reduction of surface EGF receptor was ~35% after 4 h. In addition, no detectable co-down-regulation of the cytoplasmic domain deleted T691stop was observed in Er/T691stop cells (Fig. 4*B*), correlating with the observation of the inactive heterodimer of EGFR·T691stop (Fig. 3, *E* and *F*). This finding supports the idea that receptor down-regulation is coupled to receptor tyrosine kinase activity. The formation of the inactive heterodimer between EGFR and T691stop neu proteins influenced the overall kinetics of EGFR down-regulation. Impairment of ligand-induced down-regulation of holo-EGFR by T691stop neu has also been observed in primary human cancer cells.[2]

Transforming Potency of Cells Expressing Mutant p185^{neu} Proteins with or without EGFR—We and others have showed that the transforming potency of p185^{neu} requires not only its intrinsic tyrosine kinase activity (13), but also the crucial role

[2] D. M. O'Rourke and M. I. Greene, unpublished observations.

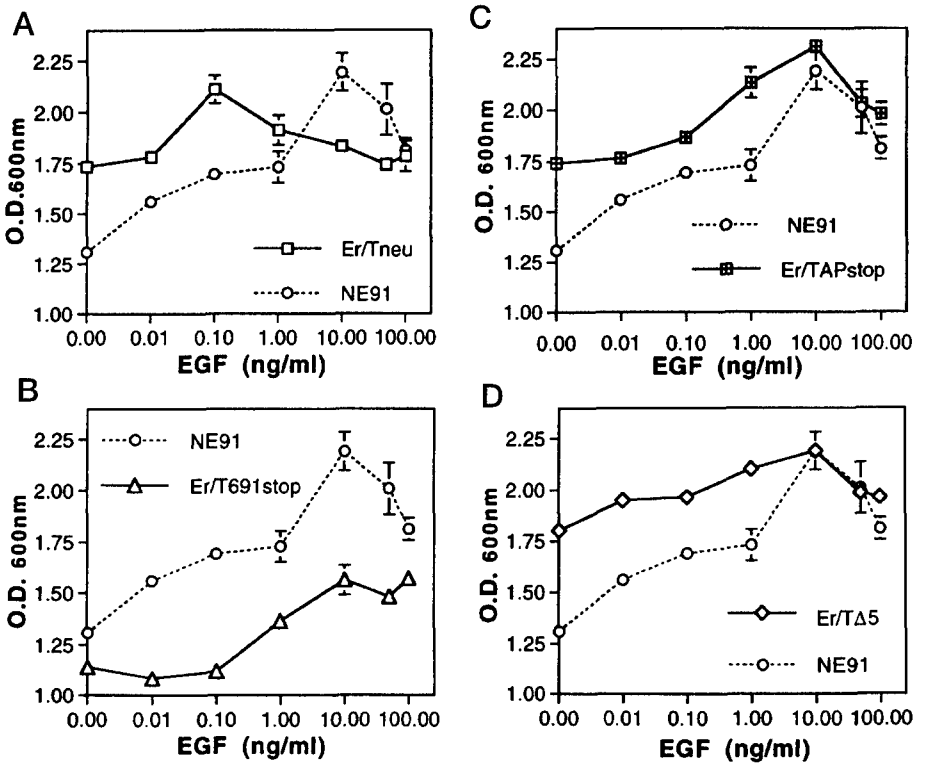

FIG. 5. **EGF-induced cell proliferation.** Cells were plated in 96-well plates (3000/well) overnight in DMEM containing 5% FBS. After starvation in serum-free media for 48 h, cells were grown in the same media supplemented with various concentrations of EGF as indicated for an additional 48-h period. Cell proliferation was determined by the MTT assay as described under "Experimental Procedures." The resultant OD_{600} was plotted against the relevant EGF concentration. NE91 cells was used as a control for the cell lines presented: *A*, Er/neu; *B*, Er/T691stop; *C*, Er/TAPstop; *D*, Er/TΔ5.

of tyrosine phosphorylation of its carboxyl terminus, as the oncogenicity of $p185^{neu}$ was greatly reduced by alteration of several tyrosine residues (41) or large structural deletions, such as seen with TAPstop (42). Transforming ability of ectodomain-deleted TΔ5 in this system was less potent than full-length $p185^{neu}$, possibly due to the reduced efficiency of forming active receptor complexes when compared with full-length oncogenic $p185^{neu}$ (27) (see Fig. 2).

We examined whether co-expression of EGFR with $p185^{neu}$ and its derivatives could enhance transforming efficiency compared with cells expressing these mutant $p185^{neu}$ proteins alone. Cell lines listed in Table I (except kinase-deficient T691stop and Er/T691stop clones) were able to form foci independent of ligand stimulation (data not shown). Co-expression of EGFR with $p185^{neu}$ in Er/neu cells increased the ability to form foci, both in density and absolute number (by greater than 3-fold). However, co-expression of EGFR with kinase-active truncated mutant TAPstop or TΔ5 did not enhance focus formation efficiency in Er/TAPstop and Er/TΔ5 cells when compared with TAP/stop and TΔ5 cells, respectively (data not shown).

The colony growth efficiency of these clones in soft agar is also summarized in Table I. B104-1-1 cells expressing high levels of $p185^{neu}$ served as a positive control, while Er/T691stop clones served as a negative control and did not exhibit transformed colonies under the same conditions. Compared with B104-1-1 cells, cells expressing lower levels of oncogenic $p185^{neu}$ formed colonies less efficiently. However, more colonies were observed in EGFR-co-expressing Er/neu cells. Co-expression of EGFR with $p185^{neu}$ still permits functional heterodimerization in addition to homodimerization of either receptor, resulting in elevated biological activity, contributing to increased transforming activity *in vitro*. Cells expressing kinase-active truncated mutant TAPstop or TΔ5 mutant proteins alone displayed reduced colony growth efficiency in soft agar when compared with control B104-1-1 cells, although the expression levels of $p185^{neu}$ variants in these cells were similar. Critically, co-expression of EGFR with TΔ5 or TAPstop did not increase colony growth efficiency in soft agar.

Tumorigenicity was studied by injection of these mutant clones individually into athymic mice. Results are presented in Table I, which summarizes receptor expression levels, tumor frequency, and tumor size. B104-1-1 cells expressing oncogenic $p185^{neu}$ were used as a positive control and tumors caused by those cells appeared and grew quickly (with a latency of 5–7 days). No tumors were observed with kinase-deficient mutant clones T691stop and Er/T691stop cells (>10 weeks observation). Co-expression of EGFR and $p185^{neu}$, each at low levels, in Er/neu cells greatly accelerated tumor appearance (~2 weeks), and the tumors grew aggressively when compared with $p185^{neu}$ cells that also expressed low level of oncogenic $p185^{neu}$ (>4–5 weeks). Cooperative signaling between EGFR and $p185^{neu}$ was thus also observed in tumorigenicity assays *in vivo*. TΔ5 protein expression was sufficient to induce tumors (latency period of 2–3 weeks), and TAPstop mutant receptor expression also resulted in tumor formation (latency of 4–5 weeks). Receptor expression levels for these two mutant proteins was close to that in B104-1-1 cells. Notably, co-expression of EGFR with these mutant proteins, *i.e.* in Er/TAPstop and in Er/TΔ5, did not promote tumor growth.

The failure of distinct endodomain interactions between $p185^{neu}$ and EGFR, caused by an ectodomain deletion (TΔ5 mutant), or the lack of a functional COOH terminus (TAPstop mutant), clearly impairs signaling needed for transformation.

EGF-dependent Cell Proliferation of Cell Lines Co-expressing EGFR and Mutant $p185^{neu}$—To analyze whether EGF-dependent heterodimerization conveys signals leading to cooperative mitogenesis, we used the MTT assay to study proliferation of various cell lines. NE91 cells expressing EGFR only served as a positive control, and showed typical EGF induction of cell growth. As expected, the maximal induction dosage of EGF was 10 ng/ml, consistent with previous observations (44). However, the maximum induction dosage of EGF in Er/neu cells was ~0.1 ng/ml, 2 orders of magnitude less than that observed in NE91 cells (Fig. 5*A*). These data suggested that $p185^{neu}$ sensitized the EGF receptor responding to ligand.

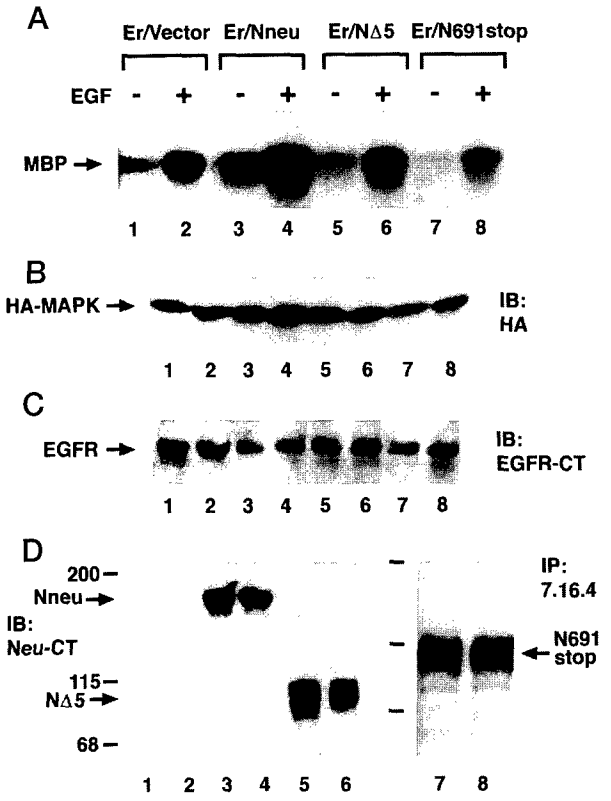

FIG. 6. **EGF-induced MAP kinase activity.** COS7 cells transiently expressing exogenous HA-MAPK, EGFR, and wild-type or mutant p185$^{c\text{-}neu}$ were treated with or without EGF (50 ng/ml) for 5 min as indicated. *A*, cells were then lysed, and anti-HA immunocomplexes were washed and underwent kinase reaction as described under "Experimental Procedures." The phosphorylation level of myelin basic protein were shown after autoradiography. *B–D*, equal amounts of cell extracts were used for examining ectopically expressed proteins. Antibodies used in immunoblot (*IB*) were indicated. Protein signals were developed by ECL. *Lanes 1–8* in these panels are correspondent to those in *panel A*. *D* (*lanes 7* and *8*), cells were metabolically labeled with [^{35}S]methionine and cell extracts were immunoprecipitated (*IP*) with 7.16.4 and analyzed in SDS-PAGE followed by autoradiography. Similar results were obtained in other two independent experiments.

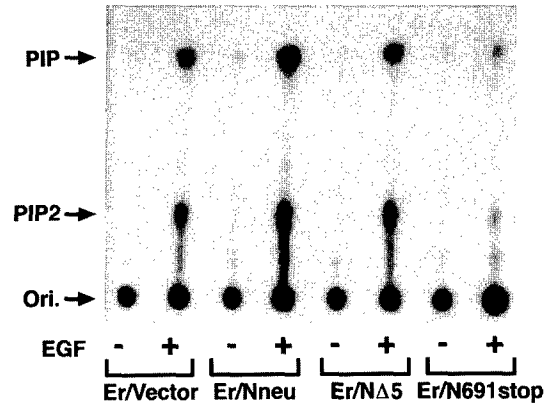

FIG. 7. **EGF-induced PI 3-kinase activity.** COS7 cells transiently expressing EGFR and wild-type or mutant p185$^{c\text{-}neu}$ (as indicated) were treated with or without EGF (50 ng/ml) for 5 min after serum starvation for 24 h. Equal amounts of cell extracts were immunoprecipitated by anti-Tyr(P) (4G10) and analyzed for PI 3-kinase activity as described under "Experimental Procedures." Autoradiogram of thin layer chromatography plate exposed overnight is shown. The positions of origin (*ori.*), phosphatidylinositol 3-phosphate (*PIP*), and phosphatidylinositol 3,4-bisphosphate (*PIP2*) were indicated by *arrows*. Data shown are representative of three individual experiments.

In contrast, the presence of T691stop in Er/T691stop cells suppressed the proliferative response to EGF, and cell growth was dramatically reduced (Fig. 5*B*). These results correlated with the inhibition of EGFR kinase (Figs. 3*E* and 4*B*). Interestingly, the EGFR in Er/TAPstop and Er/TΔ5 cells behaved normally in EGF-dependent mitogenesis when compared with that in NE91 cells, except that the basal growth level was higher (Fig. 5, *C* and *D*) due a more transformed phenotype (data not shown). These data correlated with previous observations (Figs. 2–4), suggesting that EGFR signaling is comparable in Er/TAPstop and in Er/TΔ5 clones to that seen in NE91 cells, *i.e.* neither enhanced nor suppressed. However, trans-receptor signaling was not observed due to either defective heterodimerization in Er/TAPstop cells or failure of heterodimerization in Er/TΔ5 cells.

EGF-dependent MAP Kinase and PI 3-Kinase Activation—To understand the mechanism underlying synergistic proliferative and transforming signal propagated by heteroreceptor interaction, we studied the EGF-induced MAP kinase and PI3 kinase pathways signaling phenomena. The proto-oncogenic p185 (Nneu) and its derivatives (NΔ5 or, N691stop) were co-expressed with EGFR, to evaluate EGF-dependent activation of downstream kinases, since p185^{neu} and TΔ5 are both constitutively active tyrosine kinases. An epitope-tagged HA-MAPK was also co-expressed with the combination of receptors in COS7 cells to examine downstream ERK activation.

Co-expression of p185$^{c\text{-}neu}$, but not NΔ5, with EGFR increased MAP kinase activity upon EGF stimulation. In contrast, EGFR-mediated MAP kinase activity in N691stop-co-expressing cells was suppressed when compared with cells expressing EGFR and an empty vector control (Fig. 6*A*). Equivalent protein expression levels of epitope-tagged HA-MAPK was also confirmed in these studies (Fig. 6*B*). Ectopically expressed EGFR and wild-type or mutant p185 forms were detected by immunoblot using anti-receptor specific antisera (Fig. 6, *C* and *D*). Since the intracellular domain-deleted N691stop could not be recognized by antiserum against the Nneu COOH terminus, the expression of N691stop was independently confirmed using metabolic labeled cell extracts followed by anti-neu immunoprecipitation (Fig. 6*D*, *lanes 7* and *8*).

Activation of PI-3-kinase requires phosphorylation of the Src homology 2-containing adapter p85 by receptor tyrosine kinases. Phosphatidylinositides are critical signaling intermediates and influence cell growth, differentiation, and adhesion (52). ErbB family members, notably ErbB-3, have been shown to associate with the p85 subunit of PI 3-kinase (53). To examine the influence of wild-type or mutant p185 on EGF-dependent activation of PI 3-kinase, plasmids expressing EGFR with vector or p185 variants were transiently expressed in COS7 cells. PI 3-kinase activity was examined in serum-starved cells with or without EGF stimulation. We observed a similar magnitude of the EGF-induced PI 3-kinase activity in cells expressing EGFR only or Er/NΔ5. The PI 3-kinase activity was much greater in Er/p185$^{c\text{-}neu}$ cells, and much weaker in Er/N691stop cells (Fig. 7). Expression patterns of these receptor proteins were determined (Fig. 6, *C* and *D*).

The observed super PI 3-kinase activity in Er/p185$^{c\text{-}neu}$ cells may arise through the tyrosine phosphorylation of the p85 subunit by the heteroreceptor complexes. We believe heteroreceptor complexes are more active since truncated p185 proteins alone do not seem effective at interaction with p85 (data not shown). Induced PI 3-kinase and MAPK activities therefore paralleled the heterodimerization and trans-activation events depicted in Figs. 2–4, and biological results obtained in Table I and Fig. 5. Functional heterodimerization observed in Er/neu cells permits cooperation and diversification of signaling, which contrasts with the formation of signaling-defective com-

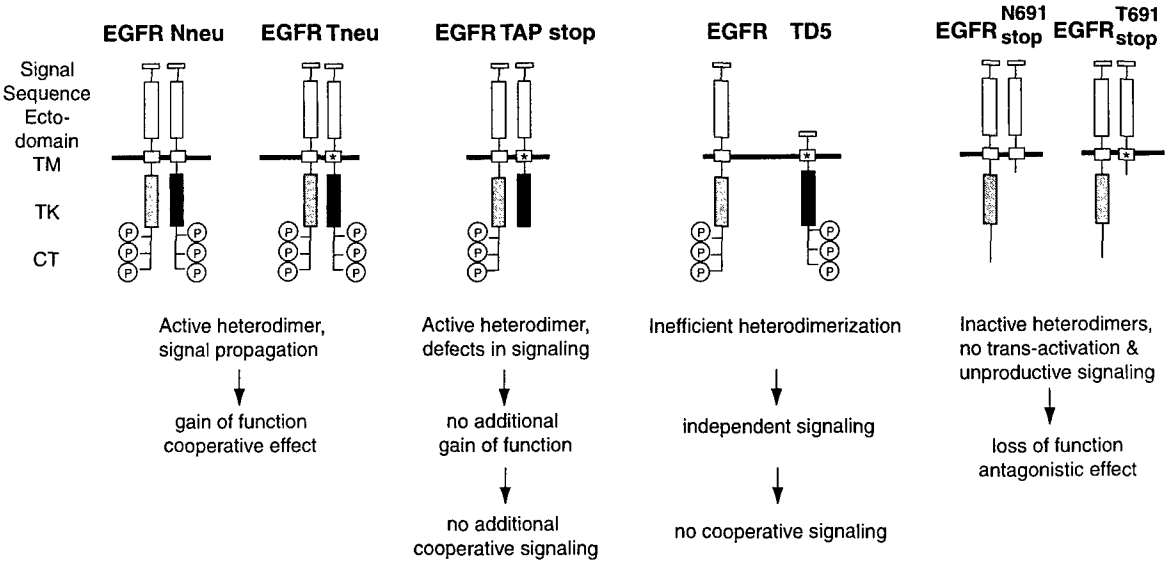

FIG. 8. **The role of p185^{neu} subdomains in heterodimerization with EGFR and resultant signaling consequences.** Functional heterodimerization requires the ectodomain for ligand-mediated physical associations, the endodomain for kinase transactivation, and the carboxyl terminus for cross-phosphorylation and combinatorial cellular signaling. Deletion of each subdomain results in inefficient heterodimerization, preventing kinase activation and defects in cooperative cellular signaling, respectively. *TD5*, TΔ5.

plexes in Er/T691stop cells or the failure of heterodimerization observed in Er/TΔ5 cells.

DISCUSSION

Using p185^{neu} mutants, which retain the capacity to homodimerize, we observed that EGF-induced heterodimerization could occur. Heterodimerization was seen in cells co-expressing EGFR with TAPstop or T691stop mutant receptors, but not with the extracellular domain-deleted TΔ5 (Fig. 2), demonstrating that the ectodomain of p185^{neu} is necessary and sufficient for heterodimerization with EGFR. Indeed, heterodimerization of the EGFR and N691stop form derived from proto-oncogenic p185^{neu} has been observed to occur preferentially to either p185$^{c\text{-}neu}$ or EGFR·EGFR homodimerization (37).

Two alternative assays confirmed trans-activation of ErbB family proteins following heterodimer formation. Anti-phosphotyrosine blotting showed that enhancement of tyrosine phosphorylation in response to EGF occurred only in cells co-expressing EGFR with the full-length p185^{neu} kinase, but not with the TAPstop or TΔ5 mutant receptors. It appears that EGFR and the T691stop neu mutant formed a kinase-inactive complex (Fig. 3), as described previously for the N691stop form (37).

An analysis of EGF-induced receptor internalization, a kinase-dependent event, also indicated that receptor trans-activation is required for efficient internalization of the EGFR found in these heteromers (Fig. 4). Full-length p185^{neu} and TAPstop proteins were modulated by EGF and showed co-internalization with EGFR efficiently, indicating an active heterodimer was formed. Co-expression of TΔ5 with EGFR did not affect normal endocytosis of EGFR since TΔ5 could not associate with EGFR, while T691stop neu expression interfered with normal EGFR down-modulation.

Recent studies have shown that the signal adapter Grb2 is required for efficient endocytosis of EGFR (54), and selective and regulated signal transduction from activated receptor tyrosine kinases may continue within the endosome (55). Interestingly, kinase-mediated activation of ERKs may also involve endocytotic trafficking since inhibition of clathrin-mediated endocytosis has been shown to impair rapid EGF-stimulated activation of ERKs (56). Therefore, it is reasonable to speculate that EGF-induced endocytosis of these receptor complexes reflects both heterodimeric kinase activity and the efficiency of activating downstream signaling components. Indeed, full-length p185^{neu}, but not other p185^{neu}-derived deletion mutants, displayed increased coupling of the Src homology 2-containing signaling molecule p85 to receptor activation (data not shown).

We previously reported that the co-expression of EGFR with p185$^{c\text{-}neu}$ (22), but not with kinase-deficient p185$^{c\text{-}neu}$ (44), synergistically transformed rodent fibroblasts. EGFR and p185$^{c\text{-}neu}$ associates into an active kinase complex (24) which upregulates EGF receptor function by increasing EGF binding affinity, ligand-induced DNA synthesis, and cell proliferation (23). In the current studies, when EGFR was co-expressed with oncogenic p185^{neu} at physiological levels (~10^4 receptors/cell), we also observed enhancement of tumor growth (4-fold) *in vivo* and anchorage-independent growth (~2-fold) *in vitro*, compared with the cells expressing p185^{neu} alone (Table I). Deletion of 122 amino acid residues from the carboxyl terminus of p185^{neu} eliminates three known tyrosine autophosphorylation sites (TAPstop mutant), and causes impaired cellular signaling and transforming potency (41). Overexpression of EGFR with the carboxyl-terminally truncated TAPstop mutant receptor, although leading to an active heterodimeric complex, did not recover the diminished transforming potency of TAPstop (Table I), indicating that signaling propagation through the carboxyl terminus of p185^{neu} could not be restored by association with full-length EGFR. These data emphasize that cooperative signaling requires not only the formation of an active kinase complex, but also a heteromeric functional carboxyl termini within the two receptor endodomains that recruit various downstream molecules required to generate signal to mediate cell growth and transformation.

The current results indicate that p185^{neu}·EGFR heterodimerization is greatly favored, even in the presence of the neu transmembrane point mutation that facilitates p185^{neu} homodimerization (12). Together with the observation that ErbB-2 is the preferred heterodimerization partner of all ErbB members (36), these studies emphasize that Neu·ErbB-2 may mediate signaling diversity through structural interactions governed by particular ectodomain sequences. For instance,

ErbB-3 is a less active kinase than other ErbB proteins (57), but serves as a binding site for Neu differentiating factor (28) and forms a potent heterodimer with ErbB-2, consequently engaging various downstream substrates. Neu·ErbB-2 may not be required for ligand binding, but may reconstitute signaling by laterally engaging other ErbB proteins in some preferred, but not well understood manner.

Kinase phosphorylation increases the affinity of binding of Src homology 2 and Src homology 3 domain-containing substrates, and initiates a variety of cascades. The binding of Grb2·Sos complexes to the active EGFR activates the Ras/Raf/MAP kinase cascade (58). Another downstream effector whose importance in cell signaling and, potentially, in tumorigenesis is becoming increasingly understood is PI 3-kinase (52). PI 3-kinase activation has also been shown to be essential for induction of DNA synthesis by EGF (59). Current studies have demonstrated that EGF-induced ErbB heterodimers activate both the ERK and PI 3-kinase pathways. Functional wild-type heterodimers, but not defective mutant heterodimers, efficiently induce both ERK and PI 3-kinase activities, which contribute to the synergistic effects on mitogenesis and cellular transformation.

As depicted in Fig. 8, these results further support the notion that cooperative signaling caused by $p185^{neu}$·EGF receptor ensembles requires the ectodomain for ligand-mediated physical association, while the intracellular domain provides contacts for efficient intermolecular kinase activation. The phosphorylated carboxyl terminus is essential for recruiting particular cellular substrates required for signal diversification.

In particular, specific ectodomain associations may therefore underlie the combinatorial interactions within the ErbB family required for signal diversification. These properties may be features that are used by many receptor ensembles involved in enzymatic signaling in cells.

REFERENCES

1. Ullrich, A., Coussens, L., Hayflick, J. S., Dull, T. J., Gray, A., Tam, A. W., Lee, J., Yarden, Y., Libermann, T. A., Schlessinger, J., Downward, J., Mayes, E. L. V., Whittle, N., Waterfield, M. D. & Seeburg, P. H. (1984) *Nature* **309,** 418–425
2. Schechter, A. L., Stern, D. F., Vaidyanathan, L., Decker, S. J., Drebin, J. A., Greene, M. I. & Weinberg, R. I. (1984) *Nature* **312,** 513–516
3. Yamamoto, T., Ikawa, S., Akiyama, T., Semba, K., Nomura, N., Miyajima, N., Saito, T. & Toyoshima, K. (1986) *Nature* **319,** 230–234
4. Kraus, M. H., Issing, W., Miki, T., Popescu, N. C. & Aaronson, S. A. (1989) *Proc. Natl. Acad. Sci. U. S. A.* **86,** 9193–9197
5. Plowman, G. D., Culouscou, J., Whitney, G. S., Green, J. M., Carlton, G. W., Foy, L., Neubauer, M. G. & Shonyab, M. (1993) *Proc. Natl. Acad. Sci. U. S. A.* **90,** 1746–1750
6. Dougall, W. C., Qian, X., Peterson, N. C., Miller, M. J., Samanta, A. & Greene, M. I. (1994) *Oncogene* **9,** 2109–2123
7. Lee, K. F., Simon, H., Chen, H., Hung, M. C. & Hauser, C. (1995) *Nature* **378,** 394–398
8. Gassmann, M., Casagranda, F., Orioli, D., Simon, H., Lai, C., Klein, R. & Lemke, G. (1995) *Nature* **378,** 390–394
9. Threadgill, D. W., Dlugose, A. A., Hansen, L. A., Tennenbaum, T., Lichti, U., Lee, D., LaMantia, C., Mourton, T., Herrup, K., Harris, R. C., Barnard, J. A., Yuspa, S. H., Coffey, R. J. & Magnuson, T. (1995) *Science* **269,** 230–234
10. O'Rourke, D. M., Zhang, X. & Greene, M. I. (1997) *Proc. Assoc. Am. Physicians* **109,** 209–219
11. Bargmann, C. I., Hung, M.-C. & Weinberg, R. A. (1986) *Cell* **45,** 649–657
12. Weiner, D. B., Liu, J., Cohen, J. A., Williams, W. V. & Greene, M. I. (1989) *Nature* **339,** 230–231
13. Weiner, D. B., Kokai, Y., Wada, T., Cohen, J. A., Williams, W. V. & Greene, M. I. (1989) *Oncogene* **4,** 1175–1183
14. Moscatello, D. K., Montgomery, R. B., Sundareshan, P., McDanel, H., Wong, M. Y. & Wong, A. J. (1996) *Oncogene* **13,** 85–96
15. O'Rourke, D. M., Nute, E. J. L., Davis, J. G., Wu, C., Lee, A., Murali, R., Zhang, H.-T., Qian, X., Kao, C.-C. & Greene, M. I. (1998) *Oncogene* **16,** 1197–1207
16. Slamon, D. J., Clark, G. M., Wong, S. G., Levin, W. J., Ullrich, A. & Mcguire, W. L. (1987) *Science* **235,** 177–182
17. Slamon, D. J., Godolphin, W., Jones, L. A., Holt, J. A., Wong, S. G., Kieth, D. E., Levin, W. J., Stuart, S. G., Udove, J., Ullrich, A. & Press, M. F. (1989) *Science* **244,** 707–712
18. Di Fiore, P. P., Pierce, J. A., Fleming, T. P., Hazan, R., Ullrich, A., King, C. R., Schlessinger, J. & Aaronson, S. A. (1987) *Cell* **51,** 1063–1070
19. Hudziak, R. M., Schlessinger, J. & Ullrich, A. (1987) *Proc. Natl. Acad. Sci. U. S. A.* **84,** 7159–7163
20. LeVea, C. M., Myers, J. N., Dougall, W. C., Qian, X. & Greene, M. I. (1993) *Receptor* **3,** 293–309
21. Samanta, A., LeVea, C. M., Dougall, W. C., Qian, X. & Greene, M. I. (1994) *Proc. Natl. Acad. Sci. U. S. A.* **91,** 1711–1715
22. Kokai, Y., Myers, J. N., Wada, T., Brown, V. I., LeVea, C. M., Davis, J. G., Dobashi, K. & Greene, M. I. (1989) *Cell* **58,** 287–292
23. Wada, T., Qian, X. & Greene, M. (1990) *Cell* **61,** 1339–1347
24. Qian, X. L., Decker, S. J. & Greene, M. I. (1992) *Proc. Natl. Acad. Sci. U. S. A.* **89,** 1330–1334
25. Goldman, R., Benlevy, R., Peles, E. & Yarden, Y. (1990) *Biochemistry* **29,** 11024–11028
26. Dougall, W. C., Qian, X., Miller, M. J. & Greene, M. I. (1996) *DNA Cell Biol.* **15,** 31–40
27. Qian, X., Dougll, W. C., Fei, Z. & Greene, M., I. (1995) *Oncogene* **10,** 211–219
28. Peles, E. & Yarden, Y. (1993) *BioEssays* **15,** 815–824
29. Carraway, K. L., III, Sliwkowski, M. X., Akita, R., Platko, J. V., Guy, P. M., Nuijens, A. A., Diamonti, J., Vandlen, R. L., Cantley, L. C. & Cerione, R. A. (1994) *J. Biol. Chem.* **269,** 14303–14306
30. Riese, D. J., van Raaij, T. M., Plowman, G. D., Andrews, G. C. & Stern, D. F. (1995) *Mol. Cell. Biol.* **15,** 5770–5776
31. Cohen, B. D., Green, J. M., Foy, L. & Fell, H. P. (1996) *J. Biol. Chem.* **271,** 4813–4818
32. Pinkas-Kramarski, R., Soussan, L., Waterman, H., Levkowitz, G., Alroy, I., Lavi, S., Seger, R., Ratzkin, B. J., Sela, M., & Yarden, Y. (1996) *EMBO J.* **15,** 2452–2467
33. Zhang, K., Sun, J., Liu, N., Wen, D., Chang, D., Thomason, A. & Yoshinaga, S. K. (1996) *J. Biol. Chem.* **271,** 3884–3890
34. Tzahar, E., Waterman, H., Chen, X., Levkowitz, G., Karunagaran, D., Lavi, S., Ratzkin, B. J. & Yarden, Y. (1996) *Mol. Cell. Biol.* **16,** 5276–5287
35. Alimandi, M., Romano, A., Curia, M. C., Muraro, R., Fedi, P., Aaronson, S. A., Di, F. P. & Kraus, M. H. (1995) *Oncogene* **10,** 1813–1821
36. Grause-Porta, D., Beerli, R. R., Daly, J. M. & Hynes, N. (1997) *EMBO J.* **16,** 1647–1655
37. Qian, X., Dougall, W. C., Hellman, M. E. & Greene, M. I. (1994)*Oncogene* **9,** 1507–1514
38. Drebin, J. A., Stern, D. F., Link, V. C., Weinberg, R. A. & Greene, M. I. (1984) *Nature* **312,** 545–548
39. Myers, J. N., LeVea, C. M., Smith, J. E., Kallen, R. G., Tung, L. & Greene, M. I. (1992) *Receptor* **2,** 1–16
40. Decker, S. J. & Harris, P. (1989) *J. Biol. Chem.* **264,** 9204–9209
41. Mikami, Y., Davis, J. G., Dobashi, K., Dougall, W. C., Myers, J. N., Brown, V. I. & Greene, M. I. (1992) *Proc. Natl. Acad. Sci. U. S. A.* **89,** 7335–7339
42. O'Rourke, D. M., Qian, X., Zhang, H. T., Davis, J. G., Nute, E., Meinkoth, J. & Greene, M. I. (1997) *Proc. Natl. Acad. Sci. U. S. A.* **94,** 3250–3255
43. Pruss, R. M. & Herschman, H. R. (1977) *Proc. Natl. Acad. Sci. U. S. A.* **74,** 3918–3921
44. Qian, X., LeVea, C. M., Freeman, J. K., Dougall, W. C. & Greene, M. T. (1994) *Proc. Natl. Acad. Sci. U. S. A.* **91,** 1500–1504
45. Moscatello, D. K., Holgado-Madrugal, M., Emlet, D. R., Montgomery, R. B. & Wong, A. J. (1998) *J. Biol. Chem.* **273,** 200–206
46. Stern, D. F. & Kamps, M. P. (1988) *EMBO J.* **7,** 995–1001
47. Akiyama, T., Saito, T., Ogawara, H., Toyoshima, K. & Yamamoto, T. (1988) *Mol. Cell. Biol.* **8,** 1019–1026
48. Kokai, Y., Dobashi, K., Weiner, D. B., Myers, J. N., Nowell, P. C. & Greene, M. I. (1988) *Proc. Natl. Acad. Sci. U. S. A.* **85,** 5389–5393
49. King, C. R., Borrello, I., Bellot, F., Comoglio, P. & Shlessinger, J. (1988) *EMBO J.* **7,** 1647–1651
50. Sorkin, A. & Waters, C. (1993) *BioEssays* **15,** 375–382
51. Segatto, O., Lonardo, F., Pierce, J. H., Bottaro, D. P. & Di Fiore, P. P. (1990) *New Biol.* **2,** 187–195
52. Hunter, T. (1997) *Cell* **88,** 333–346
53. Fedi, P., Pierce, L., Di Fiore, P. P. & Kraus, M. H. (1994) *Mol. Cell. Biol.* **14,** 492–500
54. Wang, Z. & Moran, M. F. (1996) *Science* **272,** 1935–1938
55. Bergeron, J. J., Di, G. G., Baass, P. C., Authier, F. & Posner, B. I. (1995) *Biosci. Rep.* **15,** 411–418
56. Vieira, A. V., Lamaze, C. & Schmid, S. L. (1996) *Science* **274,** 2086–2089
57. Guy, P., Platko, J. V., Cantley, L. C., Cerione, R. A. & Carraway, K. L. (1994) *Proc. Natl. Acad. Sci. U. S. A.* **91,** 8132–8136
58. Buday, L., and Downward, J. (1993) *Cell* **73,** 611–620
59. Roche, S., Koegl, M., and Courtneidge, S. A. (1994) *Proc. Natl. Acad. Sci. U. S. A.* **91,** 9185–9189

Proc. Natl. Acad. Sci. USA
Vol. 96, pp. 6434–6438, May 1999
Medical Sciences

Induction of the Tat-binding protein 1 gene accompanies the disabling of oncogenic erbB receptor tyrosine kinases

BYEONG-WOO PARK*, DONALD M. O'ROURKE*†, QIANG WANG*, JAMES G. DAVIS*, ANDREW POST*, XIAOLAN QIAN*, AND MARK I. GREENE*‡

Departments of *Pathology and Laboratory Medicine, and †Neurosurgery, Center for Receptor Biology and Cell Growth, University of Pennsylvania School of Medicine, 36th and Hamilton Walk, Philadelphia, PA 19104

Communicated by Peter C. Nowell, University of Pennsylvania School of Medicine, Philadelphia, PA, March 9, 1999 (received for review January 11, 1999)

ABSTRACT **Conversion of a malignant phenotype into a more normal one can be accomplished either by down-regulation of erbB family surface receptors or by creating inactive erbB heterodimers on the cell surface. In this report, we report the identification and cloning of differentially expressed genes from antibody-treated vs. untreated fibroblasts transformed by oncogenic p185^{neu}. We repeatedly isolated a 325-bp cDNA fragment that, as determined by Northern analysis, was expressed at higher levels in anti-p185^{neu}-treated tumor cells but not in cells expressing internalization defective p185^{neu} receptors. This cDNA fragment was identical in amino acid sequence to the recently cloned mouse Tat binding protein-1 (mTBP1), which has 98.4% homology to the HIV tat-binding protein-1 (TBP1). TBP1 mRNA levels were found to be elevated on inhibition of the oncogenic phenotype of transformed cells expressing erbB family receptors. TBP1 overexpression diminished cell proliferation, reduced the ability of the parental cells to form colonies *in vitro*, and almost completely inhibited transforming efficiency in athymic mice when stably expressed in human tumor cells containing erbB family receptors. Collectively, these results suggest that the attenuation of erbB receptor signaling seems to be associated with activation/induction or recovery of a functional tumor suppressor-like gene, *TBP1*. Disabling erbB tyrosine kinases by antibodies or by trans-inhibition represents an initial step in triggering a TBP1 pathway.**

ErbB family receptor kinases mediate oncogenic transformation by mutation, overexpression, or coexpression leading to homodimeric or heterodimeric complexes that mediate synergistic signaling (1–5). Continual expression of p185^{neu} is necessary for the maintenance of the neoplastic phenotype of neu-transformed cells (1). Incubation of oncogenic p185^{neu}-expressing tumor cells with the anti-neu mAb 7.16.4 causes phenotypic reversal *in vitro* and *in vivo* (6, 7). The mechanism of phenotypic reversal of tumor cells expressing the p185$^{neu/c\text{-}erbB2}$ oncogene occurring with anti-neu-specific mAb treatment has not been defined completely, although this mechanism has been characterized as arising as a consequence of disabling the kinase complex, a process in which a fraction of the receptors becomes down-modulated (6–8).

The binding of antibody to the extracellular domain of the p185^{neu} receptor mediates down-regulation and increases p185^{neu} oncoprotein degradation by causing the p185^{neu} complex to enter a degradation pathway. Endosomes were found to carry p185^{neu}-containing receptor aggregates to lysosomes where the complex was degraded (9).

Here, we used mRNA differential display (10, 11) to isolate genes that are specifically expressed in cells treated with the anti-p185^{neu} mAb 7.16.4. We repeatedly identified a 325-bp cDNA fragment called 3C bearing significant homology to the HIV tat-binding protein-1 (TBP1) on antibody-mediated down-regulation of the oncogenic p185^{neu} receptor associated with inhibition of transformation. The 3C fragment is completely identical to the recently cloned mouse tat binding protein-1 (mTBP1), which itself is 98% homologous to the human TBP1 over 439 aa (12). Northern blot analysis confirmed that this fragment and the TBP1 cDNA hybridized to mRNA isolated from cells undergoing phenotypic reversal by antibody treatment.

TBP1 has been reported to suppress tat-mediated transactivation of HIV replication (13). Nakamura *et al.* (12) established that full-length murine TBP1 also suppresses Tat-mediated transactivation. A TBP1-interacting protein (TBPIP), which colocalizes *in vivo* and synergistically enhances the inhibitory action of TBP1 on Tat activity *in vitro*, also has been cloned recently (14).

To investigate the biological effects of TBP1, we transfected the full length of TBP1 cDNA into a variety of human cell lines, U87MG, SK-BR-3, and MCF-7, which express erbB family genes. Ectopically expressed TBP1 was able to cause a reversion of the transformed phenotype. Additionally, basal TBP1 mRNA levels were found to be higher in phenotypically inhibited cells. These studies suggest that induction of TBP1 mediates inhibition of cell growth and transformation of erbB-inhibited cells.

MATERIALS AND METHODS

Cell Lines. B104-1-1 cells were derived from NIH 3T3 cells transfected with p185^{neu} and have been described (6). U87MG cells are human brain tumor cells; SK-BR-3 cells and MCF-7 cells are primary human breast cancer cells obtained from the American Type Culture Collection. These cells were cultured in DMEM containing 10% (vol/vol) FBS, 1% L-glutamine, and 1% penicillin/streptomycin at 37°C, 95% humidity, and 5% CO_2. The NR6TintΔ cells containing internalization-defective p185^{neu} receptors have been described (15).

Incubation of Cell Lines with mAb 7.16.4. The mAb 7.16.4 has been described (6, 7). B104-1-1 cells were grown overnight in 6-well dishes and treated with mAb 7.16.4 (10 μg/ml) for 0–4 h at 37°C. Cells were harvested, washed, stained with saturating amounts of mAb 7.16.4, and restained with anti-mouse IgG FITC. Cells were then processed for flow cytometric analysis as described (15).

RNA Isolation and mRNA Differential Display. Total RNA was purified from cell lysates by using the RNeasy Mini Kit (Qiagen, Valencia, CA) and the protocol supplied with the kit.

The publication costs of this article were defrayed in part by page charge payment. This article must therefore be hereby marked "*advertisement*" in accordance with 18 U.S.C. §1734 solely to indicate this fact.

PNAS is available online at www.pnas.org.

Abbreviations: RT-PCR, reverse transcriptase–PCR; MTT, 3-(4,5-dimethylthiazol-2-yl)-2,5-diphenyl tetrazolium bromide; EGFR, epidermal growth factor receptor.

‡To whom reprint requests should be addressed. e-mail: greene@reo.med.upenn.edu.

An mRNA Map Kit from GenHunter (Nashville, TN) was used, and the manufacturer's protocol was followed. DNase-treated total RNA (2 μg) was reverse-transcribed by using Super-Script II (United States Biochemical) with oligo(dT) primers T12MG, T12MC, or T12MA and amplified with the library 10-mers AP-3 (5′-AGGTGACCGT-3′) or AP-6 (5′-GCAATCGATG-3′) as described in the kit. The PCR products were run on a 6% sequence gel with the cDNAs that were to be compared run side-by-side. Bands representing differentially expressed genes were eluted from the gel, reamplified, subcloned into the pCRII vector as described in the TA cloning kit (Invitrogen), and sequenced on a 6% denaturing gel.

Generation of Stable TBP1 Transfectants and Confirmation of Transgene Expression by Reverse Transcriptase–PCR (RT-PCR). The TBP1 cDNA was inserted into the *Eco*RI site of the pBK-CMV (Stratagene) vector. Stable TBP1 transfectants were generated by transfecting the pBK-CMV–TBP1 plasmid into a panel of human cell lines (U87MG, SK-BR-3, and MCF-7) by using Lipofectamine (GIBCO). G418 (0.8 μg/ml; GIBCO) was used to select for the transfected cell populations, and Northern blot analysis was used to identify clones that expressed TBP1.

First-strand cDNA was prepared from 3 μg of total RNA by using the Superscript Preamplification System for first-strand cDNA Synthesis Kit (GIBCO/BRL). To confirm the integrity of the first-strand cDNAs, we amplified β-actin sequences by using the rat β-actin control amplifier set (CLONTECH), which yielded a 764-bp product. Exogenous/transfected TBP1-derived transcripts were amplified by using the pBK-CMV vector T7 primer (5′-GTAATACGCTCACTATAGGGC-3′) and a TBP1-specific primer designated C2 (5′-AGAAGAAAGCCAACCTAC-3′), which yielded a 216-bp product. After RT-PCR, the products were run on 1.8% agarose gels to evaluate the presence or absence of the amplified product.

Cell Proliferation Assay. The proliferation assay, as measured by 3-(4,5-dimethylthiazol-2-yl)-2,5-diphenyl tetrazolium bromide (MTT) incorporation, has been described (16).

***In Vitro* and *in Vivo* Tumorigenesis Assays.** Anchorage-independent growth was determined by assessing the colony-forming efficiency of cells suspended in soft agar (6, 17). For *in vivo* experiments, NCr homozygous nude mice (6–8 weeks old) were purchased from the National Cancer Institute (Bethesda, MD). Cells (1×10^6) were suspended in 0.1 ml of PBS and injected intradermally into the mid dorsum of each animal. Parental U87MG cells were injected on one side of individual animals and stably TBP1–cDNA-transfected U87/TBP1 cells were injected on the contralateral side to make direct comparisons of growth within each animal. Animals were maintained in accordance with guidelines of the Committee on Animals of the University of Pennsylvania and those of the Committee on Care and Use of Laboratory Animals of the Institute of Laboratory Animal Resources. Tumor growth was monitored twice weekly for 6–10 weeks. Tumor size was calculated by measuring tumor volume (length × width × thickness).

RESULTS

Down-Regulation of p185^{neu} Surface Receptors and Differentially Expressed Genes. Differential display provided a convenient way for us to study altered gene expression in p185^{neu}-expressing B104-1-1 murine cells treated with anti-p185^{neu}. One drawback of the differential display is its susceptibility to generating false–positive clones. To compensate, we ran two differential display trials on each of the total RNAs so that we could select bands that were present in both trials. There were nine differentially expressed bands chosen for further characterization; these bands ranged in size from 230 bp to 1,000 bp, were observed in both trials, and were not differentially expressed in NIH 3T3 cells. One of these bands represented a 325-bp cDNA termed 3C, which had 100% homology with mTBP1 (Fig. 1), which is the murine homologue of the human gene tat-binding protein 1. Northern blot analysis of 7.16.4-treated B104-1-1 cells showed increased TBP1 mRNA levels of ≈1.5 kb in size when probed by both human TBP1 cDNA (Fig. 2*A*) and 3C DNA (data not shown).

Confirmation of differential expression was achieved by comparing Northern blots of antibody-treated B104-1-1 cells and untreated cells (Fig. 2 *A* and *B*). Antibody treatment of B104-1-1 cells containing elevated levels of oncogenic p185^{neu} resulted in increased expression of the mTBP1 mRNA transcript (Fig. 2 *A* and *B*). We have shown that receptor kinase activity alone is not sufficient for the endocytic process (15). A structural element, namely an internalization sequence, is also required for both mAb- and ligand-induced receptor down-regulation (15). Importantly, NR6TintΔ cells (15), which contain an internalization-defective p185^{neu} mutant protein, TintΔ (15), and lack the ability to undergo p185^{neu} internalization, did not have an increase in mTBP1 mRNA level after 7.16.4 treatment, although the basal level of mTBP1 transcript was higher in NR6TintΔ cells (Fig. 2 *A* and *B*). Notably, B104-1-1 cells contain higher levels of transforming p185^{neu} than NR6TintΔ cells and are more oncogenic (15). The basal level of the mTBP1 transcript was, as expected, greater in the less oncogenic NR6TintΔ cell.

Because disabling erbB receptor ensembles may enable a common inhibitory pathway, we also examined cells in which EGFR was inactivated but not down-modulated by a trans-inhibitory ectodomain form of p185^{neu} (T691stop neu; refs. 17 and 18). We found that the endogenous expression of TBP1 mRNA was also higher in phenotypically inhibited U87MG-derived cells expressing the kinase-deficient T691stop neu ectodomain form compared with U87MG parental cells (Fig. 2*C*). Because T691stop inhibition of erbB kinase activity does not require erbB receptor down-modulation (17, 18), these data suggest that induction of TBP1 expression after anti-p185^{neu} mAb treatment occurs by regulation of a kinase signaling pathway (Fig. 2 *A* and *C*) and is not simply a result of receptor down-modulation and degradation (Fig. 2*C*).

Inhibition of Cell Growth and Transformation by Human TBP1. To investigate the biological effects of TBP1, we transfected, by using the pBK-CMV vector, full-length TBP1 cDNA into several different cell lines, SK-BR-3, MCF-7, and U87MG, all of which express erbB family receptors. We screened the transfected subclones by Northern blot analysis, and the expression of ectopic TBP1 in subclones was also confirmed by RT-PCR analysis (Fig. 3 *A* and *B*). We amplified a 216-bp product from all of the TBP1-cDNA-transfected clones and the pBK-CMV–TBP1 plasmid construct but not in the corresponding nontransfected parental cells (Fig. 3*A*). RT-PCR with a β-actin control amplifier set produced a 764-bp amplified product from all the cell lines except for the pBK-CMV–TBP1 plasmid construct (Fig. 3*B*).

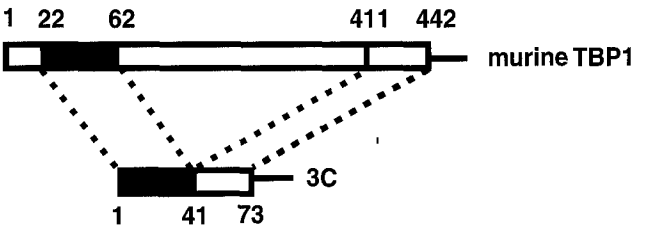

FIG. 1. Regions of homology of 3C to murine TBP1. Amino acids 1–41 of 3C correspond to amino acids 22–62 of mTBP1, and amino acids 42–73 of 3C correspond to amino acids 411–442 of mTBP1 (100% identical). The 3C C-terminal noncoding-region nucleotide sequence is 98% homologous to that of mTBP1.

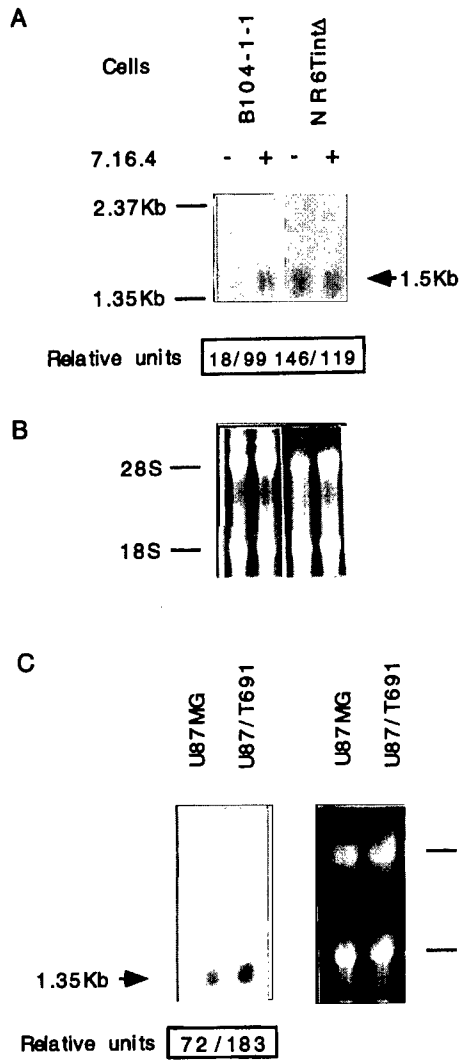

FIG. 2. Comparison and confirmation of the differentially expressed gene by Northern blot analysis and endogenous expression of TBP1 in U87MG vs. U87/T691. (*A*) B104-1-1 and NR6TintΔ cells were incubated with or without 7.16.4 (10 μg/ml) for 24 h before RNA isolation. Total RNA (10 μg) was loaded in each lane and was probed with human TBP1 cDNA probe. TBP1 expression was up-regulated with anti-p185^{neu} mAb (7.16.4) treatment in B104-1-1 cells (lanes 1 and 2) but was not changed in internalization defective NR6TintΔ cells (lanes 3 and 4). (*B*) The corresponding formaldehyde gel electrophoresis of total RNA is shown. (*C*) The U87/T691 subclone, an epidermal growth factor receptor (EGFR)-positive cell line phenotypically inhibited by the expression of a trans-inhibitory ectodomain form of p185^{neu} (T691 stop neu), showed increased endogenous levels of TBP1. Relative units are derived from scanning densitometry (Molecular Dynamics).

Cell growth of TBP1-transfected cells was evaluated by using the MTT assay (16). Transfected clones had 34–57% of proliferation inhibition compared with the corresponding parental cell lines (Fig. 4*A–C*). Cell growth was therefore greatly diminished in TBP1-transfected erbB transformed cells. The level of TBP1 mRNA in the inhibited subclones was equal to, or exceeded, the amount of mRNA detected in parental cells inhibited by antibody treatment or T691stop expression. Thus, the mRNA level was sufficiently high to play a causal role in phenotypic reversion. Transformation efficiency was assessed by using an anchorage-independent growth assay (6, 17). The ability of TBP1 transfectants to form colonies was consistently and dramatically reduced (Fig. 5*A*). Transforming efficiency of SK-BR-3/TBP1, MCF-7/TBP1, and U87MG/TBP1 subclones was inhibited 79.2 ± 3.7% (mean ± SEM), 94.2 ± 4.5%, and

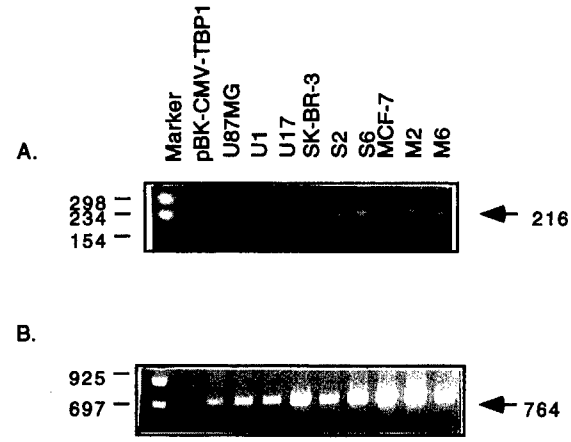

FIG. 3. Confirmation of TBP1-transfected clones by RT-PCR analysis. We made first-strand cDNA from 3 μg of each total RNA by using the Superscript Preamplification System for first-strand cDNA Synthesis Kit (GIBCO/BRL). (*A*) Amplification of the transfected TBP1 cDNA by using the pBK-CMV vector-oriented T7 primer (5′-GTAATACGCTCACTATAGGGC-3′) and the TBP1 specifically designed primer C2 (5′-AGAAGAAAGCCAACCTAC-3′) shows 216-bp product bands in only the transfected clones and the pBK-CMV–TBP1 plasmid construct and not in parental cell lines of U87MG, SK-BR-3, and MCF-7. (*B*) Amplification of actin cDNA by using the rat β-actin control amplifier set (CLONTECH) shows a 764-bp amplified product from all the cell lines except the pBK-CMV–TBP1 plasmid construct. After RT-PCR, the products were run on 1.8% agarose gel to confirm the amplified product.

65.5 ± 1.7%, respectively, as determined in three independent experiments. Transient transfection of U87MG cells with empty vector did not inhibit cell growth and transformation as determined by the MTT assay and by an anchorage-independent growth assay (data not shown).

U87/TBP1 subclones showed a profound degree of inhibition relative to U87MG parental cells after implantation into athymic mice (Fig. 5*B*). U87/TBP1 transfectants did not form appreciable tumors until 8 weeks (Fig. 5*B*), after the period of time when some animals injected with parental U87MG cells had to be killed because of excessive tumor burden. Additionally, more than 50% of the subcutaneous injections with the U87/TBP1 cell line failed to produce any palpable tumors.

DISCUSSION

Our findings indicate that disabling erbB oncoproteins with anti-erbB receptor antibodies leads to inhibition of the transformed phenotype, a feature associated with induction or recovery of TBP1 expression. Previous studies showed that kinase-deficient forms of p185^{neu} derived from the receptor ectodomain that form heterodimers with EGFR in rodent (19) and human glioblastoma cells can inhibit EGFR-dependent phenotypes contributing to transformation (17, 18). Endogenous expression of TBP1 mRNA is higher in U87MG human glioblastoma cells containing p185^{neu} kinase-deficient forms that have an inhibited phenotype. Although multiple TBP1 transfectants of three human cancer cell lines had an inhibited phenotype, all cell lines examined expressed erbB receptors. It remains possible that TBP1 induction accompanies reversion of transformation in non-erbB-containing cells. The degree to which TBP1 induction contributes to phenotypic reversion in erbB-inhibited cells is also unknown. Collectively, these observations suggest that expression of TBP1 is related to the tumorigenesis of certain malignant cells and that induction/recovery of TBP1 expression may be part of a general attenuating pathway or a specific consequence of down-regulation or attenuation of signaling from erbB family receptor tyrosine kinases.

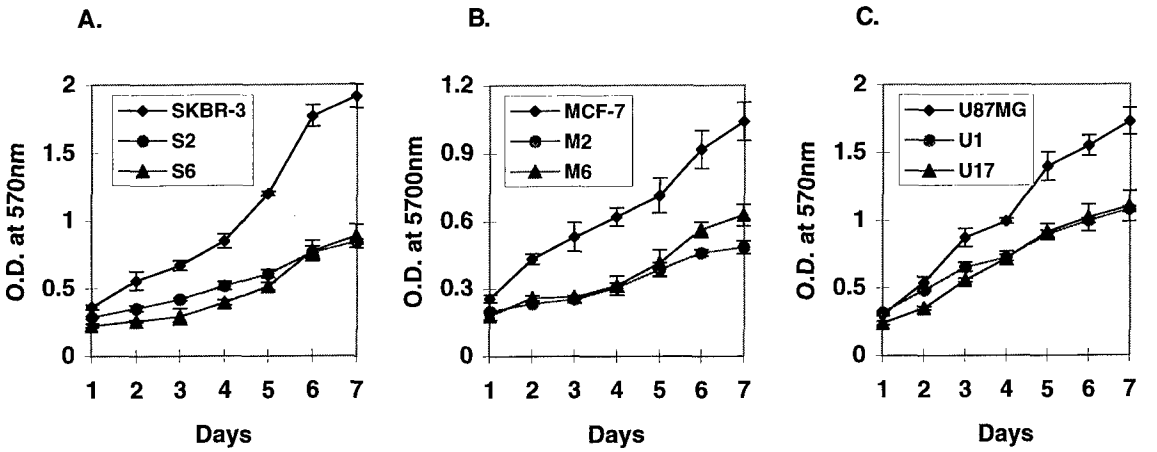

FIG. 4. Reduction of cell proliferation by expression of human TBP1 in human cancer cell lines. Cell lines were plated in 96-well plates at 4,000 cells per well in 10% DMEM and allowed to attach overnight. MTT was given to the cells for 4 h. Cells were then lysed in 50% (vol/vol) SDS/20% (vol/vol) dimethyl sulfoxide and kept at 37°C overnight. Proliferation was assessed by reading OD at 570 nm by using an ELISA reader. The number of cells used in this assay was determined to be within the linear range for this cell type. (*A*) TBP1 cDNA-transfected SK-BR-3 subclones S2 and S6 had 50% and 57% proliferation inhibition, respectively, compared with parental cells. (*B*) TBP1 cDNA-transfected MCF-7 subclones M2 and M6 had 40% and 54% proliferation inhibition, respectively, compared with parental cells. (*C*) U87MG subclones expressing elevated TBP1, U1, and U17 had 34% and 38% inhibition of proliferation, respectively, compared with parental cells.

The HIV tat protein, encoded by one of the viral regulatory genes, *tat*, is considered a powerful transactivator of viral gene expression (20–22). Human TBP1 is encoded by a 1,341-nt cDNA containing an ORF of 439 aa (23). TBP1 was originally described as a transcriptional factor of the HIV 1 by interaction with the tat protein (13, 23). TBP1 binds the HIV tat transactivator, suppressing its activity in cotransfection experiments (13). In some cases, TBP1 may also be involved in transcriptional activation (23). Nakamura *et al.* (12) isolated a full-length murine form of TBP1 that suppresses the Tat-mediated transactivation. Tanaka *et al.* (14) cloned a TBP1 interacting protein, TBPIP, that interacts with mTBP1. TBPIP colocalizes with TBP1 *in vivo* and synergistically enhances the inhibitory action of TBP1 on Tat activity *in vitro*, supporting the general concept of TBP1 ensembles that inhibit cellular functions and transcription.

We noted that TBP1 amino acids 59–63 bear 75% similarity to the motif HFRIG, and amino acids 185–189 bear 60% similarity to the motif HSRIG. The HIV gene *Vpr* contains a domain that contains two H(S/F)RIG motifs that may cause cell growth arrest and structural defects (24). *TBP1* also possesses 46% identity to *KAI1*, a metastasis suppressor gene for human prostate cancer (25). Hoyle *et al.* (26) recently localized the human *TBP1* to chromosome 11p12–13, and it has been noted that frequent loss of chromosome 11p13 occurs in a variety of cancers (27, 28). Tsuchiya *et al.* (29) reported that the tumor suppressor VHL gene product binds to TBP1. These observations suggest that the *TBP1* gene may be grouped with other possible functional tumor suppressor genes, and TBP1 may act as a negative regulator of the transcriptional elongation process by binding to tumor suppressor gene products such as pVHL.

All members of the TBP family, including TBP1, contain two highly conserved domains. One domain resembles a nucleotide-binding motif (ATP-binding site), and the other resembles a motif common to proteins with helicase activity. TBP1, TBP7, MSS1, and SUG1 are thus considered members of a large ATPase family rather than representing discrete transcriptional factors (30–33).

TBP1 has also been reported to be a component of the 26S proteasome (34), which is an essential multiprotein complex

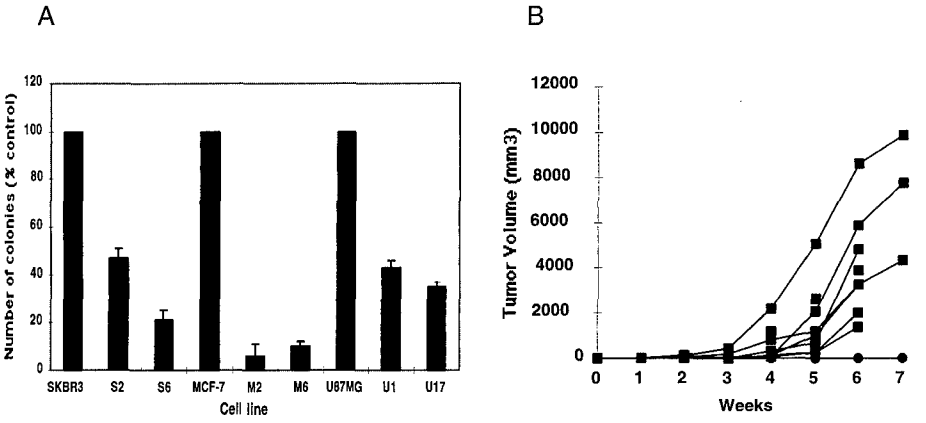

FIG. 5. Inhibition of cell growth and transformation by human TBP1. (*A*) Anchorage-independent growth. Cells of each clone (n = 1,000) were suspended in a 1-ml top layer [0.18% agarose/10% (vol/vol) FBS/10% (vol/vol) DMEM] in 6-cm culture dishes containing a 3-ml cell-free feeder layer consisting of 0.25% agarose in DMEM supplemented with 10% FBS and 20 mM Hepes (pH 7.5). Colonies (>0.3 mm) were visualized and counted on day 28 for all cell lines after staining with *p*-iodonitrotetrazolium violet (1 mg/ml). Each cell line was examined in triplicate in three separate experiments. The numbers of colonies reported represent the mean of triplicate samples. (*B*) Tumor growth in athymic mice: comparison of parental U87MG cells and U87/TBP1 transfectants. Cells of each cell line ($n = 1 \times 10^6$) were injected subcutaneously on day 0, and tumor volume was recorded weekly. These data represent individual tumor growth curves for U87MG parental cells (■) and mean tumor volumes for the U87/TBP1 subclone (●). (U87MG, n = 7; U87/TBP1, n = 8.)

that degrades ubiquitinated proteins in an ATP-dependent fashion and provides the main route for selective turnover of intracellular proteins involved with the regulation of cell growth and metabolism (35). TBP1 functions as a subunit of PA700, a nonproteasomal component of the 26S proteasome (34, 36), and a subunit of a proteasome modulator complex (34). Schnall *et al.* (37) isolated a set of 12 yeast genes, all belonging to the AAA family. Among them, the closest equivalents of the human genes *TBP1*, *TBP7*, and *MSS1* are named, respectively, *YTA1*, *YTA2*, and *YTA3*. These genes are identical or closely related to either cell cycle genes or to subunits of the 26S proteasome. We identified three proteins interacting with TBP1: p27 (34), p40 (38), and p42(SUG-2) (34, 39) in a yeast two-hybrid system by using a HeLa cell cDNA library (data not shown). Interestingly, p27 and p42 are subunits of the human proteasome 26S modulator complex, and both p40 and p42 are subunits of the regulatory proteasome PA 700. TBP1 itself is also a subunit of both the PA700 and modulator complex that enhances 26S proteasome activity (34). Moreover, DeMartino *et al.* (34) reported the purification and characterization of a proteasomal modulator complex—a trimer of TBP1, p42, and p27—which enhances proteasomal activity by as much as 8-fold. Recently, Watanabe *et al.* (40) established the association of p27, p42, and TBP1 with not only the modulator complex but also with the 26S proteasome complex. High sequence similarities of TBP1 homologues over widely different species substantiate that TBP1 function is essential *in vivo* (12). These results suggest a relationship between TBP1 expression and a protein degradation pathway.

Cell surface levels of $p185^{neu}$ and EGFR were independently down-regulated on expression of TBP1 in all subclones examined by flow cytometric analysis (B.-W.P. and M.I.G., unpublished results). These results suggest that TBP1 activity is related to inactivation of surface $p185^{neu}$ and EGFR. TBP1, as a human 26S proteasome modulator (34), may increase proteasomal activity by facilitating degradation of sequestered cell-surface proteins in addition to its role in transcriptional regulation.

This study shows that TBP1 expression was up-regulated with anti-$p185^{neu}$ mAb (7.16.4) treatment in B104-1-1 cells but not in NR6TintΔ cells expressing internalization-defective $p185^{neu}$ proteins (Fig. 2*A*). U87/T691 cells, an EGFR-disabled cell line containing a trans-inhibitory ectodomain form of $p185^{neu}$ (T691stop neu), also showed an increased endogenous level of TBP1 over that observed in parental U87MG cells (Fig. 2*C*). Our findings suggest that TBP1 expression is inversely related to the "activity" of the kinase signaling pathway (Fig. 2 *A* and *C*) and is not necessarily a direct result of the receptor degradation alone (Fig. 2*C*). Attenuation of erbB receptor signaling seems to involve the activation of a functional tumor suppressor-like gene, *TBP1*, which itself is associated with a proteasomal protein degradation pathway.

1. Dougall, W. C., Qian, X., Peterson, N. C., Miller, M. J., Samanta, A. & Greene, M. I. (1994) *Oncogene* **9,** 2109–2123.
2. Kiyokawa, N., Yan, D. H., Brown, M. E. & Hung, M. C. (1995) *Proc. Natl. Acad. Sci. USA* **92,** 1092–1096.
3. Wada, T., Qian, X. L. & Greene, M. I. (1990) *Cell* **61,** 1339–1347.
4. Alimandi, M., Romano, A., Curia, M. C., Muraro, R., Fedi, P., Aaronson, S. A., DiFiore, P. P. & Kraus, M. H. (1995) *Oncogene* **10,** 1813–1821.
5. Pinkas-Kramarski, R., Soussan, L., Waterman, H., Levkowitz, G., Alroy, I., Klapper, L., Lavi, S., Seger, R., Ratzkin, B. J., Sela, M., *et al.* (1996) *EMBO J.* **15,** 2452–2467.
6. Drebin, J. A., Link, V. C., Stern, D. F., Weinberg, R. A. & Greene, M. I. (1985) *Cell* **41,** 695–706.
7. Drebin, J. A., Link, V. C., Weinberg, R. A. & Greene, M. I. (1986) *Proc. Natl. Acad. Sci. USA* **83,** 9129–9133.
8. Katsumata, M., Okudaira, T., Samanta, A., Clark, D. P., Drebin, J. A., Jolicoeur, P. & Greene, M. I. (1995) *Nat. Med.* **1,** 644–648.
9. Brown, V. I., Shan, N., Smith, R., Hellman, M., Jarett, L., Mikami, Y., Cohen, E., Qian, X. & Greene, M. I. (1994) *DNA Cell Biol.* **13,** 193–209.
10. Liang, P. & Pardee, A. B. (1992) *Science* **257,** 967–971.
11. Liang, P., Averboukh, L. & Pardee, A. B. (1993) *Nucleic Acids Res.* **21,** 3269–3275.
12. Nakamura, T., Tanaka, T., Takagi, H. & Sato, M. (1998) *Biochim. Biophys. Acta* **1399,** 93–100.
13. Nelbock, P., Dillon, P. J., Perkins, A. & Rosen, C. A. (1990) *Science* **248,** 1650–1653.
14. Tanaka, T., Nakamura, T., Takagi, H. & Sato, M. (1997) *Biochem. Biophys. Res. Commun.* **239,** 176–181.
15. Qian, X., O'Rourke, D. M., Drebin, J., Zhao, H., Wang, Q. & Greene, M. I. (1997) *DNA Cell Biol.* **16,** 1395–1405.
16. Hansen, M. B., Nielsen, S. E. & Berg, K. (1989) *J. Immunol. Methods* **119,** 203–210.
17. O'Rourke, D. M., Qian, X., Zhang, H.-T., Davis, J. G., Nute, E., Meinkoth, J. & Greene, M. I. (1997) *Proc. Natl. Acad. Sci. USA* **94,** 3250–3255.
18. O'Rourke, D. M., Nute, E. J. L., Davis, J. G., Wu, C., Lee, A., Muralli, R., Zhang, H.-T., Qian, X., Kao, C.-C. & Greene, M. I. (1998) *Oncogene* **16,** 1197–1207.
19. Qian, X., O'Rourke, D. M., Zhao, H. & Greene, M. I. (1996) *Oncogene* **13,** 2149–2157.
20. Sodroski, J., Patarca, R., Rosen, C., Wong-Staal, F. & Haseltine, W. (1985) *Science* **229,** 74–77.
21. Sodroski, J., Goh, W. C., Rosen, C., Dayton, A., Terwilliger, E. & Haseltine, W. (1986) *Nature (London)* **321,** 412–417.
22. Feinberg, M. B., Jarrett, R. F., Aldovini, A., Gallo, R. C. & Wong-Staal, F. (1986) *Cell* **46,** 807–817.
23. Ohana, B., Moore, P. A., Ruben, S. M., Southgate, C. D., Green, M. R. & Rosen, C. A. (1993) *Proc. Natl. Acad. Sci. USA* **90,** 138–142.
24. Macreadie, I. G., Castelli, L. A., Hewish, D. R., Kirkpatrick, A., Ward, A. C. & Azad, A. A. (1995) *Proc. Natl. Acad. Sci. USA* **92,** 2770–2774.
25. Dong, J. T., Lamb, P. W., Rinker-Schaeffer, C. W., Vukanovic, J., Ichikawa, T., Isaacs, J. T. & Barrett, J. C. (1995) *Science* **268,** 884–886.
26. Hoyle, J., Tan, K. H. & Fisher, E. M. (1997) *Hum. Genet.* **99,** 285–288.
27. Bepler, G. & Garcia-Blanco, M. A. (1994) *Proc. Natl. Acad. Sci. USA* **91,** 5513–5517.
28. Shipman, R., Schraml, P., Colombi, M., Raefle, G. & Ludwig, C. U. (1993) *Hum. Genet.* **91,** 455–458.
29. Tsuchiya, H., Iseda, T. & Hino, O. (1996) *Cancer Res.* **56,** 2881–2885.
30. Dubiel, W., Ferrell, K., Pratt, G. & Rechsteiner, M. (1992) *J. Biol. Chem.* **267,** 22699–22702.
31. Dubiel, W., Ferrell, K. & Rechsteiner, M. (1994) *Biol. Chem. Hoppe-Seyler* **375,** 237–240.
32. Leeb, T., Rettenberger, G., Breech, J., Hameister, H. & Brenig, B. (1996) *Mamm. Genome* **7,** 180–185.
33. Swaffield, J. C., Melcher, K. & Johnston, S. A. (1995) *Nature (London)* **374,** 88–91.
34. DeMartino, G. N., Proske, R. J., Moomaw, C. R., Strong, A. A., Song, X., Hisamatsu, H., Tanaka, K. & Slaughter, C. A. (1996) *J. Biol. Chem.* **271,** 3112–3118.
35. Ciechanover, A. (1994) *Cell* **79,** 13–21.
36. Kominami, K., DeMartino, G. N., Moomaw, C. R., Slaughter, C. A., Shimbara, N., Fujimuro, M., Yokosawa, H., Hisamatsu, H., Tanahashi, N., Shimizu, Y., *et al.* (1995) *EMBO J.* **14,** 3105–3115.
37. Schnall, R., Mannhaupt, G., Stucka, R., Tauer, R., Ehnle, S., Schwarzlose, C., Vetter, I. & Feldmann, H. (1994) *Yeast* **10,** 1141–1155.
38. Tsurumi, C., DeMartino, G. N., Slaughter, C. A., Shimbara, N. & Tanaka, K. (1995) *Biochem. Biophys. Res. Commun.* **210,** 600–608.
39. Bauer, V. W., Swaffield, J. C., Johnston, S. A. & Andrews, M. T. (1996) *Gene* **181,** 63–69.
40. Watanabe, T. K., Saito, A., Suzuki, M., Fujiwara, T., Takahashi, E., Slaughter, C. A., DeMartino, G. N., Hendil, K. B., Chung, C. H., Tanahashi, N., *et al.* (1998) *Genomics* **50,** 241–250.

[redacted]
Manuscript: June, 2000

Inhibition of EGFR-mediated phosphoinositide-3-OH kinase (PI3-K) signaling and glioblastoma phenotype by Signal-Regulatory Proteins (SIRPs).

Chuan-jin Wu[1,5], Zhengjun Chen[4], Axel Ullrich[4], Mark I. Greene[1,3,6], & Donald M. O'Rourke[1,2,3,7]

[1]Departments of Pathology and Laboratory Medicine and [2]Neurosurgery, and [3]Cancer Center, University of Pennsylvania School of Medicine, Philadelphia, PA, 19104.
[4]Max-Planck-Institut Fur Biochemie, Am Klopferspitz 18A, 82152, Martinsried, Germany
[5] School of Life Science, University of Science and Technology of China, Hefei, Anhui 230027, P.R. China.
[6]Abramson Family Cancer Institute, University of Pennsylvania School of Medicine, Philadelphia, PA. 19104.
[7]Department of Surgery (Neurosurgery), Philadelphia Veterans Administration Medical Center, University and Woodland Avenues, Philadelphia, PA. 19104.

Keywords: apoptosis/erbB/EGFR/phosphoinositide-3-OH kinase (PI3-K)/SHP2/Signal-Regulatory Proteins (SIRPs)

Running title: *SIRP inhibits PI3-K pathway and glioblastoma phenotype.*

correspondence: Donald M. O'Rourke, 502 Stemmler Hall, 36th and Hamilton Walk, University of Pennsylvania School of Medicine, Philadelphia, PA. 19104.

Phone (215) 898-2871
Fax (215) 898-2401
Email: orourked@mail.med.upenn.edu

Several growth factors and cytokines, including EGF, are known to induce tyrosine phosphorylation of Signal Regulatory Proteins (SIRPs). Consistent with the idea that increased phosphorylation activates SIRP function, we overexpressed human SIRPα1 in U87MG glioblastoma cells in order to examine how SIRPα1 modulates EGFR signaling pathways. Endogenous EGFR proteins are overexpressed in U87MG cells and these cells exhibit survival and motility phenotypes that are influenced by EGFR kinase activity. Overexpression of the SIRPα1 cDNA diminished EGF-induced phosphoinositide-3-OH kinase (PI3-K) activation in U87MG cells. Reduced EGF-stimulated activation of PI3-K was mediated by interactions between the carboxyl terminus of SIRPα1 and the Src homology-2 (SH2)-containing phosphotyrosine phosphatase, SHP2. SIRPα1 overexpression also reduced the EGF-induced association between SHP2 and the p85 regulatory subunit of PI3-K. Inhibition of transformation and enhanced apoptosis following gamma-irradiation were observed in SIRPα1-overexpressing U87MG cells, and enhanced apoptosis was associated with reduced levels of bcl-x_L protein. Furthermore, SIRPα1-overexpressing U87MG cells displayed reduced cell migration and cell spreading that was mediated by association between SIRPα1 and SHP2. However, SIRPα1-overexpressing U87MG clonal derivatives exhibited no differences in cell growth or levels of mitogen-activated protein kinase (MAPK) activation. These data reveal a pathway that negatively regulates EGFR-induced PI3-K activation in glioblastoma cells and involves interactions between SHP2 and tyrosine phosphorylated SIRPα1. These results also suggest that negative regulation of PI3-K pathway activation by the SIRP family of transmembrane receptors may diminish EGFR-mediated motility and survival phenotypes that contribute to transformation of glioblastoma cells.

Introduction

Observations in hematopoietic cells showing that signaling from receptor tyrosine kinases (RTKs) could be attenuated by association with phosphotyrosine phosphatases led to the identification of distinct families of inhibitory receptors (reviewed in Cambier, 1997; Coggeshall, 1999). Most of the inhibitory receptors are monomeric proteins that contain multiple immunoglobin super-family (IgSF) domains in their extracellular regions (Cambier, 1997). A consensus cytoplasmic sequence found in these inhibitory receptors, referred to as the immunoreceptor tyrosine-based inhibitory motif or ITIM, binds to the SH2 domain-containing phosphotyrosine phosphatases (PTPs) SHP1 and SHP2. More recent efforts (Fujioka *et al.*, 1996; Ohnishi *et al.*, 1996; Kharitonenkov *et al.*, 1997) led to the isolation and cloning of new inhibitory receptors in neurons and epithelial cells based on their binding to SHP2. Signal-Regulatory Proteins [SIRPs (Kharitonenkov *et al.*, 1997); murine homologue SHPS-1, or SHP substrate 1 (Fujioka *et al.*, 1996)], a family of membrane glycoproteins and putative substrates of the SHP1 and SHP2 phosphatases, are unique members of the inhibitory receptor family whose members are ubiquitously expressed. While expression of SHP1 is restricted to hematopoietic cells, the distribution of SHP2 (previously called SH-PTP2, PTP2C, PTP1D, SHPTP3, and Syp) is similarly widely expressed (Ahmad *et al.*, 1993; Feng & Pawson, 1994).

The ITIM motif, (V/I/T)x Yxx(V/L) (where V is valine, I is isoleucine, T is threonine, L is leucine, Y is tyrosine, and X is any residue) was identified by sequence analysis of inhibitory receptors originally identified in hematopoietic cells (D'Ambrosio *et al.*, 1995; Daeron *et al.*, 1995). Phosphorylation of the tyrosine in ITIM triggers binding and activation of SHP1 and SHP2 and, in some cases, the phosphatidylinositol (3,4,5)P_3 5' inositol phosphatase, SHIP (Cambier, 1997; Coggeshall, 1999). Mutation of the I/V position disrupts binding of SHP1 and SHP2 (Vely *et al.*, 1997). In many systems, the binding of SH2 domain-containing phosphatases appears to be critical to the function of inhibitory receptors and PTPs may represent the effectors of inhibitory receptors. It is likely that distinct differences in the primary sequence surrounding the phosphotyrosine residue underlies differential recruitment of SH2 domain-containing proteins between positive and negative signaling receptors (Cambier, 1997; Coggeshall, 1999). Investigation of mechanisms of PTP binding to ITIM motifs may shed light on PTP functional regulation, since little is known regarding the recruitment and activation of PTPs under physiologic conditions.

SIRP/SHPS-1 proteins are tyrosine phosphorylated in response to EGF and insulin, and were originally identified in anti-SHP-2 immunoprecipitates (Fujioka *et al.*, 1996; Kharitonenkov *et al.*, 1997; Takada *et al.*, 1998). Integrin signaling also increases SHPS-1 tyrosine phosphorylation and SHP2 binding (Tsuda *et al.*, 1998), suggesting that SIRP/SHPS-1 proteins modulate cell signaling in response to both soluble growth factors and cell adhesion. Collectively, these findings suggest that multiple RTK-induced pathways may be downstream targets of SIRP. SIRP has been experimentally shown to modulate signaling of many RTKs, including the insulin receptor and the Epidermal Growth Factor Receptor (EGFR) (Kharitonenkov *et al.*, 1997; Takada *et al.*, 1998). SIRP tyrosine phosphorylation and subsequent recruitment of SHP2 to the plasma membrane have been shown to be related to SIRP functional regulation of RTK signaling (Cambier, 1997; Kharitonenkov *et al.*, 1997). Many isoforms of human SIRP and murine SHPS-1 proteins have been identified and multiple transcripts of SIRP and SHPS-1 genes have been observed in many tissues, particularly in neural cells (Fujioka *et al.*, 1996; Kharitonenkov *et al.*, 1997; Yamao *et al.*, 1997; Veillette *et al.*, 1998; Jiang *et al.*, 1999). Two subtypes of the SIRP protein family, containing at least fifteen members, have been confirmed (Kharitonenkov *et al.*, 1997). SIRPα proteins are distinguished from SIRPβ forms by the presence of an endodomain containing ITIMs (Veillette *et al.*, 1998), which bind SHP2 (Kharitonenkov *et al.*, 1997; Veillette *et al.*, 1998).

Mechanisms by which ITIM-containing receptors such as SIRP mediate their inhibitory effects, and the role of the SIRP/SHP2 complex in this process, have not been well characterized. SIRP/SHPS-1 receptors have been shown to positively or negatively regulate MAPK pathways following stimulation of many different receptors (Kharitonenkov *et al.*, 1997; Takada *et al.*, 1998). SIRPα1 overexpression in NIH3T3 cells inhibited DNA synthesis and MAPK phosphorylation following EGF or insulin stimulation (Kharitonenkov *et al.*, 1997). Genetic and biochemical studies have shown that SHP2 may positively regulate MAPK signaling in response to insulin, FGF, and EGF (Noguchi *et al.*, 1994; Tang *et al.*, 1995; Yamauchi *et al* 1995; Bennett *et al.*, 1996; Saxton *et al.*, 1997; Deb *et al.*, 1998; Shi *et al.*, 1998), but attenuate MAPK activation following PDGF and neuregulin stimulation (Saxton *et al.*, 1997; Tanowitz *et al.*, 1999). In other studies, increased SHPS-1/SHP2 complex formation resulting from overexpression of SHPS-1 potentiated the RAS-MAPK pathway in response to insulin (Takada *et al.*, 1998) or integrin stimulation (Oh *et al.*, 1999). The precise mechanisms by which

SIRP/SHPS-1 proteins regulate MAPK signaling and other signaling pathways, and how the SIRP/SHP2 complex alters RTK-induced cell signals and phenotype, have therefore not been established.

ErbB family kinases are overexpressed and/or mutated in a number of human tumors, including human glioblastomas in which erbB1/EGFR signaling pathways are deregulated (Nishikawa *et al.*, 1994; Nagane *et al.*, 1996; Huang *et al.*, 1997; O'Rourke *et al.*, 1997a; O'Rourke *et al.*, 1997b; O'Rourke *et al.*, 1998a). Mechanisms of attenuating EGFR signaling in glioblastoma cells have not been completely defined. Since tyrosine phosphorylated SIRPα1 has been shown to inhibit EGF-stimulated responses, including DNA synthesis (Kharitonenkov *et al.*, 1997), analysis of SIRP protein function may also yield insight into physiologic mechanisms of erbB1/EGFR signaling inhibition. Biochemical characterization of erbB1/EGFR inhibitory events may lead to application of receptor-based therapies for many erbB-expressing human tumors, including human glioblastomas, the most malignant and most common adult human brain tumor.

In this report, we evaluated modulation of erbB1/EGFR signaling pathways and phenotype by ectopically overexpressed SIRP proteins in human glioblastoma cells. We have used the human glioblastoma U87MG cell line as a model system to characterize EGFR-mediated transforming and survival phenotypes (Nishikawa *et al.*, 1994; Nagane *et al.*, 1996; Huang *et al.*, 1997; Nagane *et al.*, 1998; O'Rourke *et al.*, 1997a; O'Rourke *et al.*, 1998a; O'Rourke *et al.*, 1998b). Independent studies of the *PTEN* tumor suppressor protein have shown that deregulated PI3-K pathway activation alters glioblastoma survival, transformation, motility and adhesion (Furnari *et al.*, 1997; Furnari *et al.*, 1998;; Tamura *et al.*, 1998; Wick *et al.*, 1999). In this report, we demonstrate new functional roles for tyrosine phosphorylated human SIRPα1 proteins in modulating EGFR signaling pathways and phenotype of human glioblastoma cells. SIRPα1 negatively regulates EGF-induced PI3-K activation and leads to reduced transformation, reduced cell migration and cell spreading, and enhanced apoptosis following DNA damage in EGFR-containing human glioblastoma cells.

Results

SIRPα1 modulation of EGFR-mediated cell growth and transformation in human glioblastoma cells.

EGF-induced phorphorylation of the SIRP/SHPS-1 receptor (Ochi *et al.*, 1997; Tanowitz *et al.*, 1999; Yamauchi & Pessin, 1995) suggested that SIRP/SHPS-1 proteins may modulate EGFR signaling pathways. Inhibition of EGF- and insulin-induced DNA synthesis and MAPK phosphorylation was observed in NIH3T3 cells overexpressing SIRPα1 (Kharitonenkov *et al.*, 1997).

Our previous work utilized a *trans*-dominant mutant receptor derived from $p185^{neu}$ that inhibits EGFR kinase activity to show that EGFR signaling determines transforming and apoptotic phenotypes in U87MG glioblastoma cells (O'Rourke *et al.*, 1997a; O'Rourke *et al.*, 1998a; O'Rourke *et al.*, 1998b). In order to investigate the relationship between SIRP function and EGFR signaling pathways, we overexpressed the SIRPα1 cDNA in U87MG cells, which contain high endogenous levels of EGFR, but no other detectable erbB family proteins (O'Rourke *et al.*, 1997a). Stable U87MG clones expressing elevated amounts of the SIRPα1 protein were inhibited 65% in the formation of morphologically transformed foci, as compared to clones expressing vector without insert (mean number of foci ± SD: U87/pIRES 31±1.4; U87/SIRPα1 11 ± 2.8; data confirmed in three independent experiments) (Fig. 1A). Confirmation of ectopic SIRPα1 expression was confirmed by western blotting (see below, Fig.5A). These data were reproduced in other SIRPα1-overexpressing subclones. Therefore, SIRPα1 inhibited the transformed phenotype in human glioblastoma cells.

Interestingly, cell growth after 48h, as determined by the MTT assay, was unaffected by overexpression of SIRPα1 in U87MG cells (Fig. 1B). Differences in cell growth were also not observed in SIRPα1-overexpressing cells in full growth media for up to seven days (data not shown). These data suggest that inhibition of transformation mediated by SIRPα1 is not related to a reduction in cell growth *in vitro* in full growth media. The SIRPα pathway(s) in glial cells may be more relevant to transformation characteristics than mitogenic proliferation.

SIRPα1 overexpression enhances DNA damage-induced apoptosis in human glioblastoma cells.

The role of SIRP proteins in cell survival has not been evaluated. We previously showed that inhibition of erbB signaling pathways in human astrocytoma and glioblastoma cells enhanced apoptosis after irradiation-induced DNA damage (O'Rourke *et al.*, 1998b). Prolonged serum deprivation (96h) did not induce apoptosis in transformed U87MG parental cells or U87/SIRPα1 subclones (data not shown), supporting previous observations in glioma cells (O'Rourke *et al.*, 1998b). However, overexpression of the SIRPα1 cDNA conferred increased sensitivity to apoptosis following gamma-irradiation as determined by an examination of nuclear morphology following staining with 4',6-Diamidino-2-phenylindole dihydrochloride hydrate (DAPI) (O'Rourke *et al.*, 1998b). For a positive control in the analysis of apoptosis, we used U87/T691 cells engineered to express a kinase-deficient mutant $p185^{neu}$ receptor that display increased sensitivity to irradiation-induced cell death (O'Rourke *et al.*, 1998b). Apoptosis in U87/ SIRPα1 and U87/T691 cells was increased above U87/pIRES cells expressing vector without insert at both 48h and 72h following irradiation in full growth medium (mean percent apoptosis ± SD: U87/pIRES 3.6± 2.3, 48h, 5.3± 0.4, 72h; U87/ SIRPα1 14.2 ± 2.6, 48h, 15.5 ± 2.1, 72h; U87/T691 12.9 ± 0.2, 48h, 21.5 ± 0.7, 72h; these results confirmed in three independent experiments) (Figs. 2, 3A). Interestingly, apoptosis of irradiated U87/SIRPα1 cells was not enhanced by serum deprivation (data not shown), suggesting the activation of a pathway that is serum-independent.

Expression of a mutant EGFR oncoprotein in U87MG cells leads to elevated bcl-x_L protein levels and resistance to apoptotic cell death triggered by exposure to chemotherapy (Nagane *et al.*, 1998). Since EGFR stimulation modulates SIRP tyrosine phosphorylation, and SIRPα1 expression can diminish EGFR-mediated transformation in U87MG cells, we investigated the hypothesis that apoptosis occurring in SIRPα1-overexpressing cells may result from reduced levels of the bcl-x_L protein. Bcl-x_L was induced following gamma-irradiation in U87MG-derived cells (Fig. 3D). Interestingly, basal and radiation-induced levels of bcl-x_L protein were reduced in U87/SIRPα1 cells relative to controls (Fig. 3D). Bcl-x_L levels returned to baseline 72h following irradiation in U87/SIRPα1 cells, while cells expressing vector without insert showed sustained elevation in bcl-x_L protein levels 24-72h following gamma-irradiation (Fig. 3D).

Modulation of Bcl-x_L protein levels has also been shown to influence sensitivity to apoptosis in EGFR-containing keratinocytes exposed to cell death signals (Rodeck *et al.*, 1997).

Overexpressed SIRPα1 does not modulate MAPK activities in glioblastoma cells.

EGFR-dependent signaling and phenotypes in glioblastoma cells have been characterized by our laboratory (Qian *et al.*, 1996; O'Rourke *et al.*, 1997a ; O'Rourke *et al.*, 1998a; O'Rourke *et al.*, 1998b; Wu *et al.*, 1999) and others (Nishikawa *et al.*, 1994; Nagane *et al.*, 1996; Huang *et al.*, 1997; Nagane *et al.*, 1998;). Several groups have reported a modulation of MAPK activities by SIRP or SHPS-1 (refer to *Introduction*). Therefore, one mechanism by which SIRP inhibits EGFR-mediated signaling may be through modulation of MAPK activities. Unexpectedly, *in vitro* kinase assays showed that EGF-induced activation of extracellular signal-regulated kinase (ERK)-1, ERK-2, and c-jun amino-terminal kinase (JNK) were comparable in human glioblastoma cells stably expressing SIRPα1 when compared to cells expressing vector without insert (Fig. 4). Notably, basal ERK activities between U87MG parental and U87/SIRPα1 subclones were comparable (data not shown).

Ectopically expressed SIRPα1 negatively regulates EGF-induced PI3-K activation through carboxyl terminal interactions with SHP2.

In order to more precisely define the mechanism by which SIRPα1 modulates transforming and apoptotic pathways in EGFR-containing glioblastoma cells, we examined EGF-induced PI3-K activity in U87MG cells (Fig. 5). U87MG cells overexpressing wild-type SIRPα1 (U87/SIRPα1) (Fig. 5A) exhibited reduced EGF-induced PI3-K activity in anti-phosphotyrosine (anti-pTyr) immunoprecipitates when compared to U87MG cells containing vector alone (U87/pIRES) (Fig. 5B, lanes 2,4). Basal PI3-K activities in these U87MG derivatives were comparable. In order to define whether SIRPα1 attenuates EGF-induced PI3-K activation by binding SHP2, we utilized a carboxyl terminal SIRPα1 mutant (SIRPα1-4Y) in which four carboxyl terminal tyrosines have been mutated to phenylalanine, making this mutant incapable of binding to SHP2 (Kharitonenkov *et al.*, 1997) and seen below, Fig. 6A,C). Cells overexpressing the SIRPα1-4Y mutant (U87/SIRPα1-4Y) displayed EGF-induced PI3-K activation that was comparable to cells containing empty vector alone (Fig. 5B, lanes 1,2; 5,6), indicating that a SIRP/SHP2 complex

reduces EGF-induced PI3-K activity. These data were reproduced in multiple SIRPα1- and SIRPα1-4Y- overexpressing subclones.

SHP2 immunoprecipitates have been shown to contain PI3-K activity (Takahashi *et al.*, 1999). In order to examine SIRP modulation of PI3-K activity directly associated with SHP2, we assayed induced PI3-K activity contained in anti-SHP2 immunoprecipitations. In our studies, anti-SHP2 immunocomplexes contained significant amounts of PI3-K activity (Fig. 5C), suggesting that SHP2 plays an important role in regulating EGF-induced PI3-K activation in human glioblastoma cells. Interestingly, anti-SHP2 immunoprecipitates displayed the same pattern of PI3-K activation in these U87MG subclones as anti-phosphotyrosine immunocomplexes (Fig. 5 B, C). Moreover, anti-EGFR and anti-p85 (PI3-K) immunoprecipitations also displayed the same trends observed with anti-pTyr and anti-SHP2 immunoprecipitations (not shown). It is possible that SHP2 may contain the majority of PI3-K activity in EGF-stimulated glioblastoma cells, although there may be differences in affinity for tyrosine phosphorylated substrates between anti-SHP2 and anti-phosphotyrosine antibodies. Genetic studies have shown that SHP2 functions as a positive regulator of EGFR signaling and that EGFR/SHP2 interactions contribute to PI3-K modulation in mammalian cells (Qu *et al.*, 1999). Since the SIRPα1-4Y mutant protein cannot bind SHP2 (**Fig. 6**) (Kharitonenkov *et al.*, 1997), these data indicate that SIRPα1 negatively regulates EGF-induced PI3-K activation through carboxyl terminal interactions that include association with the SHP2 phosphatase.

Tyrosine phosphorylated SIRP α1 binds SHP2 and reduces SHP2/p85 association in human glioblastoma cells.

Many studies have since confirmed the observation that the SIRP receptor binds SHP2 in mammalian cells, and that this event is required for SIRPα function (Kharitonenkov *et al.*, 1997). In SHP2 immunocomplexes from U87MG subclones, overexpressed SIRPα1 was tyrosine phosphorylated and associated with SHP2 constitutively (Fig. 6 A,C, lane 3). EGF treatment increased the amount of tyrosine phosphorylated SIRP and total SIRP bound to SHP2 (Fig. 6 A,C, lanes 3, 4). Since tyrosine phosphorylation has been linked to SIRPα1 function, U87/SIRPα1 subclones therefore contain functional SIRP in the absence of EGF. Despite the level of ectopically expressed SIRPα1-4Y in U87/SIRPα1-4Y cells (Fig. 5A), anti-SHP2 immunoprecipitates did not contain SIRPα1-4Y with or without EGF stimulation (Fig. 6C, lanes

5,6). These results are consistent with data indicating that SIRPα1 binds SHP2 through carboxyl terminal sites mutated in the SIRPα1-4Y protein.

Recent studies have noted the association between SHP2 and p85 in certain cell types, including an association induced in PC12 cells by NGF (Okada *et al.*, 1996) and in cortical neurons by BDNF (Okada *et al.*, 1996; Yamada *et al.*, 1999). EGF induced the association between endogenous SHP2 and the p85 regulatory subunit of PI3-kinase in U87MG cells expressing vector without insert (Fig.6B, lanes 1,2). In U87MG/SIRPα1 cells, EGF-induced association between SHP2 and p85 was diminished (Fig.6B, lanes 3, 4). EGF-induced association between p85 and SHP2 was observed in cells expressing the mutant SIRPα1-4Y endodomain (Fig.6B, lanes 5,6), suggesting that tyrosine phosphorylated SIRPα1 must bind SHP2 to modulate PI3-K activation (Fig. 5B,C). One possibility is that functional SIRPα1 sequesters SHP2 from p85. Given the two SH2 domains and phosphotyrosine phosphatase activity in SHP2, along with the number of signaling pathways modulated by SHP2, SHP2-mediated modulation of PI3-K activation is likely to be complex. These data suggest a novel regulatory mechanism of EGF-induced PI3-K activation whereby functional SIRPα proteins may negatively modulate PI3-K activation by inhibiting an EGF-inducible SHP2/p85 association.

SIRPα1 regulates glioblastoma cell migration and cell spreading through SHP2.

Immortalized fibroblasts derived from a transgenic mouse in which the NH2-terminal SH2 site in SHP2 had been deleted exhibited phenotypic defects in cell migration and cell spreading, suggesting that SHP2 interactions may regulate attachment to cell-matrix interactions and cell migration in particular cell types (Yu *et al.*, 1998). More recent reports have illustrated that SHP2 may be a general regulator of cell motility and integrin signaling (Yu *et al.*, 1998; Oh *et al.*, 1999) and that cooperative activity between SHP2 and Fak may be important for this regulation (Manes *et al.*, 1999).

We next examined the specific role of the SIRPα1 carboxyl terminus in migration and spreading of human glioblastoma cells by using glioblastoma clones overexpressing wild-type or mutated SIRPα1. U87MG cells have a characteristic morphology and have been used for studies of cell migration and cell spreading modulated by the PTEN phosphatase mutated in many human glial tumors (Tamura *et al.*, 1998). U87MG cells expressing either empty vector, SIRPα1 or SIRPα1-

4Y were assessed for migration on fibronectin. Notably SIRP proteins are constitutively phosphorylated in the U87MG subclones used for these experiments (Fig. 6A). U87/SIRPα1 cells containing wild-type SIRPα1 exhibited a reduced rate of cell migration between 2-4h after plating when compared to U87MG clones expressing either empty vector or SIRPα1-4Y (Fig. 7). Therefore, reduced glioblastoma cell motility was observed in cells expressing elevated levels of tyrosine phosphorylated SIRPα1.

To examine the spreading efficiency of glioblastoma cells expressing wild-type or mutated SIRPα1, we collected U87MG subclones in serum-free DMEM and plated cells on fibronectin-coated cell culture dishes. Fig. 8A illustrates the progression of cell spreading following plating of the U87MG subclones. U87MG cells were well-suited for this analysis since they displayed a relatively homogeneous morphology immediately after plating. U87MG cells containing empty vector (U87/pIRES cells) initiated spreading at 10min and greater than 50% of cells had attained a flat morphology at 25min. By 60min, greater than 90% of cells were well-extended and displayed a flat morphology. Cell spreading was reduced by overexpression and tyrosine phosphorylation of wild-type SIRPα1 (Fig. 8A, B). Fewer U87/SIRPα1 cells had initiated spreading and more appeared smaller at 10min. In contrast to U87/pIRES cells, the majority of U87/SIRPα1 cells stayed round at 25min. Notably, a significant amount of U87/SIRPα1 cells were not well-extended at 60min. SIRPα1-4Y-expressing cells exhibited no apparent morphological differences from control cells. These data were reproduced in multiple SIRPα1- and SIRPα1-4Y- overexpressing subclones. Therefore, the tyrosine phosphorylated SIRPα1 carboxyl terminus reduces cell migration and cell spreading. Since the SIRPα1-4Y mutant receptor is not tyrosine phosphorylated and does not associate with SHP2 (Fig. 6), these data suggest that functional phosphorylated SIRPα1 negatively regulates cell migration and cell spreading through carboxyl terminal interactions with SH2 domains in SHP2. These data were reproduced in independent experiments using additional subclones.

Discussion

In this report, we have demonstrated several new functions for the SIRP transmembrane receptor that may begin to shed light on the mechanism by which ITIM-containing inhibitory receptors convey biological signals. In glioblastoma cells, SIRP proteins negatively regulated EGF-induced PI3-K activation by carboxyl terminal interactions with SH2 domains in SHP2. Our studies also indicate that tyrosine phosphorylated SIRPα1 inhibits an inducible association between SHP2 and the p85 regulatory subunit of PI3-K, which may interfere with activation of the p85/p110 PI3-K heterodimer. Modulation of an association between SHP2 and the p85 regulatory subunit is consistent with the role of SIRPα1 in regulating PI3-K activation. Our results support previous studies indicating a critical role for PI3-K activation in transformation, motility and survival of mammalian cells, particularly human glioblastoma cells. Phenotypic consequences of SIRP activation and diminished SHP2/p85 interaction include reduced PI3-K activation, inhibition of transformation, reduced cell migration and cell spreading and enhanced apoptosis following DNA damage. SIRP modulation of DNA damage-induced apoptosis appears to involve regulation of bcl-x_L total protein levels, a finding that has been observed by others following deregulation of EGFR signaling pathways in glioblastoma cells (Nagane *et al.*, 1998).

These studies demonstrate for the first time that tyrosine phosphorylated SIRP proteins can attenuate PI3-K activation following stimulation of EGFR. In our studies, EGF induced significant PI3-K activity in human glioblastoma cells in both antiphosphotyrosine and anti-SHP2 immunocomplexes. These results suggest that much of the EGF-induced PI3-K activation in glioblastoma cells may occur in a complex that contains SHP2. The precise role of SHP2 in regulating the PI3-K pathway in astrocytoma cells has not been resolved. Notably, anti-p85 and anti-SHP2 immunoprecipitations revealed the same trends of PI3-K activities as anti-pTyr immune complexes. Biochemical studies using chimeric murine ES cells containing mutant SHP2 alleles have shown that SHP2 is a critical mediator of EGFR signaling and that combined disruption of EGFR and SHP2 function modulates EGF-induced PI3-K activation (Qu *et al.*, 1999). Our data suggest that negative PI3-K regulation requires the formation of a SHP2/SIRP complex and that this complex may be an important mechanism of attenuating EGFR-induced PI3-K signaling. SHP2/SIRP regulation of PI3-K activation is supported by our data demonstrating that SHP2/SIRP interactions alter glioblastoma spreading and migration, two phenotypes which appear to be more related to PI3-K signaling than MAPK signaling. Our

recent experiments indicate a similar diminution of Akt/PKB phosphorylation by the functional SHP2/SIRP complex, supporting our results on PI3-K activation. SHP2/SIRP complex formation may serve to recruit and modulate PI3-K activity at the plasma membrane and may therefore represent a distinct mechanism of modulating the PI3-K pathway following stimulation of EGFR in glioblastoma cells.

SHP2 has been reported to associate inducibly with p85 in PC12 cells and primary neurons (Okada *et al.*, 1996; Yamada *et al.*, 1999) and in hematopoietic cells (Craddock & Welham, 1997; Gesbert *et al.*, 1998) and to bind inducibly the lipid phosphatase SHIP, in addition to unknown tyrosine phosphorylated proteins p100 and p120 in hematopoietic cells (Carlberg & Rohrschneider, 1997; Zhang & Broxmeyer, 1999). In human skin fibroblasts, distinct complexes involving SHP2, p85, and uncharacterized tyrosine phosphorylated proteins p115 and p105, but not including EGFR or erbB3, were found to specifically regulate EGF-induced PI3-K activity (Takahashi *et al.*, 1999). It is possible that the identified 105-115kDa proteins in these studies represent the Gab1 (Shi *et al.*, 2000) or Gab2 adaptor proteins (Gu *et al.*, 1998). However, complexes involving SHP2 and p85 may also contain SIRP/SHPS-1, since numerous SIRP/SHPS-1 proteins of 90-120kDa have been identified in different mammalian cell types, in part due tissue-specific glycosylation differences (Kharitonenkov *et al.*, 1997; Veillette *et al.*, 1998).

Cumulatively, the data suggest that a complex containing SHP2 and SIRP, and possibly other adaptor/effector proteins, modulates cell signaling following stimulation of EGFR. However, a MAPK-independent function for SIRP/SHPS-1 proteins distinct from that previously reported (Kharitonenkov *et al.*, 1997; Takada *et al.*, 1998) is suggested by our data in glioblastoma cells. Our data indicate that inhibition of transformation and reduced survival following DNA damage observed in SIRPα1-overexpressing human glioblastoma cells are not mediated by alterations in basal or EGF-induced MAPK activities. Similarly, SIRP activation does not appear to modulate mitogenic pathways in glioblastoma cells. Cell context may be critical for SIRP signaling. In COS7 cells we have been unable to document the association between SHP2 and p85 that we have consistently demonstrated in U87MG glioblastoma cells. Given that the association between SHP2 and p85 can only be documented in some cell types, e.g glioblastoma cells, it is not surprising that SIRP may preferentially regulate PI3-K signaling in some cells and MAPK

activation in others. SIRP appears to negatively modulate MAPK signaling in NIH3T3 cells (Kharitonenkov *et al.*, 1997), but diminish PI3-K activation in astrocytes.

Our data indicate that SIRP/SHP2 complexes modulate extracellular matrix-induced signals that may influence efficiency of cell transformation and cell survival. Moreover, our findings support studies indicating that PI3-K signaling pathways, rather than MAPK activation, are critical for cell motility and cell survival (Manes *et al.*, 1999; Tan *et al.*, 1999), both of which may contribute to epithelial cell transformation. Cell adhesion is critical for maintaining the integrity and topography of tissues. Proper cell adhesion requires cell-matrix adhesion and cell-cell adhesion. Cell adhesion molecules induce signals that influence cell proliferation, differentiation, motility and survival (Gumbiner, 1996). Cell spreading has been shown to be closely linked to cell survival (Re *et al.*, 1994; Chen *et al.*, 1997). Recent evidence has indicated that HRG-β-induced cell-cell adhesion (aggregation) of MCF-7 human breast cancer cells is sensitive to the PI3-K inhibitors wortmannin and LY294002, but not to the MEK1 inhibitor PD98059 (Tan *et al.*, 1999). The active signaling complex mediating this phenotype appeared to be an erbB2/erbB3 heterodimer containing more inducibly bound p85 in response to HRG-β. Others have shown that inhibition of HRG-stimulated PI3-K activation, cytoskeletal reorganization and cell migration of MCF-7 cells occurs independently of extracellular signal-regulated kinases (Adam *et al.*, 1998). Moreover, PD-98059 has been reported to have only a marginal effect on migration of MCF-7 breast cancer cells (Manes *et al.*, 1999). Our data reveal that migration and spreading of glioblastoma cells were reduced by increased SIRP tyrosine phosphorylation and binding of SHP2 in cells that also displayed reduced EGF-induced PI3-K activation. Taken together, the data suggest that SIRP/SHP2 complexes may coordinate independent signals initiated by integrins and the EGF receptor that may converge on PI3-K.

Our data also reveal increased biochemical complexity in the regulation of cell motility by SHP2. Mouse fibroblasts deficient in functional SHP2 showed defects in cell migration and spreading on fibronectin (Yu *et al.*, 1998). However, expression of catalytically-inactive SHP2 in Rat-1 fibroblasts and CHO cells increased the rate of cell attachment to and spreading on fibronectin (Inagaki *et al.*, 2000). Therefore, the mechanism by which SHP2 regulates cell motility is not clear and may require a highly complex coordination of signals that are related to cell context. Our studies indicate that binding of functional SIRPα1 to SHP2 is able to reduce motility of human glioblastoma cells. Motility-impaired glioblastoma subclones also displayed reduced

inducible association of SHP2 with p85 and reduced PI3-K activation, suggesting that the SHP2/p85 association may be critical in positively regulating cell migration and spreading through activation of the PI3-K pathway. Expression of the ΔEGFR oncoprotein in fibroblasts leads to preferential activation of PI3-K rather than MAPK (Moscatello *et al.*, 1996; Moscatello *et al.*, 1998). Furthermore, expression of the ΔEGFR oncoprotein in glioblastoma cells induces elevated constitutive PI3-K activity, enhanced SHP2/p85 association and increased cell motility (C-J Wu and D.M. O'Rourke, unpublished observations).

It is interesting that functional restoration of the PTEN phosphatase into U87MG cells leads to reduced cell migration and cell spreading (Tamura *et al.*, 1998). PTEN negatively regulates an Akt/PKB survival pathway (Stambolic *et al.*, 1998; Wu *et al.*, 1998) and is mutated or lost in many high-grade glial tumors and established glioma cell lines, including U87MG cells (Li *et al.*, 1997; Steck *et al.*, 1997). Akt/PKB is a PI3-K effector that becomes localized to sites of cell-cell and cell-matrix contact in epithelial cells in a PI3-K-dependent manner (Watton & Downward, 1999). Reintroduction of PTEN into glioma cells has been reported to increase anoikis (Davies *et al.*, 1998), a process of programmed cell death undergone by epithelial cells upon detachment from the extracellular matrix. Moreover, functional PTEN also increases sensitivity to radiation-induced apoptosis (Wick *et al.*, 1999). One might speculate that functional SHP2/SIRP complexes regulate PI3-K mediated cell survival and motility pathway(s) modulated further downstream by the PTEN tumor suppressor. Understanding the biochemical consequences of SIRP/SHP2 interactions may lead to new strategies that interfere with cell motility and survival of EGFR-overexpressing glioblastoma cells, and perhaps other erbB-containing human cancer cells.

Materials and methods

Plasmid Constructions.

The human SIRPα1 and SIRPα1-4Y cDNAs contained in pRK5(RS) (Kharitonenkov *et al.*, 1997) were modified for eukaryotic expression. The pRK5(RS) plasmids were digested with Nru I and Xho I and the fragments containing the SIRPα1 gene or its 4Y mutant gene were blunt-end ligated into the expression vector pIRES/Hyg (Clontech) previously linearized with Bam HI and blunt-ended for ligation. Derivations of the carboxyl terminal-deleted $p185^{neu}$ mutant receptor construct, T691stop, have been detailed previously (O'Rourke *et al.*, 1997a). Growth inhibitory properties of T691stop have been reported (O'Rourke *et al.*, 1997a; O'Rourke *et al.*, 1998a).

Maintenance of cells and transfection procedures.

Human U87MG glioblastoma cells were obtained from the American Type Tissue Collection (Rockville, MD) and cultured in Dulbecco's modified Eagle medium (DMEM) supplemented with 10% fetal bovine serum. For the analysis of Sirpα1 ectopic expression, U87MG cells were transfected either with empty vector (pIRESHyg), pIRESHyg/SIRPα1, or mutant pIRES/SIRPα1-4Y plasmids using lipofectamine (Gibco-BRL, Gaithersburg,MD) and were selected with 80μg/ml of hygromycin (Roche Molecular Biochemicals, Indianapolis, IN.). Positive SIRPα1- or SIRPα1-4Y- expressing subclones (U87/SIRPα1 or U87/SIRPα1-4Y) were identified by western blotting using a polyclonal antibody reactive with SIRPα1. U87MG-derived clones expressing the vector without insert were designated U87/pIRES cells. All the derived cells were maintained in DMEM containing hygromycin (35μg/ml).

Immunoprecipitation, co-immunoprecipitation and western blotting.

Cells was seeded and allowed to attach overnight. After starvation for 24h in DMEM containing 0.2% FBS, cells were treated with 50ng/ml of EGF for 5min at 37°C. The cells were then washed twice with 10mM sodium phosphate, pH7.4, 150mM NaCl, 1mM Na3VO4 and solublized in lysis buffer (50mM Tris-HCl, pH 7.5, 0.5% Triton X-100, 150mMNaCl, 2mMEGTA, 1mM sodium orthovanadate, 1mM phenylmethylsulfonyl fluoride, 10μg/ml aprotinin, 10μg/ml leupeptin).

Cell lysates were then subjected to centrifugation at 12,000xg for 15 min at 4°C. After normalization of supernatants derived from untreated cells and treated cells by protein concentration with the Dc Protein Assay kit (Bio-Rad, Hercules, CA), 500-1000μg of each cell lysate was incubated with the indicated antibody (1-3μg) on ice for 2h. Immune complexes were collected with Protein-A conjugated to Sepharose 4B (Sigma) and washed three times with 50mM Tris, pH7.5, 0.1% Triton X-100, 300mM NaCl, 2mM EGTA. The resulting immunoprecipitates were then subjected to SDS-polyacrylamide gel electrophoresis (PAGE) (6-8%), and then transferred onto nitrocellulose membranes followed by Western blot analysis with the indicated antibodies using the ECL detection system (Amersham).

For western blots evaluating Bcl-x_L protein levels, cells were harvested at the indicated time points after irradiation (10 Gy, 6min), and samples were boiled in lysis buffer, as recommended by the Bcl-x_L antibody producer's manual. After normalization by the Bio-Rad (Hercules, CA.) protein concentration assay, proteins were separated by 12% SDS-PAGE.

MAP kinase and PI3-kinase immune complex kinase assays.

Cells deprived of serum for 24h were treated with or without EGF (50ng/ml) for 5 min. For MAP kinase assays, cells were lysed with RIPA buffer (25mM Tris-HCl (pH7.5), 150mM NaCl, 1mMMgCl2, 0.2 mM EDTA, 0.5 mM dithiothreitol, 1% Triton X-100, 0.5% sodium deoxycholate, 20mM β-glycerophosphate, 1 mM sodium orthovanadate, 1mM phenylmethylsulfonyl fluoride, 10ug/ml aprotinin, 10ug/ml leupeptin). Protein concentrations were determined by the Dc Protein Assay kit (Bio-Rad). Equal amounts of proteins from cell extracts were immunoprecipitated with the indicated antibodies. After washing extensively, the immunocomplexes were then incubated with 50 μl of reaction buffer [20 mM Hepes, 50mM NaCl, 1mM sodium orthovanadate, 20mM MgCl2, 20 uM adenosine triphosphate(ATP), and 20mM β-glycerophosphate (pH 7.4) containing 2 μCi of [γ-^{32}P]ATP (NEN Life Science Products) and 2 μg of myelin basic protein (MBP) (Upstate Biotechnology Inc.) for the ERK kinase assays or 2 μg of c-Jun fusion protein (GST-jun) (Santa Cruz Biotechnology, Santa Cruz, CA.) for the JNK kinase assay. After incubation for 10 min at 30°C, kinase reactions were terminated by the addition of 3x Laemmli sample buffer. The samples were then resolved by SDS-PAGE, and phosphorylated substrates were visualized by autoradiography.

PI3-kinase assays were carried out as previously described (Qian *et al.*, 1999) with slight modifications. Cells were lysed in Nonidet P-40 lysis buffer (20mM Tris-HCl(pH 7.4), 137mM

NaCl, 1 mM MgCl2, 10% glycerol, 1% Nonidet P-40, 1mM sodium orthovanadate, 1mM phenylmethylsulfonyl fluoride, 10 μg/ml aprotinin, 1 μg/ml leupeptin). Equal amounts of protein (500μg) from cell extracts were immunoprecipitated with anti-phosphotyrosine 4G10 or anti-SHP2 for 3h. Protein A-sepharose was then added and incubated with rotation at 4°C for another 2h. Immune complexes were then washed twice with lysis buffer, twice with 0.5M LiCl in 100 mM Tris-HCl (pH 7.5) plus 100mM sodium othovanadate, and twice with reaction buffer (25mm Tris-HCl, pH7.5, 100 mM NaCl, 6.25mM MgCl2, 0.625mM disodium EDTA). The beads were resuspended in 40 μl of reaction buffer, and 10μl of substrate mixture (phosphatidylinositol and phosphatidylserine dispersed by sonication in 10 mM HEPES, 1mM EGTA, pH7.5) was added. The tubes were incubated at room temperature for 10 min and reactions were initiated by addition of 5uCi/tube [γ-^{32}P]ATP in 5μl of 100 μM of ATP and terminated by addition of 80 μl of CHCl3:CH3OH(1:1) after another 10 min. Phospholipids were extracted, desiccated, and redissolved in 12μl of CHCl3:CH3OH(2:1) and chromatographed on thin layer chromatography (TLC) plates (precoated with potassium oxalate and baked at 100°C for 1h just before use) in CHCl3:CH3OH: 2.5M NH4OH(9:7:2,v/v). Signal corresponding to phosphatidylinosital 3-phosphate (PIP) was visualized after autoradiography.

Cell growth and Transformation.

For cell growth, we utilized the MTT (3,(4,5-dimethylthiazol-2-yl)2,5-diphenyl-tetrazolium bromide) assay previously described (Hansen *et al.*, 1989; O'Rourke *et al.*, 1997a). For assays of focus formation of stably transfected subclones, previous methods were employed (Qian *et al.*, 1996).

Nuclei Staining and morphologic analysis of apoptosis.

Cells were plated onto coverslips for at least 12 hours prior to irradiation. Dose of irradiation used for this analysis was calculated to be 10 Gray for 6min. Coverslips were then washed twice with PBS at the indicated times, and fixed in 50:50 mix of ice-cold methanol/acetone for one minute. Coverslips were subsequently stained with 4',6-Diamidino-2-phenylindole dihydrochloride hydrate (DAPI) (Sigma, St. Louis, MO) at a concentration of 0.1-.25μg/ml in PBS. Inter-observer consistency in apoptosis counts of DAPI-stained nuclei were confirmed with terminal deoxynucleotidyl transferase-mediated dUTP nick end labeling (TUNEL)-staining

and by three independent observers. Statistical significance of the data was determined using the Student's *t*-test.

Cell motility assay.

Cell migration was determined as previously described (Yu *et al.*, 1998) using modified chambers containing polycarbonate membranes (tissue culture-treated, 6.5 mm diameter, 8 μm pores, transwell; Costar, Cambridge,MA). The lower sides of the membrane were coated with fibronectin (FN) (10μg/ml) for 1h at 37°C. Trypsininized cells were first washed once with DMEM containing 0.2% soybean trypsin inhibitor and then washed twice with DMEM. Cells were added to the upper chamber at $2x10^4$ cell/well in 100μl of DMEM, and the lower chamber was filled with DMEM containing 4μg/ml of FN. After incubation at 37°C for the indicated times, the membrane was fixed in methanol, and cells on the upper surface were mechanically removed. Migrated cells on the lower side of membranes were stained with Giemsa stain and counted under a microscope at 400x magnification. Two random microscopic fields were counted per well, and all experiments were performed in triplicate.

Cell spreading.

U87MG-derived glioblastoma cells were collected by trypsinization and washed twice with DMEM containing 0.2% soybean trypsin inhibitor (Sigma). Cell spreading was assessed as described previously (Yu *et al.*, 1998). Briefly, $2x\ 10^4$ cells were resuspended in DMEM and added to the wells of 24-well plates precoated with FN (10μg/ml) overnight at 4°C. Cells were allowed to spread for the indicated times at 37°C, and then photographed. Differences in morphology were found to be easiest to quantitate at 25min, therefore, this time point was chosen for quantitation of cell spreading.

Antibodies.

Rabbit polyclonal antibodies against a GST-SIRPα1 ectodomain (Ex1) fusion protein and against the SIRPα1 carboxyl terminus have been described previously (Kharitonenkov *et al.*, 1997). Anti-ERK, anti-JNK antibodies and polyclonal antibody reactive with the SHP-2 carboxyl terminus were obtained from Santa Cruz Biotechnology (Santa Cruz, CA). The anti-SHP2 antibody used for immunoblotting and the bcl-x_L polyclonal antibody were obtained from

Transduction Laboratories (Lexington, KY). The anti-phosphotyrosine mAb, 4G10, and the antibody reactive with the p85 regulatory subunit of PI3-K were obtained from Upstate Biotechnology (Lake Placid, NY).

Acknowledgments

This work was supported by grants from the Veterans Administration Merit Review Program and The Brain Tumor Society to D.M. O'Rourke. This work was also supported by grants from the National Cancer Institute, the American Cancer Society, the U.S. Army and the Abramson Family Cancer Center to M. I. Greene.

References

Adam, L., Vadlamudi, R., Kondapaka, S.B., Chernoff, J., Mendelsohn, J. & Kumar, R. (1998). *J Biol Chem*, **273,** 28238-28246.
Ahmad, S., Banville, D., Zhao, Z., Fischer, E.H. & Shen, S.H. (1993). *Proc Natl Acad Sci U S A*, **90,** 2197-2201.
Bennett, A.M., Hausdorff, S.F., O'Reilly, A.M., Freeman, R.M. & Neel, B.G. (1996). *Mol Cell Biol*, **16,** 1189-1202.
Cambier, J.C. (1997). *Proc Natl Acad Sci U S A*, **94,** 5993-5995.
Carlberg, K. & Rohrschneider, L.R. (1997). *J Biol Chem*, **272,** 15943-15950.
Chen, C.S., Mrksich, M., Huang, S., Whitesides, G.M. & Ingber, D.E. (1997). *Science*, **276,** 1425-1428.
Coggeshall, K.M. (1999). *Immunol Res*, **19,** 47-64.
Craddock, B.L. & Welham, M.J. (1997). *J Biol Chem*, **272,** 29281-29289.
D'Ambrosio, D., Hippen, K.L., Minskoff, S.A., Mellman, I., Pani, G., Siminovitch, K.A. & Cambier, J.C. (1995). *Science*, **268,** 293-297.
Daeron, M., Latour, S., Malbec, O., Espinosa, E., Pina, P., Pasmans, S. & Fridman, W.H. (1995). *Immunity*, **3,** 635-646.
Davies, M.A., Lu, Y., Sano, T., Fang, X., Tang, P., LaPushin, R., Koul, D., Bookstein, R., Stokoe, D., Yung, W.K., Mills, G.B. & Steck, P.A. (1998). *Cancer Res*, **58,** 5285-5290.
Deb, T.B., Wong, L., Salomon, D.S., Zhou, G., Dixon, J.E., Gutkind, J.S., Thompson, S.A. & Johnson, G.R. (1998). *J Biol Chem*, **273,** 16643-16646.
Feng, G.S. & Pawson, T. (1994). *Trends Genet*, **10,** 54-58.
Fujioka, Y., Matozaki, T., Noguchi, T., Iwamatsu, A., Yamao, T., Takahashi, N., Tsuda, M., Takada, T. & Kasuga, M. (1996). *Mol Cell Biol*, **16,** 6887-6899.
Furnari, F.B., Huang, H.J. & Cavenee, W.K. (1998). *Cancer Res*, **58,** 5002-5008.
Furnari, F.B., Lin, H., Huang, H.S. & Cavenee, W.K. (1997). *Proc Natl Acad Sci U S A*, **94,** 12479-12484.
Gesbert, F., Guenzi, C. & Bertoglio, J. (1998). *J Biol Chem*, **273,** 18273-18281.
Gu, H., Pratt, J.C., Burakoff, S.J. & Neel, B.G. (1998). *Mol Cell*, **2,** 729-740.
Gumbiner, B.M. (1996). *Cell*, **84,** 345-357.
Hansen, M.B., Nielsen, S.E. & Berg, K. (1989). *J Immunol Methods*, **119,** 203-210.
Huang, H.S., Nagane, M., Klingbeil, C.K., Lin, H., Nishikawa, R., Ji, X.D., Huang, C.M., Gill, G.N., Wiley, H.S. & Cavenee, W.K. (1997). *J Biol Chem*, **272,** 2927-2935.
Inagaki, K., Noguchi, T., Matozaki, T., Horikawa, T., Fukunaga, K., Tsuda, M., Ichihashi, M. & Kasuga, M. (2000). *Oncogene*, **19,** 75-84.
Jiang, P., Lagenaur, C.F. & Narayanan, V. (1999). *J Biol Chem*, **274,** 559-562.
Kharitonenkov, A., Chen, Z., Sures, I., Wang, H., Schilling, J. & Ullrich, A. (1997). *Nature*, **386,** 181-186.
Li, J., Yen, C., Liaw, D., Podsypanina, K., Bose, S., Wang, S.I., Puc, J., Miliaresis, C., Rodgers, L., McCombie, R., Bigner, S.H., Giovanella, B.C., Ittmann, M., Tycko, B., Hibshoosh, H., Wigler, M.H. & Parsons, R. (1997). *Science*, **275,** 1943-1947.
Manes, S., Mira, E., Gomez-Mouton, C., Zhao, Z.J., Lacalle, R.A. & Martinez, A.C. (1999). *Mol Cell Biol*, **19,** 3125-3135.
Moscatello, D.K., Holgado, M.M., Emlet, D.R., Montgomery, R.B. & Wong, A.J. (1998). *J Biol Chem*, **273,** 200-206.

Moscatello, D.K., Montgomery, R.B., Sundareshan, P., McDanel, H., Wong, M.Y. & Wong, A.J. (1996). *Oncogene*, **13,** 85-96.
Nagane, M., Coufal, F., Lin, H., Bogler, O., Cavenee, W.K. & Huang, H.-J.S. (1996). *Cancer Res*, **56,** 5079-5086.
Nagane, M., Levitzki, A., Gazit, A., Cavenee, W.K. & Huang, H.-J.S. (1998). *Proc. Natl. Acad. Sci. (USA)*, **95,** 5724-5729.
Nishikawa, R., Ji, X.D., Harmon, R.C., Lazar, C.S., Gill, G.N., Cavenee, W.K. & Huang, H.J. (1994). *Proc Natl Acad Sci U S A*, **91,** 7727-7731.
Noguchi, T., Matozaki, T., Horita, K., Fujioka, Y. & Kasuga, M. (1994). *Mol Cell Biol*, **14,** 6674-6682.
O'Rourke, D.M., Kao, G.D., Singh, N., Park, B.-W., Muschel, R.J., Wu, C.-J. & Greene, M.I. (1998b). *Proc Natl Acad Sci (USA)*, **95,** 10842-10847.
O'Rourke, D.M., Nute, E.J.L., Davis, J.G., Wu, C., Lee, A., Murali, R., Zhang, H.-T., Qian, X., Kao, C.-C. & Greene, M.I. (1998a). *Oncogene*, **16,** 1197-1207.
O'Rourke, D.M., Qian, X., Zhang, H.-T., Davis, J.G., Nute, E., Meinkoth, J. & Greene, M.I. (1997a). *Proc. Natl. Acad. Sci. (USA)*, **94,** 3250-3255.
O'Rourke, D.M., Zhang, X. & Greene, M.I. (1997b). *Proceedings of the Association of American Physicians*, **109,** 209-219.
Ochi, F., Matozaki, T., Noguchi, T., Fujioka, Y., Yamao, T., Takada, T., Tsuda, M., Takeda, H., Fukunaga, K., Okabayashi, Y. & Kasuga, M. (1997). *Biochem Biophys Res Commun*, **239,** 483-487.
Oh, E.S., Gu, H., Saxton, T.M., Timms, J.F., Hausdorff, S., Frevert, E.U., Kahn, B.B., Pawson, T., Neel, B.G. & Thomas, S.M. (1999). *Mol Cell Biol*, **19,** 3205-3215.
Ohnishi, H., Kubota, M., Ohtake, A., Sato, K. & Sano, S. (1996). *J Biol Chem*, **271,** 25569-25574.
Okada, N., Wada, K., Goldsmith, B.A. & Koizumi, S. (1996). *Biochem Biophys Res Commun*, **229,** 607-611.
Pruss, R.M. & Herschman, H.R. (1977). *Proc Natl Acad Sci U S A*, **74,** 3918-21.
Qian, X., O'Rourke, D.M., Fei, Z., Kao, C.-C., Zhang, H.-T. & Greene, M.I. (1999). *J Biol Chem*, **274,** 574-583.
Qian, X., O'Rourke, D.M., Zhao, H. & Greene, M.I. (1996). *Oncogene*, **13,** 2149-2157.
Qu, C.K., Yu, W.M., Azzarelli, B. & Feng, G.S. (1999). *Proc Natl Acad Sci U S A*, **96,** 8528-8533.
Re, F., Zanetti, A., Sironi, M., Polentarutti, N., Lanfrancone, L., Dejana, E. & Colotta, F. (1994). *J Cell Biol*, **127,** 537-546.
Rodeck, U., Jost, M., DuHadaway, J., Kari, C., Jensen, P.J., Risse, B. & Ewert, D.L. (1997). *Proc. Natl. Acad. Sci. USA*, **94,** 5067-5072.
Saxton, T.M., Henkemeyer, M., Gasca, S., Shen, R., Rossi, D.J., Shalaby, F., Feng, G.S. & Pawson, T. (1997). *Embo J*, **16,** 2352-2364.
Shi, Z.Q., Lu, W. & Feng, G.S. (1998). *J Biol Chem*, **273,** 4904-4908.
Shi, Z.Q., Yu, D.H., Park, M., Marshall, M. & Feng, G.S. (2000). *Mol Cell Biol*, **20**, 1526-1536.
Stambolic, V., Suzuki, A., de la Pompa, J.L., Brothers, G.M., Mirtsos, C., Sasaki, T., Ruland, J., Penninger, J.M., Siderovski, D.P. & Mak, T.W. (1998). *Cell*, **95,** 29-39.
Steck, P.A., Pershouse, M.A., Jasser, S.A., Yung, W.K., Lin, H., Ligon, A.H., Langford, L.A., Baumgard, M.L., Hattier, T., Davis, T., Frye, C., Hu, R., Swedlund, B., Teng, D.H. & Tavtigian, S.V. (1997). *Nat Genet*, **15,** 356-362.

Takada, T., Matozaki, T., Takeda, H., Fukunaga, K., Noguchi, T., Fujioka, Y., Okazaki, I., Tsuda, M., Yamao, T., Ochi, F. & Kasuga, M. (1998). *J Biol Chem*, **273,** 9234-9242.
Takahashi, Y., Akanuma, Y., Yazaki, Y. & Kadowaki, T. (1999). *J Cell Physiol*, **178,** 69-75.
Tamura, M., Gu, J., Matsumoto, K., Aota, S.-i., Parsons, R. & Yamada, K. (1998). *Science*, **280,** 1614-1617.
Tan, M., Grijalva, R. & Yu, D. (1999). *Cancer Res*, **59,** 1620-1625.
Tang, T.L., Freeman, R.M., Jr., O'Reilly, A.M., Neel, B.G. & Sokol, S.Y. (1995). *Cell*, **80,** 473-483.
Tanowitz, M., Si, J., Yu, D.H., Feng, G.S. & Mei, L. (1999). *J Neurosci*, **19,** 9426-9435.
Tsuda, M., Matozaki, T., Fukunaga, K., Fujioka, Y., Imamoto, A., Noguchi, T., Takada, T., Yamao, T., Takeda, H., Ochi, F., Yamamoto, T. & Kasuga, M. (1998). *J Biol Chem*, **273,** 13223-13229.
Veillette, A., Thibaudeau, E. & Latour, S. (1998). *J Biol Chem*, **273,** 22719-22728.
Vely, F., Olivero, S., Olcese, L., Moretta, A., Damen, J.E., Liu, L., Krystal, G., Cambier, J.C., Daeron, M. & Vivier, E. (1997). *Eur J Immunol*, **27,** 1994-2000.
Watton, S.J. & Downward, J. (1999). *Curr Biol*, **9,** 433-436.
Wick, W., Furnari, F.B., Naumann, U., Cavenee, W.K. & Weller, M. (1999). *Oncogene*, **18,** 3936-3943.
Wu, C.J., Qian, X. & O'Rourke, D.M. (1999). *DNA Cell Biol*, **18,** 731-741.
Wu, X., Senechal, K., Neshat, M.S., Whang, Y.E. & Sawyers, C.L. (1998). *Proc Natl Acad Sci U S A*, **95,** 15587-15591.
Yamada, M., Ohnishi, H., Sano, S., Araki, T., Nakatani, A., Ikeuchi, T. & Hatanaka, H. (1999). *J Neurochem*, **73,** 41-49.
Yamao, T., Matozaki, T., Amano, K., Matsuda, Y., Takahashi, N., Ochi, F., Fujioka, Y. & Kasuga, M. (1997). *Biochem Biophys Res Commun*, **231,** 61-67.
Yamauchi, K., Milarski, K.L., Saltiel, A.R. & Pessin, J.E. (1995). *Proc Natl Acad Sci U S A*, **92,** 664-668.
Yamauchi, K. & Pessin, J.E. (1995). *J Biol Chem*, **270,** 14871-14874.
Yu, D.H., Qu, C.K., Henegariu, O., Lu, X. & Feng, G.S. (1998). *J Biol Chem*, **273,** 21125-21131.
Zhang, S. & Broxmeyer, H.E. (1999). *Biochem Biophys Res Commun*, **254,** 440-445.

Figure Legends

Fig. 1. SIRP α1 inhibits EGFR-mediated transformation of U87MG human glioblastoma cells but does not affect cell proliferation. A. Transforming efficiency of SIRPα1-overexpressing U87MG-derived subclones. 200 U87MG-derived cells were plated with 10^4 NR6 cells (Pruss & Herschman, 1977) and grown in 5% FBS-DMEM for 14 days. Foci (mean ± SD) were then stained and quantitated based on triplicate dishes for each cell line. These data were confirmed by three independent experiments. B. Cell growth at 48h following overnight attachment in 10% FBS-DMEM was indistinguishable between U87/pIRES and U87/SIRPα1 cells. Results (mean ± SD) of absorbance at 570nm as determined by an ELISA reader are displayed for two cell concentrations and were in the linear range for this cell type (Hansen *et al.*, 1989). Results were confirmed in three independent experiments.

Fig. 2. SIRPα1 enhances apoptosis following gamma-irradiation in U87MG human glioblastoma cells. Mean ± SD of counts derived from two independent observers are presented as a percentage. Over 600 cells were counted in multiple fields for each sample after staining with 4',6-Diamidino-2-phenylindole dihydrochloride hydrate (DAPI) and assessing the morphologic appearance of apoptosis at 48-72h. At 72h following irradiation (10Gy, 6min), levels of apoptosis were significantly (*) higher in U87/ SIRPα1 cells ($p<.05$) and in U87/T691 cells ($p<.005$) than in control U87/pIRES cells. Results were confirmed in three independent experiments.

Fig. 3. A-C. **Morphologic assessment of apoptosis in glioblastoma subclones following gamma-irradiation (10Gy, 6min).** All cells were stained with 4',6-Diamidino-2-phenylindole dihydrochloride hydrate (DAPI) 48-72h after being exposed to gamma-irradiation. U87MG cells overexpressing empty vector (A), SIRPα1 (B), and T691stop neu mutant receptors (C) are shown. Nuclei exhibiting apoptotic morphology (O'Rourke *et al.*, 1998b) are indicated by the arrows. D. Direct western blotting of cell lysates for bcl-X_L protein at the indicated times following gamma-irradiation. Normalization of protein loading was confirmed by Coumassie blue staining.

Fig. 4. SIRPα1 does not alter ERK1, ERK2, or JNK MAPK *in vitro* kinase activities in glioblastoma subclones. Whole cell lysates taken from stably transfected U87/pIRES (empty vector) and U87/SIRPα1 cells were immunoprecipitated by antibodies preferentially

reactive with both phosphorylated and nonphosphorylated ERK1 (lanes 1,2), ERK2 (lanes 3,4) and JNK1 (lanes 5,6) forms and were then incubated with either MBP (lanes 1-4) or GST-jun (lanes 5,6) following EGF treatment (5 min, 100ng/ml, 37°C). *In vitro* kinase activities for ERK1, ERK2, and JNK1 were comparable between U87/pIRES and U87/SIRPα1 stably transfected subclones.

Fig. 5. SIRPα1 attenuates EGF-induced PI3-K activity through the SHP2 phosphatase. A. Evaluation of overexpressed SIRPα1 (lane 2) or mutated SIRPα1-4Y (lane 3) protein by direct western blotting of whole cell lysates with polyclonal antibody reactive with human SIRPα . Ectopically expressed SIRPα1 migrates at Mr=90kDa in U87MG cells. Endogenous SIRP proteins cannot be detected with the concentration of protein used for this analysis. B, C. EGF-induced PI3-K activity. U87MG human glioblastoma cells stably expressing either empty vector alone (U87/pIRES), SIRPα1 (U87/SIRPα1) or SIRPα1-4Y (U87/SIRPα1-4Y) were treated with or without EGF (50ng/ml) for 5 min after serum starvation for 24h. Equal amounts of cell extracts were immunoprecipitated by anti-pTyr (4G10) (B) or anti-SHP2 (C) antibodies and analyzed for PI3-K activity as described in *Materials and Methods*. Autoradiogram of thin layer chromatography plate exposed overnight is shown. The positions of origin (*ori*) and phosphatidylinositol 3-phosphate (*PIP*) are indicated by *arrows*. Data shown are representative of four independent experiments.

Fig. 6. SIRPα1 inhibits inducible binding of SHP2 to p85 regulatory subunit in glioblastoma cells. U87/pIRES, U87/SIRPα1, and U87/SIRPα1-4Y cells were serum-starved for 24h, followed by treatment with or without EGF (50ng/ml for 5 min). Whole cell extracts were then immunoprecipitated by an antibody reactive with SHP2 and analyzed by 8% SDS-PAGE according to *Materials and Methods*. For panels A-D, immunoblotting of SHP2 immunocomplexes was performed with the indicated antibodies and signals were visualized with the ECL detection system.

Fig. 7. SIRPα1 reduces glioblastoma cell migration through an interaction with SHP2. To measure cell motility, U87MG clones expressing either empty vector, SIRP α1, or SIRPα1-4Y were added to the upper chamber separated by a 8 μm porous membrane in a 6.5 mm Transwell chamber. The cells were incubated at 37°C for the indicated times, and allowed to migrate through the membrane into the lower side which was coated with fibronectin. Migrated cells on the lower side of the membrane were then counted. The data represent mean

± S.D of a representative experiment with all samples performed in triplicate. These data were reproduced in three additional experiments.

Fig. 8. Reduced spreading of SIRPα1-overexpressing glioblastoma cells on fibronectin. A. U87MG clones expressing either empty vector, SIRPα1 , or SIRPα1-4Y were plated on fibronectin-coated cell culture dishes, incubated at 37°C, visualized using phase contrast microscopy and then photographed at 10, 25, and 60 min. B. Quantitative comparison of cell spreading efficiency was obtained by calculating the percentage (mean ± S.D) of spread cells for U87MG-derived cell lines at 25min as indicated in *Materials and Methods*. This representative experiment was confirmed by four independent experiments.

Figure 1

A

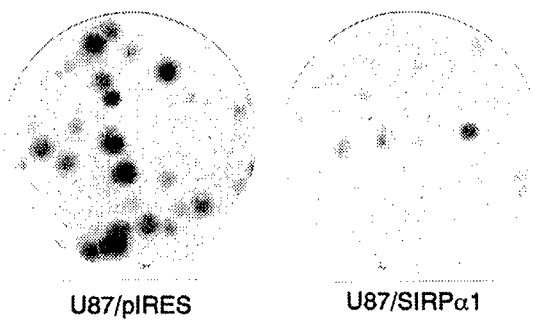
U87/pIRES
U87/SIRPα1

B

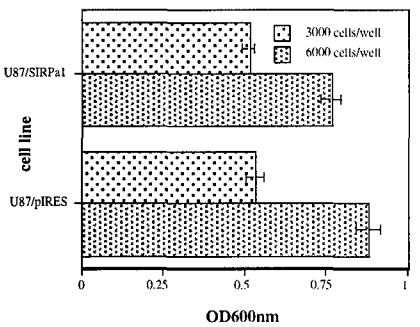
3000 cells/well
6000 cells/well
U87/SIRPa1
U87/pIRES
cell line
0
0.25
0.5
0.75
1
OD600nm

Figure 2

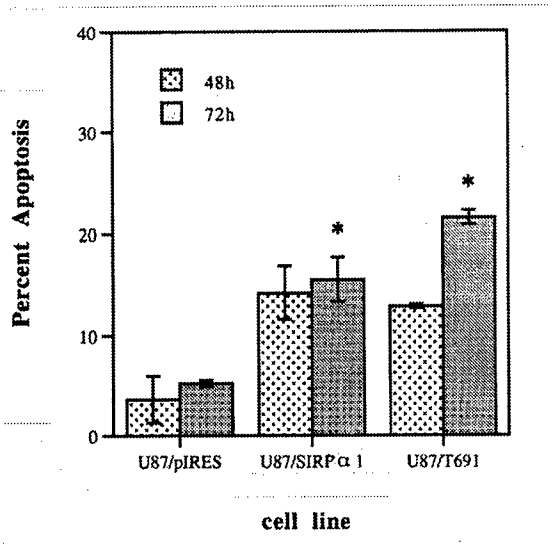
40
30
20
10
0
48h
72h
Percent Apoptosis
*
*
U87/pIRES
U87/SIRPα1
U87/T691
cell line

Figure 3

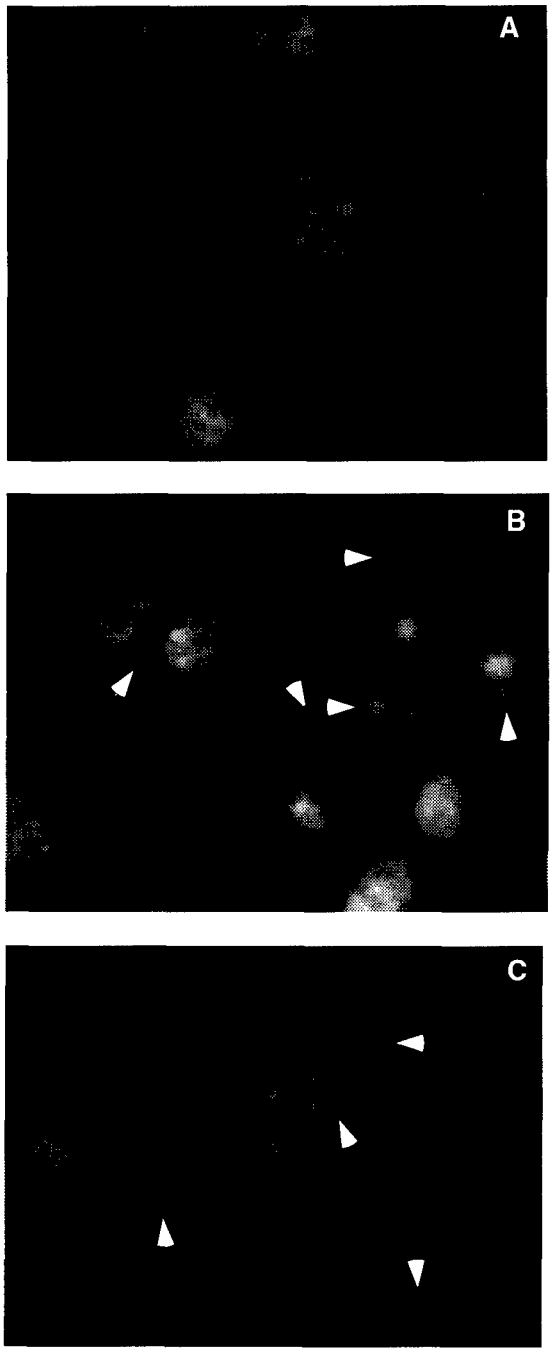
A
U87/pIRES
B
U87/SIRPα1
C
U87/T691

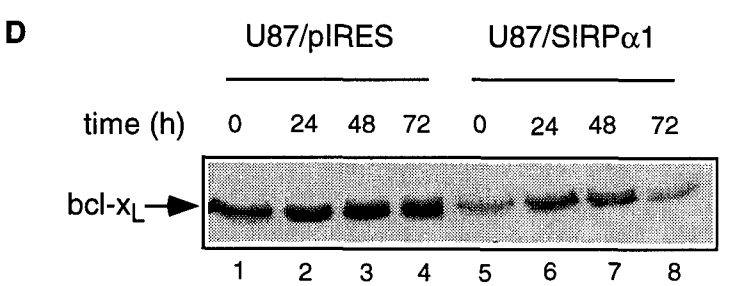
D
U87/pIRES
U87/SIRPα1
time (h)
0 24 48 72 0 24 48 72
bcl-xL
1 2 3 4 5 6 7 8

Figure 4

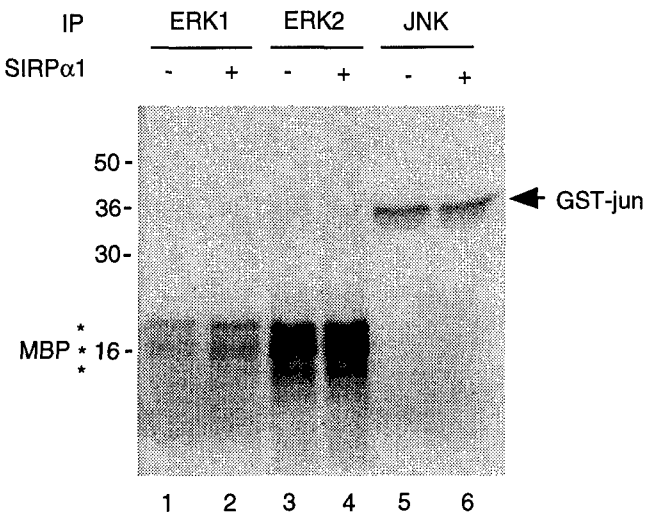

Figure 5

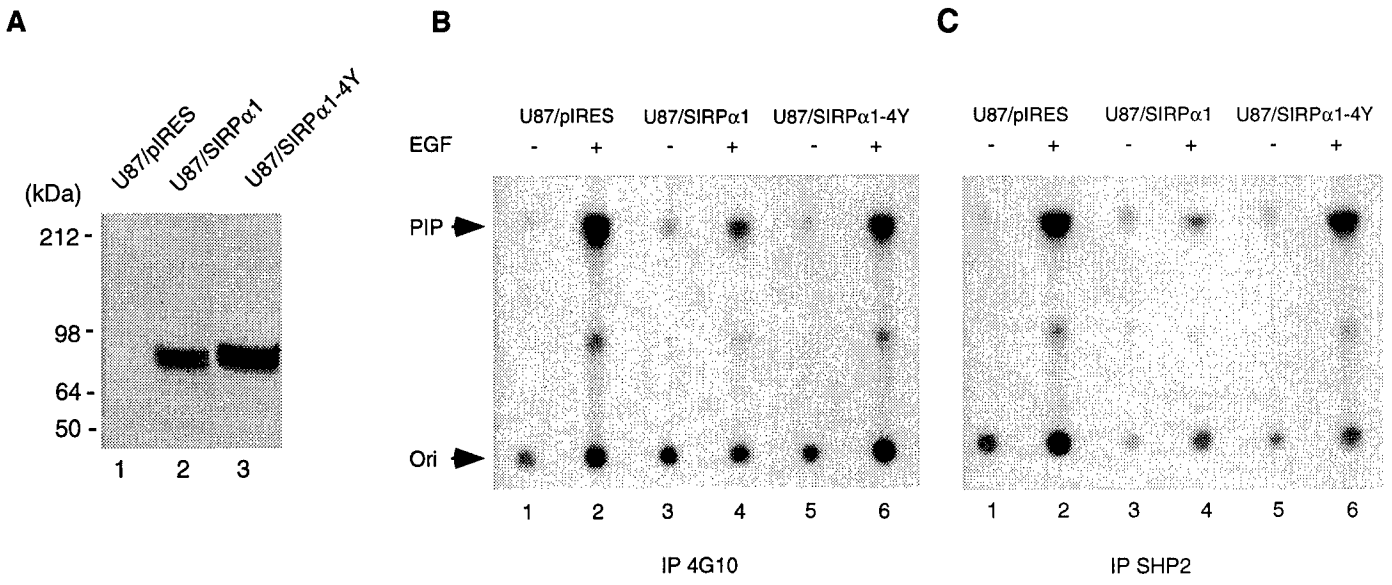
A
B
C
U87/pIRES
U87/SIRPα1
U87/SIRPα1-4Y
(kDa)
212
98
64
50
1 2 3
EGF
- + - + - +
PIP
Ori
1 2 3 4 5 6
IP 4G10
IP SHP2

Figure 6

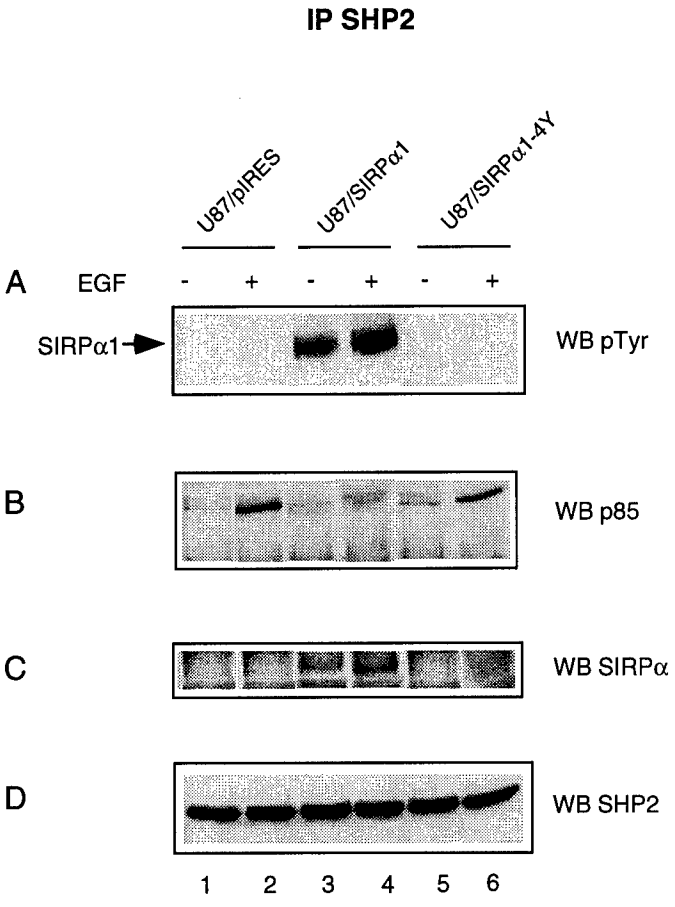
IP SHP2
U87/pIRES
U87/SIRPα1
U87/SIRPα1-4Y
A
EGF
- + - + - +
SIRPα1
WB pTyr
B
WB p85
C
WB SIRPα
D
WB SHP2
1 2 3 4 5 6

Figure 7

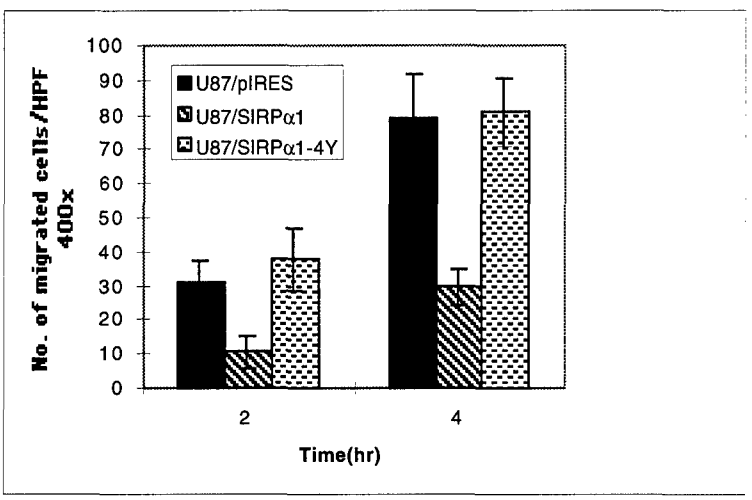
100
90
80
70
60
50
40
30
20
10
0
No. of migrated cells/HPF 400x
U87/pIRES
U87/SIRPα1
U87/SIRPα1-4Y
2
4
Time(hr)

Figure 8

A

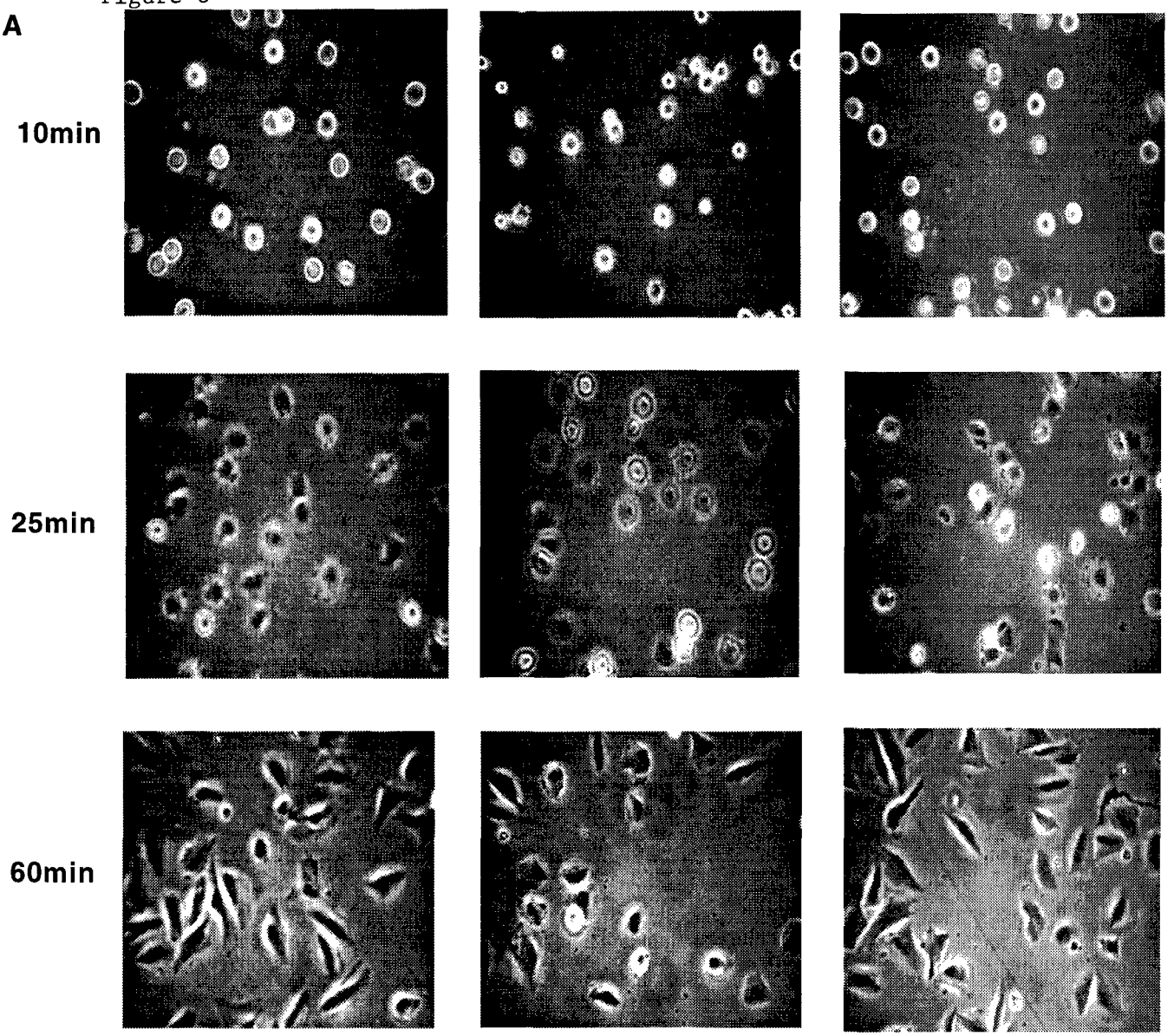
10min
25min
60min
U87/pIRES
U87/SIRPα1
U87/SIRPα1-4Y

B

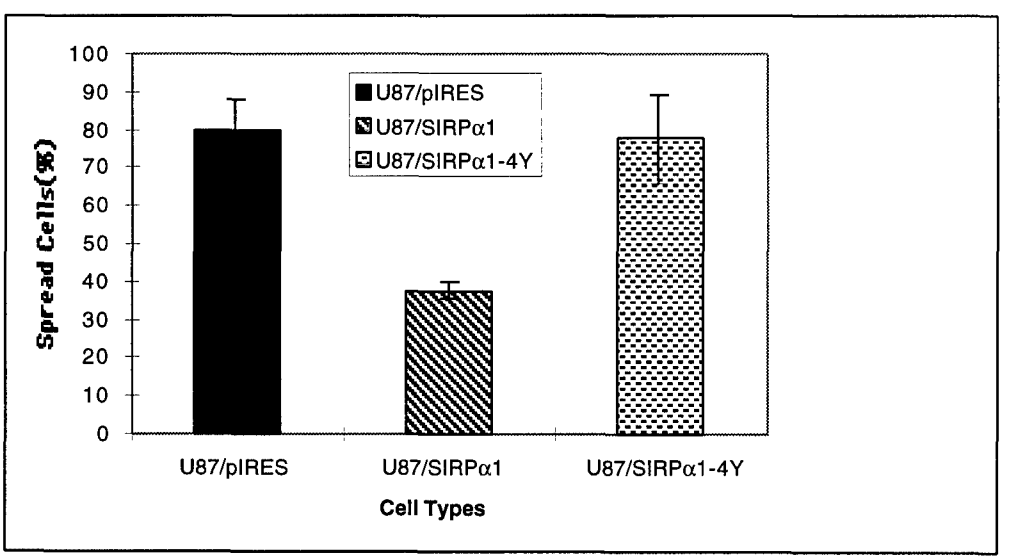
100
90
80
70
60
50
40
30
20
10
0
Spread Cells(%)
U87/pIRES
U87/SIRPα1
U87/SIRPα1-4Y
U87/pIRES
U87/SIRPα1
U87/SIRPα1-4Y
Cell Types

Rationally designed anti-HER2/neu peptide mimetic disables P185$^{HER2/neu}$ tyrosine kinases in vitro and in vivo

Byeong-Woo Park[1†], Hong-Tao Zhang[1†], Chuanjin Wu[1†], Alan Berezov[1], Xin Zhang[1], Raj Dua[2], Qiang Wang[1], Gary Kao[3], Donald M. O'Rourke[1,4], Mark I. Greene[1*], and Ramachandran Murali[1*]

*[1]Department of Pathology and Laboratory Medicine, Center for Receptor Biology and Cell Growth, University of Pennsylvania School of Medicine, 36th and Hamilton Walk, Philadelphia, PA 19104. [2]Xcyte Therapeutics, Inc., Seattle, WA, 98122. [3]Department of Radiation Oncology, University of Pennsylvania School of Medicine, 36th and Hamilton Walk, Philadelphia, PA 19104. [4]Department of Neurosurgery, University of Pennsylvania School of Medicine, 36th and Hamilton Walk, Philadelphia, PA 19104. *Corresponding authors R.M. (murali@xray.med.upenn.edu) or M.I.G. (greene@reo.med.upenn.edu). [†]These authors contributed equally to this work.*

Received 29 July 1999; accepted 14 December 1999

Monoclonal antibodies specific for the p185$^{HER2/neu}$ growth factor receptor represent a significant advance in receptor-based therapy for p185$^{HER2/neu}$-expressing human cancers. We have used a structure-based approach to develop a small (1.5 kDa) exocyclic anti-HER2/neu peptide mimic (AHNP) functionally similar to an anti-p185$^{HER2/neu}$ monoclonal antibody, 4D5 (Herceptin). The AHNP mimetic specifically binds to p185$^{HER2/neu}$ with high affinity (K_D = 300 nM). This results in inhibition of proliferation of p185$^{HER2/neu}$-overexpressing tumor cells, and inhibition of colony formation in vitro and growth of p185$^{HER2/neu}$-expressing tumors in athymic mice. In addition, the mimetic sensitizes the tumor cells to apoptosis when used in conjunction with ionizing radiation or chemotherapeutic agents. A comparison of the molar quantities of the Herceptin antibody and the AHNP mimetic required for inhibiting cell growth and anchorage-independent growth showed generally similar activities. The structure-based derivation of the AHNP represents a novel strategy for the design of receptor-specific tumor therapies.

Key Words: ErbB2, Her2, neu, mimetic, doxorubicin, Herceptin, γ-radiation, tumor therapy

The p185$^{HER2/neu}$ (also called c-erbB-2) oncoprotein is the human analog of p185^{neu}, and is overexpressed in ~25–35% of human breast, ovarian, and colon cancers[1,2]. Monoclonal antibodies to the ectodomain of p185^{neu}[3,4] and to p185$^{HER2/neu}$ (Herceptin)[5] have been shown to be effective in limiting growth of tumors in vivo. Recombinant humanized anti-HER2 monoclonal antibody[5] rhuMAb4D5 (Herceptin)[6–8] was developed as a useful anti-oncoprotein therapeutic agent based on earlier observations by Drebin and colleagues[4,9,10], showing that anti-p185^{neu} ectodomain specific antibodies reverse the malignant phenotype in vitro and in vivo.

The use of full-length monoclonal antibodies in clinical applications may be limited by: (1) the difficulty or expense of commercial-scale production (2) exclusion of monoclonal antibody from compartments such as the blood/brain barrier (3) limited ability for monoclonal antibodies to penetrate cells and tissues[11], and (4) the possibility of severe side effects such as induction of anti-idiotypic antibodies and immune complex formation.

In instances when only a defined surface of the protein mediates activity, smaller peptides represent obvious alternatives as mimics for larger macromolecular structures. Although peptide mimetics themselves are seldom used as therapeutic agents, they can be used as a template and through iterative reductions in size and increases in biological activity may lead to viable therapeutic reagents[12–17] better suited for clinical application than full-length antibody.

We have developed a structure-based procedure for designing peptidomimetics that focuses on small loops and turn reversals of members of the immunoglobulin gene family[18–20]. Using this method we have designed a 1.5 kDa anti-p185$^{HER2/neu}$ peptidomimetic, AHNP, that is comparable in potency to the full-length monoclonal antibody and exhibits biochemical and biological properties that are predictive of therapeutic use. The general approach described here may be considered a paradigm for development of specific receptor-based therapies, and AHNP may be considered a viable candidate for use in clinical trials aimed to treat p185$^{HER2/neu}$-positive human cancers.

Results and discussion

Structure of the AHNP. Structural studies of several antigen–antibody complexes have shown that of the six variable loops[21], the heavy-chain CDR3 loop often, but not always, mediates most of the contact with antigen[22,23]. Furthermore, they show that antibodies can provide a structural internal image of a given antigen[24]. Based on these observations, we have designed mimetics derived from CDR3 loops of anti-p185$^{HER2/neu}$ monoclonal antibodies.

We analyzed CDR loops from the deduced structure of the monoclonal antibody 7.16.4 (M.I.G. and P. Alzari, unpublished results) and the crystal structure of rhuMAb4D5[25,26]. Both monoclonal antibodies 7.16.4 and rhuMAb4D5 seem to bind to an overlapping epitope on the p185$^{HER2/neu}$ ectodomain[27]. The CDR3H loop of both antibodies showed 41% similarity in their primary structure, and molecular modeling revealed the predicted folding of these loops to be similar. Therefore we used heavy-chain CDR3 loops of rhuMAb4D5 and 7.16.4 as templates to design several analogs, using strategies developed earlier[15,19,20,28]. The analogs were then tested for their biological activity. Mimetics that showed activity higher than 200 μM were considered minimally active in cell growth inhibition assays and ignored (data not shown).

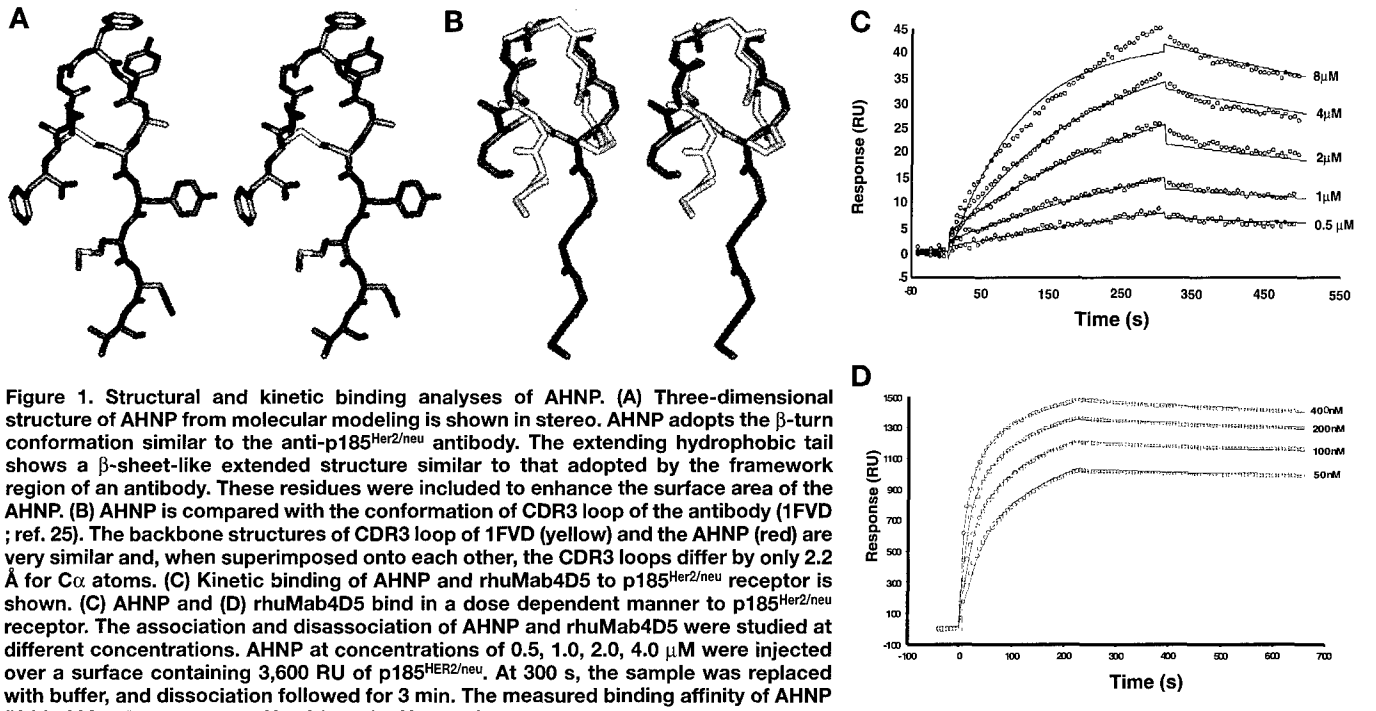

Figure 1. Structural and kinetic binding analyses of AHNP. (A) Three-dimensional structure of AHNP from molecular modeling is shown in stereo. AHNP adopts the β-turn conformation similar to the anti-p185$^{Her2/neu}$ antibody. The extending hydrophobic tail shows a β-sheet-like extended structure similar to that adopted by the framework region of an antibody. These residues were included to enhance the surface area of the AHNP. (B) AHNP is compared with the conformation of CDR3 loop of the antibody (1FVD ; ref. 25). The backbone structures of CDR3 loop of 1FVD (yellow) and the AHNP (red) are very similar and, when superimposed onto each other, the CDR3 loops differ by only 2.2 Å for Cα atoms. (C) Kinetic binding of AHNP and rhuMab4D5 to p185$^{Her2/neu}$ receptor is shown. (C) AHNP and (D) rhuMab4D5 bind in a dose dependent manner to p185$^{Her2/neu}$ receptor. The association and disassociation of AHNP and rhuMab4D5 were studied at different concentrations. AHNP at concentrations of 0.5, 1.0, 2.0, 4.0 μM were injected over a surface containing 3,600 RU of p185$^{HER2/neu}$. At 300 s, the sample was replaced with buffer, and dissociation followed for 3 min. The measured binding affinity of AHNP (K_D) is 300 nM compared to K_D of 1 nM for Herceptin.

Analysis of several analogs has shown that two structural features of the peptides seem to affect potency of cyclic peptides: (1) ring size and (2) inherent flexibility[29,30]. Residues at the C terminus also seemed critical for activity. To enhance stability, folding, and avidity, we employed aromatic modification[15,31,32]. To extend the surface area at the interface of interaction, we used extended residues (MDV) beyond the stabilizing cysteine residues in all of the AHNP species.

One of the compounds (FCGDGFYACYMDV) showed moderate activity at IC_{50} of 100 μM. High-pressure liquid chromatography (HPLC) analysis of this mimic revealed two predominant forms of the peptides, and one species had higher activity (data not shown). Upon sequencing, it was noted that the Gly3 was missing. A model without Gly3 revealed a more classical β-turn (Fig. 1A) than the original peptide. The putative contact residues of these peptide mimetics seem to have a similar relative disposition (root mean square deviation for Cα atoms is 2.2 Å) to that of the CDR3H of the parent antibody rhuMAb4D5 (Fig. 1B). Thus, exocyclic peptides that adopt rigid (compared to the original peptide mimic with extra glycine) and comparable ring sizes to β-turns may be capable of high-affinity binding activity.

Kinetic binding affinity of AHNP. Anti-HER 2/neu peptide has a 300 nM binding affinity for the p185$^{HER2/neu}$ (Fig. 1C). Based on the association and dissociation kinetics using a 1:1 Langmuir model for simple bimolecular interactions, the affinity of AHNP was shown to

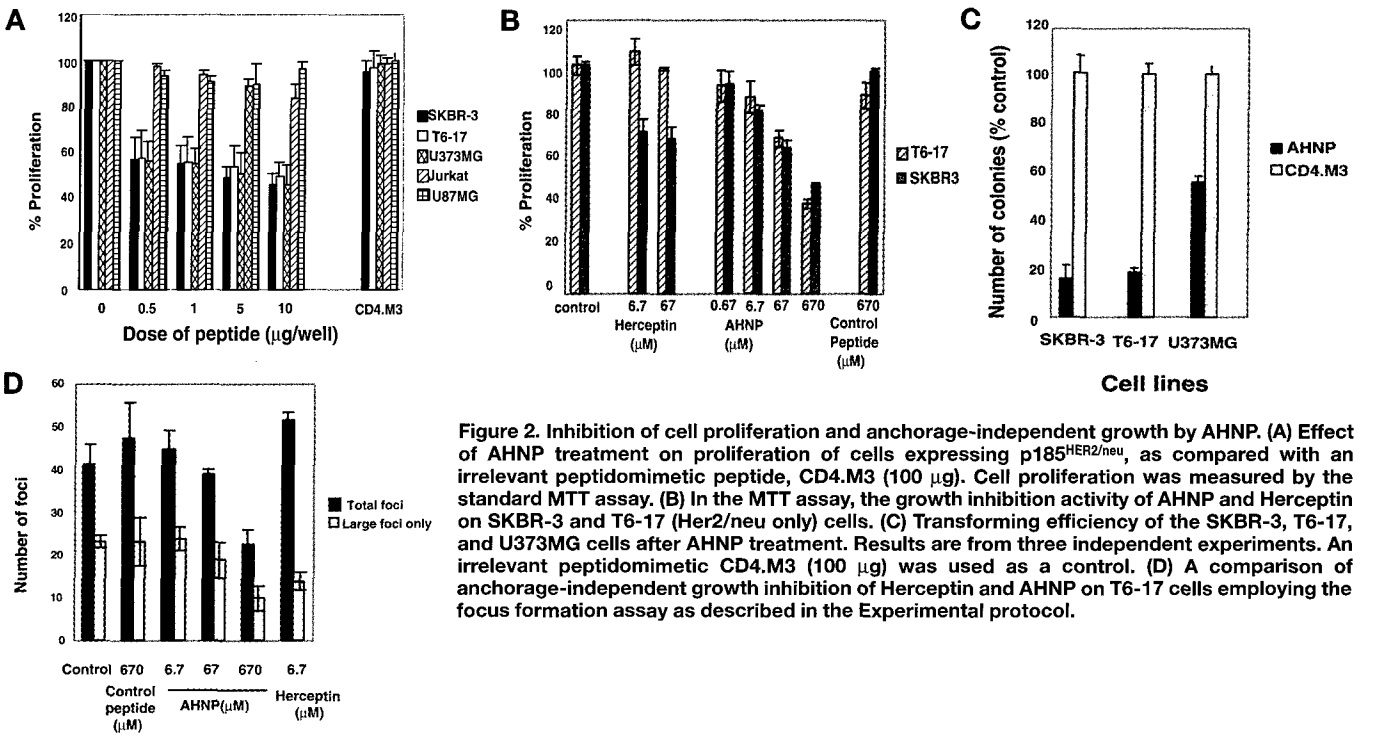

Figure 2. Inhibition of cell proliferation and anchorage-independent growth by AHNP. (A) Effect of AHNP treatment on proliferation of cells expressing p185$^{HER2/neu}$, as compared with an irrelevant peptidomimetic peptide, CD4.M3 (100 μg). Cell proliferation was measured by the standard MTT assay. (B) In the MTT assay, the growth inhibition activity of AHNP and Herceptin on SKBR-3 and T6-17 (Her2/neu only) cells. (C) Transforming efficiency of the SKBR-3, T6-17, and U373MG cells after AHNP treatment. Results are from three independent experiments. An irrelevant peptidomimetic CD4.M3 (100 μg) was used as a control. (D) A comparison of anchorage-independent growth inhibition of Herceptin and AHNP on T6-17 cells employing the focus formation assay as described in the Experimental protocol.

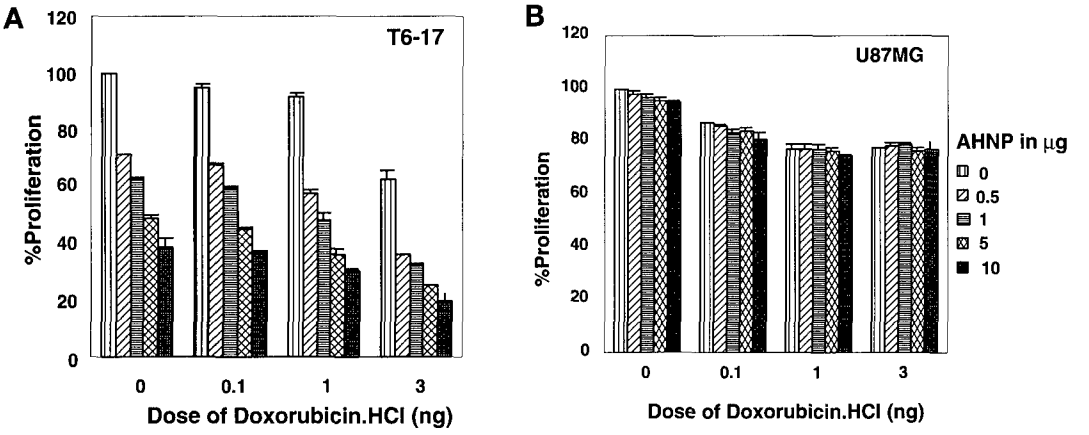

Figure 3. Combined cytotoxicity of doxorubicin and AHNP. The antiproliferation effect of doxorubicin HCl as determined by dose-dependent administration of AHNP (A) in human p185$^{HER2/neu}$-positive T6-17 cells (B) and in human U87MG cells expressing negligible concentrations of p185$^{HER2/neu}$. Results represent the mean ± s.e. of three readings.

have a K_D of 3.59×10^{-7} M. The apparent k_{on} and k_{off} rate constants were estimated to be 1.32×10^3 M^{-1} s^{-1} and 4.74×10^{-4} M^{-1} s^{-1}, respectively. Based on a bivalent model, the monoclonal antibody rhuMAb4D5 binds the p185$^{HER2/neu}$ receptor with a K_D of 1.04×10^{-9} M with k_{on} and k_{off} 1.18×10^5 M^{-1} s^{-1} and 1.23×10^{-4} M^{-1} s^{-1}, respectively.

The k_{off} value is considered as critical for kinetic binding in the development of therapeutics of biological activity [33,34] and generally correlates with potent biological effects[35]. Although the K_D of the AHNP species binds with less affinity than that of the monoclonal antibody, their k_{off} rate is very similar, which suggests that the AHNP forms a stable receptor complex. High-pressure liquid chromatography studies revealed AHNP existed as a monomer only (data not shown).

To assess the specificity of this interaction, the tumor necrosis factor receptor-(ectodomain)-Fc (TNFR-Fc) receptor was immobilized to the sensor surface. The AHNP did not bind to TNFR-Fc, indicating that AHNP polypeptide is specific for the p185$^{HER2/neu}$ ectodomain (data not shown). Calculated and experimentally observed maximum binding capacities of the commercially produced rhuMAb4D5 were comparable (Fig. 1D). No interaction of the peptide with the matrix was observed (data not shown).

Downmodulation of surface p185$^{HER2/neu}$ receptors by AHNP. Downmodulation of p185$^{Her2/neu}$ by AHNP was modest (only about 25% of total surface receptors downmodulated) and far less than with monoclonal antibody 7.16.4 treatment of p185^{neu}-expressing cells (data not shown)[36]. Mechanisms involved in downmodulation of type I receptor tyrosine kinase (RTKs) of the erbB family of receptors have not been completely defined. Efficient downmodulation of erbB receptor kinases apparently requires an intact tyrosine kinase activity as well as a structural module within the C terminus[37]. Because AHNP is able to downmodulate surface p185$^{HER2/neu}$ receptors to a smaller extent than the monoclonal antibody, downmodulation may be driven by induced conformational changes in the receptor, and this allosteric effect may trigger other inhibitory signals, which then affect phenotype.

AHNP inhibits cell proliferation and anchorage-independent growth. We analyzed the growth characteristics of peptidomimetic-treated cells using the MTT (3-(4,5-dimethylthiazol-2-yl)-2,5-diphenyltetrazolium bromide) assay for mitochondrial viability[38] in an adherent-cell assay. In three cell lines overexpressing p185$^{HER2/neu}$ at various concentrations, treatment with AHNP resulted in 33–53% inhibition of cell proliferation (Fig. 2A). The dose-dependent inhibition is best seen in Figure 2B. Adherent-cell proliferation was unaffected by AHNP or CD4.M3 treatment in Jurkat and U87MG cells that do not contain p185$^{HER2/neu}$ (Fig. 2A). These data suggest that AHNP, such as anti-p185$^{HER2/neu}$ antibodies[8,39], specifically inhibits proliferation of p185$^{HER2/neu}$-expressing cells. As seen in Figure 2B, we conducted a comparison of the molar amounts of the Herceptin antibody and AHNP required to affect the growth of cells that overexpress p185$^{HER2/neu}$ (T6-17) or that overexpress p185$^{HER2/neu}$ and EGFr (SKBR-3). Anti-HER 2/neu peptide was better at inhibiting T6-17 growth and equivalent to Herceptin at inhibiting SKBR-3 growth.

Inhibition of cell transformation was assessed using an anchorage-independent growth focus formation assay. The AHNP treatment of cells from three transformed lines inhibited the development of morphologically transformed foci (Fig. 2C). Transforming efficiencies of SKBR-3, T6-17, and U373MG cells were inhibited 84.1 ± 5.6% (mean ± s.e.m.), 81.9 ± 1.8%, and 44.2 ± 1.6%, respectively, by AHNP treatment in three independent experiments. However, treatment with an irrelevant mimetic, CD4.M3, did not result in any inhibition of transforming efficiency of the same cell lines (Fig. 2C). A comparison of Herceptin and AHNP revealed that Herceptin was slightly better at inhibiting large foci formation of T6-17 cells but less efficient than AHNP at inhibition of all sized foci (Fig. 2D).

Enhanced inhibition of cell proliferation by doxorubicin with cotreatment with AHNP. Treatment with AHNP increased doxorubicin-mediated inhibition of cell proliferation in p185$^{Her2/neu}$-overexpressing T6-17 cells (Fig. 3A). With doxorubicin alone at a dose of 3 nM, minimal inhibition of cell growth (40%) was observed. Cotreatment with AHNP resulted in additive and possibly synergistic inhibition at 5–10 μM, whereas 0.5–1 μM of AHNP resulted in inhibition that was additive with doxorubicin effects (Fig. 3A).

Anti-HER 2/neu peptide-mediated inhibition was observed at all doses of doxorubicin. However, AHNP treatment did not enhance the inhibition of cellular proliferation of U87MG cells that do not contain

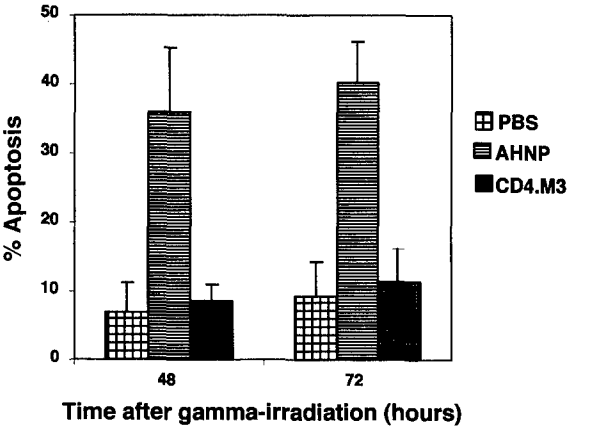

Figure 4. AHNP enhances γ-irradiation-induced apoptosis. Enhanced apoptotic cell death observed at 48 h and 72 h following γ-irradiation, after pretreatment of p185$^{HER2/neu}$-positive U373MG human astrocytoma cells with AHNP. Cells were pretreated with either PBS or a similar amount of an irrelevant peptidomimetic of identical molecular mass (CD4-M3) as controls.

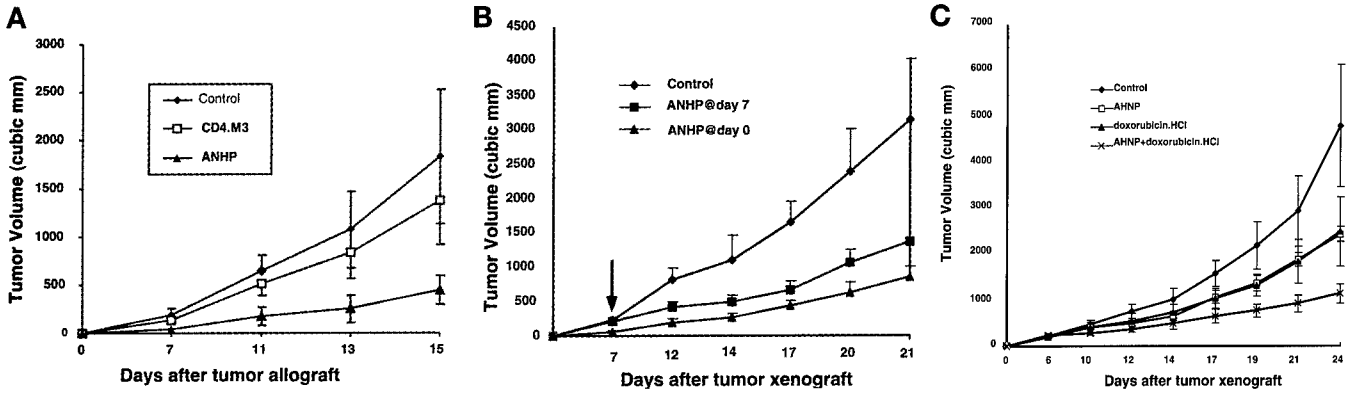

Figure 5. Inhibition of in vivo tumor growth by administration of AHNP. Tumor growth mediated by T6-17 cells was assessed in athymic mice. (A) Mice were administered 200 μg of AHNP, the irrelevant mimetic CD4.M3, or PBS by intraperitoneal injection, three times weekly beginning on the day of T6-17 cell inoculation. (B) Same experiments as in (A), except that AHNP was given to mice on the day of inoculation (AHNP@day 1) or seven days after (AHNP@day 7). (C) The effect of cotreatment with AHNP on the antitumor activity of doxorubicin against well-established T6-17 tumor xenografts. Results are given as mean tumor volume ± s.e. Tumor growth in animals treated with both reagents was significantly ($P < 0.001$) different compared to controls.

$p185^{HER2/neu}$ (Fig. 3B). U87MG cells exhibited only 20–25% inhibition of cell growth at doses of 3 nM doxorubicin. U87MG cells lack $p185^{Her2/neu}$ and contain elevated concentrations of endogenous epidermal growth factor receptor (EGFR)[40], in addition to low concentrations of erbB3 and erbB4 proteins (data not shown). These data indicate that AHNP selectively inhibits proliferation of $p185^{HER2/neu}$-expressing cells in which p185 is contributing to the transformed phenotype.

AHNP increases tumor cell death in response to γ-irradiation. Induction of apoptosis rather than cell cycle arrest may underlie successful anticancer treatment[40,41]. Therefore we examined whether AHNP could enhance cell death induced by radiation.

Incubation with AHNP of U373MG cells containing elevated EGFR concentrations and moderately elevated concentrations of $p185^{HER2/neu}$ followed by γ-irradiation resulted in 36% and 40% cell death at 48 h and 72 h, respectively, compared to cell death fractions of about 10% observed at all time points in untreated U373MG cells (Fig. 4). As a control, an irrelevant peptide mimetic of equivalent molecular mass, CD4.M3, was shown to not enhance radiation-induced apoptosis.

Inhibition of in vivo tumor growth by AHNP. Small exocyclic peptides have short half-lives and may be cleared before they can induce biological changes. However, we have found that AHNP is an active molecule in in vivo assays. In an athymic mouse model, monoclonal antibody 4D5 was shown to localize at the site of tumors in vivo and inhibit the growth of human tumor xenografts that overexpress $p185^{HER2/}$neu (ref. 39).

In vivo growth of T6-17 transfected fibroblasts expressing human $p185^{Her2/neu}$ was evaluated in athymic mice. In the first set of studies, AHNP was administered intraperitoneally three times weekly following inoculation of tumor cells in the flank. Sustained treatment with AHNP resulted in inhibition of tumor xenograft formation. Administration of a size-matched irrelevant peptidomimetic peptide, CD4.M3, or phosphate-buffered saline (PBS) had no effect on tumor growth (Fig. 5A). We then AHNP administered intraperitoneally after the development of small palpable tumors derived from the T6-17 fibroblast. AHNP also inhibited progression of tumor formation in these animals, indicating that AHNP could inhibit progression of growth of established tumors (Fig. 5B).

As with studies using the full-length rhuMAb4D5 in our hands, growth delay alone was observed because tumors eventually grew in all treated animals. This result suggests that the action of the AHNP is cytostatic, and not cytotoxic, a feature described in previous reports using full-length antireceptor antibodies[10,42].

Inhibition of in vivo tumor growth is enhanced by coadministration of doxorubicin and AHNP. Although AHNP and doxorubicin independently showed inhibition of established tumor growth, administration of both AHNP and doxorubicin increased growth inhibition of tumor xenografts in an additive manner (Fig 5C). Similar concentrations of inhibition were observed in vivo with either AHNP or doxorubicin. Inhibition of tumor cell growth in vivo by treatment of U373MG cells with AHNP alone revealed that the AHNP could inhibit tumor growth in cells expressing $p185^{HER2/neu}$ in combination with EGFR and other erbB proteins (data not shown).

In summary, we have reduced the macromolecular structure of a monoclonal antibody to a small secondary structure mimetic that has high affinity and in vivo activity against tumor growth, creating a true "antibody mimic." This small molecule has comparable affinity and molar activities as the parental Herceptin antibody. Creation of such small antibody mimics not only eliminates the laborious humanization of antibodies, but also provides a new avenue in the design of antibody-based therapy.

Experimental protocol

Design of AHNP. We analyzed the crystal structure of anti-$p185^{HER2/neu}$ receptor antibody (1FVD[25,26]) and the structural model of an anti-$p185^{neu}$ antibody (7.16.4) that binds rodent and human p185 and compared all of the CDRs of both monoclonals for sequence and structural similarity using a variety of software including BLAST, CLUSTALV, and AbM (Oxford Molecular, Mountain View, CA). Details of the procedure in the design of peptidomimetic are described in Takasaki and coworkers[20]. Molecular modeling and the structural analyses were carried out using both QUANTA and INSIGHT (Molecular Simulation, San Diego, CA).

Kinetic binding analysis. Biosensor experiments were carried out on both Biacore X and Biacore 2000 (Biacore AG, Uppsala, Sweden) instruments at 25°C. Recombinant purified $p185^{HER2/neu}$ receptors composed of the ectodomain of $p185^{HER2/neu}$ fused to the Fc of human IgG (provided by Dr. Che Law, Xcyte Therapeutics, Seattle, WA) were immobilized to the dextran hydrogel on the sensor surface (Biacore CM5 sensor chip) with a surface density of 3,600 resonance units (RU). Surface plasmon resonance (SPR) measurements were carried out under a continuous flow of 20 ml^{-1} min^{-1}. The surface was regenerated to remove all bound analyte among binding cycles using a mixture of organic solvents composed of dimethyl sulfoxide (DMSO), acetonitrile, 1-butanol, formamide, and ethanol, each at 0.2% (v/v) concentration in water. The apparent rate constants (k_{on} and k_{off}) and the equilibrium-binding constant (K_D) for the receptor–peptide binding interaction were estimated from the kinetic analysis of sensorgrams, using the BIA evaluation 3.0 software (Biacore International AB, Uppsala, Sweden).

Cell lines. We used several human tumor cells expressing variable concentrations of $p185^{HER2/neu}$ receptors all of which we characterized for $p185^{HER2/neu}$ concentrations by flow cytometric analysis and quantitative immunoprecipitation: (a) U87MG cells and Jurkat cells (negligible $p185^{HER2/neu}$) (b) U373MG cells expressing low–moderate $p185^{HER2/neu}$ (c) SK-BR-3 and T6-17 (NIH3T3 cells stably transfected with $p185^{HER2/neu}$, provided by J. Pierce, National

Cancer Institute) cells (high concentration of $p185^{HER2/neu}$). NE91 murine fibroblasts expressing human EGFR have been described[43]. These cells were cultured and maintained in Dulbecco's modified Eagle's medium (DMEM) containing: 10% fetal bovine serum (FBS), 1% L-glutamine, and 1% penicillin/streptomycin at 37°C, 95% humidity, and 5% CO_2.

Cell proliferation. Proliferation was measured by standard MTT assay[38]. Cell lines were plated in 96-well plates (4,000 cells/well) in DMEM–10% FBS with indicated amount of AHNP or irrelevant CD4.M3, and were incubated for 24 h. Then MTT was given to the cells for 4 h. Cells were lysed in 50% SDS–20% DMSO and kept at 37°C overnight. Proliferation was assessed by taking optical density readings at 600 nm, using an ELISA reader. The number of cells used in these assays was determined to be within the linear range for this cell type.

Anchorage-independent growth. For the focus formation assay, 10^3 T6-17 cells were plated with 2×10^3 NR6 cells onto a 60 mm dish in DMEM medium with 2% FBS. Media, with or without antibodies or mimetics, were changed every three days. Fourteen days after plating, foci were scored after cells were fixed with 10% formalin and stained with hematoxylin. All experiments were done in triplicate and two or three independent studies were done. The next day, colonies were counted using an Alpha-imager system (Alpha Innotech, San Leandro, CA) for automatic counting. Large colonies were determined by automatic scaling for colonies >3 mm^2.

Apoptosis estimation by morphology and flow cytometry. For morphologic analysis, 30,000 cells were allowed to attach to coverslips overnight in six-well plates. Cells were incubated with 25 μg/ml of AHNP, or CD4.M3 (an irrelevant peptide mimetic of equivalent molecular mass) for 24 h before γ-irradiation. γ-Irradiation (10 Gy) was applied and cells were incubated at 37°C for the indicated time periods. Nuclear morphology characteristic of apoptosis was assessed following staining with DAPI (4,6-diamidino-2-phenylindole) at the following time points after irradiation: 12, 24, 48, and 72 h. Statistical significance of the data was determined using Student's *t*-test, as previously used. For flow cytometry analysis, 200,000 cells were plated onto six-well dishes and allowed to attach overnight. Cells were then incubated with 25 μg/ml of AHNP, or irrelevant mimetic CD4/M3, for 2 h, and the indicated amount of doxorubicin was then added.

In vivo studies. NCr homozygous athymic (nude) mice (six to eight weeks-old) were purchased from the National Cancer Institute. An aliquot of 2×10^6 T6-17 cells were suspended in 200 μl of PBS and injected subdermally in the right thigh of each animals. Six days after tumor xenograft, tumors reached ~200–230 mm^3 in volume. Animals were regrouped into four treatment groups: control, AHNP alone, doxorubicin alone, and AHNP in combination with doxorubicin. At day 6 and again at day 20, 100 μg of doxorubicin were given. Anti-HER 2/neu peptide was administered (200 μg) intraperitoneally three times a week from day 6 after tumor xenograft. Animals were maintained in accordance with guidelines of the Institutional Animal Care and Use Committee (IACUC) of the University of Pennsylvania. Tumor growth was monitored three times weekly for four weeks. Tumor volume was calculated by the formula: $\pi/6 \times (\text{larger diameter}) \times (\text{smaller diameter})^2$.

Acknowledgments

This work was supported by grants awarded to M.I.G. from the Abramson Cancer Institute, National Cancer Institute, NIH, and the US Army.

1. Slamon, D.J. et al. Human breast cancer: correlation of relapse and survival with amplification of the HER-2/neu oncogene. *Science* **235**, 177–182 (1987).
2. Cohen, J.A. et al. Expression pattern of the *neu* (NGL) gene-encoded growth factor receptor protein (p185neu) in normal and transformed epithelial tissues of the digestive tract. *Oncogene* **4**, 81–88 (1989).
3. Drebin, J.A., Link, V.C., Stern, D.F., Weinberg, R.A. & Greene, M.I. Development of monoclonal antibodies reactive with the product of the *neu* oncogene. *Symp. Fund. Cancer Res.* **38**, 277–289 (1986).
4. Drebin, J.A., Link, V.C. & Greene, M.I. Monoclonal antibodies specific for the *neu* oncogene product directly mediate anti-tumor effects in vivo. *Oncogene* **2**, 387–394 (1988).
5. Baselga, J., Norton, L., Albanell, J., Kim, Y.M. & Mendelsohn, J. Recombinant humanized anti-HER2 antibody (Herceptin) enhances the antitumor activity of paclitaxel and doxorubicin against HER2/neu overexpressing human breast cancer xenografts. *Cancer Res.* **58**, 2825–2831 (1998).
6. Carter, P. et al. Humanization of an anti-p185HER2 antibody for human cancer therapy. *Proc. Natl. Acad. Sci. USA* **89**, 4285–4289 (1992).
7. Fendly, B.M. et al. Characterization of murine monoclonal antibodies reactive to either the human epidermal growth factor receptor or HER2/neu gene product. *Cancer Res.* **50**, 1550–1558 (1990).
8. Hudziak, R.M. et al. p185HER2 monoclonal antibody has antiproliferative effects in vitro and sensitizes human breast tumor cells to tumor necrosis factor. *Mol. Cell Biol.* **9**, 1165–1172 (1989).
9. Drebin, J.A., Stern, D.F., Link, V.C., Weinberg, R.A. & Greene, M.I. Monoclonal antibodies identify a cell-surface antigen associated with an activated cellular oncogene. *Nature* **312**, 545–548 (1984).
10. Drebin, J.A., Link, V.C., Weinberg, R.A. & Greene, M.I. Inhibition of tumor growth by a monoclonal antibody reactive with an oncogene-encoded tumor antigen. *Proc. Natl. Acad. Sci. USA* **83**, 9129–9133 (1986).
11. Cho, M.J. & Juliano, R. Macromolecular versus small-molecule therapeutics: drug discovery, development and clinical considerations. *Trends Biotechnol.* **14**, 153–158 (1996).
12. Hruby, V.J. Conformational and topographical considerations in the design of biologically active peptides. *Biopolymers* **33**, 1073–1082 (1993).
13. Langston, S. Peptidomimetics and small molecule design. *Drug Discov. Today* **2**, 254–256 (1997).
14. Qabar, M., Urban, J., Sia, C., Klein, M. & Kahn, M. Pharmaceutical applications of peptidomimetics. *Lett. Pept. Sci.* **3**, 25–30 (1996).
15. Murali, R. & Greene, M.I. Structure-based design of immunologically active therapeutic peptides. *Immunol. Res.* **17**, 163–169 (1998).
16. Moore, G.J. Designing peptide mimetics. *Trends Pharmacol. Sci.* **15**, 124–129 (1994).
17. KieberEmmons, T., Murali, R. & Greene, M.I. Therapeutic peptides and peptidomimetics. *Curr. Opin. Biotechnol.* **8**, 435–441 (1997).
18. Saragovi, H.U. et al. Design and synthesis of a mimetic from an antibody complementarity-determining region. *Science* **253**, 792–795 (1991).
19. Zhang, X. et al. Synthetic Cd4 exocyclic peptides antagonize Cd4 holoreceptor binding and T-cell activation. *Nat. Biotechnol.* **14**, 472–475. (1996).
20. Takasaki, W., Kajino, Y., Kajino, K., Murali, R. & Greene, M.I. Structure-based design and characterization of exocyclic peptidomimetics that inhibit TNF alpha binding to its receptor. *Nat. Biotechnol.* **15**, 1266–1270 (1997).
21. Chothia, C. & Lesk, A.M. Canonical structures for the hypervariable regions of immunoglobulins. *J. Mol. Biol.* **196**, 901–917 (1987).
22. MacCallum, R.M., Martin, A.C. & Thornton, J.M. Antibody-antigen interactions: contact analysis and binding site topography. *J. Mol. Biol.* **262**, 732–745 (1996).
23. Mariuzza, R.A., Phillips, S.E. & Poljak, R.J. The structural basis of antigen-antibody recognition. *Annu. Rev. Biophys. Biophys. Chem.* **16**, 139–159 (1987).
24. Bruck, C. et al. Nucleic acid sequence of an internal image-bearing monoclonal anti-idiotype and its comparison to the sequence of the external antigen. *Proc. Natl. Acad. Sci. USA* **83**, 6578–6582 (1986).
25. Eigenbrot, C., Randal, M., Presta, L., Carter, P. & Kossiakoff, A.A. X-ray structures of the antigen-binding domains from three variants of humanized anti-p185HER2 antibody 4D5 and comparison with molecular modeling. *J. Mol. Biol.* **229**, 969–995 (1993).
26. Eigenbrot, C. et al. X-ray structures of fragments from binding and nonbinding versions of a humanized anti-CD18 antibody: structural indications of the key role of VH residues 59 to 65. *Proteins* **18**, 49–62 (1994).
27. Zhang, H. et al. Pathobiological features of shared antigenic epitopes and biological functions of distinct and humanized anti-p185her2/neu monoclonal antibodies. *Exp. Mol. Pathol.* **67**, 15–25 (1999).
28. Zhang, X. et al. Synthetic Cd4 exocyclics inhibit binding of human-immunodeficiency-virus type-1 envelope to Cd4 and virus-replication in T-lymphocytes. *Nat. Biotechnol.* **15**, 150–154. (1997).
29. Adang, A.E.P., Hermkens, P.H.H., Linders, J.T.M., Ottenheijm, H.C.J. & van Staveren, C.J. Case histories of peptidomimetics: progression from peptides to drugs. *Recl. Trav. Chim. Pays-Bas.* **113**, 63–78 (1994).
30. Akamatsu, M. et al. Potent inhibition of protein-tyrosine phosphatase by phosphotyrosine-mimic containing cyclic peptides. *Bioorg. Med. Chem.* **5**, 157–163 (1997).
31. Graciani, N.R., Tsang, K.Y., McCutchen, S.L. & Kelly, J.W. Amino acids that specify structure through hydrophobic clustering and histidine-aromatic interactions lead to biologically active peptidomimetics. *Bioorg. Med. Chem.* **2**, 999–1006 (1994).
32. McDonnell, J.M., Fushman, D., Cahill, S.M., Sutton, B.J. & Cowburn, D. Solution structures of Fc epsilon RI alpha-chain mimics: a beta-hairpin peptide and its retroenantiomer. *J. Am. Chem. Soc.* **119**, 5321–5328 (1997).
33. Yiallouros, I. et al. Phosphinic peptides, the first potent inhibitors of astacin, behave as extremely slow-binding inhibitors. *Biochem. J.* **331**, 375–379 (1998).
34. Benveniste, M. & Mayer, M.L. Structure-activity analysis of binding kinetics for NMDA receptor competitive antagonists: the influence of conformational restriction. *Br. J. Pharmacol.* **104**, 207–221 (1991).
35. Moosmayer, D. et al. Characterization of different soluble TNF receptor (TNFR80) derivatives: positive influence of the intracellular domain on receptor/ligand interaction and TNF neutralization capacity. *J. Interf. Cytok. Res.* **16**, 471–477 (1996).
36. Drebin, J.A., Link, V.C., Stern, D.F., Weinberg, R.A. & Greene, M.I. Down-modulation of an oncogene protein product and reversion of the transformed phenotype by monoclonal antibodies. *Cell* **41**, 697–706 (1985).
37. Qian, X. et al. Identification of p185neu sequences required for monoclonal antibody- or ligand-mediated receptor signal attenuation. *DNA Cell Biol.* **16**, 1395–1405 (1997).
38. Hansen, M.B., Nielsen, S.E. & Berg, K. Re-examination and further development of a precise and rapid dye method for measuring cell growth/cell kill. *J. Immunol. Methods* **119**, 203–210 (1989).
39. Shepard, H.M. et al. Monoclonal antibody therapy of human cancer: taking the HER2 protooncogene to the clinic. [Review]. *J. Clin. Immunol.* **11**, 117–127 (1991).
40. O'Rourke, D.M. et al. Conversion of a radioresistant phenotype to a more sensitive one by disabling erbB receptor signaling in human cancer cells. *Proc. Natl. Acad. Sci. USA* **95**, 10842–10847 (1998).
41. Waldman, T. et al. Cell-cycle arrest versus cell death in cancer therapy. *Nat. Med.* **3**, 1034–1036 (1997).
42. Katsumata, M. et al. Prevention of breast tumour development in vivo by down-regulation of the p185neu receptor. *Nat. Med.* **1**, 644–648 (1995).
43. Qian, X., Dougall, W.C., Hellman, M.E. & Greene, M.I. Kinase-deficient neu proteins suppress epidermal growth factor receptor function and abolish cell transformation. *Oncogene* **9**, 1507–1514 (1994).

DEPARTMENT OF THE ARMY
US ARMY MEDICAL RESEARCH AND MATERIEL COMMAND
504 SCOTT STREET
FORT DETRICK, MARYLAND 21702-5012

REPLY TO
ATTENTION OF:

MCMR-RMI-S (70-1y)

1 JUN 2001

MEMORANDUM FOR Administrator, Defense Technical Information Center (DTIC-OCA), 8725 John J. Kingman Road, Fort Belvoir, VA 22060-6218

SUBJECT: Request Change in Distribution Statement

1. The U.S. Army Medical Research and Materiel Command has reexamined the need for the limitation assigned to technical reports. Request the limited distribution statement for reports on the enclosed list be changed to "Approved for public release; distribution unlimited." These reports should be released to the National Technical Information Service.

2. Point of contact for this request is Ms. Judy Pawlus at DSN 343-7322 or by e-mail at judy.pawlus@det.amedd.army.mil.

FOR THE COMMANDER:

Encl

PHYLLIS M. RINEHART
Deputy Chief of Staff for
Information Management

DAMD17-94-J-4413	ADB261602
DAMD17-96-1-6112	ADB233138
DAMD17-96-1-6112	ADB241664
DAMD17-96-1-6112	ADB259038
DAMD17-97-1-7084	ADB238008
DAMD17-97-1-7084	ADB251635
DAMD17-97-1-7084	ADB258430
DAMD17-98-1-8069	ADB259879
DAMD17-98-1-8069	ADB259953
DAMD17-97-C-7066	ADB242427
DAMD17-97-C-7066	ADB260252
DAMD17-97-1-7165	ADB249668
DAMD17-97-1-7165	ADB258879
DAMD17-97-1-7153	ADB248345
DAMD17-97-1-7153	ADB258834
DAMD17-96-1-6102	ADB240188
DAMD17-96-1-6102	ADB257406
DAMD17-97-1-7080	ADB240660
DAMD17-97-1-7080	ADB252910
DAMD17-96-1-6295	ADB249407
DAMD17-96-1-6295	ADB259330
DAMD17-96-1-6284	ADB240578
DAMD17-96-1-6284	ADB259036
DAMD17-97-1-7140	ADB251634
DAMD17-97-1-7140	ADB259959
DAMD17-96-1-6066	ADB235510
DAMD17-96-1-6029	ADB259877
DAMD17-96-1-6020	ADB244256
DAMD17-96-1-6023	ADB231769
DAMD17-94-J-4475	ADB258846
DAMD17-99-1-9048	ADB258562
DAMD17-99-1-9035	ADB261532
DAMD17-98-C-8029	ADB261408
DAMD17-97-1-7299	ADB258750
DAMD17-97-1-7060	ADB257715
DAMD17-97-1-7009	ADB252283
DAMD17-96-1-6152	ADB228766
DAMD17-96-1-6146	ADB253635
DAMD17-96-1-6098	ADB239338
DAMD17-94-J-4370	ADB235501
DAMD17-94-J-4360	ADB220023
DAMD17-94-J-4317	ADB222726
DAMD17-94-J-4055	ADB220035
DAMD17-94-J-4112	ADB222127
DAMD17-94-J-4391	ADB219964
DAMD17-94-J-4391	ADB233754